UNIVERSITAT DE BARCELONA

Oncogenes in aggressive B cell lymphomas:
dissecting the mechanisms of their aberrant expression and tumorigenic role

Marta Sureda Gómez

Oncogenes in aggressive B cell lymphomas: dissecting the mechanisms of their aberrant expression and tumorigenic role

Doctoral thesis presented by **Marta Sureda Gómez**

PhD Program in Biomedicine

FACULTY OF MEDICINE, UNIVERSITY OF BARCELONA

Doctoral supervisor: **Dr. Virginia Amador Espinosa**

Tutor: **Prof. Elias Campo Guerri**

Functional characterization of oncogenic mechanisms in lymphomagenesis

Fundació de Recerca Clínic Barcelona - Institut d'Investigacions Biomèdiques August Pi i Sunyer

Barcelona, 2023

Thesis presented by:

Marta Sureda Gómez

Doctoral supervisor: Dr. Virginia Amador Espinosa

Tutor: Prof. Elias Campo Guerri

This doctoral thesis was supported by a pre-doctoral fellowship FI-2018 grant for the recruitment of novel researchers (grant 2018FI_B_00632) from the "Agència de Gestió d'Ajuts Universitaris i de Recerca de Catalunya" (AGAUR). The work presented in this thesis was funded by grants from the "Ministerio de Ciencia, Innovación y Universidades" (MCIU) (project numbers BFU2015-64879-R and RTI2018-099793-B-I00) and from the "Fundació La Marató de TVE3" (project number 75/C/2019). This work was carried out at the Center Esther Koplowitz (CEK).

A mis padres

A mis hermanos

A Edu, y a la nueva vida que estamos formando juntos

“No siempre podemos hacer grandes cosas,

pero sí cosas pequeñas con gran amor.”

Madre Teresa de Calcuta

ABSTRACT

B cell lymphomas are a heterogeneous group of hematological neoplasms. The first tumorigenic events in B cell lymphomagenesis are usually translocations involving defined oncogenes that often lead a block on normal B cell differentiation. However, pre-tumoral cells need secondary hits involving other oncogenes to progress. The principal aims of this Thesis were to explore the functional role of specific oncogenes in aggressive B cell lymphomas, as well as to unravel the mechanisms that underlie their aberrant expression in lymphoid malignancies. Our final aim was to identify more effective targeted therapies against new specific oncogenic pathways to improve the outcome and life quality of patients with aggressive lymphomas.

In the **Study 1** of this thesis, I focused on mantle cell lymphoma (MCL), one of the most aggressive mature B cell neoplasms. Two subgroups of the disease with distinct clinical, biological and molecular features have been described. SOX11 transcription factor is aberrantly overexpressed in conventional MCL (cMCL) and negative or very weakly expressed in the nnMCL subtype. SOX11 has an oncogenic role in the pathogenesis of MCL. Patients with MCL expressing the SOX11 transcription factor have been shown to have worse prognoses compared to those that do not express SOX11, likely due to shorter responses to treatment and a higher incidence of relapse to current therapies. This might be attributed to the role of SOX11 regulating progenitors and stem cells proliferation and differentiation in various tissues. Additionally, SOX11 has been shown to enhance cancer stem cell (CSC) properties and to promote drug resistance in several cancer cell types. Thus, the aims for **Study 1** were to identify SOX11-dependent stemness-related factors as possible prognostic biomarkers for relapsed MCL, and to find therapeutic interventions targeting CSC-related genes for treatment of aggressive MCL.

In **Study 1**, I found that SOX11+ MCLs showed enrichment of hematopoietic and leukemic stem cell-related gene signatures, compared to SOX11- MCL primary cases and cell lines. Moreover, I identified Musashi-2 (MSI2) RNA-binding protein as one of the most significant stem cell-related genes upregulated in SOX11+ MCLs compared to SOX11- MCLs. *MSI2* expression correlated with worse overall survival in MCL. In

addition, *MSI2* expression was directly regulated by SOX11, and was associated with active intronic superenhancers. MSI2 upregulation might contribute to the maintenance of stem cell properties in MCL cells by promoting translation of stemness-related genes and downregulating apoptotic factors, since MSI2 knockdown and inhibition with Ro 08-2750 (RO) small molecule impaired self-renewal capabilities, such as clonogenic growth and aldehyde dehydrogenase (ALDH) activity, and decreased cell survival and chemoresistance. Finally, MSI2 knockdown inhibited tumoral cell dissemination and growth in MCL xenotransplanted mice models. Unfortunately, RO showed toxicity in our MCL mouse model, impairing us to test the efficacy of MSI2 inhibition in vivo. Therefore, our results open a new perspective for treatment, highlighting MSI2 oncogene as a potential therapeutic target to inhibit drug resistance and relapse in aggressive MCLs.

In the **Study 2** of this thesis, I focused on Burkitt lymphoma (BL), a highly proliferative B cell neoplasm that originates from germinal center B cells. Three clinical variants are distinguished: endemic (eBL), sporadic (sBL) and immunodeficiency-related BL. eBL is usually positive for Epstein-Barr virus (EBV) infection and presents with jaw or facial bone involvement. sBL shows lower frequency of EBV infection, and usually involves abdomen (Peyer's patches). One of the genetic hallmarks of BL is the t(8;14), leading to MYC overexpression. However, MYC overexpression is not enough to develop a BL. Several studies have revealed genetic and molecular differences depending on the clinical variant and the EBV status of BL patients. For instance, EBV+ BLs show lower driver mutations than EBV- BLs. Approximately 25-50% of BL patients show SOX11 overexpression. Although SOX11 has an impact on MCL prognosis, no association between SOX11 expression and survival has been found in BL. Several studies have shown the oncogenic role of SOX11 in the pathogenesis of MCL, but the contribution of SOX11 to BL pathogenesis and clinical evolution remains unknown. Thus, the aims for the **Study 2** were to understand the clinical relevance of SOX11 expression in BL, and to shed light on the functional role of SOX11 in the development of BL.

In **Study 2**, I have observed that EBV infection and SOX11 expression were mutually exclusive, and that SOX11+ BLs mainly exhibited *IG-MYC* translocations

acquired during class switch recombination (CSR), rather than somatic hypermutation (SHM), the process predominantly observed in SOX11- and EBV+ BL cases. In addition, SOX11+ BLs showed lower levels of *BCL6* and *AICDA*, alongside a distinct mutational landscape characterized by a higher frequency of *SMARCA4*, *ID3* and *RFX7* mutations, and a lower frequency of mutations in *DDX3X* gene, compared to EBV+ and SOX11- BLs. The previously described *SOX11* distal enhancer regions associated to SOX11 expression in MCL were not observed in BL. There were similarities in the transcriptional program regulated by SOX11 in BL and MCL, including upregulation of chemokine receptors. However, SOX11+ BL cells did not show differences in tumor cell migration or adhesion towards stromal cells compared to SOX11- BL cell lines. Instead, BL SOX11+ cells showed more adhesion to VCAM-1, associated to homing through the Peyer's patches. Therefore, I hypothesize that BL transformation could take place at different stages during germinal center differentiation and by distinct pathogenic mechanisms according to SOX11 expression or EBV infection in BLs. The molecular dichotomy observed between SOX11 and EBV suggests that both might play a role in early stages of BL tumorigenic transformation. However, due to limited functional effects observed upon ectopic overexpression of SOX11 in our BL cell line models compared to SOX11- BL cells, I hypothesize that SOX11 might not have a key role in the maintenance of this lymphoma in later stages.

Overall, I have described the role of two oncogenes, MSI2 and SOX11, in two non-Hodgkin lymphomas, MCL and BL, respectively. I have unraveled the mechanisms by which MSI2 is overexpressed and how exerts its tumorigenic function in MCL, highlighting MSI2 as a new possible target for therapeutic interventions to overcome drug resistance in aggressive MCL. I have also given some insights into the functional role of SOX11 in BL, demonstrating a clear dichotomy between EBV and SOX11, and suggesting different B cell of origin and pathogenic mechanisms between them in the pathogenic early transformation of mature B cells in BL. These findings have improved our understanding of the molecular mechanisms underlying these lymphomas and might guide the development of future therapies.

RESUMEN

Los linfomas de células B son un grupo heterogéneo de neoplasias hematológicas. Los primeros eventos en la linfomagénesis B son translocaciones que involucran ciertos oncogenes, resultando en un bloqueo de la diferenciación normal de las células B en las células tumorales. Sin embargo, las células pretumorales necesitan mecanismos secundarios que involucren a otros oncogenes para progresar. Los objetivos generales de esta tesis fueron explorar el papel funcional de ciertos oncogenes en los linfomas de células B agresivos, así como desentrañar los mecanismos que subyacen a su expresión aberrante en neoplasias linfoides. Nuestro objetivo final es poder desarrollar en el futuro terapias dirigidas más efectivas que aprovechen las vulnerabilidades de ciertas vías oncogénicas y mejorar la supervivencia y la calidad de vida de los pacientes con linfomas agresivos.

El **Estudio 1** de esta tesis versa sobre el linfoma de células del manto (LCM), una de las neoplasias de células B maduras más agresivas. Existen dos subgrupos de la enfermedad con distintas características clínicas, biológicas y moleculares. El factor de transcripción SOX11 se sobreexpresa de forma anómala en el subtipo de LCM convencional, pero se expresa negativa o muy débilmente en el subgrupo no nodal. SOX11 tiene un papel oncogénico en la patogénesis del LCM. Se ha demostrado que los pacientes con LCM que expresan el factor de transcripción SOX11 tienen peor pronóstico en comparación con aquellos que no expresan SOX11, probablemente debido a respuestas más cortas al tratamiento y una mayor incidencia de recaída con las terapias actuales. Esto puede atribuirse al papel de SOX11 en la regulación de la proliferación y diferenciación de progenitores y células madre en varios tejidos. Además, se ha demostrado que SOX11 promueve propiedades de células madre cancerosas (CSC) (*stemness*) y resistencia a las terapias en varios tumores. Por lo tanto, los objetivos del **Estudio 1** fueron identificar factores relacionados con *stemness* regulados por SOX11 como posibles biomarcadores pronósticos para el LCM recidivante, y desarrollar terapias dirigidas hacia los genes relacionados con las CSC para el tratamiento del LCM agresivo.

En el **Estudio 1**, observé que los LCM SOX11+ mostraban un enriquecimiento de firmas genéticas relacionadas con células madre hematopoyéticas y leucémicas, en comparación con los casos y líneas celulares primarios de LCM SOX11-. Además, identifiqué la proteína de unión al ARN Musashi-2 (MSI2) como uno de los genes relacionados con la *stemness* más importantes regulados al alza en los LCM SOX11+ en comparación con los SOX11-. La expresión de MSI2 se correlacionaba con una peor supervivencia global en los pacientes con LCM. Además, la expresión de MSI2 estaba regulada directamente por SOX11 y se asociaba con superpotenciadores intrónicos activos. El incremento de la expresión de MSI2 podría contribuir al mantenimiento de las propiedades de las células madre en las células del LCM mediante el incremento de la traducción de genes relacionados con la *stemness* y el descenso de factores pro-apoptóticos, ya que el silenciamiento y la inhibición de MSI2 con el fármaco Ro 08-2750 (RO) perjudican las capacidades de autorrenovación, como el crecimiento clonogénico y la actividad de la aldehído deshidrogenasa (ALDH), y disminuyen la supervivencia celular y la quimiorresistencia de las células del LCM. Finalmente, la eliminación de MSI2 inhibió la diseminación y el crecimiento de células tumorales en modelos de ratones xenotrasplantados con células de LCM. Desafortunadamente, el fármaco RO mostró toxicidad en nuestro modelo de ratón de LCM, lo que nos impidió comprobar la eficacia de la inhibición de MSI2 in vivo. Por lo tanto, nuestros resultados abren una nueva perspectiva para el tratamiento, destacando el oncogén MSI2 como una diana terapéutica potencial para inhibir la resistencia a los medicamentos y la recaída en los pacientes con LCM agresivo.

El **Estudio 2** de esta tesis versa sobre el linfoma de Burkitt (BL), una neoplasia de células B altamente proliferativa que se origina a partir de las células B del centro germinal. Se distinguen tres variantes clínicas: BL endémico (eBL), BL esporádico (sBL) y BL relacionado con inmunodeficiencia. El eBL suele presentar infección del virus de Epstein-Barr (EBV) y afecta generalmente la mandíbula o el hueso facial. El sBL muestra una frecuencia más baja de infección por EBV y generalmente se desarrolla en el abdomen (placas de Peyer). Una de las características genéticas de BL es la t(8;14), que conduce a

la sobreexpresión de MYC. Sin embargo, la sobreexpresión del oncogén MYC no es suficiente para desarrollar un BL. Varios estudios han revelado diferencias genéticas y moleculares según la variante clínica y el estado del EBV de los pacientes con BL. Por ejemplo, los BL que son EBV+ muestran mutaciones "*driver*" en menor proporción que los BL que son EBV-. Aproximadamente el 25-50% de los pacientes con BL muestran sobreexpresión del factor de transcripción SOX11. Aunque SOX11 tiene un impacto en el pronóstico del LCM, no se ha encontrado asociación entre la expresión de SOX11 y la supervivencia en los pacientes de BL. Varios estudios han demostrado el papel oncogénico de SOX11 en la patogénesis del LCM, pero se desconoce la contribución de SOX11 a la evolución clínica del BL. Por lo tanto, los objetivos del **Estudio 2** fueron comprender la relevancia clínica de la expresión de SOX11 en BL e investigar sobre el papel funcional de SOX11 en el desarrollo del BL.

En el **Estudio 2**, observé que la infección por EBV y la expresión de SOX11 eran mutuamente excluyentes, y que los BL SOX11+ exhibían principalmente translocaciones *IG-MYC* adquiridas durante el mecanismo de conmutation del isotipo (CSR), en lugar de durante la hipermutación somática (SHM), como ocurre en los casos de BL SOX11- y EBV+. Además, los BL SOX11+ mostraron niveles más bajos de *BCL6* y *AICDA*, junto con un paisaje mutacional distintivo caracterizado por una frecuencia más alta de mutaciones en *SMARCA4*, *ID3* y *RFX7*, y una frecuencia más baja de mutaciones en el gen *DDX3X*, en comparación con los BL EBV+ y SOX11-. Las regiones potenciadoras distales de *SOX11* descritas anteriormente asociadas a la expresión de SOX11 en el LCM no se observaron en el BL. Había similitudes en el programa transcripcional regulado por SOX11 en BL y MCL, incluida la regulación positiva de los receptores de quimiocinas. Sin embargo, las células SOX11+ BL no mostraron diferencias en la migración o adhesión de las células tumorales hacia las células del estroma en comparación con las líneas celulares SOX11-. En cambio, las células BL SOX11+ mostraron más adhesión a VCAM-1, que promueve la migración de las células B hacia las placas de Peyer. Por lo tanto, la transformación del BL podría tener lugar en diferentes etapas durante la diferenciación del centro germinal y mediante distintos mecanismos patogénicos según la expresión de

SOX11 y la infección por EBV en los BL. La dicotomía molecular observada entre SOX11 y EBV sugiere que ambos podrían desempeñar un papel relevante en las primeras etapas de la transformación tumorigénica de BL. Sin embargo, los limitados efectos funcionales observados en nuestros modelos celulares de BL SOX11+ sugieren que SOX11 podría no tener un papel clave en el mantenimiento de este linfoma en etapas posteriores.

En general, en esta tesis se ha descrito el papel de dos oncogenes, MSI2 y SOX11, en el LCM y el BL, respectivamente. He desentrañado los mecanismos por los cuales MSI2 se sobreexpresa y cómo ejerce su función tumorigénica en el LCM, destacando MSI2 como una nueva diana terapéutica para vencer la resistencia a los medicamentos en el LCM agresivo. También se han aportado algunas ideas sobre el papel funcional de SOX11 en el BL, demostrando una clara dicotomía entre EBV y SOX11, y sugiriendo diferentes mecanismos patogénicos y diferencias en las células B de origen entre ellos en la transformación temprana del BL. Estos hallazgos han mejorado nuestra comprensión de los mecanismos moleculares subyacentes a estos linfomas y podrían guiar el desarrollo de futuras terapias.

LIST OF SELECTED ABBREVIATIONS

4-OHT	4-hydrohytamoxifene
AICDA	Activation-induced cytidine deaminase
ALDH	Aldehyde dehydrogenase
AML	Acute myeloid leukemia
B-ALL	B acute lymphoblastic leukemia
BCR	B cell receptor
BL	Burkitt lymphoma
BMSC	Bone marrow stromal cells
BSA	Bovine serum albumin
CAM-DR	Cell adhesion mediated drug resistance
CAMs	Cell adhesion molecules
CCL19	C-C motif chemokine ligand 19
CCL21	C-C motif chemokine ligand 21
CCND1	Cyclin D1
CCND2	Cyclin D2
CCND3	Cyclin D3
CCR7	C-C motif chemokine receptor 7
CDK6	Cyclin dependent kinase 6
ChIP	Chromatin immunoprecipitation
ChIP-chip	Chromatin immunoprecipitation on DNA microarray
CLL	Chronic lymphocytic leukemia
cMCL	Conventional MCL
CML	Chronic myeloid leukemia
CMPs	Common myeloid progenitors
CNA	Copy number alterations
CNS	Central nervous system
CSCs	Cancer stem cells
CSR	Class switch recombination

CXCR4	C-X-C motif chemokine receptor 4
CXCR5	C-X-C motif chemokine receptor 5
DCIS	Ductal carcinoma in situ
DLBCL	Diffuse large B cell lymphoma
DMSO	Dimethyl sulfoxide
DNMTs	DNA methyl transferases
EBER	EBV-encoded small nuclear RNA
eBL	Endemic BL
EBV	Epstein-Barr virus
ER	Estrogen Receptor
ESCs	Embryonic stem cells
FBS	Fetal bovine serum
FC	Flow Cytometry
FDC	Follicular dendritic cells
FFPE	Formalin fixed, paraffin embedded
FISH	Fluorescence in situ hybridization
FITC	Fluorescein isothiocyanate
FL	Follicular lymphoma
GMP	Granulocyte-monocyte progenitor
gRNA	Guide RNA
GSEA	Gene set enrichment analysis
HEVs	High endothelial venules
HIV	Human immunodeficiency virus
HMG	High mobility group
HSC	Hematopoietic stem cells
iBL	Immunodeficiency-related BL
IG	Immunoglobulin
IGH	Immunoglobulin heavy gene
IGK	Immunoglobulin kappa gene
IGL	Immunoglobulin lambda gene

IHC	Immunohistochemistry
IL7R	Receptor for IL-7 interleukin
iPSCs	Induced pluripotent stem cells
ISH	In situ hybridization
KLF4	Kruppel-like factor 4
KO	Knock out
LMPPs	Lymphoid-primed multipotent progenitors
LSK	Lin-Sca-1+c-Kit+
LT-HSCs	Long term-hematopoietic stem cells
MAdCAM	Mucosal addressin cell adhesion molecule
MALT	Mucosa-associated lymphoid tissue
MCL	Mantle cell lymphoma
MDS	Myelodysplastic syndromes
MEP	Megakaryocyte-erythrocyte progenitor
MFI	Mean fluorescence intensity
MIPI-c	Combined MCL international prognostic index
MLL	Mixed-lineage leukemia
MSCs	Mesenchymal stem cells
MSI2	Musashi-2
MSI2KD	MSI2-knockdown
NHL	Non-Hodgkin's lymphomas
nnMCL	Non-nodal MCL
NANOG	Nanog Homeobox
NPC	Neural progenitor cell
OCT4	Octamer-binding transcription factor 4
OS	Overall survival
PAX5	Paired box protein Pax-5
PBS	Phosphate-buffered saline
PCA	Principal component analysis
PDGF	Platelet-derived growth factors

PI	Propidium Iodide
PRMT5	Protein arginine methyltransferase 5
RAG1/RAG2	Recombination-activating proteins 1 and 2
RBPs	RNA binding proteins
R-CHOP	Rituximab, cyclophosphamide, doxorubicin, vincristine, and prednisone
RIP	RNA immunoprecipitation
RBD	RNA binding domain
RNAi	RNA interference
RNA-seq	RNA-sequencing
Ro 08-2750	Ro
RSS	Recombination signal sequence
sBL	Sporadic BL
SHM	Somatic hypermutation
SNV	Single nucleotide variant
SOX11	Sex-determining region Y-box11
SOX4	SRY-box transcription factor 4
SRY	Sex-determining region Y
ST-HSCs	Short term-hematopoietic stem cells
SV	Structural variants
T-ALL	T acute lymphoblastic leukemia
TdT	Terminal deoxynucleotidyl transferase
TGF-β1	Transforming growth factor beta 1
T_H	Helper T cells
TSS	Transcription start site
VCAM	Vascular cell adhesion molecule
VEGF	Vascular endothelial growth factors
WB	Western Blot
WGBS	Whole genome bisulfite sequencing
WGS	Whole-genome sequencing
WHO	World Health Organization

TABLE OF CONTENTS

INTRODUCTION

1. B CELL NON-HODGKIN'S LYMPHOMAS

1.1 General concepts

Non-Hodgkin's lymphomas (NHLs) are a heterogeneous group of hematological neoplasms that arise from any type of lymphocyte, including immature or mature B, T or NK lymphoid cells (Swerdlow et al., 2017). NHLs primarily affect the organs of the lymphatic system, but they vary widely in their clinical presentation, progression and treatment (Armitage et al., 2017). The World Health Organization (WHO) has developed a detailed classification system for NHLs to better stratify patients, improve their diagnosis and provide them with more accurate treatments. An integration of several techniques, such as morphology, immunophenotyping and genetics, is usually needed to resolve this classification in lymphoma patients (Swerdlow et al., 2017; Campo et al., 2022).

1.2 General aspects of lymphomagenesis

Mature B cell lymphomas account for the majority (85-90%) of NHLs and are more common in developed countries, except for certain subtypes. Several factors, including infections, genetics and immune disorders, increase the risk of developing B cell lymphomas (Armitage et al., 2017). For instance, human immunodeficiency virus (HIV) or Epstein-Barr virus (EBV) infection are associated with the development of Burkitt lymphoma (BL) or diffuse large B cell lymphoma (DLBCL) (Saha & Robertson, 2011; Carbone et al., 2022; Molyneux et al., 2012).

However, the initial events leading to B cell lymphomagenesis are usually translocations involving immunoglobulin gene regions (*IG*) and a specific oncogene partner, that occur during B cell receptor (BCR) generation and maturation as part of the normal B cell differentiation process (Küppers & Dalla-Favera, 2001; Dalla-Favera & Gaidano, 2001; Willis & Dyer, 2000). If these processes fail, a translocation can be produced, juxtaposing the regulatory regions of *IG* genes to a specific partner gene. Since *IG* genes are highly expressed in B cells, translocations involving *IG* regulatory regions lead to overexpression of the partner gene.

However, not all humans with *IG* aberrant translocations develop hematologic neoplasms (Schüler et al., 2009; Müller et al., 1995), and there are several checkpoints in B cells to avoid inefficient B cell maturation (Melchers, 2015), indicating that secondary hits are required for pre-tumoral B cells to progress into a lymphoma (Shaffer et al., 2012). Once this occurs, tumor B cell differentiation is generally blocked, remaining in a particular “B cell stage” (Küppers et al., 1999; Greaves, 1986). The broad spectrum of B cell lymphomas reflects the normal B cell differentiation process, with each specific lymphoma sharing immunophenotypic and genetic characteristics with its cell of origin (Swerdlow et al., 2017). Therefore, the biology of different lymphomas depends not only on their B cell of origin but also on the genetic, epigenetic and molecular alterations required to overcome tumor suppression mechanisms (Jaffe et al., 2008; Shaffer et al., 2002; Scott & Gascoyne, 2014).

Thus, understanding the generation and differentiation of immune cells is crucial for comprehending the biological differences between hematologic neoplasms.

1.3 Immune system

1.3.1 General overview

Throughout their lives, humans are exposed to a wide range of harmful pathogens. To protect against these threats, the immune system is composed of numerous cells and molecules that work together in a complex and dynamic network. The immune cells are organized into primary and secondary lymphoid organs, with the bone marrow and thymus serving as the primary sites where lymphocytes are generated and matured. Mature lymphocytes then move through the bloodstream to secondary lymphoid organs such as lymph nodes, spleen, or mucosa-associated lymphoid tissue (MALT), where they interact with antigens.

The immune system's diversity is essential for recognizing and eliminating exogenous organisms and abnormal or damaged endogenous cells. In order to achieve this, the immune system must be highly adaptable, diversified, and capable of "remembering" previous pathogens. As a result, certain immune cells remain after an

infection to recognize future pathogenic threats, while others are continually replaced, requiring a continuous production of hematopoietic cells.

1.3.2 Hematopoiesis

Hematopoiesis is the process that generates the totality of the cells composing the hematopoietic system (Orkin, 1995). It initially takes place in the fetal liver and is later taken over by the bone marrow for the rest of an individual's life (Melchers, 2015). Hematopoiesis is critical for homeostasis and correct function of the immune system. The hematopoietic system is the paradigm of a hierarchical cell model, with hematopoietic stem cells (HSCs) at the top of the hierarchy.

1.3.2.1 Hierarchy of HSCs

HSCs have the unique ability to generate all different types of hematopoietic cells, including erythrocytes, monocytes, and lymphocytes, due to their intrinsic properties of self-renewal and pluripotency (Till & McCulloch, 1961). In other words, HSCs can divide to produce another HSC without differentiation, while simultaneously generating a large number of differentiated cells.

Long term-HSCs (LT-HSCs) first generate multipotent progenitors named short term-HSCs (ST-HSCs), which have lost the ability to self-renew but still maintain the potential to differentiate into all cell lineages. From ST-HSCs derive two different cells, the lymphoid-primed multipotent progenitors (LMPPs) and the common myeloid progenitors (CMPs), which constitute the lymphoid and the myeloid lineages (Figure 1). The CMPs divides into two intermediate cells, the megakaryocyte-erythrocyte progenitor (MEP), that gives rise to platelets and erythrocytes, and the granulocyte-monocyte progenitor (GMP), that generates granulocytes and monocytes, the cells composing the innate immune system. Regarding the LMPPs, they differentiate into B and T lymphocytes, that constitute the adaptive immune system, and into NK lymphocytes (Cedar & Bergman, 2011; Orkin & Zon, 2008). This process is thoroughly coordinated by several components, including the regulated expression of several transcription factors, and the cytokines and growth factors secreted by the bone marrow niche (Orkin, 2000; Zon, 2008; Orkin & Zon, 2008).

For example, the proper function of adult HSCs is affected by Wnt/β-catenin and Notch-Delta signaling pathways, that induce expression of specific target genes (Figure 1). The addition of Wnt3a protein to HSCs increases their self-renewal, measured as the engraftment into irradiated recipient mice (Reya et al., 2003), although a continuous activation of Wnt pathway leads to HSC exhaustion (Scheller et al., 2006). Besides, the activation of Notch signaling boosts HSC activity and cooperates with Wnt pathway to increase the self-renewal (Duncan et al., 2005). Notch-1, one of the members of Notch family receptors, regulates the cell fate of hematopoietic progenitors (Pui et al., 1999), but also suppresses the differentiation of hematopoietic progenitors, probably through the regulation of cell cycle (Stier et al., 2002; Carlesso et al., 1999).

Cell cycle kinetics is important for the maintenance of HSCs, as it is needed a balance between quiescent and proliferating states. One of the proteins regulating this process is cyclin dependent kinase 6 (CDK6), which is not expressed in LT-HSCs but becomes highly expressed after the differentiation of LT-HSCs to ST-HSCs, enabling a quick entrance into cell cycle (Laurenti et al., 2015) (Figure 1). Thus, several factors are involved in the regulation of self-renewal and differentiation of HSCs.

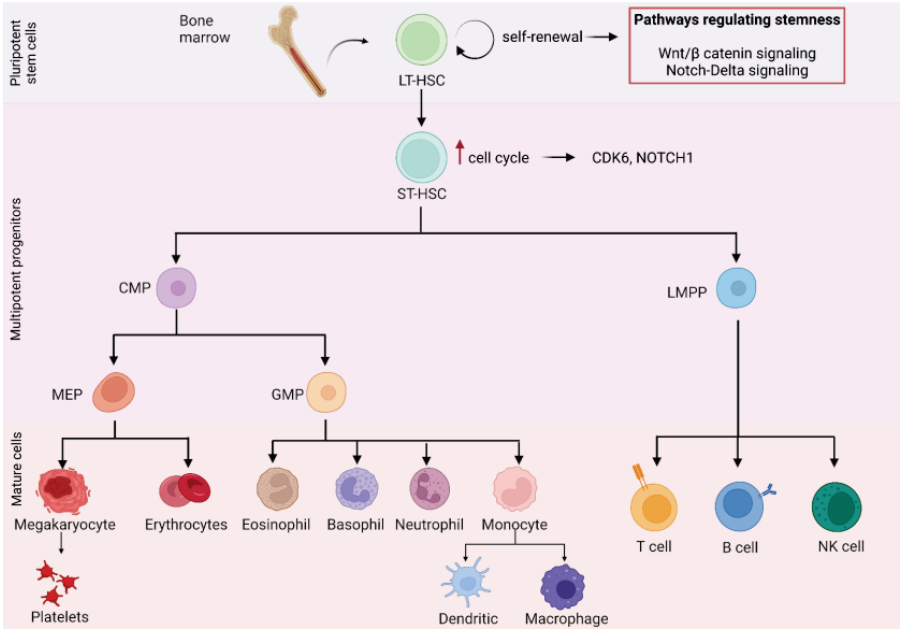

Figure 1. Schematic representation of hematopoiesis. Pluripotent stem cells, multipotent progenitors and mature cells generated during hematopoiesis, and relevant pathways. Figure adapted from Orkin & Zon, 2008.

As this thesis is focused on B cell lymphomas, the B cell differentiation process is explained in detail below.

1.3.2.2 B cell differentiation

The final fate of B cell differentiation is to generate effector cells capable to identifying antigens and neutralizing the exogenous or endogenous pathogenic elements through an antibody response. The differentiation of B cells from their precursor cells is a complex process that involves several stages (Figure 2).

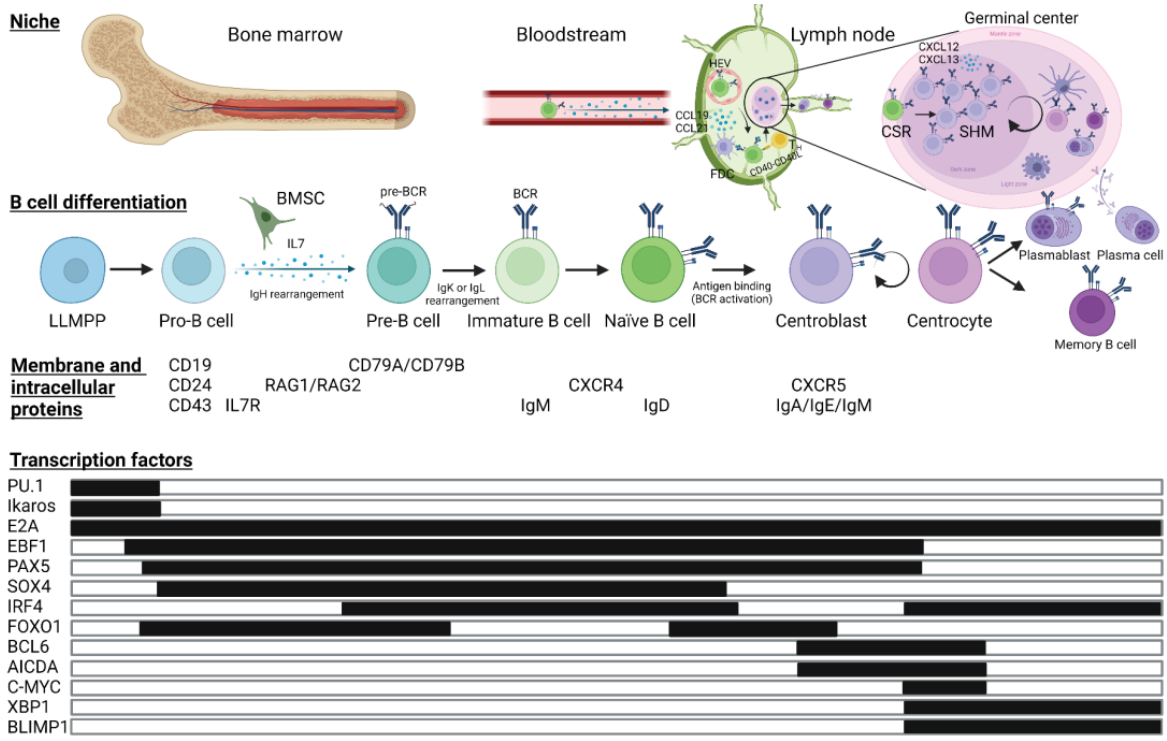

Figure 2. Graphical scheme of B cell differentiation process. Representation of the different B cell stages, their niche, the mechanisms produced, the membrane and intracellular proteins, and the transcription factors expressed during B cell differentiation.

1.3.2.2.1 Initial steps

The initial steps of B cell differentiation occur in the bone marrow. There, the LMPPs give rise to pro-B cells, characterized by the expression of the CD19, CD24 and CD43 cell surface markers, and the absence of immunoglobulin molecules (Figure 2). The interaction between bone marrow stromal cells (BMSC) and pro-B cells promotes the expression of the receptor for IL-7 interleukin (*IL7R*). The IL-7 secreted by the BMSC

induced the maturation of the pro-B cells, that start to express specific transcription factors (Chaplin, 2010; Nagasawa, 2006). This epigenetic change leads to the transcription of V(D)J recombination-activating proteins 1 and 2 (*RAG1* and *RAG2)*, and consequently, to the recombination of *IG* variable segments (VDJ recombination) to obtain a functional antibody.

1.3.2.2.2 VDJ recombination

The antibodies are constituted by two Ig heavy (*IGH*) and two Ig light chains [kappa (*IGK*) or lambda (*IGL*)]. Each of these chains has a constant and a variable region. The variable region of the heavy chain is itself composed of multiple V_H, D_H and J_H segments, and the light chain of V_L and J_L segments (Chaplin, 2010). The constant region of heavy chain contains 9 different exons, used to generate the different Ig isotypes (IgM, IgD, IgG, IgA and IgE), while the constant region of light chains contains a single exon (Bonilla & Oettgen, 2010). The constant region outlines the effector function of the antibody, while the variable region provides specificity and variability for the recognition of the antigen (Pieper et al., 2013).

During VDJ recombination, RAG1 and RAG2 proteins recognize specific sequences located near the start and the end of the V(D)J segments named recombination signal sequence (RSS), inducing a break and a subsequent deletion of the genomic sequences between them, and maintaining only a subset of these V(D)J segments (Schroeder & Cavacini, 2010) (Figure 3). The rearrangement is first induced in the *IG* heavy chain gene, with a recombination between D_H and J_H segments. Then, the pro-B cell starts to express a heterodimer of Ig-α (CD79A) and Ig-β (CD79B) (Figure 2). When the V_H and D_HJ_H are finally rearranged, the pro-B differentiates into a pre-B cell expressing a pre-BCR. If the rearrangement fails, the other allele will follow the same process. If not, an allele exclusion is produced to have a unique heavy chain for each B cell (Melchers, 2015). Only during the Ig heavy rearrangement is expressed the terminal deoxynucleotidyl transferase (TdT), which add random nucleotides at D_H-J_H and V_H-D_HJ_H coding junctions (Chaplin, 2010) (Figure 3).

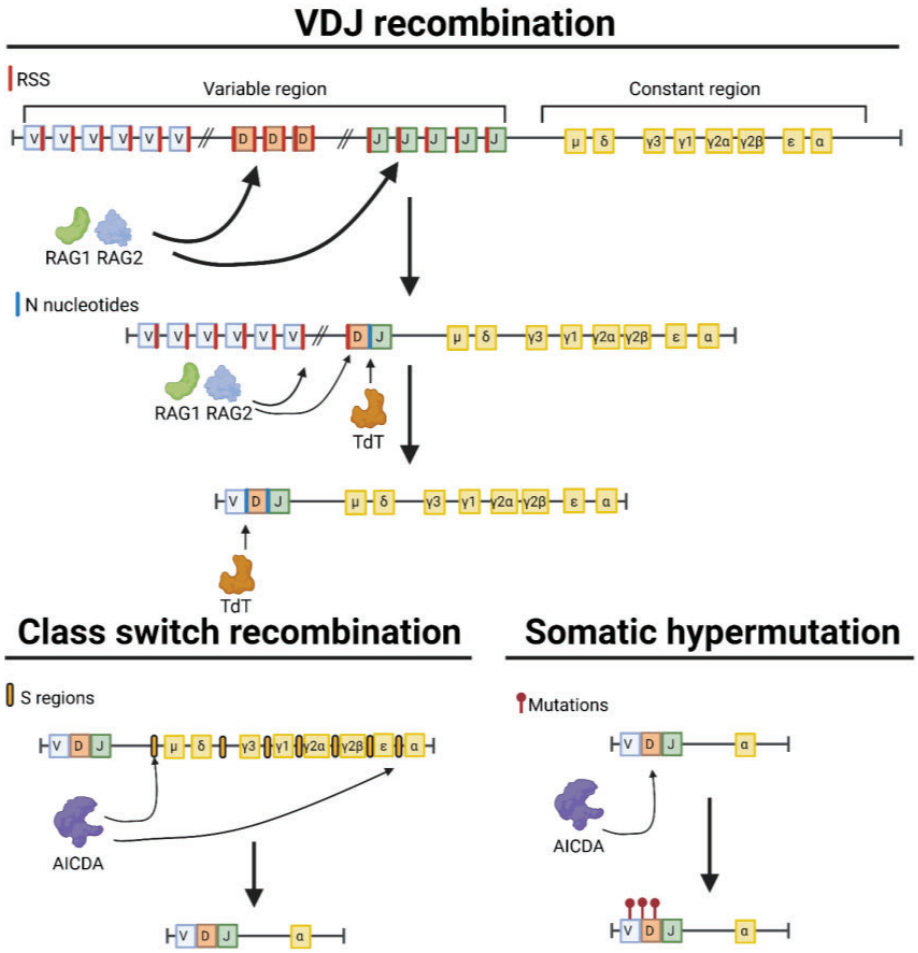

Figure 3. Schemating representation of rearrangement and affinity maturation of immunoglobulin heavy chain. Variable regions of *IG* heavy and light chains are rearranged during VDJ recombination process, and constant regions are switched by class switch recombination. Then, affinity maturation is achieved by somatic hypermutation process that adds mutations in the VDJ region.

Then, a specific *IG* light chain gene will be rearranged, generating an immature B cell expressing the complete BCR (Ig-α, Ig-β and IgM) (Figure 2). If some of these processes fail or the cell becomes auto-reactive (recognition of self-antigens), the B cell will be eliminated. Then the immature B cell enters to bloodstream differentiating into a naïve B cell expressing IgM and IgD surface immunoglobulins in search of an antigen (Melchers, 2015; Chaplin, 2010) (Figure 2).

1.3.2.2.3 Lymphocyte migration to secondary lymphoid organs

Naïve B cells migrate to secondary lymphoid organs through high endothelial venules (HEVs), following several chemoattractants that bind to their G protein-coupled chemoreceptors (Springer, 1994) (Figure 2). C-X-C motif chemokine receptor 4 (CXCR4), 5 (CXCR5) and C-C motif chemokine receptor 7 (CCR7) are some of the chemoreceptors expressed in naïve B cells, and bind to C-X-C motif chemokine ligand 12 (CXCL12), 13 (CXCL13), and C-C motif chemokine ligand 19 (CCL19) and 21 (CCL21) chemokines, respectively (Stein & Nombela-Arrieta, 2005). Different types of cells secrete several chemokines. For example, stromal cells secrete CXCL12 and CXCL13 and HEVs secrete CCL19 and CCL21 to guide lymphocytes within different secondary lymphatic tissues (Table 1) (Figure 2).

The activation of chemoreceptors induces conformational changes and aggregation of cell surface integrins (Stein & Nombela-Arrieta, 2005). The adhesion between integrins and cell adhesion molecules (CAMs) of the Ig superfamily is required to produce lymphocyte extravasation in the endothelium (Springer, 1994). The HEVs express different types of CAMs of the selectin, mucin and Ig families, that bind to lymphocyte integrins. For example, MAdCAM-1, VCAM-1 and fibronectin CAM molecules expressed by HEVs are necessary for the B and T cell homing into Peyer's patches, which are one of the main components of MALT, through the direct binding to α4β7, and also regulate the homing to other locations together with different CAMs (Ruegg et al., 1992; Berlin et al., 1993; Drillenburg & Pals, 2000) (Table 1).

Table 1. Lymphocyte chemoreceptors and cell adhesion molecules implicated in lymphocyte homing.

Receptor	Expression on Lymphocytes	Ligands	Ligands secreted by	Predominant Role in Homing
Chemoreceptors				
CXCR4	T and B cells	CXCL12	Stromal cells, Endothelial cells	Homing to bone marrow and lymph nodes
CXCR5	B cells Follicular helper T cells	CXCL13	FDC	Homing to lymphoid follicles
CCR7	T and B cells	CCL19 CCL21	Stromal cells, HEV	Homing to secondary lymphoid organs

Receptor	Expression on Lymphocytes	Ligands	Interacting Cells/ Substrates	Predominant Role in Homing
CAM				
L-selectin	T and B cells	PNAd GlyCAM CD34 (MAdCAM-1)	HEV	Peripheral lymph node-homing
αLβ2 (LFA-1)	T and B cells	ICAM-1 ICAM-2 ICAM-3	Endothelium, HEV, Dendritic cells, FDC, Activated epithelium	Broad function in lymphocyte homing
α4β1 (VLA-4)	T and B cells	VCAM-1 Fibronectin (CS-1)	Activated endothelium, Dendritic cells, FDC	Homing to inflammatory sites
α4β7	Naive T and B cells Memory T-cell subset Peripheral B-cell subset	MAdCAM-1 (VCAM-1) (Fibronectin)	Endothelium of intestinal mucosa, Peyer patches, mesenteric lymph node, HEV	Gut-homing

FDC: follicular dendritic cells; HEV: high endothelial venules; GlyCAM: glycosylation-dependent cell adhesion molecule; ICAM: intercellular adhesion molecule; LFA: lymphocyte function-associated; MAdCAM: mucosal addressin cell adhesion molecule; VCAM, vascular cell adhesion molecule; VLA: very late antigens.

1.3.2.2.4 Germinal center reaction

Naïve B cells migrate to secondary lymphoid organs to establish contact with an antigen. They initially reside in primary lymphoid follicles along with other immune cells such as helper T cells (T_H) and follicular dendritic cells (FDC) (Figure 2). After recognizing an antigen presented by FDC, the B cells undergo clonal selection, resulting in their activation and proliferation via BCR signaling. This leads to the formation of a secondary lymphoid follicle that contains proliferating B cells called centroblasts surrounded by resting B cells that form the mantle zone (Klein & Dalla-Favera, 2008).

If a T_H cell provides co-stimulation to these activated B cells by CD40-CD40L interaction (T cell dependent humoral response), it can result in a change in the antibody isotype as well as an increase in its affinity (Figure 2). Here starts the so-called germinal center reaction. B cells may be also activated in an independent T cell manner in the marginal zone of the follicles (T cell independent response), but the antibodies generated are of low diversity because the germinal center reaction is not produced (De Silva &

Klein, 2015). In the germinal center, different cytokines secreted by T cells and dendritic cells induce the class switch recombination (CSR) process, promoting the Ig change into a particular isotype. For example, transforming growth factor beta 1 (TGF-β1) present in the microenvironment of Peyer's patches induces a class switch towards IgA isotype, which is specialized in protecting mucosal barriers (Cerutti & Rescigno, 2008) (Figure 4).

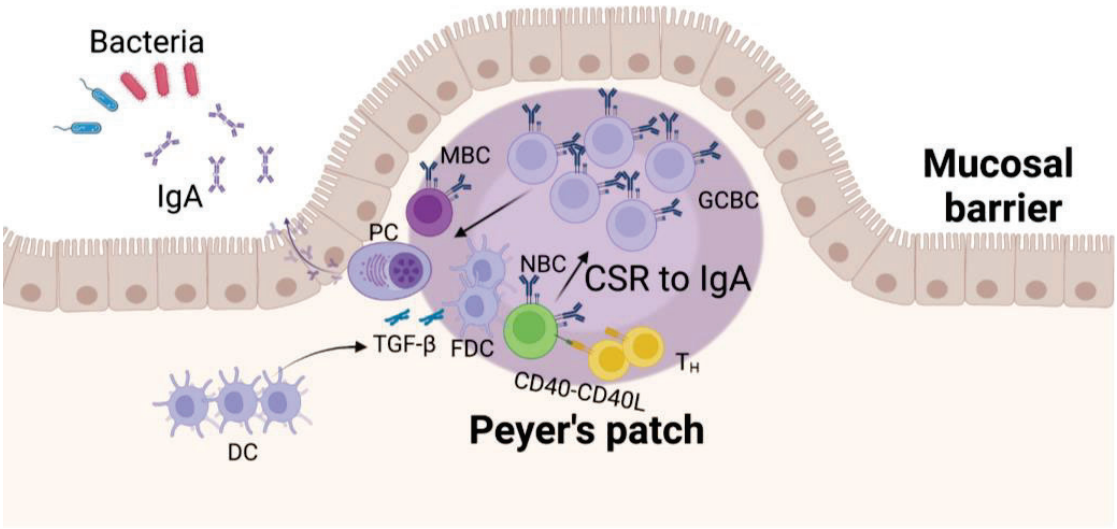

Figure 4. Specific class switch into IgA isotype in Peyer's patches. Dendritic cells and T cells induced IgA class switching by activating B cells present in the Peyer's patches through TGF-β and CD40L. Then, IgA antibodies are secreted into the lumen of intestinal tract. Figure adapted from Cerutti & Rescigno, 2008.

CSR is regulated by activation-induced cytidine deaminase (AICDA), which induces breaks around switch regions flanking the exons of the constant region of *IGH* (μ, δ, γ, ε and α) (Okazaki et al., 2002) (Figure 3). This is resolved by recombination, deleting the DNA sequences between S regions, and results in the expression of a different Ig isotype (Schroeder & Cavacini, 2010). However, a recent study suggests that the CSR process may occur outside the follicle, prior to the germinal center reaction, which contradicts previous beliefs (Roco et al., 2019).

After CSR, B cells undergo somatic hypermutation (SHM), a process also regulated by AICDA, that induces mutations around VDJ segments to increase the antibody affinity for the antigen (Figure 3). If the affinity increases, the BCR signaling will be more active, leading to the survival of the lymphocyte. Otherwise, the pro-survival

signals decrease, conducing to the apoptosis of the cell (Victora & Nussenzweig, 2022). Afterwards, the centroblasts become centrocytes, cells with lower rates of proliferation.

Centroblasts and centrocytes are localized in opposite poles in the germinal center, called dark and light zones, respectively. However, centrocytes can re-enter the dark zone multiple times to undergo several rounds of germinal center reaction to increase their affinity for the antigen (De Silva & Klein, 2015) (Figure 2). If the centrocyte is finally positively selected, it differentiates into effector memory or plasma cells, which will return to the bloodstream in search of infection sites where they must act. Plasma cells are short-life specialized effector B cells that secrete high amounts of antibodies, while memory cells have a longer lifespan and can rapidly differentiate into plasma cells in a future immune response against the same antigen (Akkaya et al., 2020). To ensure an adequate and rapid effector response to infection, careful regulation of the B cell differentiation process is necessary. This involves a series of epigenetic and transcriptional changes that drive each step of B cell differentiation.

1.3.2.2.5 Transcriptional and epigenetic regulation of B cell differentiation

The B cell differentiation process requires lineage-specific transcription factors and epigenetic modification that direct cells' fate decisions in a stepwise manner. Disruptions in this process can result in various diseases, ranging from benign lymphoproliferative disorders to malignant conditions such as leukemia and lymphoma.

The differentiation of MPPs to LMPPs is controlled by three key transcription factors: PU.1 (SPI1), Ikaros (IKZF1) and E2A (also named TCF3) (Figure 2). Moreover, E2A regulates the expression of Early B cell factor (EBF1) and Paired box protein Pax-5 (PAX5), that are essential for the transition of LMPPs to pro-B cells rather than T or NK cell lineages (Rothenberg, 2014; Fischer et al., 2020). PAX5 together with SRY-box transcription factor 4 (SOX4) are also necessary to enable rearrangement of *IGH* variable regions and to facilitate the formation of signaling complexes that allow the cells to receive signals from the BCR (Cobaleda et al., 2007; Mallampati et al., 2014) (Figure 2). Other transcription factors, such as Interferon regulator factor-4 (IRF4) and Forkhead box O transcription factor-1 (FOXO1), are required to promote the VDJ recombination in pro-

B cells, but they have additional roles in other stages of B cell differentiation (Dengler et al., 2008; Bevington & Boyes, 2013).

Once naïve B cell is activated, it starts to express B-cell lymphoma 6 protein (BCL6) (Figure 2). BCL6 is the master transcriptional repressor during germinal center reaction. BCL6 prevents an early differentiation from germinal center B cells to plasma cells and induces toleration through DNA break to permit CSR and SHM process (Basso & Dalla-Favera, 2012). The centrocyte re-entry to the dark zone is induced by c-MYC (MYC), which activates cyclin D2 (*CCND2)* and cyclin D3 (*CCND3)* leading to CCND2-dependent proliferation. On the other hand, MYC is suppressed in the centroblasts, and E2A becomes responsible for sustaining proliferation via *CCND3* and *E2F2* activation (De Silva & Klein, 2015). FOXO1 is also necessary in this stage to induce CSR through *AICDA* upregulation (Dengler et al., 2008). Finally, the differentiation into plasma cells is achieved by upregulation of IRF4, X-box-binding protein 1 (XBP1) and B-lymphocyte-induced maturation protein 1 (BLIMP1), that repress B cell programs promoting Ig secretion and an exit of cell cycle (Shapiro-Shelef & Calame, 2005) (Figure 2).

The genome-wide binding patterns of all these transcription factors must be modulated during B cell differentiation. This is possible due to the action of many epigenetic regulators that open or close the chromatin through changes in histone modifications, levels of DNA methylation or DNA strands disruption, among others (E. Li, 2002). Some important epigenetic regulators in B cells are SMARCA4, EZH2 and DNMT1, that control the access of B cell-specific transcription factors to regions that must be activated or repressed during B cell differentiation (Bossen et al., 2015; Guo et al., 2018; Shaknovich et al., 2011).

2. ONCOGENIC MECHANISMS IN B CELL LYMPHOMAS

Tumorigenic cells need different functional capabilities in their way from normal B cells to malignant tumors. This is known as the hallmarks of cancer, defined for the first time by Hanahan and Weinberg in 2000 (Hanahan & Weinberg, 2000). The hallmarks of cancer have been continuously updating as the research has progressed (Hanahan & Weinberg, 2011; Hanahan, 2022). Several hallmarks have been described, and some have

important roles in B cell lymphomagenesis, such as the genomic instability and mutation, the sustaining proliferative signaling, the resistance to cell death, the induction of angiogenesis and the evasion of the immune system (Figure 5).

Errors during the normal B cell differentiation process that lead to effector B cells often induce the first tumorigenic mechanisms in B cell lymphomas. B cell lymphomas not only highjack many of the intrinsic mechanisms used by normal B cells during their differentiation, but also acquire new capabilities to progress (Shaffer et al., 2012) (Figure 5). Next, some brushstrokes will be given about the main mechanisms and intrinsic features involved in the tumorigenicity of B cell lymphomas.

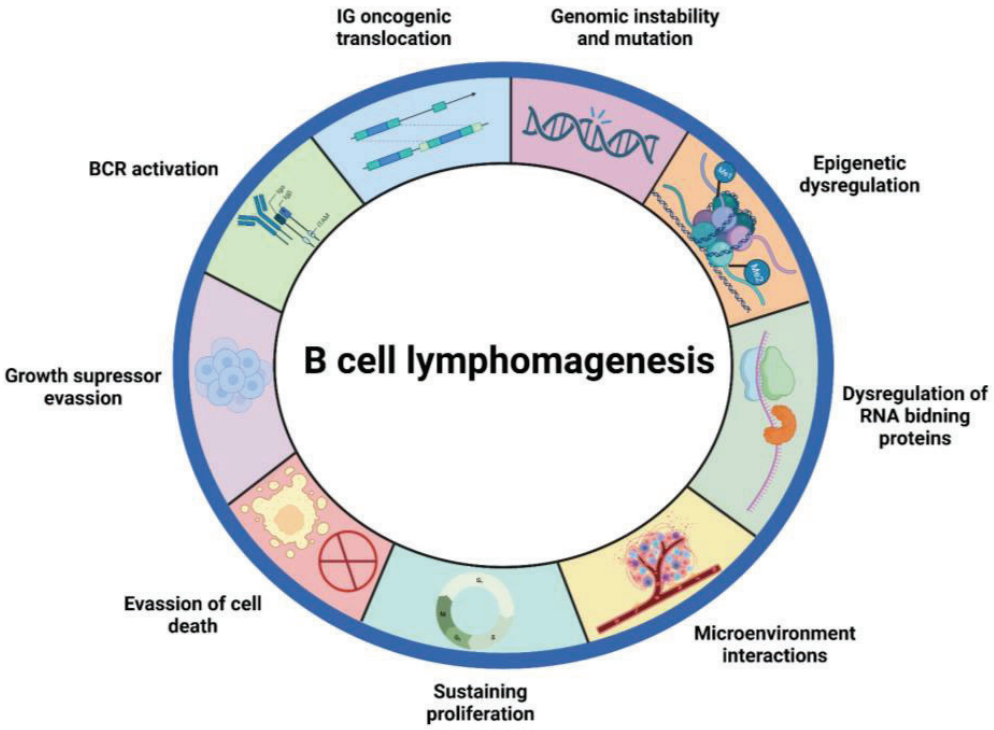

Figure 5. Schematic representation of the main mechanisms involved in B cell lymphomagenesis. Some of the mechanisms involved in the malignant transformation of B cells, including genomic instability and mutation, epigenetic dysregulation and sustaining proliferation, among others, are showed.

2.1 B cell of origin imprints

B cell lymphomas can be divided into three types regarding their normal cell counterpart: pre-germinal center, germinal center and post-germinal center neoplasms

(Figure 6). Pre-germinal center hematologic neoplasms, like B acute lymphoblastic leukemia (B-ALL), are characterized by the absence of mutations in the variable region of *IG*. By contrast, germinal center and post-germinal center derived hematologic neoplasms show imprints of SHM. Germinal center derived lymphomas usually present ongoing SHM in the tumor clones, while post-germinal center lymphomas do not. Some examples of germinal center derived lymphomas are BL, follicular lymphoma (FL) and GCB-DLBCL, whereas multiple myeloma and ABC-DLBCL are considered post-germinal center derived lymphomas (Küppers et al., 1999). Interestingly, mantle cell lymphoma (MCL) and chronic lymphocytic leukemia's (CLL) show two different patterns: non-nodal MCL (nnMCL) and mutated-CLL (mCLL) present SHM imprints, while conventional MCL (cMCL) and unmutated-CLL (uCLL) do not (Navarro et al., 2012; Seifert et al., 2012). Thus, cMCL and uCLL derive from pre-germinal center B cells and nnMCL and mCLL from post-germinal center B cells (Figure 6).

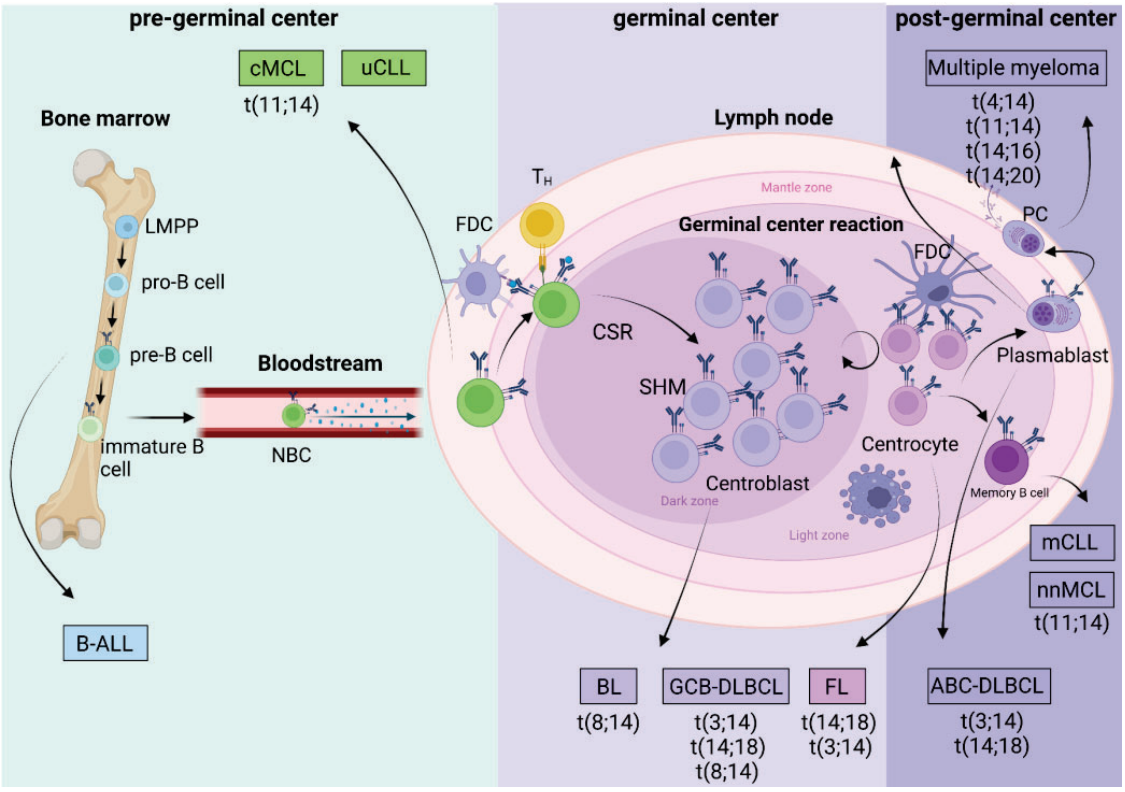

Figure 6. B cell origin of Non-Hodgkin's lymphomas. Representation of the B cell differentiation process and the derived B cell neoplasms. The recurrent translocations for each lymphoma and the origin in the light of germinal center reaction (pre-germinal, germinal and post-germinal) are indicated.

Depending on the B cell origin of the hematologic neoplasm, tumor cells will express specific factors and activate certain pathways that will influence their pathogenesis. Moreover, determination of the B cell of origin is crucial in some hematologic neoplasms such as MCL, CLL and DLBCL, because different prognosis is observed in the patients depending on the B cell of origin (Royo et al., 2012; Seifert et al., 2012; Alizadeh et al., 2000). For instance, cMCL patients show worse prognosis compared to nnMCLs.

2.2 *IG* chromosomal translocations

Chromosomal translocations are recurrently found in B cell lymphomas, being *IG* aberrant translocations one of the first tumorigenic events. The *IG* translocations involved different partners among the B cell lymphomas, leading to oncogene overexpression.

Some of the recurrent *IG* translocations are the t(11;14) in MCL and the t(8;14) in BL, which lead to the overexpression of cyclin D1 (CCND1) and MYC, respectively (Raffeld & Jaffe, 1991; Zech et al., 1976) (Figure 6). The overactivation of these two genes explains the pathogenesis of both lymphomas. Cyclin D1 is a cell cycle regulator which promotes the G_1-S transition, and the sustained proliferative signaling is a hallmark of MCL. Regarding MYC, it is a global transcription factor that regulates proliferation, cell growth and apoptosis, which are some of the pathways dysregulated in BL. Other oncogenes involved in translocations in B cell lymphomas are *BCL2* [t(14;18)] and *BCL6* [t(3;14)] (Figure 6), that are involved in apoptosis and in the germinal center reaction, respectively. In addition, the *IG* partner in the translocations can also be less frequently one of the *IG* light chains (kappa and lambda), which are located in chromosomes 2 and 22, respectively.

These malignant translocations can occur at different moments of the B cell differentiation process: during VDJ recombination, produced by RAG1 and RAG2, or during SHM and CSR mechanisms, induced by AICDA (Figure 3). If the translocation is acquired during VDJ recombination, the breakpoint of the translocation is found in the RSS signals that flank each segment. When there is an abnormal process of CSR, the

breakpoints of the *IG* aberrant translocation tend to occur in the switch regions of the constant gene segments that code for the different immunoglobulin isotypes. On the other hand, when there is an abnormal process of SHM, the breakpoints occur either within or near the rearranged V(D)J segments.

2.3 Aberrant somatic hypermutation

SHM is a normal mechanism in the B cell differentiation that if it is active in tumoral cells (aberrant SHM) lead to acquisition of a higher number of mutations (mutational burden). AICDA not only produces mutations in specific and accessible DNA motifs that are found in *IG*, but also genome-wide. The constant activation of AICDA in germinal center-derived lymphomas leads to SHM hotspot mutations in the partner genes involved in the malignant *IG* translocations and in other genes and genomic regions, particularly in regulatory regions around transcription start sites (TSS). If these mutations are produced in oncogenes or tumor suppressors, they may provide an evolutionary advantage to the tumor cell, causing an expansion of the tumor cell clone. For example, SHM hotspot mutations have been found in *MYC*, *CCND1*, *BCL2*, and other common translocated genes (Pasqualucci et al., 2001; Gaidano et al., 2003; Jiang et al., 2012; Grande et al., 2019; Nadeu et al., 2020).

2.4 Epigenetic dysregulation

As mentioned in 1.3.2.2.5 section, epigenetic regulation is relevant for B cell development. Epigenetics consists in the regulation of gene transcription and RNA translation without changes in the DNA sequence. The most important mechanisms in epigenetics are DNA methylation, chromatin accessibility and histone modifications. Before going into the epigenetic dysregulation mechanisms of lymphomas, a brief description of these epigenetic mechanisms is shown below.

DNA methylation is usually produced in CpG sites and consists in the addition of a methyl group in the C-5 position of a cytosine by DNA methyl transferases (DNMTs) (Figure 7). With some exceptions, it is general accepted that an increase in DNA methylation in promoter and enhancer regions of tumor cells derives into a repression of

gene expression, while hypomethylation permit the binding of transcription factors, activating gene expression (Esteller, 2008). DNA methylation can be measured with different techniques, like whole genome bisulfite sequencing (WGBS).

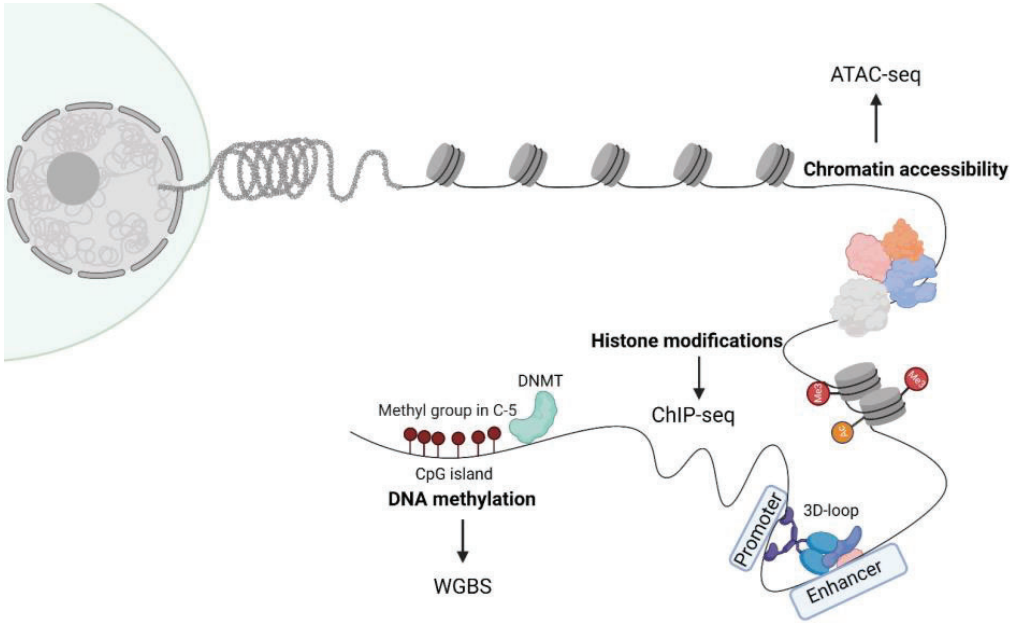

Figure 7. Schematic representation of epigenetic mechanisms involved in chromatin remodeling. Chromatin accessibility, histone modifications and DNA methylation epigenetic mechanisms are represented. The techniques used for the analysis of these mechanisms are indicated.

Regarding chromatin accessibility, it is described as the degree to which nuclear complexes are capable of binding to the DNA chromatin. This accessibility depends on the occupancy, the topological organization of nucleosomes and the presence of chromatin-binding factors. Open chromatin permits the binding of transcription factors to promoter and enhancer regions, which in turn regulates the transcription of several genes. ATAC-seq is one of the most popular methods used to measure chromatin accessibility (Klemm et al., 2019) (Figure 7).

Finally, histones can acquire different chemical modifications to regulate the chromatin, nucleosome packaging and transcription (Figure 7). Each type of histone modification is associated with specific chromatin functions (active promoters, strong or weak transcription, strong or weak enhancers, heterochromatin, …) (Bannister & Kouzarides, 2011; Kouzarides, 2007). The capture of histone modifications can be

achieved by ChIP-seq technique (O'Geen et al., 2011), and bioinformatics tools allow to determine these "chromatin states" based on the combination of different histone marks present in specific DNA regions (Ernst et al., 2011; Ernst & Kellis, 2017) (Figure 8).

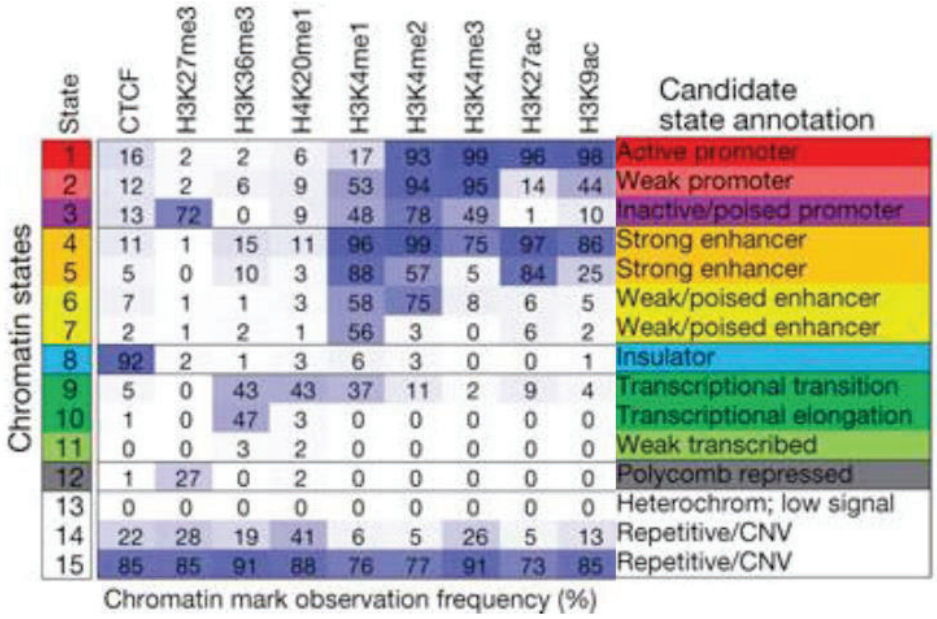

Figure 8. Chromatin states definition. Emission parameters on the basis of genome-wide recurrent combinations of chromatin marks. Each entry of the table denotes the frequency with which a given mark is found at genomic positions corresponding to the chromatin state (right). Figure modified from Ernst et al., 2011.

Epigenetic dysregulation is a known oncogenic mechanism in B cell lymphomas. In fact, mutations and gene expression deregulation have been found in several epigenetic modifiers. For instance, *KMTD* gene coding lysine methyltransferases is often mutated in MCL, BL, DLBCL and follicular lymphoma (FL) (Beà et al., 2013; Grande et al., 2019; J. Zhang et al., 2015). Mutations in components of the SWI/SNF chromatin remodeler complex, like *SMARCA4* and *ARID1A*, are also found in these lymphomas (Lunning & Green, 2015; J. Zhang et al., 2014; Love et al., 2012). Besides, *DNTM1* expression is upregulated in BL and DLBCL patients (De Falco et al., 2015; Loo et al., 2018), and is higher in MCL patients which have extensive methylation changes, increased proliferation signature and worse prognosis (Enjuanes et al., 2013). Notably, FL is the paradigm of a B cell lymphoma predisposed to epigenetic dysregulation, as nearly all FL

patients show mutations in some epigenetic modifier (Pasqualucci et al., 2014; Okosun et al., 2014). Thus, epigenetics plays a substantial role in B cell lymphomas.

2.5 RNA binding proteins

RNA binding proteins (RBPs) are a diverse group of proteins that interact with RNA molecules to regulate post-transcriptional gene expression (Gebauer et al., 2020). Dysregulation of RBPs has been linked to various hematological malignancies. RBPs can regulate RNA splicing, stability, transport, localization, and translation, and their dysfunction can lead to aberrant gene expression (Dreyfuss et al., 2002) (Figure 9).

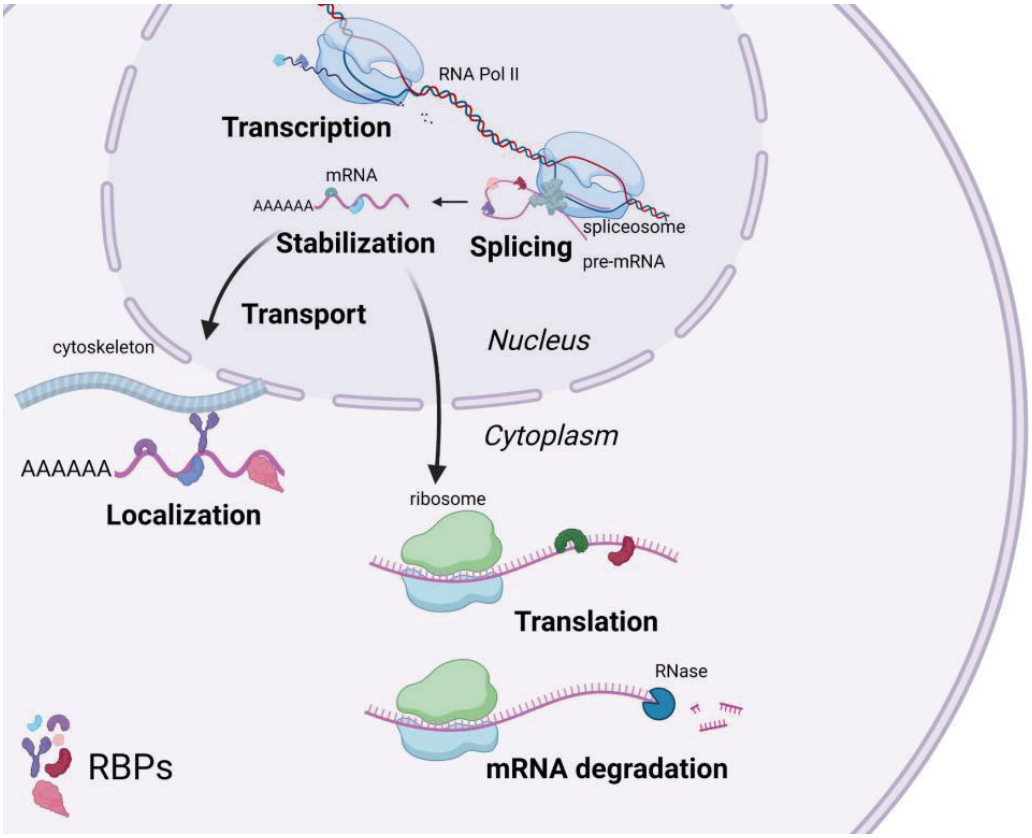

Figure 9. RNA-binding proteins control post-transcriptional regulation of RNAs. Representation of some of the processes regulated by RBPs, including transcription, splicing, stabilization, transport, localization, translation and mRNA degradation. Figure adapted from Gebauer et al., 2020.

One of the key steps in post-transcriptional regulation is alternative splicing (Figure 9), where introns are removed from pre-mRNA and exons are spliced together by spliceosome complex, composed of small nuclear ribonucleoproteins and specific RBPs,

including SF3B1. After splicing, mature mRNA is transported to cytoplasm and is further associated with RBPs, which dictate its fate. Some RBPs, such as HuR and IGF2BP3, stabilize mRNA and protect it from degradation, while others, such as Musashi-2 (MSI2), enhance or inhibit the translation of their mRNA targets (Prieto & Kharas, 2020). RBPs have RNA binding domains (RBD) specialized in recognizing certain RNA sequences, providing specificity for mRNAs.

Specific RBPs have been implicated in the pathogenesis of leukemia and lymphoma, including SF3B1, which is mutated in CLL, producing aberrant splicing and worse prognosis (L. Wang et al., 2011), and HuR and IGF2BP family proteins, which are overexpressed in acute myeloid leukemia (AML), MCL and other B cell lymphomas (Hartmann et al., 2012; Natkunam et al., 2007; Elcheva et al., 2020). MSI2 is also overexpressed in many hematologic neoplasms, such as CLL, B-ALL and myeloid malignancies, correlating with worse survival and promoting leukemic progression and stem cell renewal (Palacios et al., 2021; Aly & Ghazy, 2015; Ito et al., 2010).

Thus, RBPs are promising therapeutic targets for leukemia and lymphoma, and several preclinical and clinical studies have targeted RBPs to treat these diseases (Prieto & Kharas, 2020).

2.6 Microenvironment interactions

The tumor microenvironment comprises a complex network of cells, molecules, and extracellular matrix components that interact with tumor cells and influence their behavior. Cancer cells can modulate the tumor microenvironment to induce the secretion of growth factors, the formation of new blood vessels, the presence of immunosuppressive cells and the absence of cytotoxic cells, which contribute to increased proliferation, higher supply of nutrients and oxygen, higher dissemination and increased immune escape in the tumor (Burger et al., 2009; Y. Liu et al., 2021; Scott & Gascoyne, 2014) (Figure 10).

Some B cell lymphomas show a high dependence on tumor microenvironment interactions, while others do not. For instance, the overexpression of *MYC* and the tonic activation of the BCR in BL drives it independence of interactions with immune cells of

the germinal center (Schmitz et al., 2012), although the presence of macrophages engulfing apoptotic BL cells is a pathogenic mechanism in this lymphoma (Ogden et al., 2005).

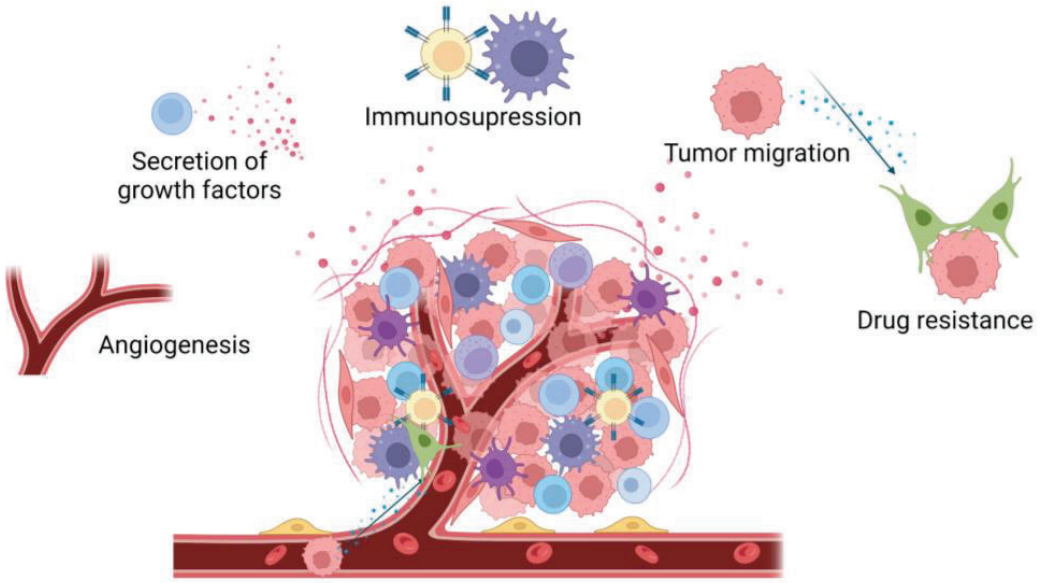

Figure 10. Representative illustration of the tumor microenvironment of B cell lymphomas. Some of the processes involved in the crosstalk between tumor cells and their microenvironment are included, such as angiogenesis and tumor migration.

Depending on the immune organ, the malignant B cells have a specific crosstalk with different cell types, and several chemokines, cytokines and CAMs allow tumor B cells homing to access supportive microenvironmental niches (Scott & Gascoyne, 2014). For example, in the bone marrow microenvironment, BMSCs produce a high flux of CXCL12 which may attract tumor cells with high expression of CXCR4 to the bone marrow niche (Burger & Kipps, 2009). In fact, the overexpression of chemokine receptors is usually observed in several B cell lymphomas, such as CXCR4 and CXCR5 in MCL (Kurtova et al., 2009), or CXCR5 in BL (Dobner et al., 1992). The activation of the signaling pathways of these receptors provide tumor cells with higher survival, proliferation, migration and resistance to drugs (Burger et al., 2009).

In the context of secondary lymphoid organs, the crosstalk between tumor and endothelial cells plays an important role in B cell lymphomas. This oncogenic pathway called angiogenesis is regulated by the production of specific growth factors by the tumor

cells or their tumor microenvironment. Vascular endothelial growth factors (VEGF) and platelet-derived growth factors (PDGF) are the main players in the new creation of blood vessels, leading to tumor growth and dissemination (Cacciatore et al., 2012; Carmeliet & Jain, 2011). In BL, MYC seems important for the production of new blood vessels during tumor progression (Ruddell et al., 2003). In MCL, VEGF and PDGFA are highly expressed, contributing to an angiogenic switch (Potti et al., 2002; Palomero et al., 2014).

2.7 Aberrant signaling pathways

Several signaling pathways regulate the tumorigenicity of B cell lymphomas. The activation or inhibition of these pathways can be achieved by different mechanisms: mutations produced in driver genes [single nucleotide variant (SNV), structural variants (SV), copy number alterations (CNA) and small insertions or deletions (indels)] (Campbell et al., 2020), gene expression dysregulation due to transcription changes, RNA processing or translation changes (epigenetics, non-coding RNAs, transcription factors and RBPs, among others, can affect these processes) (White & Sharrocks, 2010), and tumor microenvironment interactions (Scott & Gascoyne, 2014). Some pathways especially relevant for B cell lymphomas will be briefly described below.

The blockade of the DNA damage response, characterized by loss-of-function mutations and loss of *TP53* (17p) and *ATM* (11q), as well as downregulation of *CHK1* and *CHK2*, induce genomic instability in some B cell lymphomas, such as MCL, BL or DLBCL, promoting the acquisition of chromosomal aberrations and mutations (Beà et al., 1999; Camacho et al., 2002; Tort et al., 2005; Klumb et al., 2003; Grønbaek et al., 2002). AICDA also induces genomic instability through SHM (Mlynarczyk et al., 2019).

In addition, the sustaining proliferation and growth suppressor evasion can be achieved through loss-of-function mutations in cell cycle inhibitors, as *CDKN2A* and *CDKN2B* genes codifying for p16 and p15 proteins, respectively (Grønbæk et al., 1998; Pinyol et al., 1997). The overexpression or activation of *CCND1*, *CCND3, TCF3*, *MYC* and *NOTCH1* in MCL, BL and other lymphomas as a consequence of translocations, gain-of-function mutations or amplifications, also support the proliferation of malignant B cells

(Navarro et al., 2020; Beà et al., 2013; Kridel et al., 2012; Richter et al., 2012; Schmitz et al., 2012; Love et al., 2012).

The inhibition of cell death is another oncogenic pathway important for B cell lymphomas. Upregulation of anti-apoptotic Bcl-2 family proteins, like *BCL2*, by translocations, gene overexpression or amplifications, and downregulation of pro-apoptotic proteins, like *BCL2L11* and *FAS*, by chromosomic loss or mutations, are some of the mechanisms used by malignant B cells to overcome apoptosis (Beà et al., 2009; Shaffer et al., 2002).

The activation of the BCR pathway is a hallmark of most B cell lymphomas. This pathway is intrinsic of B cells and is hijacked by the malignant cells. In normal B cells, BCR activation induce a cascade of phosphorylation by LYN, SYK, FYN, BLK and BTK kinases, which in turns activate different pathways, such as PI3K-Akt, NFκB, MAPK and actin cytoskeleton pathways, inducing cell proliferation, survival and migration (Tanaka & Baba, 2020). Some B cell lymphomas show chronic activation of BCR signaling mediated by NFκB (Shaffer et al., 2012), while others, like BL, tonic BCR signaling, which is antigen-independent and mediated by PI3K (Srinivasan et al., 2009). In BL and DLBCL, many genes of this pathway are mutated, like *FOXO1*, *PTEN*, *CARD11* or *CD79A/B*. Moreover, the inhibition of BTK by ibrutinib treatment improves patient survival in many B cell lymphomas, corroborating the importance of BCR signaling for malignant B cells (Saba et al., 2016; Young et al., 2019).

Aberrant expression of different transcription factors regulating many of these oncogenic mechanisms has been found in B cell lymphomas. One example is the SRY (sex-determining region Y)-box11 (SOX11) transcription factor, which belong to SOX family factors.

3. SOX FAMILY FACTORS

SOX family transcription factors were discovered through their homology to the high mobility group (HMG) domain of the Sry mammalian testis-determining factor (Sinclair et al., 1990). The HMG domain of SOX factors provides them with the capacity of binding to specific DNA motif TTGT with a few variable flanking bases, that is located

in the minor groove of DNA (Hou et al., 2017). SOX factors have domains other than HMG, like transactivation, transrepression or dimerization domains. The binding of SOX factors to DNA induces sharp bending of DNA helices due to the singular structure of the HMG domain (Lefebvre et al., 2007).

In addition, Dodonova and colleagues established that some SOX factors, like SOX2 and SOX11, may act as pioneer transcription factors, since they can bound to nucleosomes producing a detachment of nucleosomal DNA from the histone octamer, increasing DNA accessibility, similarly to chromatin remodelers (Dodonova et al., 2020) (Figure 11). Indeed, it has been suggested that SOX factors may promote the formation of protein complexes in enhancer regions due to their interactions with other proteins and transcription factors (Lefebvre et al., 2007). It has been shown that the interaction with other proteins increases DNA binding specificity and affinity (Bernard & Harley, 2010). Interestingly, most of the known interactor proteins of SOX factors are other HMG proteins and chromatin remodelers, confirming the architectural role of SOX proteins.

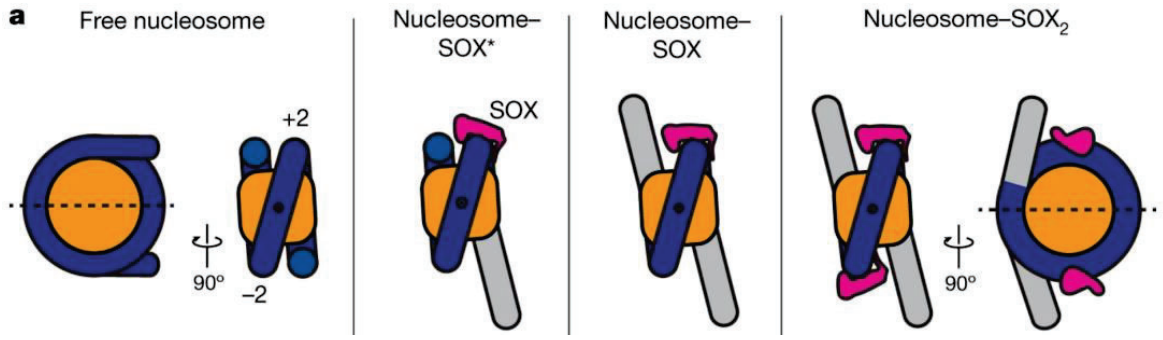

Figure 11. SOX2 and SOX11 are pioneer transcription factors. Nucleosome invasion by SOX factors and terminal DNA detachment. The histone octamer is shown in orange, SOX in pink and DNA in blue. Detached DNA is shown in grey. Figure from Dodonova et al., 2020.

Nine distinct groups of SOX transcription factors have been identified based on their shared homology in the HMG domain (at least 70%) (Figure 12). SOX proteins that belong to the same group exhibit significant homology in their HMG domain and outside it. Conversely, proteins from different groups display homology only within the HMG domain. These groups are denoted as SOX- A to H, with two groups inside the SOXB (Sarkar & Hochedlinger, 2013). SOX factors belonging to the same group share not only

homology but also similar biochemical properties and functions that often overlap, showing redundancy in specific processes (Wegner, 2010).

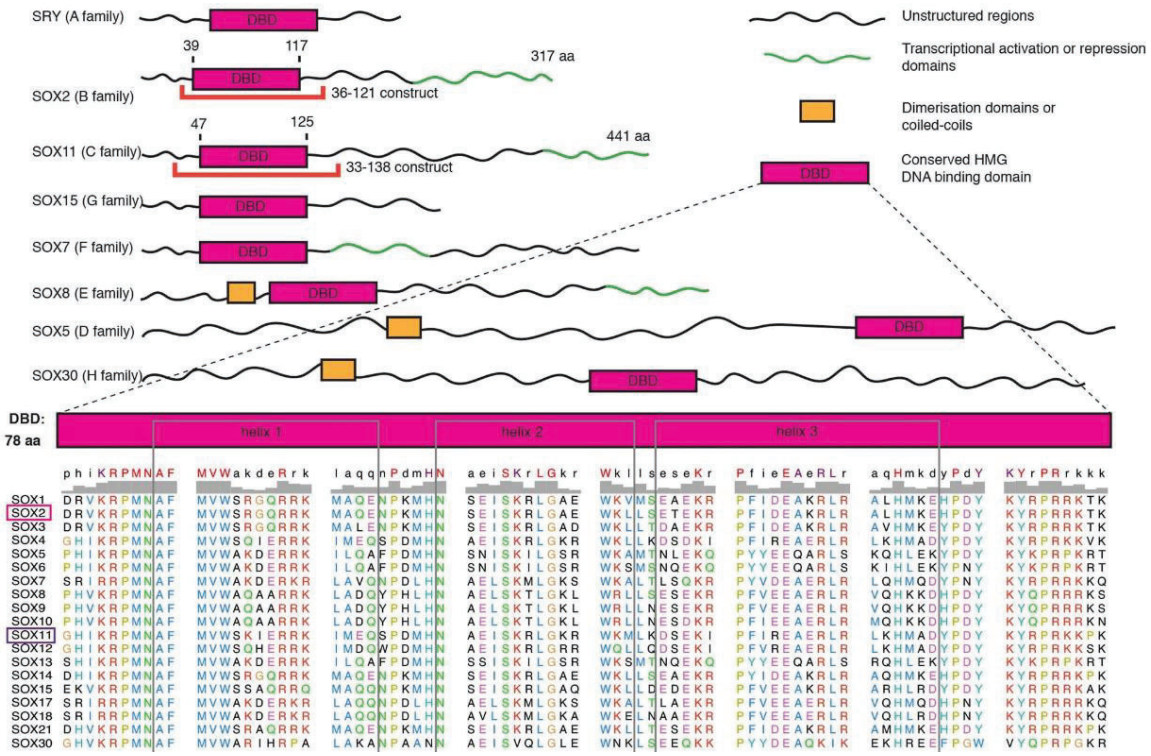

Figure 12. Conservation of SOX-family DNA binding domains sequence and structure. Domain organization of the human SOX protein family. The alignment of DNA binding domain sequences (produced using Clustal Omega) is shown below. Figure from Dodonova et al., 2020.

3.1 SOX factors in stemness and development

Typically, SOX transcription factors control cell fate and differentiation decisions in a broad amounts of processes, such as male differentiation, neurogenesis, skeletogenesis, hematopoiesis and stem cell maintenance.

SOX2 SOXB1 factor is one of the most studied SOX proteins due to its role during embryonic development. The blastocyst is the embryonic structure composed of the inner mass cell and the trophectoderm, which contains pluripotent and multipotent stem cells, and gives raise to all embryonic lineages and the placenta, respectively (Rossant & Tam, 2009). Deleting *SOX2* in zygotes causes early embryonic death due to a failure to form the pluripotent epiblast, leading the trophectoderm unaffected (Avilion et al., 2003). However, subsequent studies revealed that maternal Sox2 protein remains

present in preimplantation embryos, potentially concealing a phenotype in the trophectoderm in zygotic *SOX2* mutants (Keramari et al., 2010). Depleting both maternal and zygotic transcripts by RNA interference (RNAi) leads to the arrest of embryos at the morula stage and a failure to form the trophectoderm, indicating that Sox2 is necessary for the segregation of trophectoderm and the inner cell mass. SOX2 is required for the pluripotency maintenance of embryonic stem cells (ESCs), collaborating closely with Octamer-binding transcription factor 4 (OCT4) and Nanog Homeobox (NANOG) to bind to DNA and recruit other factors critical for gene activation (Boyer et al., 2005). Indeed, SOX2 along with the transcription factors OCT4, Kruppel-like factor 4 (KLF4) and c-MYC act as reprogramming factors during induced pluripotent stem cells (iPSCs) generation (Takahashi & Yamanaka, 2006). Thus, SOX2 is a master regulator of stemness.

SOX2 also regulates the differentiation of ESCs to specific cell lineages. For instance, during the initial stages of in vitro differentiation of ESCs towards the neural lineage, *SOX2* is expressed, indicating its involvement in neural commitment (Zhao et al., 2004). SOX2 promotes neural induction and differentiation by repressing regulators of other lineages (Thomson et al., 2011). It also maintains neural progenitor stem cell self-renewal in vitro and in vivo. *SOX2* is highly expressed in proliferating neural progenitor cells (NPC) but downregulated during differentiation to neurons and glia. Reducing *SOX2* impairs self-renewal and proliferation, leading to earlier exit from the cell cycle and differentiation. Overexpressing *SOX2* inhibits NPC differentiation into neurons and glia (Bylund et al., 2003). However, the expression of the SOX1 and SOX3 SOXB1 proteins also keep neural cells undifferentiated, demonstrating the redundancy of SOX proteins (Bylund et al., 2003). By contrast, SOX21 SOXB2 protein counteracts promoting the differentiation of neuronal progenitors into neurons (Sandberg et al., 2005). Other SOX factors, such as SOX4 and SOX11 SOXC proteins, have a central role in the maturation of neurons (Bergsland et al., 2006). Other nervous system lineage regulated by SOX is the oligodendrocyte lineage. SOXD transcription factors SOX5 and SOX6 repress differentiation in oligodendrocyte progenitors, whereas SOXE proteins SOX9 and SOX10 act in the opposite way, promoting terminal differentiation (Stolt et al., 2006).

The sequential action of Sox proteins from early pluripotent stem cells to neurons and glia was elegantly studied in (Bergsland et al., 2011), where it was found an overlap between Sox2, Sox3 and Sox11 bound genes that seemed to be poised at early stages but activated at differentiation of NPC by Sox11 (Figure 13). Thus, neural differentiation is the paradigm of how SOX proteins act as pioneer factors occupying and maintaining target genes in a silenced state until they are ready to be activated during subsequent stages of differentiation by other SOX factors. As cells become competent to differentiate, the SOX members that maintain stemness are downregulated, while other SOX members assume their functions and oversee the differentiation process.

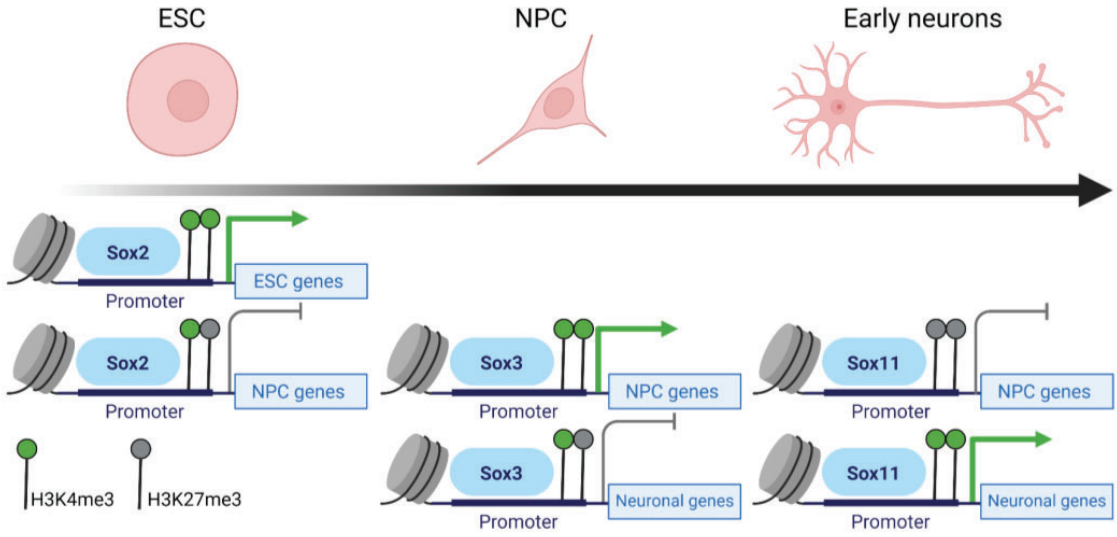

Figure 13. Sequential action of Sox proteins in the differentiation from ESC to early neurons in mice. Sequential binding of Sox proteins to common downstream genes in stem cells differentiation along the neural lineage, highlighting the association between Sox prebinding and histone modifications. Figure adapted from Bergsland et al., 2011.

Special relevant for hematopoiesis is SOX4 transcription factor, that is expressed in immature B and T cells in adult tissues (Van De Wetering et al., 1993) and is necessary for the proper differentiation and survival of pro-B cells (Schilham et al., 1996; Sun et al., 2013). Interestingly, SOX4 is the only SOX factor expressed during B cell differentiation. Besides, it upregulates the expression of *RAG1* and *RAG2*, activating the VDJ recombination process, and also regulates Wnt pathway (Mallampati et al., 2014).

Indeed, several SOX factors regulate Wnt pathway. For instance, SOX17 and SOX3 interact with β-catenin inhibiting its activity, which leads to corepression of Wnt targets transcription by TCF/LEF factors (Zorn et al., 1999). On the other hand, SOX4, SOX5 and SOX11 enhance β-catenin activity, promoting their entrance into the nucleus, the inhibition of TCF/LEF corepressors and the transcription of Wnt targets (Sinner et al., 2007). Moreover, the synergistic stabilization of β-catenin through the SOXC/canonical Wnt pathway plays a crucial role in efficiently repressing SOX9 expression in perichondrium cells, ensuring proper delineation and articulation of skeletal primordia (Bhattaram et al., 2014). As it was explained in "1.3.2.1 Hierarchy of HSCs" section, Wnt pathway is important for stem cells, evidencing the importance of SOX factors in stemness.

3.2 SOX11 regulation of development and progenitor cells

SOX11 belongs to SOXC group of transcription factors, together with *SOX4* and *SOX12*, and is located at chromosome 2p25.2. SOXC transcription factors share high homology, with similar transactivation and HMG domains. According to studies conducted on mice, it was found that the deletion of *Sox4* or *Sox11* did not significantly affect neurogenesis, indicating that the SoxC proteins may have a redundant function in this process (M. Cheung et al., 2000; Sock et al., 2004). This assumption was supported by further research that showed that the simultaneous deletion of both SoxC factors resulted in widespread apoptosis in the developing nervous system, primarily affecting immature neurons (Bhattaram et al., 2010; Thein et al., 2010). Besides, *Sox11*- and *Sox4*-deficiencies in embryos are incompatible with life, as mice die at birth with serious developmental abnormalities. SoxC triple-null embryos also die during midgestation with no external changes but display normal patterning and lineage specification while having a significant amount of dying neural and mesenchymal progenitor cells (Bhattaram et al., 2010). Thus, SOX11 together with SOX4 and SOX12 have an important role in developmental processes.

SOX11 also plays a role during adulthood. For instance, neurogenic niches of adult brains show *SOX11* expression, specifically in neuronal committed precursors and

immature neurons (Haslinger et al., 2009). In addition, *SOX11* overexpression in adult neural stem cells induces their differentiation into immature neurons (Haslinger et al., 2009; Feng et al., 2013). *SOX11* is expressed in human mesenchymal stem cells (MSCs) and its knockdown impairs the self-renewal in these multipotent cells (Kubo et al., 2009), and also their proliferation and osteogenic differentiation potential (Larson et al., 2010). Indeed, *SOX11* levels decreased with the progressive differentiation of MSCs. Moreover, other studies show that Wnt7b increase self-renewal and osteogenic differentiation of MSCs by activating *Sox11* expression in mice (Yu et al., 2020). Therefore, the expression of *SOX11* in multiple progenitors, combined with the discovery of *de novo SOX11* expression following the reprogramming of hematopoietic cells into induced pluripotent stem cells (iPSC) (Vegliante et al., 2011), suggests a potential involvement of SOX11 in stemness.

3.3 SOX11 role in cancer: focus in cancer stem cells

SOX11 aberrant upregulation is observed in a number of lymphoid and solid tumors including MCL, BL, B- and T-ALL, hairy cell leukemias, glioblastoma, medulloblastoma, ovarian cancer and breast cancer (Ek et al., 2008; Dictor et al., 2009; Y. H. Chen et al., 2009; Weigle et al., 2005; De Bont et al., 2008; D. J. Brennan et al., 2009; Zvelebil et al., 2013). However, the prognostic value of *SOX11* expression varies depending on the cell context. While it is associated with improved survival in ovarian and gastric cancer (D. J. Brennan et al., 2009; Qu et al., 2014), it is linked to reduced survival in MCL and breast cancer (Fernàndez et al., 2010; Zvelebil et al., 2013). Whereas mutations of *SOX11* are not common in primary cancers, they can be found in individuals diagnosed with Coffin-Siris syndrome (Tsurusaki et al., 2014). *SOX11* is not found in normal mature postnatal breast tissue but is expressed in about 80% of basal-like breast cancers, a subtype associated with poor prognosis (Zvelebil et al., 2013). Inhibition of *SOX11* reduces the growth, the migration and the invasion of several basal-like breast cancers cell lines, suggesting that SOX11 is a potential therapeutic target for this cancer (Shepherd et al., 2016). Additionally, high levels of *SOX11* expression are associated with

poor overall survival and increased formation of metastasis in breast cancer patients and cell lines (Zvelebil et al., 2013; Oliemuller et al., 2020).

Cancer stem cells (CSCs) account for a little percentage of the tumor population of some cancers. CSCs share traits with normal stem cells, such as the ability to self-renew and differentiate, and also show higher resistance to chemotherapy (Kreso & Dick, 2014). *SOX11* is expressed in 59% of ductal carcinoma in situ (DCIS) preinvasive lesions in breast, and its constitutive expression in DCIS cells promotes the expansion of a specific type of breast CSC population characterized by increased formation of mammospheres and aldehyde dehydrogenase (ALDH) activity (Oliemuller et al., 2017), features of cancer and normal stem cells (Mani et al., 2008; Ma & Allan, 2011). Besides, reducing *SOX11* levels affected the proliferative state, stem cell activity, and lineage marker expression in embryonic mammary progenitor cells (Tsang et al., 2021). The results of a study using single cell RNA-sequencing (RNA-seq) indicate that *SOX11* is highly expressed in a rare subpopulation of undifferentiated cells in oligodendrogliomas that show stem cell-related gene signatures and higher proliferation (Tirosh et al., 2016). In addition, *SOX11* silencing in MCL cell lines shows dysregulation of stem cell-related genes (Vegliante et al., 2013). Therefore, SOX11 is associated with stemness in different cancers.

It is worth mentioning that other SOX factors have been also involved in CSCs. For instance, *SOX2* and *SOX4* are expressed in CSCs populations of several cancers, showing higher resistance to treatments and self-renewal (Pouremamali et al., 2022).

This thesis is focused on the study of SOX11 and downstream oncogenes in lymphomas. Specifically, it explores their regulation and oncogenic functions. Since SOX11 is primarily found in MCL and BL, this thesis provides below a comprehensive description of the main features of these two lymphomas, including their pathogenesis and oncogenic mechanisms.

4. MANTLE CELL LYMPHOMA

MCL is a monoclonal B cell neoplasm characterized by the expansion of mature B cells present in the mantle zone of the follicles, which tend to spread to lymphoid

tissues, bone marrow, peripheral blood and extranodal sites (Swerdlow et al., 2017). MCL is considered an aggressive and incurable lymphoma. Nevertheless, MCL cases display high clinical heterogeneity, from patients with clinical symptoms and short overall survival to patients with indolent clinical course and needless treatment at diagnose. Therefore, correct classification of cases and prediction of outcome is essential in this lymphoma.

4.1 Epidemiology, clinical and biological characteristics

MCL accounts for 3-10% of adult NHL cases in western countries and has a higher incidence in males (male-to-female ratio of 3:1). The incidence of MCL increases with age, with a median age at the time of diagnosis in the mid-60s (Swerdlow et al., 2017; B. Sander et al., 2022).

MCL patients are usually diagnosed at advanced stages, and can present a wide variety of symptoms, including lymphadenopathies, hepatosplenomegaly and bone marrow involvement. Extranodal and peripheral blood involvement are also common in MCL patients and can involve gastrointestinal tract and the central nervous system (CNS) (Swerdlow et al., 2017). Three cytological variants have been described: blastoid/pleomorphic, classic and small cell, being the former the most aggressive variant. MCL is linked with a median survival rate ranging from 4 to 5 years, and unfortunately, most patients cannot be completely cured even with the employment of advanced therapeutic approaches available today, as they often relapse with a more aggressive disease (Vose, 2017).

The hallmark of MCL is the t(11;14), leading to the overexpression of cyclin D1 and a subsequent deregulation of the cell cycle. MCL cases also exhibit numerous genetic and epigenetic alterations that contribute to the potential tumorigenicity of the cells. MCL cells show positive expression of several B cell markers, such as IgD/IgM, CD19, CD20, CD22, CD79A and CD5, and lack of other like CD23, BCL6 or MUM1 (IRF4), although some patients can be negative for CD5, and positive for BCL6 or MUM1 (Swerdlow et al., 2017).

4.2 cMCL and nnMCL: two spectrums of the disease

The cell of origin of MCL has been postulated a pre-B cell that acquires the t(11;14) during VDJ recombination process (Jares et al., 2007; Nadeu et al., 2020). Then, tumor cells acquire secondary alterations in B cell mature stages. This mature B cell can follow two distinct fates, which give rise to two clinical, molecular and biological subtypes of the disease, now known as cMCL and nnMCL (Swerdlow et al., 2016).

The nnMCL cases were first defined as indolent cases with leukemic presentation, splenomegaly and absence of lymphadenopathies (Angelopoulou et al., 2002). Since this first description, several studies compared the clinicopathologic features, gene expression and genomic profile of patients with aggressive conventional and indolent disease (then renamed as nnMCL). First, it was found that cMCL cases had non-mutated *IGHV*, complex karyotypes, high expression of a gene signature which includes *SOX11*, and gene expression profiles resembling naïve B cells, whereas nnMCLs had mutated *IGHV* genes, lack of genomic alterations, SOX11 low or negative expression and gene expression profile resembling memory B cells (Fernàndez et al., 2010; Royo et al., 2012; Navarro et al., 2012). Then, these observations were validated in a study of the methylome of MCL and normal B cells. Queirós and colleagues found two clusters of MCLs with differential methylation of CpG which resemble naïve and memory B cells, respectively (Queirós et al., 2016) (Figure 14).

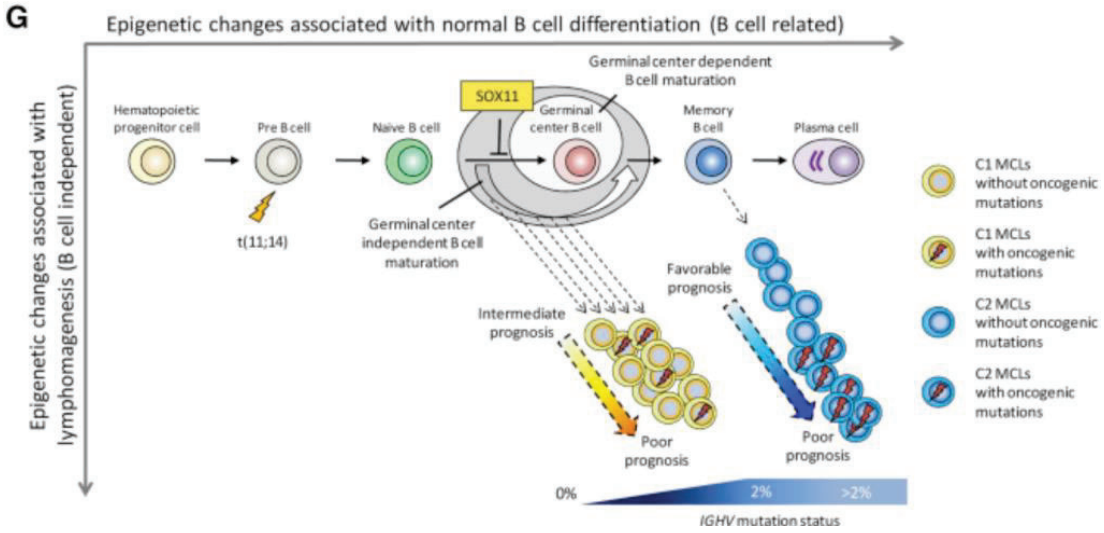

Figure 14. Proposed epi(genetic) model of MCL pathogenesis. cMCL cases (yellow) with intermediate to poor prognosis arise from naïve B cells that bypass the germinal center reaction. Germinal center B cell maturation gives rise to nnMCL cases (blue). The acquisition of mutations and CNA lead to poor prognosis in both subtypes. Figure from Queirós et al., 2016.

Clinically, cMCL presents with generalized lymphadenopathy and tends to have an aggressive course, with poor responses to treatment and frequent relapses (Figure 15). Instead, nnMCLs present peripheral blood involvement with or without splenomegaly, and the clinical course may be indolent for extended periods without need of treatment, although eventually some tumors can progress and exhibit more aggressive behavior, usually for the acquisition of *TP53* mutations (Navarro et al., 2012; Royo et al., 2012; Swerdlow et al., 2016).

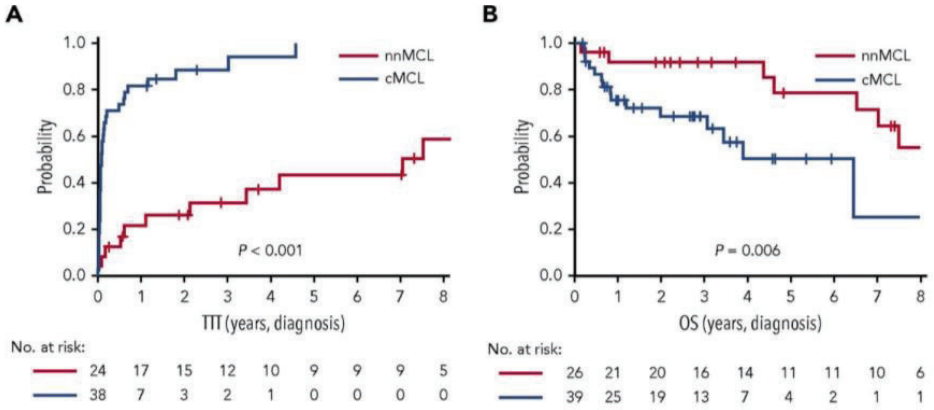

Figure 15. Prognostic impact of MCL clinical subtypes. Kaplan meier curves of time to first treatment (TTT) **(A)** and overall survival (OS) **(B)** from diagnosis date of the nnMCL and cMCL subgroups identified by the L-MCL16 assay. Figure from Clot et al., 2018.

4.3 SOX11 is an oncogenic factor in MCL

The oncogenic role of SOX11 has been well described in MCL. Ek and colleagues were the first to report the specific aberrant nuclear expression of SOX11 in MCL patients in comparison to other lymphomas and lymphoid cells (Ek et al., 2008). The aforementioned observation has established SOX11 as a useful marker for the diagnose of MCL, including challenging cases as "in situ" MCLs and patients that lack the t(11;14) and do not express cyclin D1 (Carvajal-Cuenca et al., 2012; Mozos et al., 2009). Interestingly, "in situ" MCLs constituted preliminary manifestations of MCL, suggesting that SOX11 expression may be an early event in this lymphoma (Adam et al., 2012).

Approximately 90% of MCL patients are positive for SOX11 expression, but SOX11 is also expressed in a limited number of hematologic neoplasms, including BL, B- and T-ALL, and hairy-cell leukemias (Dictor et al., 2009; Mozos et al., 2009). However, another study contradicts the SOX11 expression in ALL and hairy-cell leukemia using a monoclonal specific SOX11 antibody (Nordström et al., 2012). Instead, the SOX11 expression has been validated in BL using other cohorts of patients and antibodies, confirming positive expression in around 30-50% of patients (Wästerlid et al., 2017; Richter et al., 2022; Nakashima et al., 2014). Moreover, several studies have described the prognostic role of SOX11 in MCL (Fernàndez et al., 2010; Royo et al., 2012; Beekman, Amador, et al., 2018) (Figure 16).

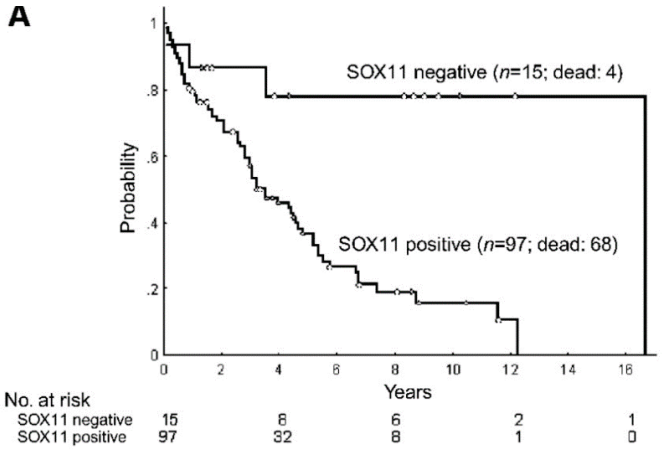

Figure 16. SOX11 positive expression associates with poor prognosis in MCL. Kaplan-Meier curves of overall survival (in years) of 112 MCLs according to SOX11 expression ($P < 0.001$). Figure from Fernàndez et al., 2010.

4.3.1 SOX11 in MCL: friend or foe?

Fernandez and colleagues established for the first time an association between SOX11 expression and aggressive behavior of MCL. Comparing the gene expression profile of aggressive cMCL cases to indolent nnMCLs they discovered a set of genes highly expressed in the aggressive ones, including SOX11 (Figure 17). Indeed, SOX11 was highly specific of cMCL aggressive cases, being weak or negatively express in nnMCL cases (Fernàndez et al., 2010; Navarro et al., 2012).

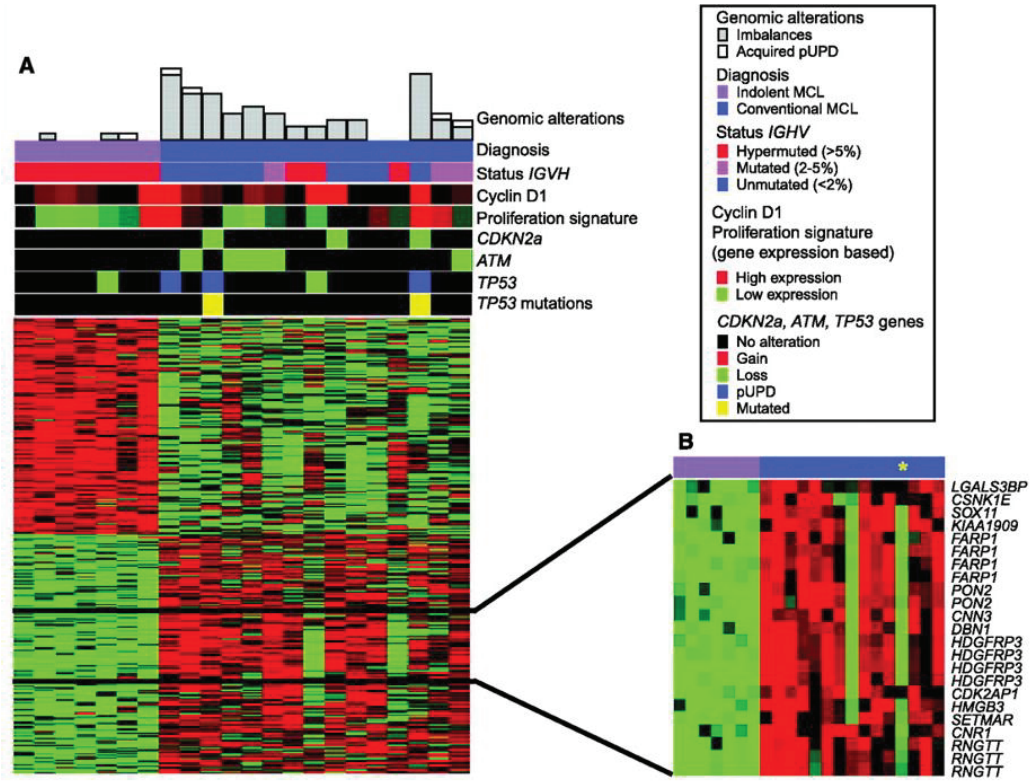

Figure 17. Differential gene expression profile between cMCL and nnMCL cases. (A) The genomic complexity is illustrated at top panel. Different characteristics, including IGHV status, CCND1 expression, proliferation signature and molecular alterations are indicated for each case. Heatmap of differential gene expression signature between cMCL and nnMCL cases is shown. Red indicates high expression and green low expression. **(B)** Selected probe sets higher expressed in cMCL than in nnMCL are shown, including SOX11 probe. Figure from Fernàndez et al., 2010.

The prognostic role of SOX11 was controversial for a long time, as some studies showed lower survival in SOX11- MCL patients compared to SOX11+ (X. Wang et al., 2008; Nygren et al., 2012; Nordström et al., 2014; Kuo et al., 2015). However, the presence of a considerable number of SOX11- patients with *TP53* mutations, together

with the difficulties to establish an optimal cut-off for SOX11 positivity, the cross-reactivity of some SOX11 antibodies with other SOXC factors such as SOX4, and the heterogeneity of treatments in the MCL analyzed cohorts, may explain the incongruences exposed (B. Sander et al., 2022; Beekman, Amador, et al., 2018; Nordström et al., 2014). Besides, studies in MCL mice models support SOX11 association with aggressive phenotypes, as SOX11 silencing decrease the tumor growth and dissemination to bone marrow and lymph nodes in subcutaneous and intravenous MCL xenotransplanted mice (Vegliante et al., 2013; Balsas et al., 2017), and SOX11 overexpression specifically in mice B cells leads to a "MCL-like" tumor, characterized by proliferation of CD5+ B1 cells (Kuo et al., 2018). On the other hand, Conrotto and colleagues conclude that SOX11 knockdown xenograft mice have lower tumorigenicity than SOX11 controls. However, they build this result on suggestive and unclear observations, specifically on the measure of disease symptoms in mice (Conrotto et al., 2011).

To gain a deeper understanding of SOX11 oncogenic role in MCL, several studies have investigated the transcriptional program that SOX11 regulates in this context, revealing crucial targets and oncogenic pathways involved in B cell differentiation and interactions with the tumor microenvironment, among other processes.

4.3.2 Regulation of B cell differentiation program by SOX11 in MCL

Through the combination of SOX11 chromatin immunoprecipitation on DNA microarray analysis (ChIP-chip) and gene expression profiling upon SOX11 silencing in MCL cell lines, two studies conducted in our group revealed evidence for the regulation of B cell differentiation transcriptional program by SOX11 (Vegliante et al., 2013; Palomero et al., 2016).

First, PAX5, one of the master regulators of B cell differentiation, was discovered to be directly activated by SOX11 (Figure 18) (Vegliante et al., 2013). Besides, SOX11 knockdown not only produces the downregulation of PAX5, but also the upregulation of some plasmacytic transcription factors such as BLIMP1, and the downregulation of B cell markers CD20 and CD24. Concordantly, plasmablast gene signature was found enriched in SOX11- MCL patients, and evidence of plasmacytic differentiation was found in a high

number of SOX11- MCL primary cases but not in SOX11+ MCLs (Vegliante et al., 2013; Ribera-Cortada et al., 2015). In addition, the entrance to the germinal center may be blocked by SOX11 through direct inhibition of BCL6 (Palomero et al., 2016), explaining why nnMCLs carry *IGHV* mutations but not cMCLs, as well as the different B cell of origin of both MCL subtypes (Navarro et al., 2012; Queirós et al., 2016) (Figure 18).

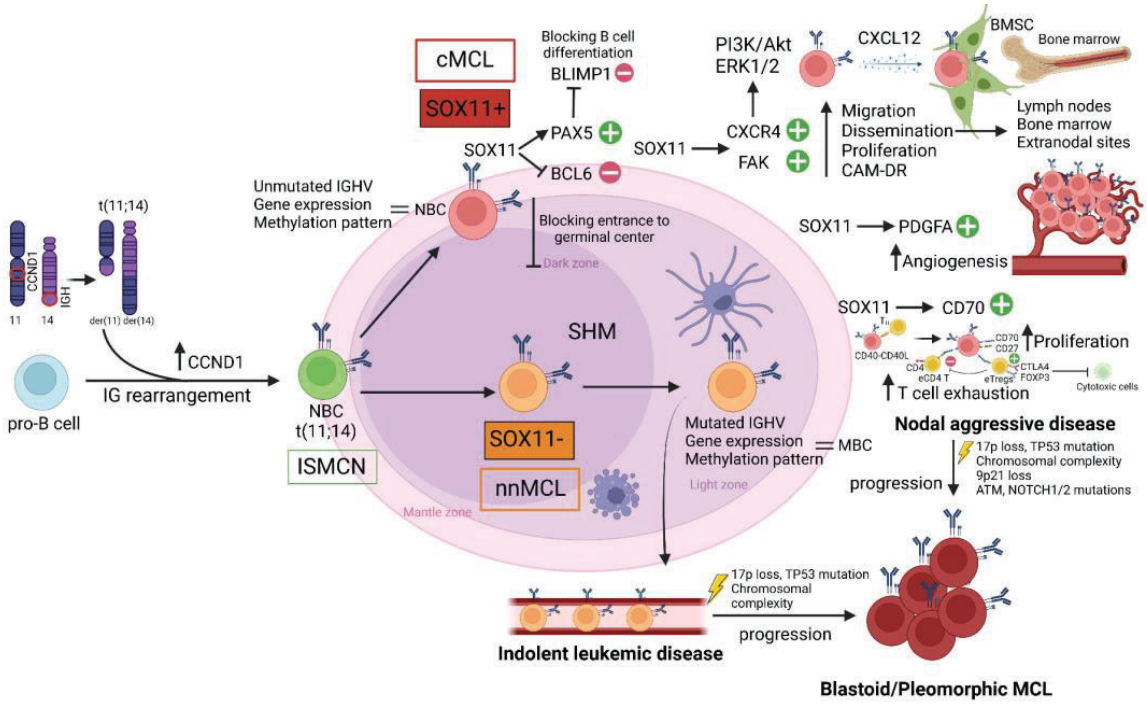

Figure 18. SOX11 oncogenic role in MCL. *IG-CCND1* translocation is acquired during VDJ recombination process in pro-B cells. Naïve B cells with the t(11;14) may transform into an in situ mantle cell neoplasia (ISMCN), a preliminary manifestation of MCL, or in cMCL or nnMCL neoplasms. In cMCL, the SOX11 expression may block the B cell differentiation process and the entrance to the germinal center through activation of PAX5 and inhibition of BCL6. Moreover, SOX11 activates CXCR4 and FAK, promoting increased migration, proliferation and drug resistance mediated by adhesion to stromal cells, as well as dissemination through lymph nodes, bone marrow and extranodal sites. SOX11 may promote increased angiogenesis through activation of PDGFA, and increased proliferation and T cell effector exhaustion by activating CD70. Thus, cMCL is a nodal aggressive disease. Conversely, nnMCL cases are SOX11- and show imprints of germinal center reaction, resembling memory B cells. Both subtypes can progress to blastoid/pleomorphic variants by acquisition of alterations. Figure adapted from Beekman, Amador, et al., 2018, and Balsas et al., 2021.

Thus, SOX11 may regulate the B cell differentiation program by activating PAX5 and inhibiting BCL6, blocking the terminal B cell differentiation and the entrance to the germinal center.

4.3.3 SOX11 interacts with MCL tumor microenvironment

Several studies performed in our group revealed a connection between SOX11 and the tumor microenvironment in MCL (Palomero et al., 2014; Balsas et al., 2017, 2021). The first study found enrichment of angiogenic gene signatures and increased formation of blood vessels in SOX11+ MCL patients (Palomero et al., 2014). The higher microvascular development of SOX11+ MCLs was also validated in another study and correlates with poor overall survival, suggesting an angiogenic switch and aggressive phenotype in SOX11+ tumors (Petrakis et al., 2019). In vitro and in vivo experiments showed that SOX11 is inducing blood vessel growth and migration of endothelial cells through the direct activation of PDGFA in MCL cells and mice models, but this angiogenic switch can be reverted by imatinib PDFGR inhibitor in vivo (Palomero et al., 2014).

In addition, MCL SOX11+ cells interact with other elements of the tumor microenvironment to acquire cell adhesion mediated drug resistance (CAM-DR) and proliferation (Balsas et al., 2017) (Figure 18). Specifically, SOX11 directly activates the expression of CXCR4 and PTK2 (encoding for focal adhesion kinase, FAK) and the corresponding downstream pathways PI3K/Akt and ERK1/2 promoting higher migration of MCL cells through high fluxes of CXCL12 chemokine, which are observed in lymph nodes and bone marrow (Figure 18). Besides, MCL cells can interact with stromal cells like BMSCs to activate proliferation signaling and to remain protected against therapies. This crosstalk with stromal cells can be reverted by FAK and CXCR4 inhibition with specific drugs, reducing proliferation, cell adhesion and CAM-DR in MCL cells and mice models (Balsas et al., 2017; Rudelius et al., 2018). These results are in agreement with the different tumor presentation of cMCL and nnMCL, with a disseminated disease in the former and a leukemic presentation in the last one.

Recently, another study suggested cell interactions between MCL and T cells. CD70 overexpression, which induces immune evasion by promoting differentiation and proliferation of T regulatory cells, and exhaustion of T cytotoxic cells, is activated by SOX11 after CD40L stimulation in MCL (Balsas et al., 2021) (Figure 18). CD70 expression is higher in SOX11+ MCLs, correlating with poor overall survival, and associates with lower infiltration of T cytotoxic cells. Thus, SOX11/CD70 axis may modulate the tumor microenvironment in MCL, promoting immunosuppression.

4.3.4 Other pathways regulated by SOX11

Other researchers have studied complementary functions associated with SOX11 in MCL. For example, SOX11 knockdown in MCL cells produces a modest increased in proliferation and in fraction of cells in S phase, while SOX11 overexpression inhibits proliferation (Conrotto et al., 2011; Yang et al., 2017; Gustavsson et al., 2010; Kuo et al., 2015). These results are in agreement with recent results in our laboratory showing a stop in G1 phase after 24h of SOX11 induction in MCL and lymphoproliferative cell lines. Based in our observations, it seems that at a short time of SOX11 induction MCL cells need to manage the exogenous SOX11 expression, but finally they remain stable and tumorigenic, without significant differences in cell cycle. Indeed, other study shows no differences in proliferation rates upon SOX11 downregulation in MCL cells (X. Wang et al., 2010).

BCR signaling is an important pathway in MCL and other B cell lymphomas, as it can be deduced by the effectiveness of ibrutinib and other BTK inhibitors (Colomer & Campo, 2014). Kuo and coworkers generated a transgenic immunocompetent mouse model aberrantly expressing Sox11 under the regulation of IgH-Eμ enhancer, only found in B cell populations (Kuo et al., 2018). They observed an oligoclonal B cell lymphoproliferative disorder that mimics some of the MCL features, such as expression of CD5 and CD19 and absence of CD23 markers (Figure 19). The authors found that these lymphoproliferative cells show activation of BCR pathway based on the increased phosphorylation levels of some downstream proteins, such as BTK or PLCγ2. Thus, SOX11 might activate the BCR pathway in MCL.

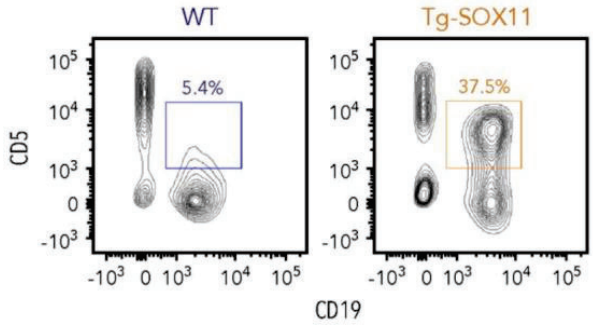

Figure 19. Transgenic immunocompetent mice expressing Sox11 under the regulation of IgH-Eμ enhancer mimics MCL features. CD5+/CD19+ cell fraction in splenocytes of sublethally irradiated recipients of bone marrow from Eμ-SOX11-EGFP donors is increased compared with recipients of bone marrow from WT donors. Figure from Kuo et al., 2018.

Another pathway that has been suggested regulated by SOX11 in MCL is the Wnt pathway (Kuo et al., 2015). The authors performed SOX11 ChIP-seq in MCL cells and observed several SOX11 target genes involved in Wnt pathway. Besides, they show inhibition of Wnt pathway upon SOX11 overexpression in MCL cells. However, they used an antibody that shows cross-reactivity with SOX4, which is also expressed in MCL, in the ChIP-seq experiment. Moreover, slight SOX11 peaks were found in promoter regions (only a 3.7% of total peaks), which is strange for transcription factors, and SOX11 overexpression in vitro experiments were performed in a MCL cell line that already expresses high levels of SOX11. Therefore, these results must be interpreted with that caveat in mind.

4.3.5 Mechanism of aberrant SOX11 transcriptional regulation in MCL

The regulation of SOX11 in MCL has been a mystery that little by little begins to be sight. Contrary to SOX4, SOX11 is not expressed in normal B cells, and mutations in this transcription factor which could explain its aberrant expression have not been found in MCL and other neoplasms. First studies show a negative correlation between SOX11 levels and its promoter methylation (Gustavsson et al., 2010; Vegliante et al., 2011; Wasik et al., 2013), suggesting that epigenetics could be the answer for this enigma. However, adult stem cells and hematopoietic cells are unmethylated in the *SOX11* promoter and do not express this transcription factor. Instead, activating histone marks in *SOX11* promoter are only observed in SOX11+ cells (Vegliante et al., 2011).

Interestingly, Queirós and colleagues described the presence of a DNA three-dimensional (3D) loop affecting *SOX11* promoter region and a distal enhancer only in SOX11+ MCLs, by 4C-sequencing (Queirós et al., 2016) (Figure 20). They proposed that this 3D loop puts the *SOX11* promoter in contact with the distal enhancer promoting the activation of SOX11 in this lymphoma. In addition, Vilarrasa-Blasi et al. elegantly validated the proximity of the *SOX11* promoter and distal enhancer region in MCL samples using fluorescent in situ hybridization (FISH) probes (Vilarrasa-Blasi et al., 2022) (Figure 20).

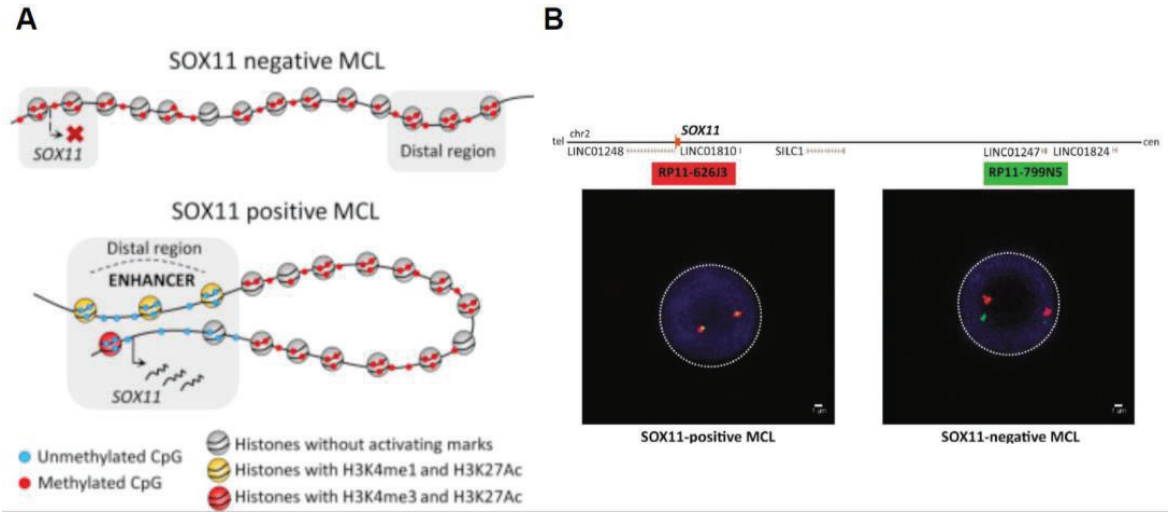

Figure 20. The *SOX11* promoter region and a distal enhancer contact through a DNA 3D loop in SOX11+ MCLs. (A) Model of the *SOX11* locus in SOX11- MCL (upper) and SOX11+ MCL (lower). **(B)** 3D FISH experiments in SOX11+ and SOX11- MCL primary cases using a probe that hybridizes to *SOX11* promoter region (in red) and another to *SOX11* distal enhancer region (in green). Figures from Queirós et al., 2016 and from Vilarrasa-Blasi et al., 2021.

Nonetheless, which factors are involved in this chromatin remodeling? Mohanty and coworkers tried to answer this question, and proposed cyclin D1 and STAT3 as regulators of SOX11 in MCL, by hijacking histone deacetylases located in the SOX11 promoter and by direct binding to the promoter and distal enhancer, respectively (Mohanty et al., 2019). Nevertheless, the authors did not demonstrate the direct binding of cyclin D1 to the *SOX11* promoter; they only show a higher presence of activating histone marks in this region upon cyclin D1 overexpression, and the interaction between cyclin D1 and histone deacetylases. In addition, SOX11 is not expressed in nnMCL cases which also show t(11;14) and cyclin D1 overexpression, and it is expressed in a subset of

CCND1- MCLs, contradicting the hypothesis of SOX11 regulation by cyclin D1. Besides, the results obtained in a cyclin D1 ChIP-seq experiment performed in MCL cells by Albero et al do not show cyclin D1 peaks in this *SOX11* region (Albero et al., 2018). Regarding STAT3, the researchers showed that this transcription factor is binding to the distal enhancer region found in Queirós et al. 2016, which contact with *SOX11* promoter. However, the exact location of STAT3 in the context of this enhancer is in accessible peak regions which are also activated and accessible in SOX11- MCLs and normal B cells (Vilarrasa-Blasi et al., 2022). The interrogated amplicon regions in the ChIP of STAT3 were exactly located in the called peaks 3 and 5 in Vilarrasa-Blasi et al. 2022 study (Figure 21). On the other hand, Vilarrasa-Blasi and colleagues found PAX5 binding to peak 1, which is specific of SOX11+ MCLs, and they proposed that this transcription factor and not cyclin D1 or STAT3 may be activating SOX11 in MCL (Vilarrasa-Blasi et al., 2022). However, future studies are needed to validate this hypothesis and completely decipher the complex regulation of SOX11 in MCL.

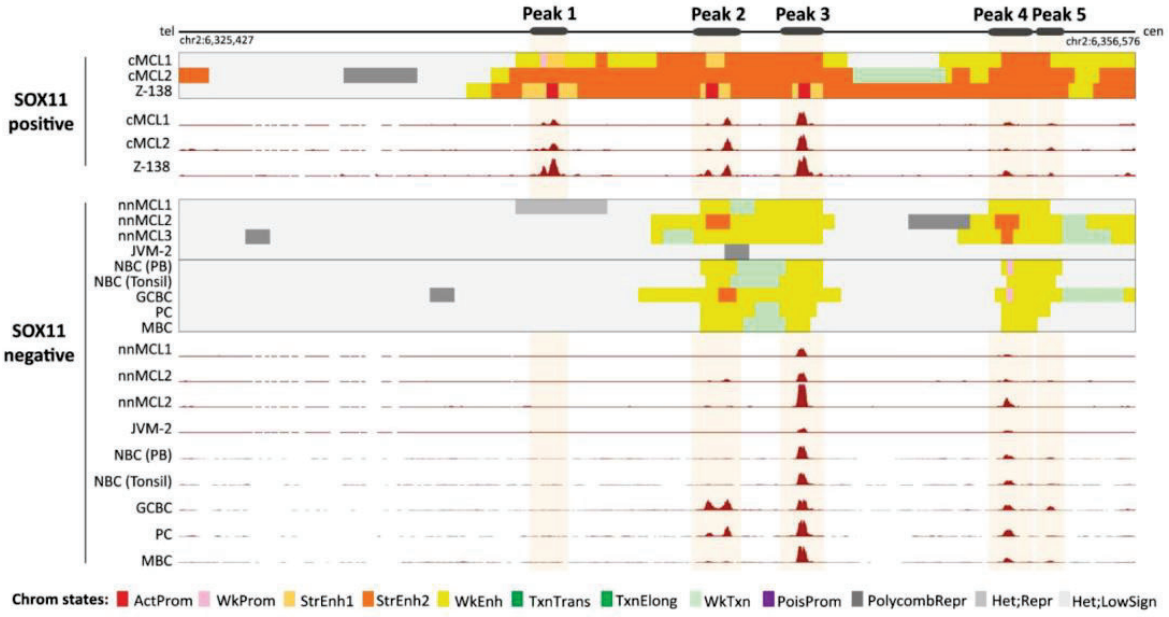

Figure 21. Multi-omics dissection of the *SOX11* super-enhancer region. Chromatin states and chromatin accessibility data from SOX11+ cMCL primary cases and cell lines (Z138), SOX11- nnMCL primary samples, cell line (JVM2) and normal B cells, including naïve B cells (NBC), germinal center B cells (GCBC), plasma cells (PC) and memory B cells (MBC). Figure from Vilarrasa-Blasi et al., 2021.

4.4 Pathogenesis in MCL

The pathogenesis of MCL is characterized by the overexpression of cyclin D1 and SOX11 (reviewed at "4.3 SOX11 is an oncogenic factor in MCL" section), and diverse chromosomal alterations and mutations that dysregulate cell cycle, apoptosis, DNA damage response and epigenetics (Navarro et al., 2020).

4.4.1 Role of cyclin D1

The t(11;14) is the main oncogenic event in MCL, which juxtaposes *CCND1* with *IG* enhancer region, leading to a constitutive overexpression of cyclin D1. This translocation is found in 95% of the MCL cases. However, a small fraction of cases shows cyclin D1 negative expression and *IG* translocation with other partners like *CCND2* or *CCND3* (Martín-Garcia et al., 2019). Cyclin D1 overexpression could disturb the G_1/S cell cycle progression and trigger the malignant transformation of B cells. In addition to its established role in the cell cycle, there are increasing evidences suggesting that cyclin D1 is involved in other cellular processes, such as transcription and DNA damage response (Aggarwal et al., 2010; Bienvenu et al., 2010; Jirawatnotai et al., 2012; Beltran et al., 2011; Albero et al., 2018).

4.4.2 Dysregulation of cell cycle, cell growth and apoptosis

Tumor cells need to proliferate, growth and bypass apoptosis to overcome the tumor suppressor mechanisms of the cells. In MCL, overexpression of cyclin D1 due to the t(11;14) is the first hit giving tumor cells a fitness advantage through its binding to CDK4, promoting the phosphorylation of RB1, the release of E2F and the subsequent G_1/S transition in the cell cycle (Table 2). Alternatively, *CCND2* and *CCND3* rearrangements with *IGH* may lead to the overexpression of these cyclin proteins. In addition, several alterations affecting cell cycle, growth and apoptosis have been described in MCL (Table 2) (Beà & Amador, 2017). For instance, 12q13 amplification is found in 20% of MCL cases, leading to *CDK4* overexpression and increased proliferation (Hernández et al., 2005). Another recurrent chromosomal alteration is the 9p21 deletion, found in 25% of MCL patients. This deletion involved the *CDKN2A* cell cycle inhibitor, encoding for p16 and p14 proteins, which inhibits CDK4 and CDK6 kinases and stabilizes

p53 protein preventing MDM2 degradation, respectively (Hernández et al., 2005). Thus, *CDKN2A* deletion promotes more proliferation and inhibition of the cell cycle checkpoints. Amplification of 10p12 affecting BMI1 is less common, but acts as an alternative to 9p21 deletion, as BMI1 is a transcriptional repressor of CDKN2A (Beà et al., 1999). Other MCL cases show loss-of-function mutations and deletions in *RB1* (Pinyol et al., 2007), deletions in *CUL4A* and *ING1* cell cycle suppressors by loss of 13q34 (Hartmann et al., 2010), and amplifications in *MYC* (Beà et al., 1999; Hu et al., 2017).

Regarding cell death, amplifications or overexpression of anti-apoptotic genes like *BCL2* or *BCLX,* together with loss of 2q13 affecting *BCL2L11* pro-apoptotic gene, are the main mechanisms to reduce apoptosis by MCL cells (Beà et al., 2009). *NOTCH1* and *NOTCH2* loss-of-function mutations are also relevant in blastoid variant, deregulating apoptosis, cell proliferation, cell migration and angiogenesis in MCL cells (Kridel et al., 2012; Beà et al., 2013; Silkenstedt et al., 2019).

Table 2. Recurrent primary and secondary somatic genetic alterations in primary MCL. Table modified from Beà & Amador, 2017.

Region	Gene	Frequency	Function
Primary genetic alterations			
Rearrangement 11q13	IG-*CCND1*	95%	Cell cycle
Rearrangement 12p13	IG-*CCND2*	2–4%	Cell cycle
Rearrangement 6p21	IG-*CCND3*	Occasional	Cell cycle
Secondary genetic alterations			
Loss 1p21-p22	–	17–55%	
Loss 2q13	*BCL2L11* (*BIM*)	3–17%	Apoptosis
Loss 2q37.1	*SP100*, *SP140*	15–33%	DNA damage
Loss 6q23-q25	*TNFAIP3*/*LATS1*	19–37%	NF-KB inhibitor/cell cycle
Loss 8p21-pter	*MCPH1*/*FBXO25*	17–34%	DNA damage/apoptosis
Loss 9p21	*CDKN2A*, *CDKN2B*, *MTAP*/*MOBKL2B*	10–36%	Cell cycle
Loss 9q22	*CDC14B*, *FANCC*…	17–31%	
Loss 10p14-p13	–	18–28%	

Loss 11q22-q23	*ATM, BIRC3*	11–57%	DNA damage/NF-KB signaling
Loss 13q14	*RB1*	25–55%	Cell cycle
Loss 13q34	*CUL4A/ING1*	16–54%	Cell cycle/DNA damage
Loss 17p13	*TP53*	21–45%	Cell cycle, DNA damage
Gain 3q25-qter	–	28–50%	
Gain 12q13	*CDK4/MDM2*	20%	Cell cycle, DNA damage
Gain 7p21-p22	*IGF2BP3* (*IMP3*)	8–31%	Insulin-like growth pathway
Gain 8q21-qter	*MYC*	6–32%	Proliferation
Gain 10p12	*BMI1*	6–12%	Epigenetic modifier, cell cycle
Gain 15q23	–	10–23%	
Gain 18q21	*BCL2*	3–17%	Apoptosis
Somatic mutations			
11q22.3	*ATM*	41–61%	DNA repair/genomic integrity
17p13.1	*TP53*	14–31%	Cell cycle, DNA damage
11q13.3	*CCND1*	14–34%	Cell cycle
12q13.12	*KMT2D* (*MLL2*)	12–23%	Epigenetic modifier
7q36.1	*KMT2C* (*MLL3*)	5–16%	Epigenetic modifier
4p16.3	*NSD2 (WHSC1, MMSET)*	10–13%	Epigenetic modifier
19p13	*SMARCA4*	10%	Epigenetic modifier
11q22.2	*BIRC3*	6–10%	NF-KB signaling pathway
6p21.1	*NFKBIE*	5%	NF-KB signaling pathway
9q34.3	*TRAF2*	7%	NF-KB signaling pathway
9q34.3	*NOTCH1*	5–14%	Notch signaling pathway
1p12	*NOTCH2*	5%	Notch signaling pathway

8q22.3	*UBR5*	7–18%	Ubiquitin-proteasome system
7p22.2	*CARD11*	3–15%	B-cell receptor signaling pathway
1p21.2	*S1PR1*	3–15%	Lymphocyte migration
5q14.3	*MEF2B*	3–7%	Transcription factor
4q31.3	*TLR2*	7%	Toll-like receptor

4.4.3 Genomic instability

MCL cells tend to accumulate several chromosomal alterations, mainly the cMCL subtype, which carries complex genomes. In normal cells, there are several checkpoints to induce cell cycle arrest, apoptosis and senescence when the DNA of cells become compromised, a process called DNA damage response. However, *ATM* and *TP53* mutations, present in most MCL cases, inhibit these checkpoints and permit the accumulation of several chromosomal alterations (Beà et al., 1999; Camacho et al., 2002) (Table 2). Besides, downregulation of *CHK1* and *CHK2*, effectors of the DNA damage response, is an alternative mechanism to bypass this pathway (Tort et al., 2002, 2005). Thus, genomic instability is an important cancer hallmark of MCL.

4.4.4 Immune dysregulation

As described in "4.3.3 SOX11 interacts with MCL tumor microenvironment" section, SOX11 is an important factor in the crosstalk between MCL and the tumor microenvironment, especially with BMSCs, endothelial cells and T cells (Balsas et al., 2017; Palomero et al., 2014; Balsas et al., 2021). In addition, SOX11 might activate BCR pathway in MCL (Kuo et al., 2018). BCR is an important pathway in MCL, as it promotes survival and proliferation of tumor cells. Amplifications or activation of several protein kinases of the BCR pathway have been observed in MCL, like LYN, SYK or BTK, and BTK inhibition with ibrutinib show good responses in MCL patients (Rinaldi et al., 2006; M. L. Wang et al., 2013; Colomer & Campo, 2014). Some of the pathways regulated by the activation of the BCR, such as PI3K/Akt and NFκB pathways, have an important role in angiogenesis, migration, cell growth and survival of MCL cells (Saba et al., 2016; Balsas et al., 2017; Pham et al., 2003; Rosich et al., 2014). MCL cases also show loss-of-

function mutations and deletions in proteins of the NFκB pathway (Rahal et al., 2014; Nadeu et al., 2020) (Table 2).

4.4.5 Epigenetic dysregulation

Epigenetic dysregulation is an important mechanism of oncogenesis in MCL. Proof of this are the numerous mutations in epigenetic regulators found in MCL patients (Table 2). Moreover, MCL cases show DNA methylation changes compared to their normal counterparts correlating with worse overall survival and more driver mutations (Queirós et al., 2016). Typical mutations found in MCL related to epigenetics are targeting the SWI/SNF complex, specifically *SMARCA4* and *ARID1A* (J. Zhang et al., 2014; Nadeu et al., 2020). Other genes frequently mutated are *KMT2D*, *KMT2C* and *NSD2* lysine methyltransferases, and *BMI1* polycomb transcriptional repressor.

4.4.6 Cancer stem cells

MCL typically shows a positive response to the initial treatment, but resistance often emerges later, leading to relapse with a more aggressive form of the disease. The resistance to chemotherapy has been linked, at least in part, to the existence of CSCs present in certain types of tumors (Zhou et al., 2021). Despite the lack of agreement on a specific phenotype of CSCs in MCL, a number of research teams have successfully isolated MCL-CSC through the use of single or combined CSC markers (Medina et al., 2014; Jung et al., 2011; Kim et al., 2015; Z. Chen et al., 2010). For instance, Medina and colleagues show that CD133+/CD19- cobblestone area forming cells from MCL patients have a quiescent phenotype, increased drug resistance and higher engraftment in mice after limiting dilution assays compared to CD133-/CD19+ MCL cells (Medina et al., 2014). Other studies show that CD45+/CD19- MCL primary cell population has higher engraftment in mice, is highly resistant to combined chemotherapeutic regimens and increases in percentage in MCL patients upon relapse (Z. Chen et al., 2010; Jung et al., 2011; Kim et al., 2015). Besides, it has been observed that MCL cell lines and cells derived from a MCL mouse model show populations with increased self-renewal, chemoresistance, ALDH activity, clonogenic growth in vitro and tumorigenicity in vivo (Luanpitpong et al., 2018; Vega et al., 2010; Teshima et al., 2014; S. K. Brennan et al., 2010). Although frontline treatments for MCL appear to yield satisfactory rates of

complete remission, the resistance of isolated MCL-CSCs to standard therapies might explain why MCL remains an incurable lymphoma (Prichard et al., 2009; Zaja et al., 2014). However, the lack of consensus in MCL-CSC markers is an unsolved problem that bothers the study of potential stemness in MCL cells.

4.5 Prognostic factors

MCL is a heterogeneous lymphoma, with a very variable disease course. Some patients require immediate treatment while others need strategies of wait and watch. For this reason, prognostic factors have been considered useful in this lymphoma to predict the outcomes, responses to treatments or possibility of relapse in patients. Some of the first biomarkers used in MCL were SOX11 and *IGHV* mutational status, both associated to poor overall survival and cMCL subtype (Fernàndez et al., 2010; Ribera-Cortada et al., 2015; Navarro et al., 2012). In addition, NanoString platform's L-MCL16 assay has been used to differentiate between cMCL and nnMCL subgroups among patients with leukemic involvement. When combined with genomic complexity and *TP53* alterations, the assay can anticipate patient outcomes (Clot et al., 2018).

One of the most used scores for risk stratification is the combined MCL international prognostic index (MIPI-c), which includes age, performance status, lactate dehydrogenase, leucocyte count and Ki-67 variables (Hoster et al., 2008, 2014, 2016). The prognosis power of cytological variants has been also studied, finding that blastoid/pleomorphic variants are more aggressive.

Chromosomal alterations impact the outcome of MCL patients. Proof of this is that a greater genome complexity and increased CNA determine worse survival in MCL patients (Sarkozy et al., 2014; Clot et al., 2018). Specific chromosomal alterations have been associated with poor prognosis, such as *TP53* and *CDKN2A* alterations or mutations, which have prognostic value independent of MIPI-c (Delfau-Larue et al., 2015; K. J. J. Cheung et al., 2009).

Despite the fact that many prognostic factors already exist, there is a need to improve prognostic and potentially predictive clinical scoring systems due to the clinical diversity and increasing number of therapeutic options available for MCL.

4.6 Treatment and management of MCL patients

The treatment and management of MCL depend on several factors, including the age of the patients, the overall health status, the disease stage and some genetic features. In some cases, a watch and wait approach is used for MCL patients, especially for those with asymptomatic disease, as nnMCLs (Martin et al., 2009). Chemotherapy is a cornerstone of MCL treatment and is often used as the first-line therapy for patients with advanced stage disease. The standard of care for MCL is the combination chemotherapy regimen that include rituximab, cyclophosphamide, doxorubicin, vincristine, and prednisone drugs (R-CHOP) (Lenz et al., 2005). However, some elderly patients cannot receive these intense regimens. Instead, they can be treated with targeted therapies. Several targeted therapies have been approved for MCL, including BTK, PI3K, CDK4/6 and BCL2 inhibitors, such as ibrutinib, idelalisib, abemaciclib and venetoclax, respectively (Jain & Wang, 2022; Dreyling et al., 2014). However, resistance to these agents is observed in several patients (Zhao et al., 2020; Jain et al., 2018). Finally, stem cell transplantation is an option for younger MCL patients with good health, that gives good results (Gianni et al., 2003; Dreyling et al., 2005).

Although numerous therapies are available for MCL patients, there are still patients who relapse or do not respond to standard therapies, called relapsed/refractory MCL (Dreyling et al., 2018). The management of these patients is a challenge nowadays. Thus, the study of new therapies capable of overcoming resistance to therapy in MCL patients is urgent.

5. BURKITT LYMPHOMA

BL is an aggressive and highly proliferative B cell neoplasm that often presents in extranodal sites or as acute leukemia in children, adults and elderly (Swerdlow et al., 2017). It was described for the first time in 1958 by the missionary surgeon Denis Burkitt

as a rapid growing sarcoma that affects the jaws of several African children (Burkitt, 1958). Despite its aggressiveness, patients are usually cured with intense chemotherapeutic regimens due to the strong chemosensitivity of the BL cells.

The translocation t(8;14), which involves *IG* enhancer regions and *MYC* oncogene, is considered the hallmark of BL, as it is virtually present in all cases, and is believed to be an early event in the pathogenesis of the disease. However, MYC overexpression is not enough to develop completely the BL pathogenesis, as observed in the transgenic mice generated by Sung and colleagues, characterized by *MYC* insertion into *IGH* enhancer region (Sung et al., 2005). This result together with the pro-apoptotic effects induced by MYC overactivation (Hoffman & Liebermann, 2008) suggest that additional oncogenic mechanisms are involved in this lymphoma.

Other B cell lymphomas may also exhibit the *IG-MYC* translocation, such as DLBCL or other high-grade lymphomas (Dave et al., 2006; Hummel et al., 2006). Therefore, the accurate diagnosis of BL relies on a combination of the immunophenotype, and clinical, histological and molecular features.

5.1 Morphology and immunophenotype of BL cells

The tumor cells in BL are medium-sized B cells that display monomorphic characteristics, exhibiting multiple mitosis and apoptosis. These cells are highly proliferative and susceptible to apoptosis due to MYC overexpression. As a result, tumor cells typically exhibit a Ki-67 index greater than 95%. On hematoxylin and eosin stains, the presence of macrophages that engulf apoptotic tumor cells results in a "starry sky" appearance (Figure 22).

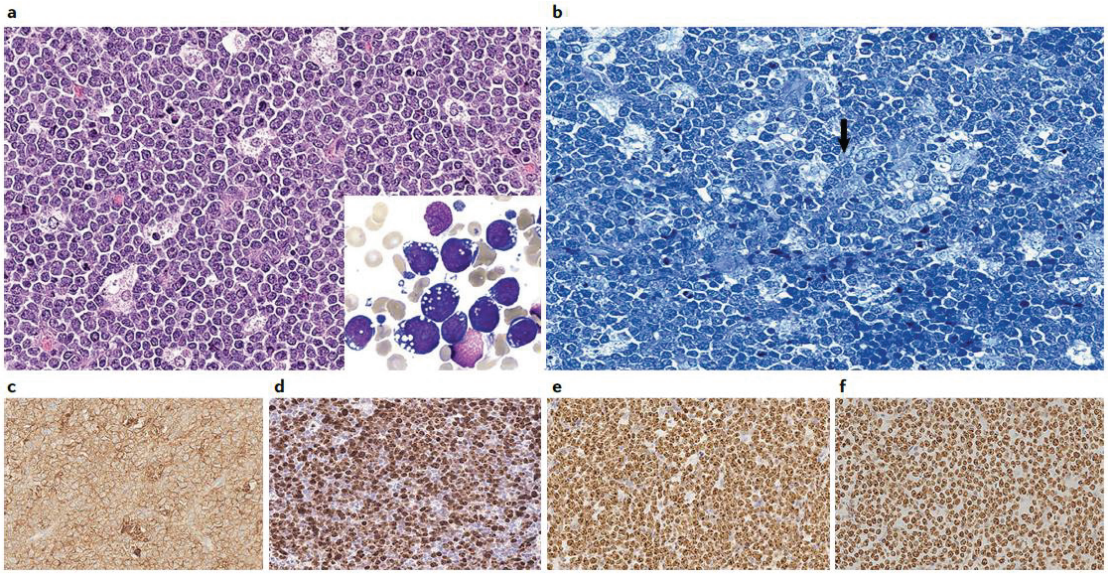

Figure 22. Morphology and immunophenotype of classic BL. Haematoxylin and eosin-stained **(a)** and Giemsa-stained **(b)** tumor sections showing morphological features of classic Burkitt lymphoma, including the diffuse proliferation of monomorphic B cells and the starry sky pattern. Cytoplasmic lipid vacuoles can be seen in cytological preparations **(a, inset)**. Neoplastic cells are usually CD10+ **(c)** or BCL6+ **(d)**, with strong MYC expression **(e)** and a high proliferation rate demonstrated by Ki-67 expression **(f)**. All images, ×20. Figure from López et al., 2022.

BL cells express several B cell antigens, including CD19, CD20, CD79A, CD22, PAX5 and IgM, in addition to germinal center markers like CD10 and BCL6, and MYC (Figure 22). However, they lack certain B cell antigens such as CD5, CD23, CD138, CD44, BCL2 and TdT (Roschewski et al., 2022; Swerdlow et al., 2017).

5.2 BL epidemiology and clinical features

There are three recognized variants of BL that differ in their geographic distribution, clinical presentation, and molecular features. These variants include endemic BL (eBL), sporadic BL (sBL), and immunodeficiency-related BL (iBL) (Table 3). eBL is most prevalent in regions where malaria is endemic, such as equatorial Africa and Papua New Guinea, and is associated with EBV infection (Swerdlow et al., 2017). Indeed, it is widely believed that eBL is caused by concomitant EBV and malaria infection (De-Thé et al., 1978; Johnston et al., 2014; Robbiani et al., 2015). In these endemic regions, BL accounts for 30-50% of pediatric cancers and is the most common lymphoma (Roschewski et al., 2022). sBL, on the other hand, occurs in regions outside of the malaria

belt and constitutes 30-50% of childhood lymphomas and 1-2% of adult lymphomas. iBL is associated with HIV infection due to the consequent immunosuppression and is distributed worldwide. Overall, there is a higher incidence in males than in females (2-4:1 male to female ratio) (López et al., 2022).

Each of the BL variants also displays differences in their clinical presentation. eBL often presents with jaw or facial involvement, but patients may also exhibit tumor masses in the abdomen, kidneys, ovaries, breasts, or other locations. sBL typically presents in the Peyer's patches of the abdominal ileocecal region, as well as the head and neck, while iBL shows a more nodal pattern and commonly involves the bone marrow (Swerdlow et al., 2017).

Table 3. Differences in epidemiology, clinical and molecular characteristics of BL variants.

Feature	Endemic BL	Sporadic BL	Immunodeficiency-associated BL
Geographical regions	Equatorial Africa and Papua New Guinea (Malaria regions)	Worldwide	Worldwide
Incidence	30–50% of all childhood cancers; 90% of lymphomas in high-risk areas	30–50% of all childhood cancers; 1-2% of adult lymphoms	40% of lymphomas associated to HIV
Age	Mainly children (incidence peak between 4-7 years)	Mainly children, adolescents and adults (incidence peak at 10, 40 and 75 years)	Mainly adults (40-45 years)
Male to female ratio	2:1	2-3:1	1:1
EBV infection	>95% of cases	15-30% of cases	25-40% of cases
Clinical presentation	Jaw, facial bones, abdomen, kidneys	Abdomen (Peyer's patches of ileum)	Lymph nodes and bone marrow
Mechanism of t(8;14) acquisition	SHM and CSR (SHM predominance)	SHM and CSR (CSR predominance)	SHM and CSR (CSR predominance)

Despite these striking differences, recent studies suggest that a classification based on the EBV status of BL patients better explains the observed molecular differences in this lymphoma (Grande et al., 2019; Kaymaz et al., 2017; Thomas et al., 2022). In fact, the 5th revision of the WHO recommends a BL classification based on the EBV status (Alaggio et al., 2022).

5.3 The role of EBV in BL

BL disease is strongly associated with the presence of EBV infection, a gamma-herpesvirus linked to a number of lymphoid malignancies and other diseases. EBV is detected in >95% of eBL tumors, in 15-30% of sBL tumors and in 25-40% of iBL, indicating that EBV status determines the BL clinical variant (Table 3) (López et al., 2022; Roschewski et al., 2022). In sBL, EBV infection is more prevalent in adults than in children (Satou et al., 2015; Richter et al., 2022).

The impact of EBV on the development of BL is multifaceted. EBV infection in B cells leads to the generation of proliferating and immortalized lymphoblastoid cell lines in vitro by induction of changes in the transcriptional profile, especially in RNA synthesis, metabolic, cell division, migration and immune response pathways (Mrozek-Gorska et al., 2019). In EBV+ BLs, the virus usually presents at latency I and II types, characterized by the expression of cellular microRNAs and LMP proteins, respectively (Figure 23), which counteract the apoptosis induced by MYC overexpression (Leucci et al., 2010; Vereide et al., 2014). A unique pattern of EBV latency has been also observed in selected cases in which the virus expresses both LMP2 and lytic genes (Tierney et al., 2015; Abate et al., 2015). LMP2 has been shown to contribute to the reprogramming of B cell function and the enhancement of MYC-driven lymphomagenesis by activating the PI3K pathway (Fish et al., 2014). In addition, LMP1 can mimic CD40 function inducing proliferation in B cells (Lam & Sugden, 2003). However, the expression of the latency pattern is heterogeneous in BL. This heterogeneity exists not only from case to case but also within the same patient (Kelly et al., 2013). Besides, using high sensitivity methods, EBV traces are found in some EBV- BL diagnosed cases by conventional methods (Mundo et al., 2020).

All of these observations suggest that the tumor is subject to a selective pressure and indicate a "hit-and-run" model (Figure 23). In this model, EBV initially facilitates tumor progression but gradually limits its latency programs and may ultimately be lost due to the presence of heritable changes induced by the virus and/or the acquisition of somatic mutations in oncogenes and tumor suppressor genes.

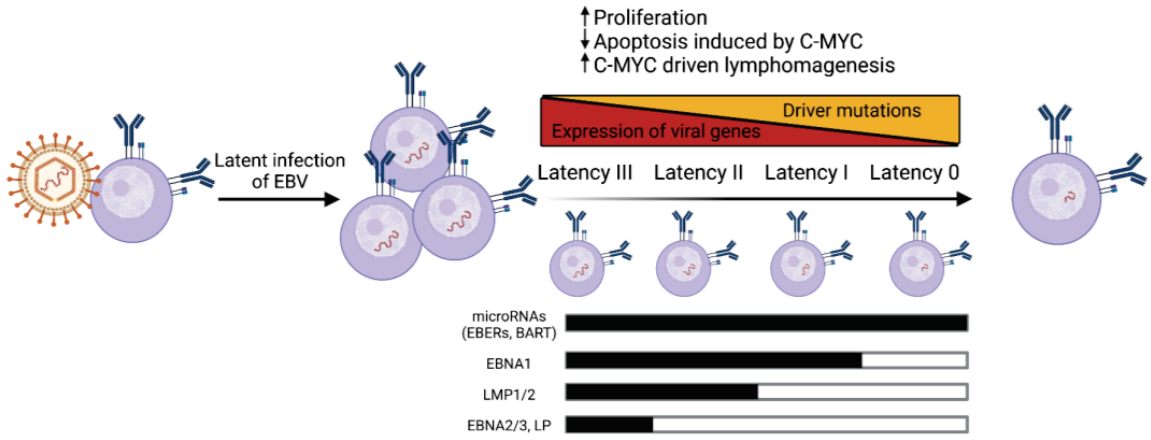

Figure 23. "Hit-and-run" model of EBV infection. B cells are infected by EBV, which promotes proliferation and c-MYC driven lymphomagenesis, and counteracts the apoptosis induced by c-MYC. EBV progressively downregulates viral gene expression through the changes in latency patterns and tumor B cells increase in acquisition of driver mutations. Finally, EBV genome may be lost.

5.4 Molecular biology and genetics in the light of EBV status

The postulated cell of origin of BL is a germinal center B cell from the dark zone, as tumor cells have undergone SHM process and show expression patterns of dark zone cells (Klein et al., 1995; Hummel et al., 2006; Caron et al., 2009; Piccaluga et al., 2011; Victora et al., 2012). However, differences in the mechanism of acquisition of *IG-MYC* translocation, in tumor mutational burden and in driver mutations regarding the EBV status suggest differences in the B cell of origin or in the acquired mechanisms driving oncogenesis in both subtypes of BLs. For instance, López and colleagues proposed that the B cell of origin of a subset of sBLs may be a germinal center B cell poised to express IgA (López et al., 2019). This specific class switch is frequently found in Peyer's patches (Figure 4), the prevalent localization for sBL (Table 3), corroborating their hypothesis.

5.4.1 IG-MYC translocation

The *IG-MYC* rearrangement is considered an early event in the development of BL. The translocation involves the chromosomic region 8q24 where *MYC* is located and the chromosomic regions of *IGH* (14q32), *IGL* (22q11*)* or *IGK* (2p12) (López et al., 2022) (Figure 24). The translocation is acquired during SHM and CSR, processes governed by AICDA. sBL and EBV- BLs mainly acquire the *IG-MYC* translocation by CSR process, while eBL and EBV+ BLs by SHM (López et al., 2019; Bellan et al., 2005; Thomas et al., 2022) (Figure 24 and Table 3).

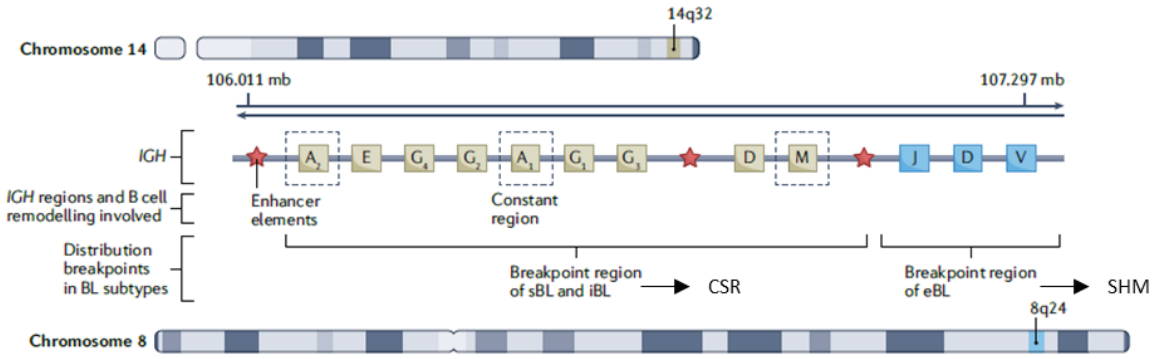

Figure 24. *IG-MYC* translocation is a hallmark of BL. *IGH* gene (14q32) is typically rearranged into *MYC* gene region (8q24) in BL primary cases. In sBL and iBL the breakpoint is usually located in the class-switch regions and in the eBL in the VDJ region, suggesting that CSR and SHM processes are involved in the acquisition of the translocation, respectively. Figure modified from López et al., 2022.

The result of the translocation is the overexpression of *MYC* oncogene through enhancer hijacking. MYC plays an important role in the global regulation of gene expression in BL, and is involved in several cellular processes, including cell cycle regulation, metabolism, protein biosynthesis, DNA replication and apoptosis. For instance, MYC activates some genes related to cell cycle progression, such as *CDK6* and *CDC6*, and others related to apoptosis, like *TP53*, *DAXX* and *DAP3*. For that reason, BL tumors acquire additional driver gene mutations in several pathways, including apoptosis and BCR/PI3K signaling, to overcome the "toxic" effects of MYC (Z. Li et al., 2003).

5.4.2 Molecular signature

The gene and the microRNA expression profile of BL is quite homogeneous, allowing it to be distinguished from other similar lymphomas, such as DLBCL (Piccaluga

et al., 2011; Hummel et al., 2006; Dave et al., 2006; Lenze et al., 2011). These studies defined BL gene expression signatures characterized by upregulation of *MYC* and its target genes, as well as *BCL6* and other germinal center B cell genes, and a downregulation of histocompatibility-complex class I genes and NFκB target genes, compared to related B cell lymphomas. Molecular BL signatures may identify BL cases with atypical morphologies, but also can include other high-grade B cell lymphomas and DLBCL cases (Figure 25).

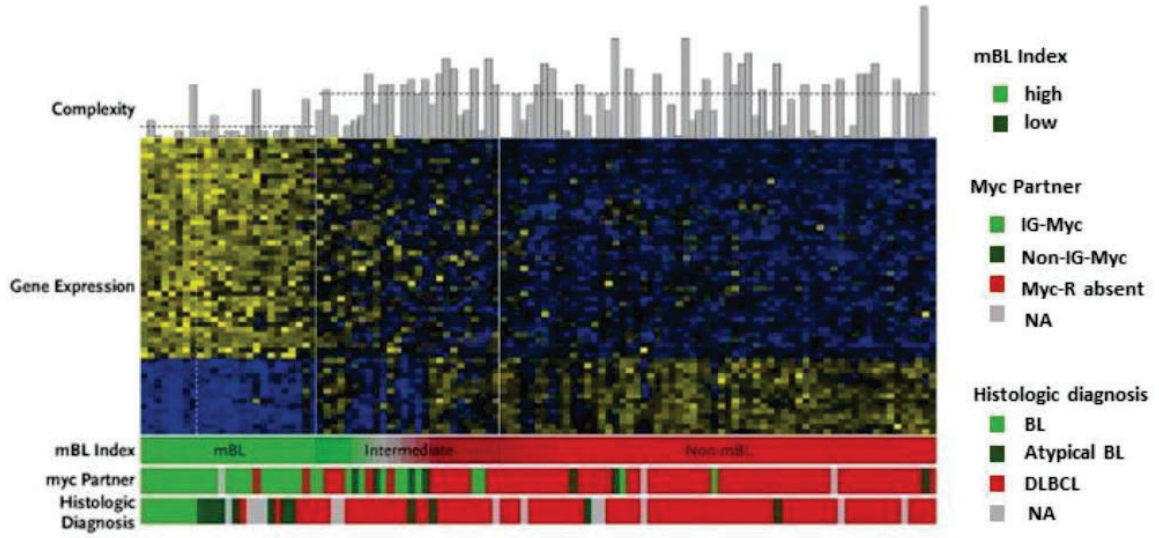

Figure 25. Molecular BL gene signature. The gene expression of the molecular BL signature is shown for 105 BL and DLBCL cases. Genomic complexity is illustrated in the top panel. Blue indicates high expression and yellow low expression. Clinical characteristics are shown in the bottom panel. Figure modified from Hummel et al., 2006.

Regarding the clinical variants or EBV status, slight differences in the gene expression profile have been shown (Lenze et al., 2011; Piccaluga et al., 2011). Kaymaz and colleagues showed gene expression differences in the PTEN/PI3K/mTOR pathway between EBV+ and EBV- BL tumors (Kaymaz et al., 2017). In addition, Grande and coworkers found increased *AICDA* expression in EBV+ compared to EBV- BLs.

5.4.3 Pathogenesis and genomic landscape

Genetic and epigenetic studies have identified several pathways dysregulated in BL. Tonic BCR, survival, proliferation, SWI/SNF complex and sphingosine-1-phosphate are some of the signaling pathways deregulated in this lymphoma (Figure 26) (López et

al., 2022; Schmitz et al., 2014). For instance, the module TCF3/ID3 is frequently mutated in BL patients. *ID3* loss-of-function mutations have been identified in 50-70% of patients, and *TCF3* gain-of-function mutations in around 10-25% (Schmitz et al., 2012; Richter et al., 2012; Love et al., 2012; López et al., 2019). In addition, inactivating *CCND3* and *TP53* mutations are also frequently found in BL patients (40% and 50% of patients, respectively). *CDKN2A* inactivating mutations or loss are less frequently found, in around 10% of BLs (Schmitz et al., 2012). *RFX7*, which act as a tumor suppressor in response to p53 (Coronel et al., 2021), is also mutated in BL (López et al., 2019; Grande et al., 2019). All these mutations contribute to enhance the growth and survival of the tumor cells through sustaining the cell cycle and evading apoptosis.

The most altered gene in BL is *MYC* (70% of patients) due to its susceptibility to SHM machinery, especially in its transactivation domain (Schmitz et al., 2012; Richter et al., 2012; Love et al., 2012). These alterations can contribute to higher proliferation rates but also to activate BCR signaling through PI3K pathway, an essential pathway for the BL pathogenesis (S. Sander et al., 2012). Indeed, several genes that participate in this pathway are mutated, although at low frequencies. For example, *FOXO1*, inhibited by PI3K to promote cell survival and growth, is mutated in 15% of BLs (Schmitz et al., 2012). Moreover, the negative and the positive regulators of PI3K, *PTEN* and *MIR17HG*, respectively, are mutated in 5-10% of the BLs (Grande et al., 2019).

Other pathways involved in the pathogenesis of BL are the sphingosine-1-phosphate and the SWI/SNF complex. Mutations in *P2RY8*, *GNA13* and *RHOA* are found in 10-20% of BLs, which results in increased cell migration (Figure 26). Besides, inactivating mutations in several components of the SWI/SNF chromatin-remodeling complex have been identified, especially mutations in *SMARCA4* (40%) and *ARID1A* (20-30%) ATP-dependent helicases (Schmitz et al., 2012; Richter et al., 2012; Love et al., 2012; López et al., 2019; Grande et al., 2019; Giulino-Roth et al., 2012). Another helicase frequently mutated in BL is *DDX3X*, which is required for RNA biogenesis.

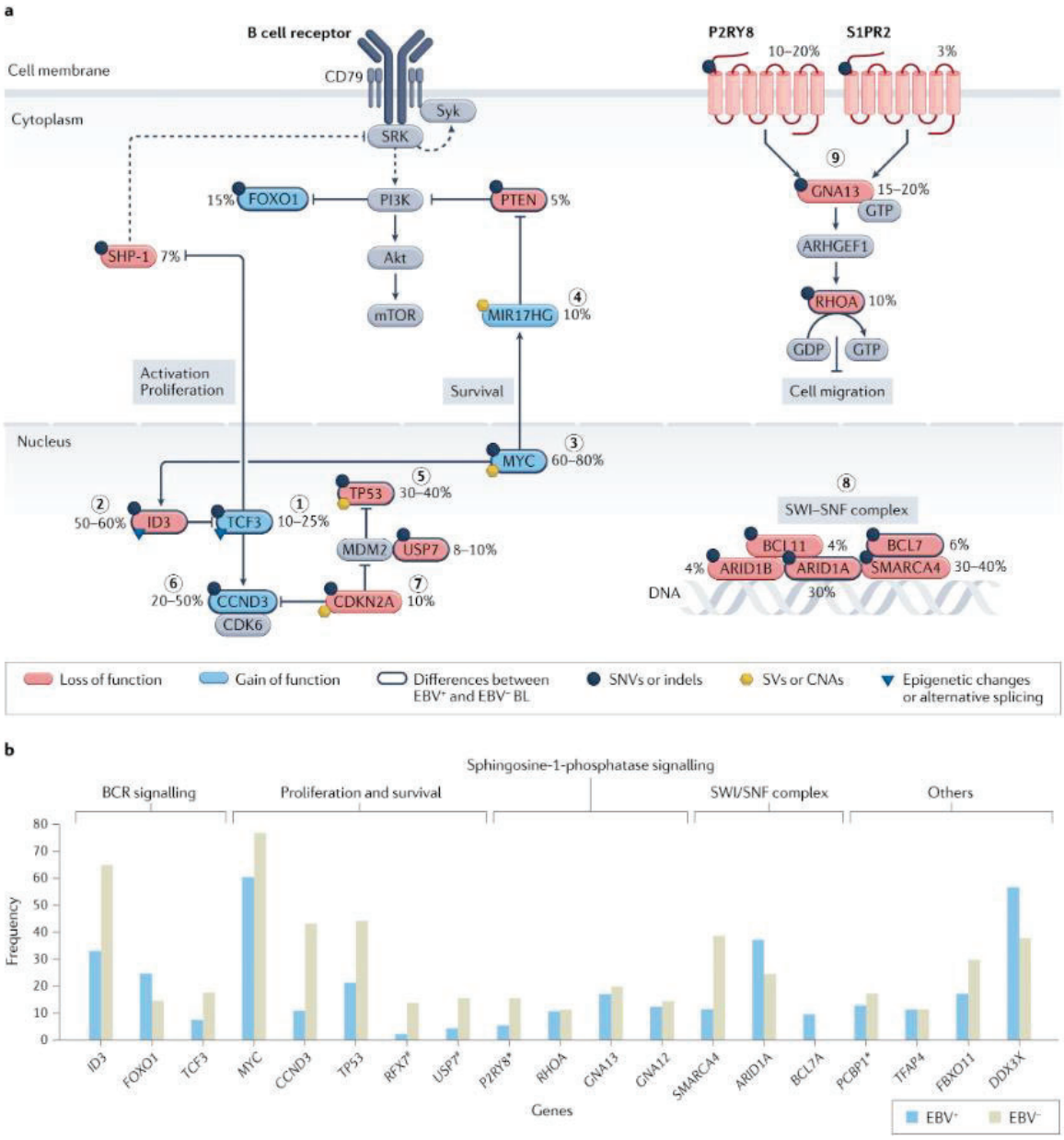

Figure 26. Recurrent pathways and genes altered in BL primary cases. (a) Frequency of mutations and alterations in genes found in BL (SNVs and indels labelled with dark blue circles, SVs and CNAs labelled with gold hexagons, and epigenetic changes and alternative splicing labelled with blue triangles). Gain-of-function mutations are labelled in blue and loss-of-function mutations in red. The altered genes with different frequencies between EBV+ and EBV- BL are indicated with a dark border. The altered genes and pathways are labelled (1) to (9), corresponding to TCF3–ID3 module (1 and 2), cell cycle and proliferation (3 to 7), the SWI–SNF complex (8), and sphingosine-1-phosphate signalling (9). **(b)** Frequencies of somatic genes affected in BL according to the EBV status obtained from Grande et al. 2019, Kaymaz et al. 2017 and López et al. 2019 (the alteration frequencies of the two genes labelled with an asterisk are available in only two studies (Grande et al. 2019 and López et al. 2019)). Genes included are those recurrently

mutated in at least 10% of cases and identified in more than one study. Figure from López et al., 2022.

Significant differences have been described between the genome landscape of eBL or EBV+ BLs and sBL or EBV- BLs. Despite eBLs having increased tumor mutational burden due to AICDA hyperactivation, they show lower mutations in driver genes, including *ID3*, *TCF3*, *CCND3*, *TP53*, *MYC*, *FOXO1* and *SMARCA4,* than sBL (Figure 26) (Kaymaz et al., 2017; Grande et al., 2019; Thomas et al., 2022). This result suggests that sBLs may achieve increased cell growth and survival through driver gene mutations in relevant genes, while eBLs may take advantage of the survival advantage provided by EBV infection.

5.4.4 SOX11 in BL

Despite the established oncogenic role of SOX11 in MCL, there is limited understanding of its function in BL. SOX11 overexpression is observed in 25-50% of BL patients (Dictor et al., 2009; Mozos et al., 2009; Wästerlid et al., 2017), and its expression is mainly detected in pediatric cases at diagnosis (Wästerlid et al., 2017; Richter et al., 2022; Deffenbacher et al., 2012). Furthermore, SOX11 is included in one of the transcriptional molecular signatures that distinguish molecular BLs (Hummel et al., 2006) (Figure 25). While SOX11 expression has been shown to impact MCL prognosis, its association with survival in BL remains unclear (Wästerlid et al., 2017). Additionally, although SOX11 silencing in BL cell lines has been shown to increase tumor cell proliferation, the experiment was only performed on two cells, and statistical significance was not achieved (Wästerlid et al., 2017). As a result, the contribution of SOX11 to the pathogenesis and clinical progression of BL remains unidentified.

AIMS

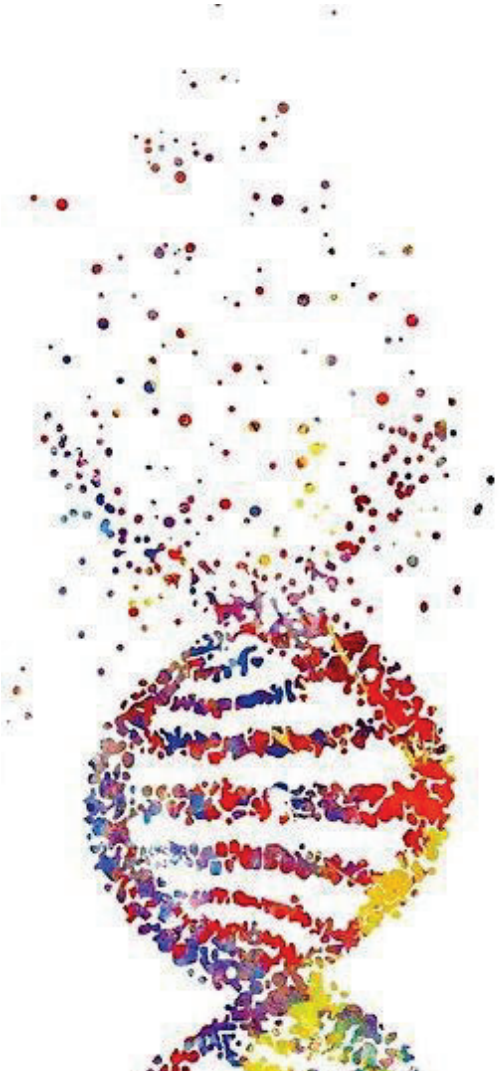

The overall aim of this thesis was to explore the functional role of specific oncogenes in aggressive B cell lymphomas, as well as to unravel the mechanisms that underlie their aberrant expression in lymphoid malignancies. By studying oncogenic drivers promoting tumor growth and survival in these lymphomas, we aimed to develop more effective targeted therapies that exploit the vulnerabilities of specific oncogenic pathways.

Hypothesis 1

Patients with MCL expressing the SOX11 transcription factor have worse prognoses compared to those that do not express SOX11, due to shorter responses to treatment and a higher incidence of relapse with current therapies. This may be attributed to the role of SOX11 in regulating progenitors and stem cells proliferation and differentiation in various tissues. Additionally, SOX11 enhances CSC properties and promotes drug resistance in multiple cancer cell types. Our hypothesis was that SOX11 could promote stem cell-like properties through the activation of stem cell-related genes in MCL, supporting tumor survival, self-renewal, and resistance to treatments. To achieve the study 1 of this thesis, the following aims were proposed:

AIM 1. To identify SOX11-dependent stemness-related factors as possible prognostic biomarkers for relapsed/refractory MCL.

AIM 2. To evaluate the CSC-related role of SOX11-direct target genes by loss-of-function experiments using in vitro MCL cell lines and in vivo MCL xenograft mice models.

AIM 3. To identify potential therapeutic interventions targeting CSC-related genes for the treatment of aggressive MCL.

- Investigating the efficacy of specific inhibitors targeting CSC-related genes through in vitro experiments to reduce clonogenic growth, tumor proliferation, and survival in MCL cell line models.

- Evaluating the therapeutic potential of CSC-related inhibitors through in vivo experiments to reduce self-renewal and engraftment in xenograft MCL mice models.

Hypothesis 2

While MYC oncogene overexpression is known to be a hallmark of BL, several studies confirm that it may not be sufficient for disease development. Overexpression of SOX11, which has been implicated in the pathogenesis of MCL, is found in a wide range of BL patients. Therefore, we hypothesize that SOX11 may also play an oncogenic role in BL, similar to that seen in MCL, and contributes to the pathogenesis of the disease. In order to achieve the study 2 of this thesis, the following specific aims were proposed:

AIM 1. To understand the clinical relevance of SOX11 expression in BL.

- Investigating the association between SOX11 expression and BL clinical features (EBV infection, sporadic/endemic presentation).

- Comparing the mechanism involved in the *IG-MYC* break between SOX11+ and SOX11- BL patients.

- Analyzing the mutational status of recurrent mutated genes in BL, comparing SOX11+ and SOX11- cases.

AIM 2. To shed light on the functional role of SOX11 in the development of BL.

- Identifying SOX11-specific gene expression profiles upon SOX11 overexpression and knockout in BL cell lines.

- Analyzing SOX11-specific molecular signatures in pediatric and adult BL cases.

- Identifying common genes and pathways regulated by SOX11 in BL and MCL

- Investigating the functional and mechanistic role of SOX11 in BL using SOX11-overexpression and knockout cell lines.

MATERIALS AND METHODS

1. BIOLOGICAL SAMPLES

1.1 Cell lines

The MCL cell lines Z138, Granta-519, JeKo-1 and HBL-2 (ATCC CRL-3001, DSMZ ACC 342, ATCC CRL-3006, and kindly provided by Dr. Colomer (Hospital Clinic, Barcelona, Spain) respectively, all SOX11+) and JVM2 (ATCC CRL-3002, SOX11-), the B-prolymphocytic leukemia cell line JVM13 (ATCC CRL-3003), the BL cell lines Ramos, DG-75 (ATCC CRL-1596 and ATCC CRL-2625, respectively, all SOX11-) and BL-2 (DSMZ ACC 625, SOX11+), the epithelial-like 293T cell line (ATCC CRL-3216) and the bone marrow stromal SNKT cells (Kawano et al., 2003), were used for this thesis.

Cells were cultured at 37 ºC and 5% CO_2 in RPMI 1640 with L-glutamine (Corning), DMEM with L-glutamine (Lonza) (only Granta-519 and HEK-293T) or SNKT medium (only SNKT), which contains MEM alpha medium (Life Technologies) with 2 µM of L-glutamine, 10% of horse serum (Life Technologies), 50 µM of hidrocortisone (Sigma) and 100 µM of beta-mercaptoetanol (Sigma). The three medium were supplemented with 10% of fetal bovine serum (FBS) (Gibco), 100 µg/ml streptomycin and 100 U/ml penicillin (Gibco).

Cells in suspension were counted by using a Neubauer chamber and trypan blue, and passaged two or three times per week adding cell media to dilute cells to $0.5x10^6$ cells/ml. Cell media was renewed once a week by centrifuging cells for 5 minutes at 300g. 293T and SNKT adherent cells were passaged when they reached 90% of confluence by washing cells with phosphate-buffered saline (PBS) and incubating them with trypsin for 5 minutes at 37 ºC and 5% CO_2 to detach cells. Then, DMEM or SNKT medium was added to dilute trypsin and cells were split into several plates. Adherent and suspension cells were passaged the day before the experiment to assure exponential growth. Cell line authentication was performed by qCell Identity (qGenomics) and *Mycoplasma* contamination was regularly tested.

For cryopreservation, $5x10^6$ cells were centrifuged for 5 minutes at 300g and freezing media containing FBS and 20% of dimethyl sulfoxide (DMSO) was added drop by drop to cells. Cryovials were stored in a cell freezing container for 2 days at -80 ºC, and then cryovials were stored in liquid nitrogen at -196 ºC.

1.2 MCL primary samples

MCL primary cells were collected from peripheral blood or lymph node samples of MCL patients diagnosed according to previous defined criteria (Swerdlow et al., 2017). MCL cells were isolated by Ficoll-Hypaque density gradient centrifugation (GE Healthcare) and cryopreserved in the Hospital Clínic/IDIBAPS tumor Biobank (Barcelona, Spain). The tumor cells were highly purified (>95% of purity), carried the t(11;14) and overexpressed cyclin D1. MCL cells were defrosted, washed in RPMI 1640, and cultured at 37 ºC and 5% CO_2 in RPMI 1640 supplemented with 10% FBS, 100 µg/ml streptomycin and 100 U/ml penicillin.

1.3 MCL and BL patient's cohorts

In the first study, the gene expression profile of 54 leukemic purified (>95%) tumor cells from MCL primary cases (Table 4), obtained previously by Affymetrix GeneChip Human Genome U133 Plus 2.0 (GSE79196) (Navarro et al., 2017), was used for gene set enrichment analysis (GSEA), differential expression analysis and survival analysis. Molecular characterization was performed as described in "3.2 Molecular profiling" methods section. For survival analysis, samples obtained after treatment (n = 7) and from patients that received an allogeneic stem cell transplant (n = 2) were discarded. Follow-up information was missing in 5 patients.

We also used the gene expression profile of a validation series containing 39 MCL primary cases from lymph node or peripheral blood samples, previously obtained using Affymetrix U219 microarrays (Nadeu et al., 2020). We performed RNA-seq on 12 purified leukemic or lymph node tumor cells from MCL patients of both cohorts (8 SOX11+ and 4 SOX11-) (Table 4). We integrated this information with previously

published RNA-seq data from 2 SOX11+ and 2 SOX11- MCL primary cases (Table 4), obtained from the BLUEPRINT consortium (Queirós et al., 2016; Vilarrasa-Blasi et al., 2021). MCL purified primary cells were also used for in vitro experiments (n=8) (Table 4).

MCL cases were classified as SOX11+ and SOX11- by immunohistochemistry and/or L-MCL16 assay, as previously described (Navarro et al., 2012; Clot et al., 2018). To obtain MSI2 mRNA levels from HG-U133 Plus 2.0 microarray, only 4 out of 10 probe sets, that showed a good expression and correlation (225237_s_at, 225238_at, 225240_at and 226134_s_at), were averaged together.

The study was approved by the Institutional Review Board of the Hospital Clínic, Barcelona, Spain.

Table 4. MCL primary cases used in this thesis for gene expression microarray, RNA sequencing and in vitro experiments.

Gene expression microarray		
Variable	**cMCL (n = 30)**	**nnMCL (n= 24)**
Clinical data (at diagnosis)		
Age yr, median (range)	73 (56-99)	64 (45-82)
Male (%)	23/30 (77)	12/24 (50)
Molecular data		
SOX11+ (%)	30/30 (100)	0/24 (0)
MSI2 High	25/30 (83)	11/24 (46)
Pretreatment sample (%)	26/30 (87)	21/24 (88)
TP53 alterations (%)	10/25 (40)	7/21 (33)
CDKN2A alterations (%)	6/27 (22)	0/21 (0)
CNA		
CNA High (%)	16/30 (53)	3/24 (12)
CNA Low (%)	11/30 (37)	18/24 (75)
Follow-up data (n = 40)		
2-yr OS, % (95% CI)	38 (21-70)	88 (74-100)
n dead, n censored	14, 9	5, 12

RNA sequencing		
Variable	**cMCL (n=10)**	**nnMCL (n = 6)**
Male (%)	9/10 (90)	5/6 (83)
Sample type PB (%)	6/10 (60)	6/6 (100)
Sample type LN (%)	4/10 (40)	0/6 (0)
SOX11+ (%)	10/10 (100)	0/6 (0)
In vitro experiments		
Variable	**MSI2 High (n = 3)**	**MSI2 Low (n = 5)**
Male (%)	3/3 (100)	4/5 (80)
SOX11+ (%)	3/3 (100)	2/5 (40)
cMCL, nnMCL	3, 0	2, 3

cMCL: Conventional mantle cell lymphoma, nnMCL: Non-nodal mantle cell lymphoma, PB: Peripheral blood, LN: Lymph node, MSI2 High > 8.46 units of mRNA expression or >0.51 relative mRNA expression, CNA: Copy number alterations (High >6 CNA), OS: Overall survival, CI: Confidence interval

Several previously published BL patient cohorts were used for the second study of this thesis (Grande et al., 2019; Richter et al., 2012; López et al., 2019; Burkhardt et al., 2022; Hummel et al., 2006). The first cohort includes 117 pediatric BL patients (96 endemic and 21 sporadic) with available RNA-seq, clinical and molecular data (EBV status, breakpoint of *IG-MYC* and recurrently mutated genes) (Grande et al., 2019). The second cohort includes 162 sBL patients (92 children and 70 adults), some with available SOX11 immunohistochemistry (IHC), EBV-encoded small nuclear RNA (EBER) in situ hybridization (ISH) and targeted DNA sequencing data (Richter et al., 2022). The third series includes 51 pediatric sBL selected cases from Burkhardt et al. study (Burkhardt et al., 2011) with available deep targeted DNA sequencing data, in which SOX11 IHC and EBER ISH was performed. The fourth series includes 24 pediatric sBL selected cases with available SOX11 IHC, whole-genome sequencing (WGS) data and EBV status (López et al., 2019). The last series includes 45 sBL cases considered molecular BLs, with available microarray expression data (Hummel et al., 2006).

2. GENERATION OF CELL LINE MODELS

The cell line models generated by lentiviral transduction and/or used in this thesis are summarized in Table 5.

Table 5. Cell line models generated by lentiviral transduction with its corresponding selection.

Cell lines	Lenviral plasmid	Transduced model	Selection
Z138	pL-CRISPR.EFS.GFP	Z138CT	GFP sorting
	pL-CRISPR.SOX11.1.EFS.GFP	Z138-SOX11KO	GFP sorting
	shCT	Z138shCT	Puromicin
	sh2MSI2	Z138sh2MSI2	Puromicin
	sh4MSI2	Z138sh4MSI2	Puromicin
	sh5MSI2	Z138sh5MSI2	Puromicin
Granta-519	shCT	GrantashCT	Puromicin
	sh4MSI2	Grantash4MSI2	Puromicin
	sh5MSI2	Grantash5MSI2	Puromicin
JVM2	pCDH-MCS-T2A-Puro-MSCV	JVM2CT*	Puromicin
	pCDH-MCS-T2A-Puro-MSCV-Flag-SOX11	JVM2-SOX11+*	Puromicin
Z138shCT	pLV430G-oFL-T2A-eGFP	Z138shCT-Luc	GFP sorting
Z138sh5MSI2	pLV430G-oFL-T2A-eGFP	Z138sh5MSI2-Luc	GFP sorting
Z138-SOX11KO	pCDH-MCS-T2A-Puro-MSCV	Z138-SOX11KO CT	Puromicin
	pCDH-MCS-T2A-Puro-MSCV-Flag-SOX11	Z138-SOX11KO SOX11+	Puromicin
	sh5MSI2	Z138-SOX11KO-sh5MSI2	Puromicin
Z138sh4MSI2	pLV-Neo-EF1A	Z138sh4 EF1A Ø	G418
	pLV-Neo-EF1A-hMSI2-FLAG	Z138sh4 EF1A MSI2-FLAG	G418
Z138sh5MSI2	pLV-Neo-EF1A	Z138sh5 EF1A Ø	G418
	pLV-Neo-EF1A-hMSI2-FLAG	Z138sh5 EF1A MSI2-FLAG	G418
Ramos	pCDH-MCS-T2A-Puro-MSCV	Ramos-CT	Puromicin
	pCDH-MCS-T2A-Puro-MSCV-Flag-SOX11	Ramos-SOX11	Puromicin

* *Generated in* (Balsas et al., 2017)

DG75 ER and ER-SOX11, and BL2-CT and -SOX11KO BL cell lines were stable transfected by electroporation with pEF1α-IRES-ER-(HA-SOX11)-AcGFP1, and a specific guide RNA (gRNA) against SOX11 together with Cas9 protein, respectively.

2.1 Plasmid generation

The gRNA for SOX11 knockout (KO) genome editing in Z138 MCL cell line using CRISPR-Cas9 technology was designed using E-CRISP tool (Heigwer et al., 2014). The gRNA (Table 6) was amplified by PCR and cloned in pL-CRISPR.EFS.GFP lentiviral plasmid (Addgene #57818) by restriction enzyme digest with BsmBI, generating pL-CRISPR.SOX11.1.EFS.GFP. The plasmid pCDH-MCS-T2A-Puro-MSCV-FLAG-SOX11, obtained previously (Balsas et al., 2017), was used for SOX11 overexpression, and the empty plasmid pCDH-MCS-T2A-Puro-MSCV (CD522A-1; System Bioscience) was used as control.

MSI2 MISSION shRNA Plasmids TRCN0000423713, TRCN0000062811 and TRCN0000417428 (Sigma Aldrich) were used for MSI2-knockdown (MSI2KD), generating sh2MSI2, sh4MSI2 and sh5MSI2 cell lines, respectively (Table 6). Scramble shRNA lentiviral particles (Santa Cruz Biotechnology) were used as control (shCT). Experiments performed with the MSI2KD and control cell lines were done at a short time of silencing to avoid compensation effects. Lentiviral transductions were repeated to have at least n = 3 number of experiments for each assay in MSI2KD and control cell lines. Z138sh5MSI2 and Z138shCT cells were stable transduced with the lentiviral vector pLV430G-oFL-T2A-eGFP (kindly provided by Beatriz Martin-Antonio (Perez-Amill et al., 2021)) expressing the luciferase and green fluorescent proteins (GFP), generating the Z138shCT-Luc and Z138sh5MSI2-Luc cell lines. Plasmids pLV-Neo-EF1A empty or expressing hMSI2(NM_138962.4)-FLAG were customized by VectorBuilder.

ER-SOX11 expression was achieved using the pEF1α-IRES-AcGFP1 vector (Clontech). Briefly, both SOX11 ORF and the sequence of the hormone-binding domain of the mouse Estrogen Receptor (ER) carrying mutations that increase its affinity for the synthetic drug 4-hydrohytamoxifene (4-OHT) (Littlewood et al., 1995) were amplified by

PCR and cloned in the vector using unique restriction sites. The ER sequence was amplified from a plasmid expressing the Myc-ER gene fusion (Iaccarino et al., 2003) with primers adding the unique restriction sites NheI and HindIII and an improved Kozak sequence. SOX11 sequence was amplified by PCR from the plasmid pcDNA3-SOX11-HA (Vegliante et al., 2013) with primers removing the starting ATG and adding the unique restriction sites HindIII and BamHI.

Table 6. Sequences for short hairpin RNAs MSI2 silencing and guide RNA for SOX11-KO.

RNA	Name	Commercial number	Sequence
shRNA	sh2MSI2	TRCN0000423713	CTTCGGATCGAGGGTTGACTA
shRNA	sh4MSI2	TRCN0000062811	CCCAACTTCGTGGCGACCTAT
shRNA	sh5MSI2	TRCN0000417428	TGCAATGCTGATGTTTGATAA
gRNA	SOX11.1	No commercial	GTTCCCCGACTACTGCACGC

2.2 Generation of lentivirus and lentiviral transduction

HEK-293T were transfected at 60-70% of confluence with lentiviral packaging and envelope plasmids psPAX2 and pCMV-VSV-G (Addgene #12260 and #8454, respectively), and the corresponding plasmid of interest (see 2.1 Plasmid generation and Table 5) by using Lipotransfectin (Niborlab). Viral supernatants were collected 48 h after transfection, filtrated and concentrated adding Lenti-X Concentrator (Takara) at 1/10 following manufacturer's instructions. $1.5x10^6$ MCL and BL cells (Table 5) were transduced with 300 µl of concentrated lentivirus or 30 µl of commercial Control shRNA Lentiviral Particles (sc-108080; Santa Cruz Biotechnology) by centrifugation for 90 minutes at 32 ºC and 2500 rpm. Cells were incubated with lentivirus for 24 hours.

2.3 Cell selection and sorting

After 48 h of lentiviral transduction, transduced MCL and BL cells were selected with 0.5 µg/ml of puromycin (Gibco) or 500 µg/ml of G-418 (Sigma) (Table 5), for 3 to 7 days. For selection by GFP (Table 5), GFP+ cells were sorted 72 h after transduction in FACSAria II Cell Sorter (BD). For DG75 cell line models, two days after transfection cells were incubated with G418 for two weeks, to select for stable transfectant. Pools of

stably transfected cells were sorted by FACS to purify only the cells expressing acGFP, and therefore either ER-SOX11 or ER-only.

2.4 CRISPR pool validation

Z138-SOX11KO GFP+ cells were seeded at 500 cells/well in order to obtain pools with SOX11KO. Disruption of *SOX11* locus using CRISPR/Cas9 technology was verified by using the Genomic Cleavage Detection Kit (GeneArt) following manufacturer's indications and by PCR using specific primers (Appendix Table 1) followed by Sanger Sequencing (Figure 27).

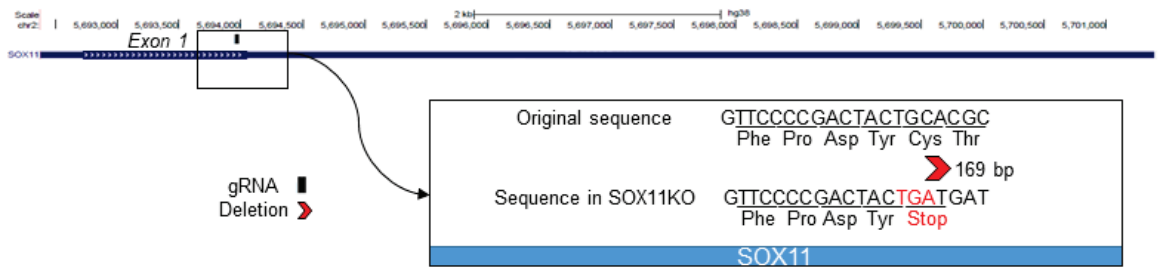

Figure 27. CRISPR/Cas9 strategy to knock out SOX11 in Z138 MCL cell line. Guide RNA (gRNA) targets exon 1 of the *SOX11* coding sequence and deletes a region of 169 bp, which results in addition of a stop codon that truncates the SOX11 protein.

For BL2-SOX11KO, RNA-seq read aligned to the human genome (GRCh38/hg38) was used to validate SOX11 knockout.

3. HIGH-THROUGPUT PROFILING AND SEQUENCING

3.1 Gene expression microarrays

Previously published microarrays (Navarro et al., 2017; Nadeu et al., 2020; Hummel et al., 2006) were preprocessed by fRMA (McCall et al., 2010) or RMA (Irizarry et al., 2003) algorithm using R (version 3.6.3, https://www.r-project.org). For differential expression analysis in microarray data, gene filtering was done with featureFilter in order to maintain only probes sets with Entrez Gene ID and with the highest interquartile range of the probe sets annotated by the same Entrez Gene ID. Differential expressed genes

were obtained by linear models and empirical Bayes methods with limma package (3.42.2). P-values were adjusted with Benjamini and Hochberg method. Genes with an adjusted P-value <0.05 and absolute $\log_2$ fold change >0.7 were selected. To obtain mRNA levels of genes, all the probe sets were averaged together, except for MSI2 on the HG-U133 Plus 2.0 microarray (see "1.3 MCL and BL patient's cohorts methods" section). To obtain the stem cell signature score, the mean of the probe sets with the highest interquartile range for each stem cell-related gene enriched in SOX11+ MCLs GSEA was used.

3.2 Molecular profiling

Molecular profiling of MCL primary cases was performed as described below. *TP53* alterations were considered when *TP53* was mutated and/or deleted. *TP53* mutations were obtained by Sanger sequencing (Royo et al., 2012) or whole-exome sequencing (Beà et al., 2013). *CDKN2A* alterations were considered when *CDKN2A* was deleted (homozygous or heterozygous). CNA were detected using Affymetrix Genome-Wide SNP 6.0 arrays and analyzed by Nexus BioDiscovery (version 9) (Beà et al., 2013). CNA high was defined as >6 CNA and indicates high genomic complexity.

To identify the partner and the mechanism involved in the *IG-MYC* translocation of BL cases (Grande et al., 2019), the breakpoint was analyzed in detail in order to detect the *IG* partner and the *IG* region involved in the translocation.

For mutational analysis in BL primary cases, lists of mutated driver genes were obtained from the different studies (Grande et al., 2019; López et al., 2019; Richter et al., 2022; Burkhardt et al., 2022). Some of the data was obtained by WGS and other by targeted mutational analysis. Only the genes that were present in more than 5% of the BL cases were used for oncoprint analysis and comparisons between groups.

3.3 RNA-seq

RNA from MCL and BL cell lines and primary cases was extracted as described in "5.2 RNA extraction" methods section. RNA quantity and quality were examined using

NanoDrop (Thermo Scientific) and RNA 6000 Nano Assay on the Agilent 2100 Bioanalyzer (Agilent Technologies). RNA samples from cell lines or primary cases with RIN higher than 8 were selected to generate mRNA or total RNA libraries using the TruSeq RNA Sample Prep Kit v2 or the TruSeq Stranded Total RNA kit with Ribo-Zero Gold (Illumina), respectively, following manufacturer's specifications. RNA-seq libraries were amplified, pooled and sequenced on a HiSeq2500 or NovaSeq sequencer (Illumina) to generate 75 bp paired-end, 50 bp single-end or paired-end reads (Samples information, RNA extraction, library and sequencing conditions are shown in Appendix Table 2). More than 30 million of reads were sequenced for each sample.

MCL sequencing reads were quality checked with FastQC (version 0.11.9), depleted from rRNA reads with SortMeRNA (version 4.3.2), trimmed to remove adapters and low-quality reads with trimmomatic (version 0.40), and pseudo-aligned to reference human genome GRCh38.p13 version with kallisto (version 0.46.1) to extract gene-level counts (Ensembl release 100). RNA-seq data from BL cell lines were analyzed using the open-source web-based Galaxy (Afgan et al., 2018): paired fastq files were aligned to the human genome (GRCh38) using HISAT2 and counts files were generated with featureCounts using GRCh38.102.gtf as gene annotation file.

Gene level counts were imported to R (version 3.6.3, https://www.r-project.org) using tximport (version 1.12.3). Differential expression was conducted using DESeq2 package (version 1.24.0), shrinking the size factor with apeglm method. Variance stabilized expression matrix were obtained for GSEA and clustering. Lists of differential expressed genes were used for pathway over-representation analysis. To classify BL pediatric cases (Grande et al., 2019) in SOX11- and SOX11+, a cut-off of 10.5 (in $\log_2$ transformed values) was done. To obtain the SOX11 specific signature in BL, differentially expressed genes in the analysis between DG75 ER and DG75 ER-SOX11 4-OHT treated cells (adjusted P-value <0.1 and absolute log2-transformed fold change >0.65), and in the analysis between Ramos CT and Ramos SOX11 (adjusted P-value <0.15 and absolute log2-transformed fold change >0.5), were overlapped.

For Z138CT and Z138-SOX11KO or JVM2CT and JVM2-SOX11+, samples were sequenced per triplicate. For MSI2 silencing, 4 samples from Z138shCT, 2 from Z138sh2MSI2, Z138sh4MSI2 and Z138sh5MSI2 were sequenced. For Ro inhibitory experiments, Z138 cell line was independently treated per triplicate with Ro 08-2750 20 μM or DMSO 0.1% for 4 hours and samples were sequenced. For SOX11 overexpression in BL, DG75 CT and DG75 ER-SOX11 were treated for triplicated with 150 nM of 4-OHT or ethanol for 8 and 24 hours, and Ramos CT and Ramos SOX11 were sequenced for duplicated. For SOX11KO in BL, 2 selected clones of SOX11KO and CT BL cells were sequenced for duplicated. Previously published RNA-seq data from MCL primary cases, cell lines and normal B-cells were obtained from BLUEPRINT consortium (Queirós et al., 2016; Vilarrasa-Blasi et al., 2021; Beekman, Chapaprieta, et al., 2018). RNA-seq data for BL primary cases was obtained from the National Cancer Institute's Genome Data Commons Publication Page (https://gdc.cancer.gov/about-data/publications/CGCI-BLGSP-2019) (Grande et al., 2019).

3.4 Reference epigenomes

Reference epigenomes of five MCL cases (2 SOX11+ and 3 SOX11-), 2 MCL cell lines (Z138 and JVM2), as well as sorted naïve, germinal center, memory and plasma B cells from 3 healthy donors were mined from previously published reports (Queirós et al., 2016; Vilarrasa-Blasi et al., 2021). Reference epigenomes were made out of chromatin states derived from ChIP-seq of six different histone modifications (H3K27ac, H3K4me1, H3K4me3, H3K36me3, H3K9me3, H3K27me3), chromatin accessibility (ATAC-seq), DNA methylation at the whole genome scale, and gene expression (RNA-seq). Chromatin states from BL2 SOX11+ and DG75 SOX11- BL cells was obtained from BLUEPRINT consortium. The data was generated and processed as described in (http://dcc.blueprint-epigenome.eu/#/md/methods) (Queirós et al., 2016; Vilarrasa-Blasi et al., 2021; Beekman, Chapaprieta, et al., 2018). The 12 different chromatin states were generated at 200 bp interval using the chromHMM software (Ernst & Kellis, 2012), as previously described (Beekman, Chapaprieta, et al., 2018).

4. CELL CYTOMETRY

The flow cytometer raw data was analyzed by using FACSDiva and FlowJo v.10 (BD) softwares to plot percentages of populations or the mean fluorescence intensity (MFI) when indicated, depending on the experiment. Singlets gating was done in all the experiments by plotting FSC-A and FSC-H and selection of the cells in the diagonal (Figure 28). All the experiments were performed in FACSCanto II flow cytometer (BD).

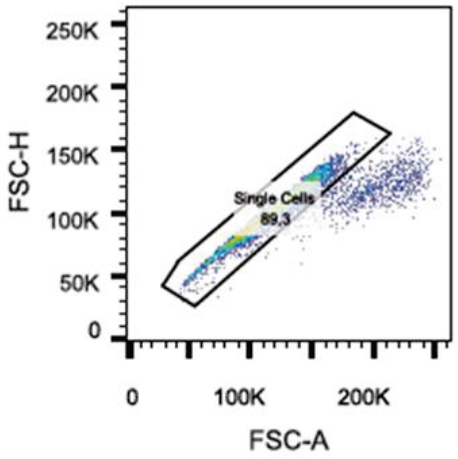

Figure 28. Gating strategy to obtain single cells. Singlets were obtained by gating the cells of the diagonal in the FSC-A vs FCS-H plot.

4.1 Apoptosis analysis

Apoptosis was analyzed by using Annexin V Apoptosis Detection Kit FITC (eBioscience). Briefly, we centrifuged $5x10^4$ growing MCL transduced untreated cells, MCL wild type cells treated with Ro 08-2750 (Ro) (Tocris Bioscience) at 1 µM or 5 µM during 24, 48 or 72 h, or MCL transduced cells treated with 0.05 µM (Z138) and 3 µM (Granta-519) of Doxorubicin (Selleckchem) for 24 hours. Cells were incubated with 100 µl of Annexin Binding Buffer mixed with 1.5 µl of Propidium Iodide (PI) and/or 0.4 µl of Annexin V conjugated to fluorescein isothiocyanate (FITC) for 15 minutes to analyze apoptosis (Figure 29). Technical triplicates were performed for each experiment, and the experiments were repeated at least 3 times.

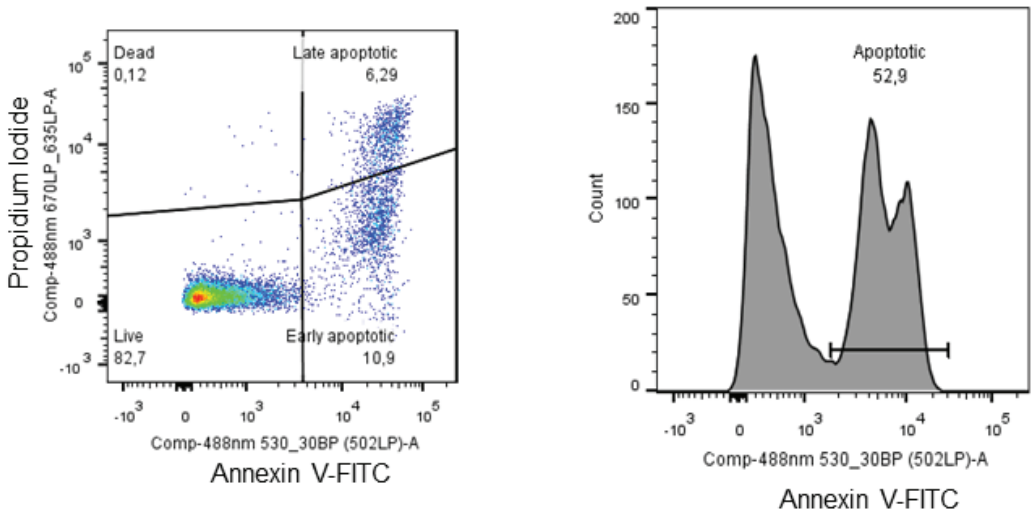

Figure 29. Gating strategy in apoptosis analysis. Flow cytometry gating strategy for apoptosis analysis using Propidium Iodide and Annexin V-FITC (left), or only Annexin V-FITC (right) fluorophores.

4.2 Cell cycle analysis

For cell cycle analysis, Click-iT Plus EdU Pacific Blue Flow Cytometry Assay Kit (ThermoFisher) was used following manufacturer's instructions. Briefly, 0.5-1x10^6 exponential growing cells were incubated 1 hour with 20 µM of EdU. Cells were washed with PBS, fixed by adding 300 µl of PBS and 700 µl of absolute ethanol drop by drop and stored at -20 ºC overnight. Fixed cells were permeabilized and blocked with 0.1% Tween and 1% bovine serum albumin (BSA) for 10 minutes. Click-it reaction was performed during 30 minutes. Then, cells were incubated with PI staining solution (2.5 µg PI and 100 µg RNase A) for 30 minutes and analyzed by flow cytometry. The experiment was repeated at least 3 times.

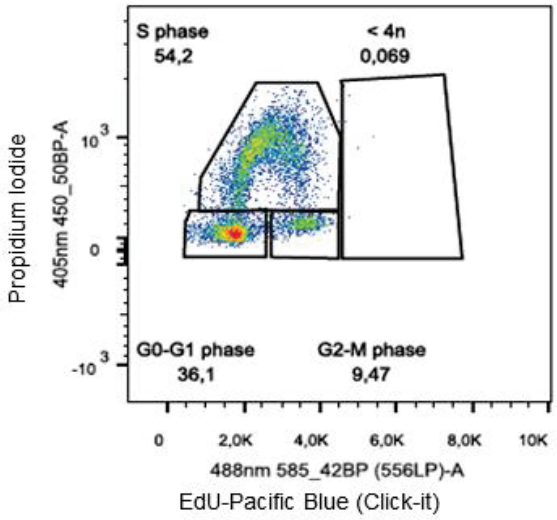

Figure 30. Gating strategy for cell cycle analysis. Cell cycle analysis using Propidium Iodide and EdU-Pacific Blue fluorophores for detection of G_0-G_1, S and G_2-M phases.

4.3 Intracellular and extracellular staining

For intracellular staining of cleaved caspase 3, $2x10^5$ growing MCL cells were fixed with paraformaldehyde 4% for 15 minutes. Cells were washed with PBS, permeabilized with Triton 0.5% and FBS 5%, and stained with 10 µl of active caspase 3 antibody conjugated with FITC (Appendix Table 3) for 30 minutes at 4 ºC. Cells were washed with PBS and analyzed in FACSCanto II flow cytometer (BD).

For extracellular staining of FAS and CD24, $2x10^5$ growing MCL cells were washed with PBS and FBS 5%, and stained with 2 µl of FAS, 2.5 µl of CD24 or isotype antibodies conjugated with fluorophores (Appendix Table 3) for 20-30 minutes at 4 ºC. Cells were washed with PBS and analyzed. Technical duplicates were performed for each experiment, and the experiments were repeated at least 3 times. To plot the results of Fas and CD24 staining, MFI was used.

4.4 ALDEFLUOR assay

For ALDEFLUOR assay (STEMCELL Technologies), $5x10^5$ MCL primary cells were incubated with 1, 5 µM of Ro or DMSO 0.05% for 24 h. Then, we washed cells with 1 ml of ALDEFLUOR Assay Buffer and added 5 µl of ALDEFLUOR Reagent to the

cells, mixing them. Immediately, 0.5 ml of the cell mixture was separated into another tube containing 5 µl of ALDEFLUOR DEAB Reagent. Cells were incubated with shaking for 40 minutes at 37°C. Cells were washed with ALDEFLUOR Assay Buffer and analyzed in flow cytometer. ALDEFLUOR+DEAB samples were used as negative controls. For plot the results of ALDEFLUOR assay, MFI was used.

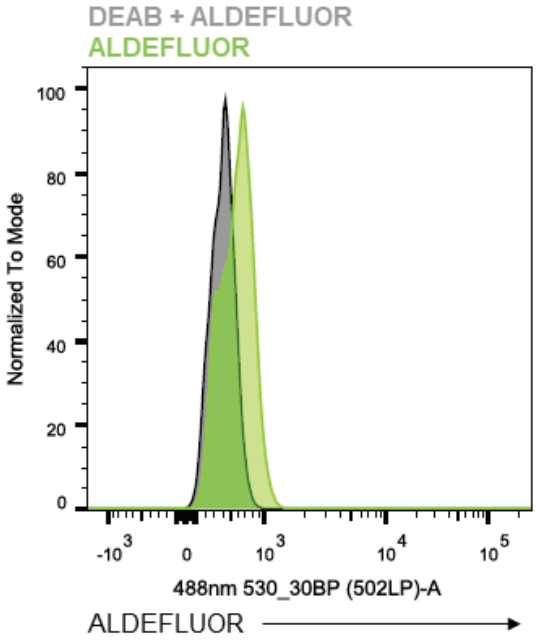

Figure 31. Gating strategy for ALDEFLUOR assay. ALDEFLUOR analysis measuring MFI of ALDEFLUOR samples comparing to DEAB + ALDEFLUOR control negative samples

4.5 Migration assay towards CXCL13

BL cells (SOX11-expressing and control DG75 [after 24 hours of 4-OHT 150 nM induction] and Ramos cells) were cultured during 90 minutes in RPMI supplemented with 0.5% FBS, to induce cell starving. Then, $5x10^5$ of BL cells were added on top of transwells embedded in a 24-well plate containing 1 µg/ml of CXCL13 chemokine. Cells were cultured overnight and next day transwells were extracted, mixing the medium and collecting 400 µl of cells. We added 50 µl of CountBright beads (Invitrogen) to count the total number of cells that migrated towards CXCL13 stimuli for each sample by flow cytometry, with the following formula:

$$Absolute\ count\ \left(\frac{cells}{\mu l}\right) = \frac{Cell\ count\ x\ Beads\ volume}{Beads\ count\ x\ Cell\ volume}\ x\ Counting\ beads\ (\frac{beads}{\mu l})$$

The migration index towards CXCL13 was measured as the absolute count of cells migrating through CXCL13 divided by the absolute count of cells migrating in an unspecific way (without CXCL13).

4.6 Pseudoemperipolesis

BL cells (SOX11-expressing DG75 [after 24 hours of 4-OHT 150 nM induction] and Ramos, and their controls) were added on top of a confluent SNKT cell layer (1:5 SNKT/BL ratio), and were incubated overnight. Supernatant was removed (unattached BL cells), and three washes with PBS were performed in the adhered cells. Then, cells were tripsinized and BL cells that migrated to the SNKT layer were distinguished by cell size and counted by flow cytometry by adding 50 µl of CountBright beads, with the formula showed previously.

5. NUCLEIC ACID AND PROTEIN ANALYSIS

5.1 DNA extraction

Bacterial glycerol stocks were grown in LB medium supplemented with ampicillin overnight. Plasmid DNA was obtained from 200 ml of bacteria culture by using EndoFree Plasmid Maxi Kit (Qiagen) and genomic DNA was obtained from $5x10^6$ Z138-SOX11KO cells by QIAmp DNA Mini Kit. For Maxis, pellets were resuspended in Buffer P1 and lysed in buffer P2 for 5 minutes. Then, we stopped the lysis by addition of Buffer P3. Lysates were filtered with QIAfilte Cartridge and incubated with Buffer ER for 30 minutes on ice. Then, columns were equilibrated with Buffet QBT and lysates were added to columns, washed several times and eluted with Buffer QN. DNA was precipitated overnight by addition of isopropanol, and next day we washed the DNA pellet with 70% ethanol and we eluted the DNA in Buffer TE. For Minis, cell pellets were incubated with Proteinase K and Buffer AL for 10 minutes at 56 ºC. Absolute ethanol was added and

sample was transferred to the QIAmp MiniElute Column. After centrifugation, columns were washed with Buffer AW1 and AW2, and DNA was eluted in Buffer AE.

5.2 RNA extraction

RNA from MCL and BL cell lines and primary cases was extracted with TRIZOL (Life Technologies) or by using RNeasy Plus kit (QIAGEN). Immunoprecipitated RNA (see 5.3 RNA immunoprecipitation method below) was purified by Phenol:Chloroform:Isoamyl Alcohol (125:24:1) method.

For TRIZOL method, after washing pellets, we incubated the cells with 1 ml of TRIZOL for 5 minutes. Then, we centrifuged the cells at 11400 rpm for 15 minutes. We transferred the aqueous phase to another tube, and we added the same volume rescued of isopropanol. We precipitated the RNA overnight at -80 ºC. Next day, we centrifuged at 11400 rpm for 25 minutes, we washed twice the pellet with 70% ethanol and we eluted the RNA in RNase-free water.

For RNeasy Plus kit, we lysed $5x10^6$ cells with 350 µl of RLT Plus buffer and we transferred the lysate to gDNA eliminator column, saving the supernatant. Then, we added 70% ethanol and we transferred the lysate to RNeasy column. After washing with RW1 and RPE, we eluted the RNA in RNase-free water.

For Phenol:Chloroform:Isoamyl Alcohol method in RNA immunoprecipitation experiment, we added 400 µl of phenol:choloform:isoamyl alcohol to samples, and after vigorous shaking in Phase Lock Gel Heavy tubes (Quantabio), samples were centrifuged at 14000 rpm for 10 minutes at room temperature. Then, we added 400 µl of chloroform and after vigorous shaking, samples were centrifuged at 14000 rpm for 10 minutes at room temperature. After that, 400 µl of sample was recovered in a new tube, precipitating the RNA by addition of Salt Solutions I and II, Precipitate Enhancer (Magna RIP RNA-binding protein immunoprecipitation kit; Millipore) and ethanol 85% overnight at -80 ºC. Next day, RNA was washed with ethanol 80% and eluted with 12 µl of RNase-free water.

5.3 RNA immunoprecipitation

For RNA immunoprecipitation (RIP), Magna RIP RNA-binding protein immunoprecipitation kit (Millipore) was used following manufacturer's instructions. MCL growing cells were lysed for 5 minutes at 4 ºC and stored at -80 ºC for 2 hours. Magnetic beads protein A/G were washed and incubated with 3 µg of MSI2 or normal Rabbit IgG antibody (Appendix Table 3) on rotating wheel for 1 hour at 4 ºC. Then, lysates were incubated with each immune-complex ($30x10^6$ cells per 3 µg of antibody bound to beads) on rotating wheel overnight at 4 ºC, separating a 10% of input fraction before antibody-beads addition. Supernatants (unbound fractions) were saved for western blot experiment. Immuno-complexes bound to lysates were washed 6 times. One sample incubated with MSI2 antibody was used for western blot analysis adding 25 ul of Sample Buffer mixed with DTT and incubating at 95 ºC for 10 minutes. Remaining samples incubated with MSI2 and IgG antibodies and input fraction were used for protein digestion with Proteinase K Buffer at 55 °C for 30 minutes with shaking. Then, purification of RNA was done by Phenol:Chloroform:Isoamyl Alcohol (125:24:1) method (see "5.2 RNA extraction" method) by using Phase Lock Gel Heavy tubes (Quantabio). NanoDrop (Thermofisher) was used for RNA quantification. RNA from input fraction (1 µg) and the whole RNA eluted from MSI2 and IgG RIP (< 1 µg) were used for cDNA generation by using Verso cDNA Synthesis Kit (Thermofisher) following manufacturer's guidelines and using a blend of oligo dT primers and random hexamers. *CDK6*, *NOTCH1* and *GUSB* mRNA enrichment was analyzed by qPCR in StepOnePlus (Thermofisher) using Fast SYBR Green Master Mix (Applied Byosistems) and specific primers (Appendix Table 1), as described in next section "5.4 RT-qPCR". To quantify relative abundance of each mRNA, Ct of qPCR curves normalized with adjusted input Ct (ΔCt [normalized RIP] = (Ct [RIP] - (Ct [Input] + log2 (% of input/100)) were calculated with the following formula: mRNA enrichment (%) = 100*2ΔCt [normalized RIP].

5.4 RT-qPCR

RNA from MCL leukemic primary cases, and MCL and BL cell lines, was extracted using RNeasy Plus kit (QIAGEN) (see "5.2 RNA extraction" methods section). RNA quantity and quality were examined using NanoDrop (Thermo Scientific). cDNA was generated using qScript cDNA Synthesis Kit (Quantabio). Briefly, 500 ng of RNA were mixed with 4 µl of qScript Reaction Mix and 1 µl of qScript RT. Then, samples were retrotranscribed by using the next program in a thermocycler: 1 cycle 22 ºC 5 min, 1 cycle 42 ºC 30 min and 1 cycle 85 ºC 5 min. cDNA samples were analyzed by RT-qPCR using Fast SYBR Green Master Mix or TaqMan Fast Advanced Master Mix (Applied Biosystems) and specific primers or probes (Appendix Table 1) following the next reaction mix: 5 µl of SYBR Mix or 12.5 µl of TaqMan buffer, 0.25 µl of Primer F and R or 1.25 µl of TaqMan probe, and 1 µl of cDNA (except for RIP method, in which we amplified 2 µl of cDNA), respectively. The plate was amplified in Step One Real-Time PCR system (Applied Biosystems).

5.5 EBER ISH

Formalin fixed, paraffin embedded (FFPE) biopsy specimens were cut and stained for EBER ISH using Leica Bond-MAX staining systems and reagents (Leica). EBV-positivity was defined as the majority of tumor cells being positive.

5.6 RNAscope for *EBNA1* mRNA

RNAscope is an ISH assay that uses a multiple probe pair design strategy to detect viral gene expression more sensitively than standard ISH. The method involves the hybridization of two independent probes (double Z probes) to the target sequence in tandem for signal amplification, which improves the signal-to-noise ratio. The assay uses a cascade of hybridization of a nucleic acid preamplifier followed by multiple amplifiers that serve as a substrate for the subsequent binding of chromogenic molecules to the numerous binding sites in each amplifier.

In this study, RNA ISH was performed on FFPE tissue sections using the RNAscope 2.0 HD Red Chromogenic Reagent Kit and V-EBV-EBNA1 target probe (Advanced Cell Diagnostics), following manufacturer's indications. Each sample was quality-controlled for RNA integrity with a probe specific to the housekeeping *PPIB* mRNA used as a positive control, as previously described (Mundo et al., 2020).

Briefly, FFPE tissue sections were baked, deparaffinized, and dehydrated. The tissues were then air-dried and treated with a peroxidase blocker before boiling in Target Retrieval Reagent solution. Protease Plus was then applied before hybridizing target probes for 2 hours at 40 °C, followed by a series of signal amplification steps, each separated by two washes. Signal detection was performed by hybridizing the FastRed probe mix on each sample and counterstaining the section with hematoxylin. RNA staining signals were identified as red punctate dots. Background staining was evaluated using a negative control probe specific for bacterial *dapB*; all lymphoma cases analyzed did not show any dots for *dapB* in any cells.

5.7 Protein extraction and western blot

For protein extraction, 3-5x10^6 growing cells were washed with PBS and lysed in RIPA Buffer (Sigma-Aldrich) with Protease and Phosphatase inhibitor cocktail (Thermo Fisher Scientific) for 20 minutes at 4 ºC. Lysates were obtained by centrifugation at 13000 rpm for 15 min, collecting the supernatant. Protein was quantified by Protein Assay (Bio Rad) in Sinergy HT spectrophotometer (BioTek) (λ595 nm) and 50-70 μg of total protein mixed with Sample Buffer 5X and DTT was used for western blot.

Protein extracts were separated by 6–9% SDS–PAGE, transferring them to a 0.45 μm nitrocellulose membrane. Membranes were blocked with 5% of milk powder, BSA or 2.5% of PhosphoBLOCKER (for detection of phosphorylated proteins) (Cell Biolabs) in TBS-T for 1 h and incubated overnight at 4 ºC with specific antibodies (Appendix Table 3). After incubation, membranes were washed 3 times with TBS-T and incubated 1 h with the corresponding secondary antibody (Appendix Table 3). After washing, the membrane was incubated with Pierce ECL reagent (Thermo Fisher Scientific) to detect the proteins

in ImageQuant LAS4000 (Fujifilm). Protein quantification was performed with MultiGauge Software (Fujifilm).

5.8 Immunofluorescence

DG75 ER and DG75 ER-SOX11 cells induced or not with 150 nM of 4-OHT for 24 hours were centrifuged at 1500 rpm for 5 minutes at room temperature. The pellet of $1x10^6$ cells was then resuspended in 0.5 ml of RPMI (supplemented with 10% FBS) and incubated for 30 minutes into a coverslip pre-treated with poly-L-lysine (Sigma-Aldrich). Then, cells were fixed with 4% of paraformaldehyde for 15 minutes at room temperature. Coverslips were washed twice with PBS and permeabilized for 20 minutes at room temperature with blocking solution (PBS with 5% FBS and 0.5% Triton), and incubated for 1 hour at room temperature with SOX11 primary antibody (Appendix Table 3). Cells were washed twice with PBS and incubated for 1 hour at room temperature with secondary antibody (Appendix Table 3). Coverslips were washed twice with PBS and once with MiliQ water, and then were dried. A minimal volume of Mounting Medium with DAPI (DUO82040) was added, and the edges of the coverslips were sealed with nail polish and stored at -20ºC protected from light until observation in Nikon Eclipse 50i microscope.

5.9 Immunohistochemistry

IHC of SOX11 for cases from Burkhardt and colleagues (Burkhardt et al., 2022) was performed on an automated stainer (Leica) by using a mouse monoclonal antibody (Appendix Table 3) and a pH 6 antigen retrieval solution, as previously described (Aukema et al., 2018; Croci et al., 2020).

6. MCL XENOGRAFT MICE MODELS

6.1 MSI2 knockdown in MCL xenograft mouse model

For the generation of MSICTLuc+ and MSI2KDLuc+ xenograft mice models, NSG mice (NOD.Cg-Prkdc^{scid}Il2rg^{tm1Wjl}/SzJ, Janvier LABS) were intravenously inoculated into their tail veins with 10x10^6 cells of Z138shCT-Luc and Z138sh5MSI2-Luc cells (5 mice per group). Mice were intraperitoneally injected with 112 mg/kg of D-Luciferin (tebu-bio) and anesthetized with isofluorane (Esteve). Tumor dissemination and growth was captured by luciferase bioimage (LBI) twice a week for 5 weeks. Bioluminiscence was captured 10 min after the injection of D-luciferin by IVIS Lumina III In Vivo Imaging System (PerkinElmer) and total flux (photons/s) from the tumoral cells was quantified using Living Image Software.

MSICT-Luc+ and MSI2KD-Luc+ MCL xenograft mice models were euthanized at 35 days post inoculation. Animals were euthanized according to institutional guidelines. Peripheral blood was collected with capillary action blood collection tubes (SAI Infusion Technologies) from tail vein. Spleens were obtained, photographed, weighed, homogenized and filtered through 70 μm nylon cell strainers (Fisher Scientific). Femur and tibias were extracted, cleaned of all connective tissues, and flushed with PBS and EDTA using a 27-gauge needle (Becton Dickinson). Bones were grinded with a mortar and filtered along with the bone marrow flushes by using a 70 μm nylon cell strainer. Erythrocytes from peripheral blood, spleens and bone marrow were lysed incubating samples with ACK buffer (Quality Biological) for 10 minutes. Samples were washed with PBS and the process was repeated until pellets remained white. Cells were filtered and resuspended in PBS to determine the percentage of MCL cells measuring GFP+ cells fluorescence by flow cytometry.

6.2 Ro 08-2750 therapy in MCL xenograft mouse model

For in vivo MSI2 inhibition experiments with Ro small molecule, 10x10^6 Z138shCT-Luc cells were pretreated with 1 μM of Ro or DMSO 0.005% for 1 hour and

were intravenously injected into NSG mice tail veins (5-6 mice per group). NSG mice were treated twice a week during 2 weeks for a total of 3 doses of Ro 13.75 mg/kg or DMSO solvent (5 mice per group), and twice a week during 3 weeks for a total of 5 doses of Ro 7 mg/kg or DMSO solvent (6 mice per group), both intraperitoneally injected. Tumor growth was monitored by LBI, mice of groups Ro 13.75 mg/kg or DMSO, and Ro 7 mg/kg or DMSO were euthanized at days 12 and 19, respectively, and MCL tumor engraftment was analyzed as explained in "6.1 MSI2 knockdown in MCL xenograft mouse model" from the methods section.

7. STATISTICAL ANALYSIS

7.1 Gene set enrichment analysis

For GSEA, C2 curated gene sets from the Molecular Signatures Database were used in gene expression profiling data. Additionally, several gene sets derived from differential expression analysis in RNA-seq data (Z138 treated with Ro 08-2750 vs Z138 treated with DMSO, cMCL vs nnMCL, Z138 SOX11KO vs Z138 CT) were generated for GSEA.

GSEA was performed on preprocessed microarray data by fRMA (GSE79196) or RMA (EGAD00010001842), and in variance stabilized expression matrices from RNA-seq data with GSEA v2.2.4 or v4.0.3. For the analyses, data was randomized by 1000 permutations phenotype (datasets with >7 samples per phenotype) or gene_set (datasets with <7 samples per phenotype). For microarray data, probes were collapsed to Gene Symbol using Max-probe. The metric for ranking genes was Diff_of_Classes, which uses the difference of class means to calculate fold change for log scale data. Gene sets with <15 and >500 genes were filtered out. Enrichment of gene sets in the two corresponding phenotype labels was considered at P-value <0.05 and FDR <0.2.

7.2 FIMO analysis

FIMO analysis (https://meme-suite.org/meme/doc/fimo.html) was done using the sequence from the 4 SOX11+ MCL specific ATAC-seq peaks found and SOX family

consensus binding motifs from JASPAR CORE vertebrates database (Fornes et al., 2020). ATAC-seq peaks regions: ATAC_peak_1: chr17: 57,440,795-57,441,325; ATAC_peak_2: chr17: 57,463,187-57,463,603; ATAC_peak_3: chr17: 57,499,225-57,500,470; ATAC_peak_4: chr17: 57,525,240-57,527,912.

7.3 SOX11 motif enrichment analysis

PMWScan (https://ccg.epfl.ch/pwmtools/pwmscan.php) was used to scan SOX11 human motif from Hocomoco v11 collection (Kulakovskiy et al., 2018) through the human genome (GRCh38/hg38) obtaining SOX11 binding motifs. UCSC Genome browser (https://genome.ucsc.edu/) was used to display SOX11 binding motifs in *MSI2* locus.

7.4 Pathway over-representation analysis

For pathway over-representation analysis, we used two different softwares, DAVID Functional Annotation Tool (https://david.ncifcrf.gov/home.jsp) and PANTHER (http://www.pantherdb.org/). For DAVID, list of differentially expressed genes (in ENSMBL identifier) was used to find statistically significant (p value < 0.05) over-represented pathways from KEGG PATHWAY and BioCarta databases, and biological processes from Gene Ontology project. For PANTHER, list of differentially expressed genes (in Gene Symbol identifier) was used to find statistically significant (p value < 0.05) over-representated pathways from PANTHER database.

7.5 Statistics

Normal distribution and variances were tested with Shapiro-Wilk and Levene tests, respectively. Differences between continuous variables in more than two groups were tested with ANOVA (variables with normal distribution and equal variance) or Kruskal-Wallis (variables without normal distribution and/or different variances) methods. To compare continuous variables between two groups, unpaired two-tailed Student t-test (normal distribution) or Wilcoxon test (non-parametric test) were done. For analysis in MCL primary samples before and after treatment with Ro 08-2750, a paired

one-tailed Student t-test was done. Welch's correction was applied to compare samples with different variances. To compare categorical variables between groups, Fisher test was performed, and pairwise comparisons were applied when needed. For correlation between continuous variables, Pearson correlation was used. Overall survival calculated from time of sampling was used for Kaplan-Meier curves, and log-rank test was performed to measure the association of overall survival with categorical variables. Maximally selected rank statistics were applied to obtain cutoffs of continuous variables for Kaplan Meier curves (maxstat R package 0.7-25). For univariate and bivariate analysis, Cox regression was used to evaluate the prognostic value of the variables. P-values were adjusted with the Benjamini and Hochberg method or FDR, correcting for multiple testing. Ro EC50 was obtained fitting the dose-response curve with non-linear regression methods (log(agonist) vs. response - Variable slope). Statistical tests were performed using R statistical software (version 3.6.9) or GraphPad Prism 5 software.

8. OTHER TECHNIQUES

8.1 Colony assay

For colony assay, 500 growing cells were mixed with 1 ml of Human Methylcellulose Complete Media (R&D System) and plated in a 24-well plate for triplicated. For in vitro MSI2 inhibition experiments, cells were treated with Ro 08-2750 or 0.05% DMSO, before mixing them with Methylcellulose media. Two weeks later, number of colonies formed were counted (1 colony >50 cells). One week later, the Cytation 5 Imaging Reader (BioTek) was used to obtain bright field images of the colonies stitching 88 images.

8.2 Luciferase assay

MSI2 promoter region (chr17:57,257,388-57,257,837) was amplified by PCR using specific primers (Appendix Table 1) and cloned in pGL4.23 plasmid containing luciferase reporter gene. Reporter constructs in cotransfection with SOX11 full-length (pcDNA3-HA-SOX11) or the truncated SOX11 protein (pcDNA3-HA-SOX11ΔHMG)

expression vectors were used for luciferase assay experiments in HEK-293T cells, performed as previously described (Vegliante et al., 2013).

8.3 Cytotoxicity assay

MCL cells were plated into 96-well plate at $5x10^4$/well density and treated with increasing concentrations of Ro (1:2-1:10 serial dilutions up to 100 µM, in quadruplicated) for 24 hours. Cells were incubated with 10 µl of 12 mM MTT (Invitrogen) during 2-3 hours. Formazan crystals were solubilized with 100 µl of Isopropanol:HCl 1M (24:1). Absorbance was quantified in a Sinergy HT spectrophotometer, measuring at λ570 and λ655. Relative viability was calculated with the next formula:

$$\text{Viability (\%)} = \frac{(\text{Abs570} - \text{Abs570 RPMI}) - (\text{Abs655} - \text{Abs655 RPMI}) \text{ with Ro}}{(\text{Abs570} - \text{Abs570 RPMI}) - (\text{Abs655} - \text{Abs655 RPMI}) \text{ without Ro}}$$

8.4 Adhesion assay to VCAM-1

Untreated wells of a 96-well microplate were coated with 500 ng/ml of VCAM-1 or with BSA 0.5% in RPMI medium overnight at 4ºC. Next day, BL cells (SOX11-overexpressing and control DG75 (induced with 150 nM of 4-OHT during 24h) and Ramos cells) were stained with 1 µM of Calcein AM Viability dye (eBioscience) for 30 minutes. Then, cells were centrifuged and $2x10^5$ BL cells were plated in wells coated with VCAM-1 or BSA 0.5% and incubated during 1 hour. After incubation, wells were gently washed three times with PBS and cells were incubated in 50 µl of RPMI + 50 µl of Triton 2% for 30 minutes. Finally, cells were transferred to a black 96-well microplate and fluorescence emitted by calcein (λ535 nm) was measured in Sinergy HT spectrophotometer. Relative adhesion was measured as the calcein emitted fluorescence by cells coated with VCAM-1 divided by the fluorescence emitted by calcein-labelled cells adhered in an unspecific way to the well (with BSA 0.5%).

8.5 BCR stimulation

BL cells (SOX11-expressing DG75 [after 24 hours of 4-OHT 150 nM induction] and Ramos, and their controls) were cultured during 90 minutes in RPMI supplemented

with 0.5% FBS, to induce cell starving. Then, $1x10^6$/ml of cells were stimulated with 10 µg/ml of Goat $F(ab')_2$ anti-human IgM (Southern Biotech). Cells were centrifuged at 0 and 15 minutes of induction and protein extraction was performed to do western blot analysis of pSYK protein (Appendix Table 3).

STUDY 1

Deciphering the role of Musashi-2 as a regulator of stem-like properties in aggressive mantle cell lymphoma

The results of this study have been published:

Sureda-Gómez M, Balsas P, Rodríguez ML, Nadeu F, De Bolòs A, Eguileor Á, Kulis M, Castellano G, López C, Giné E, Demajo S, Jares P, Martín-Subero JI, Beà S, Campo E, Amador V. Tumorigenic role of Musashi-2 in aggressive mantle cell lymphoma. Leukemia. 2023 Feb;37(2):408-421.

1. INTRODUCTION

MCL is a highly aggressive type of mature B cell cancer that is driven by a specific genetic abnormality, the t(11;14) oncogenic event. MCL can be classified into two subtypes based on clinical, biological, and molecular features: cMCL and nnMCL. Patients with cMCL have lymph node involvement, short responses to current therapies, a higher risk of relapse and adverse outcomes. On the other hand, nnMCL is characterized by peripheral blood involvement without lymph node enlargement, longer survival, and often no need for treatment for long periods. cMCL arises from naive-like B cells, while nnMCL develops from more differentiated memory-like B cells that have undergone germinal center experience.

Although MCL initially responds to treatment, it often develops resistance and becomes more aggressive upon relapse. Tumor chemoresistance is partly attributed to the presence of CSC in some tumors. Several studies have identified MCL-CSCs with self-renewal capacity, ALDH activity, clonogenicity, increased tumorigenicity in vivo and resistance to standard therapies, which could explain why MCL remains an incurable lymphoma despite achieving complete remission.

SOX11 is a SOX family member that is overexpressed in cMCL but negative or weakly expressed in nnMCL. SOX11 plays an oncogenic role in MCL. SOX family members regulate the proliferation and differentiation of stem and progenitor cells. For example, SOX2 is essential for embryonic development as it is required for the pluripotency maintenance of ESCs. Along with OCT4 and NANOG, SOX2 acts as a master regulator of stemness, collaborating to bind to DNA and recruit other factors critical for gene activation. SOX proteins are also important in controlling cell fate and differentiation decisions. Indeed, SOX proteins act as pioneer factors that occupy and maintain target genes in a silenced state until they are ready to be activated by other SOX proteins during subsequent stages of differentiation. In particular, SOX11 plays an important role in neuronal development. In addition, SOX11 is expressed in several progenitor and stem cells, indicating its potential involvement in stemness. SOX11 is also

expressed in the CSC population of oligodendrogliomas, and promotes CSC properties, increasing ALDH activity, mammosphere formation, and drug resistance, in mammary cells. However, the stemness role of SOX11 in MCL remains unknown.

In this first study, we have searched for stem cell-related genes in MCL and their possible relationship to SOX11 expression and contribution to MCL oncogenic and clinical evolution. We have identified MSI2 as a stem cell-related gene orchestrating chemoresistance, tumor survival and self-renewal in aggressive MCL.

2. RESULTS

2.1 Enrichment of stem cell-related gene signatures in SOX11+ MCL primary cases

To study the possible relationship between SOX11 transcription factor and stemness features in MCL, we analyzed differences in the expression of stem cell-related gene signatures between 30 SOX11+ and 24 SOX11- leukemic MCL primary cases (GSE79196), by GSEA. We observed that SOX11+ MCL primary cases were enriched in genes upregulated in hematopoietic and leukemic stem cells (LSCs), and in genes directly regulated by NANOG, OCT4 and SOX2 (NOS) pluripotent transcription factors, among other gene signatures, compared to SOX11- MCLs (Figure 32A, Appendix Table 4). The gene expression profile of an independent cohort from leukemic and lymph node samples (26 SOX11+ and 13 SOX11-) (EGAD00010001842), obtained by microarray, was used to validate the enrichment of HSC, LSC and NOS gene sets in SOX11+ MCLs (Figure 32B). Besides, we performed RNA-seq of 16 samples from both cohorts (10 SOX11+ and 6 SOX11-) that confirmed the enrichment of stem cell related gene sets in SOX11+ MCLs (Figure 32C). This result suggests that SOX11 may be regulating stem cell-related gene signatures.

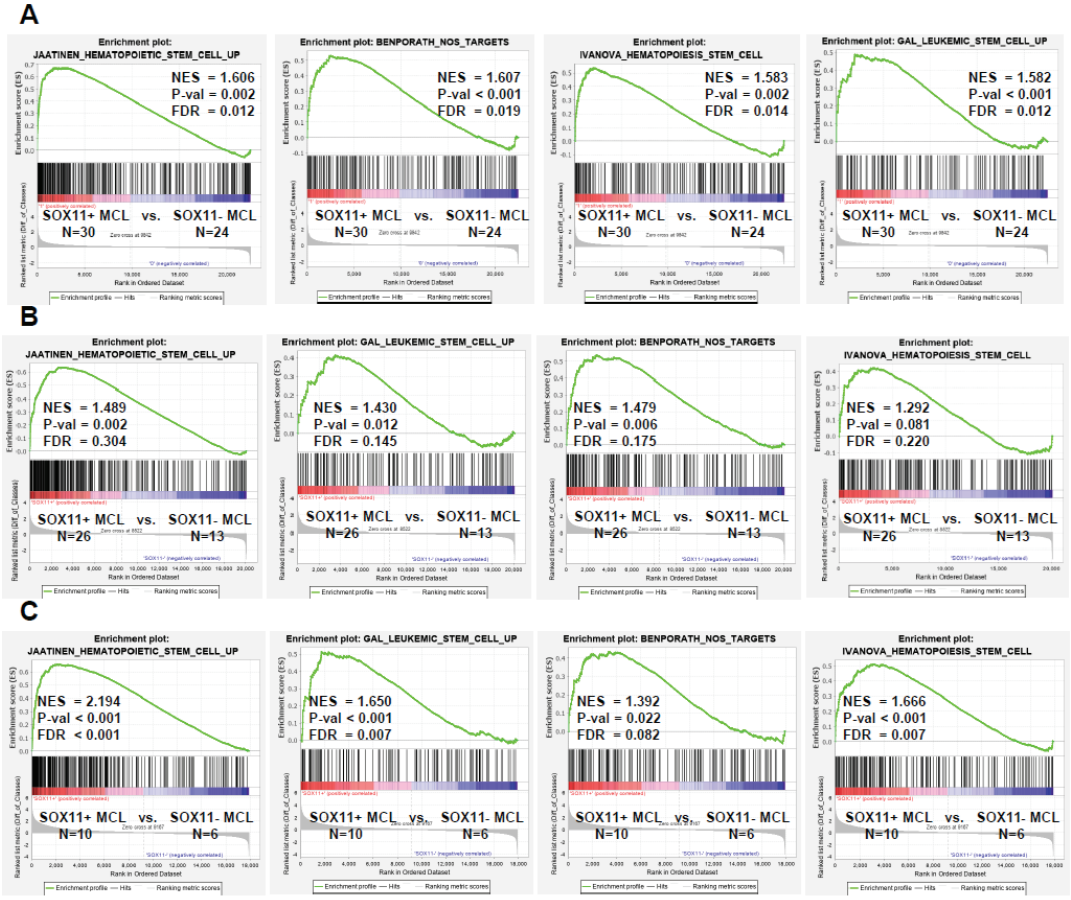

Figure 32. Up-regulation of genes associated to stem cells in SOX11+ compared to SOX11- MCL primary cases. Enrichment plots obtained by GSEA using gene expression profile microarray data from 30 SOX11+ and 24 SOX11- (GSE79196) **(A)** and from 26 SOX11+ and 13 SOX11- (EGAD00010001842) **(B)**, and RNA-seq data from 10 SOX11+ and 6 SOX11- **(C)** MCL primary tumors, showing significant enrichment of HSCs, LSCs and NOS (pluripotent transcription factors NANOG, OCT4 and SOX2) target gene sets in SOX11+. Normalized enrichment score (NES), P-value (P-val) and false discovery rate (FDR) are shown.

Then, we used the genes differentially upregulated in SOX11+ MCLs from the gene signatures of Figure 32A in order to search for MCL cases expressing high values of this specific stem cell-related gene signature. Whereas SOX11- group had uniformly low expression of the stem cell-related gene signature (Cluster 3), we found two well differentiated clusters in the SOX11+ group, one (Cluster 1) expressing higher values than the other (Cluster 2) (Figure 33A-B). We compared the overall survival of these three clusters to assess the clinical impact of this stem cell-related signature in our MCL cohort using gene expression (GSE79196) and available clinical data of some patients. No

differences in overall survival between Clusters 2 and 3 were found (Figure 33C), suggesting that this gene signature had no clinical impact in SOX11+ MCLs, while Cluster 1 (all SOX11- MCL cases) showed higher overall survival than the others due to the indolent disease of nnMCL/SOX11- patients. This result led us to focus on genes that had a validated function on stemness rather than signatures overexpressed in stem cell populations.

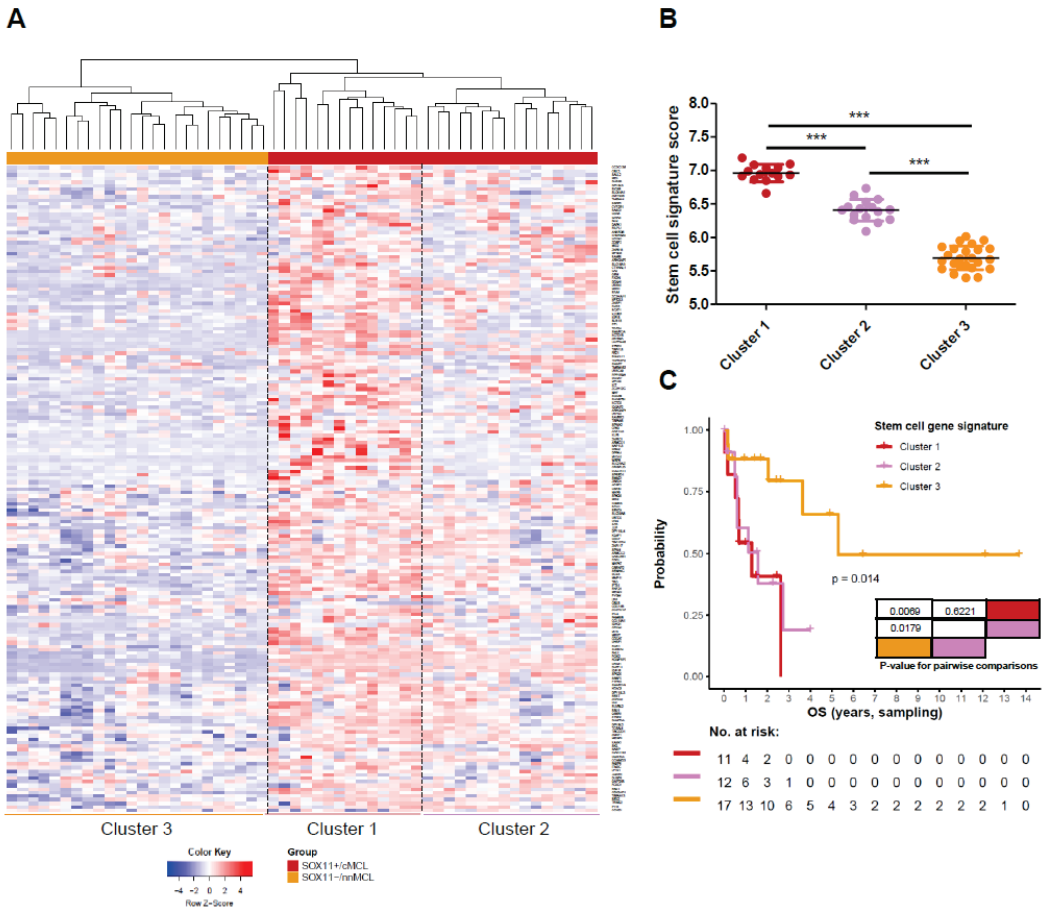

Figure 33. Stem cell-related gene signature in MCL patients. (A) Scaled expression of 181 upregulated genes (the probe with higher interquartile range for each gene was used) from the top 4 gene sets related to stem cells enriched in SOX11+ vs. SOX11- MCL primary cases (GSE79196), showed in Figure 32A. Dashed line separates the three clusters, highlighted below the heatmap. **(B)** Stem cell-related gene signature score (mean of the 181 genes showed in Figure 33A) in the three different clusters obtained from Figure 33A. Statistical significance was obtained by unpaired two-tailed Student t-test: *** P value < 0.001. **(C)** Kaplan-Meier curve showing overall survival (OS) in the three MCL clusters. The P-value of log-rank test (p), the risk table (No. at risk) and the p value for pairwise comparisons are shown.

2.2 MSI2 stem cell gene is upregulated in SOX11+ MCL primary cases and associates with poor survival in MCL

To identify specific genes involved in stem cell features directly regulated by SOX11, we overlapped the list of genes differentially expressed between SOX11+ and SOX11- MCL primary cases (GSE79196) (DEG SOX11+ vs SOX11-, Appendix Table 5) with genes directly regulated by SOX11 in MCL by chromatin immunoprecipitation on chip (GSE35021) (ChIP-chip, SOX11-bound genes), and genes with a validated stemness function by the Gene Ontology project (GO stem cell-related genes, Appendix Table 6). The Venn diagram showed that of the 816 genes differentially expressed between SOX11+ and SOX11- MCL cases, 22 genes were related to stemness functions, and 74 overlapped with SOX11-bound genes (Figure 34A). Besides, approximately 3% (57 genes) of the SOX11 target genes were considered stem cell-related genes, but only 4 genes (*PROX1*, *PRDM15*, *MSI2* and *SOX5*) overlapped with the differential expressed genes between SOX11+ and SOX11- MCLs (Figure 34A). Out of these 4 genes, *PROX1*, *PRDM15* and *MSI2* were significantly upregulated, and *SOX5* downregulated, in SOX11+ MCLs (Figure 34B). Significant differences in *PROX1*, *MSI2* and *SOX5* mRNA levels between SOX11+ and SOX11- MCLs were found in our MCL validation cohorts, by microarray and RNA-seq (Figure 34C-D, respectively).

Then, we generated SOX11 knockout (Z138-SOX11KO) and overexpressing (JVM2-SOX11+) (Balsas et al., 2017) MCL cell lines transducing a SOX11+ and a SOX11- cell line, respectively, and performed RNA-seq. As observed in SOX11+ MCL cases, GSEA showed an enrichment of NOS targets and/or HSC gene signatures in SOX11+ (Z138CT and JVM2-SOX11+) compared to their respective SOX11- MCL cell lines (Z138-SOX11KO and JVM2CT) (Figure 35A). This result reinforces the idea that SOX11 may regulate stem cell features in MCL.

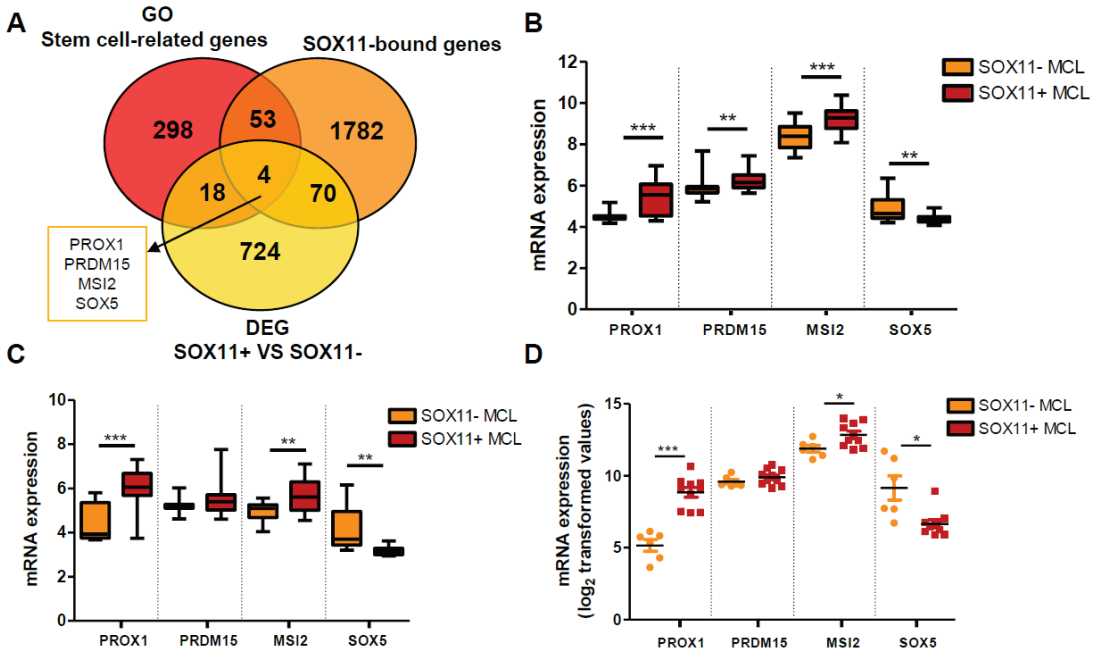

Figure 34. SOX11 target genes differentially expressed between SOX11+ and SOX11- MCLs and related to stemness functions. (A) Venn diagram illustrating the overlap between genes whose gene ontology biological process definition is related to stem cells (GO stem cell-related genes) (red circle, 373 genes; see Appendix Table 6), SOX11-bound genes (GSE35021) (orange circle, 1909 genes found by SOX11-specific ChIP-chip in MCL cell lines) and differential expressed genes (DEG) between SOX11+ and SOX11- MCL primary cases (GSE79196) (yellow circle, 747 genes with adjusted P-value <0.05 and absolute log2 fold change >0.7; see Appendix Table 5). **(B-D)** mRNA expression levels of *PROX1*, *PRDM15*, *MSI2* and *SOX5* in 30 SOX11+ and 24 SOX11- (GSE79196) **(B)** and in an independent cohort of 26 SOX11+ and 13 SOX11- (EGAD00010001842) **(C)** MCL microarrays, validated in 10 SOX11+ and 6 SOX11- MCL cases by RNA-seq **(D)**. The significance of difference was determined by unpaired two-tailed Student t-test (Welch's correction was applied to compare samples with different variances): * P-value <0.05, ** P-value <0.01, *** P-value <0.001.

Interestingly, SOX11 target genes related to stemness functions found previously in Figure 34 (*PROX1*, *PRDM15*, *MSI2* and *SOX5*) were also differentially expressed upon SOX11 knockout or overexpression in MCL cell lines compared to their respective controls (Figure 35B).

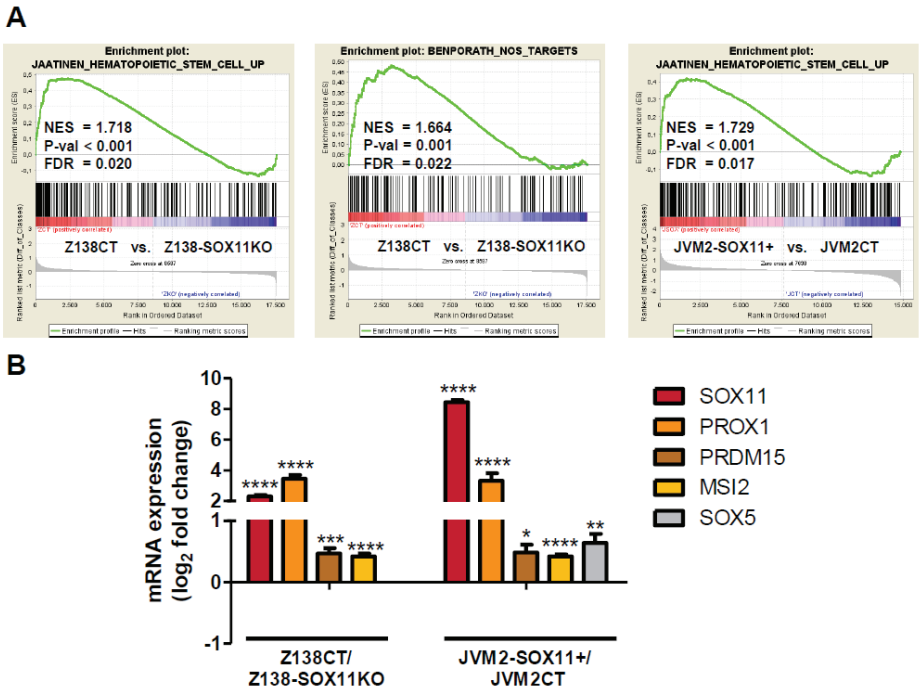

Figure 35. SOX11 expression in MCL cell lines associates to increased enrichment in stem cell-related gene signatures. (A) GSEA using RNA-seq data from Z138CT vs Z138-SOX11KO, and JVM2CT vs JVM2-SOX11+ cell lines on HSC-related gene sets and NOS (pluripotent transcription factors NANOG, OCT4 and SOX2)-target genes. Normalized enrichment score (NES), P-value (P-val) and false discovery rate (FDR) are shown. **(B)** *SOX11*, *PROX1*, *PRDM15*, *MSI2* and *SOX5* mRNA expression in $\log_2$ fold change between Z138CT and Z138-SOX11KO, or JVM2-SOX11+ and JVM2CT MCL cell lines, from RNA-seq data (3 samples per group). Statistical significance is determined by Wald test: * P-value <0.05, ** P-value <0.01, *** P-value <0.001, **** P-value <0.0001.

This result encouraged us to analyze if the upregulation or downregulation of these 4 genes was translating into a clinical impact in our initial MCL cohort with gene expression and clinical data. High *MSI2* and low *PRDM15* and *SOX5* mRNA levels were significantly associated with shorter overall survival of patients. Nonetheless, no association between *PROX1* expression and overall survival was found (Figure 36). In bivariate COX regression analyses, *MSI2* mRNA levels but not *PRDM15* or *SOX5* levels had an overall survival prognostic value independent of common high-risk prognostic MCL factors, such as SOX11 expression, high CNA, and 17p/*TP53* and 9p/*CDKN2A* alterations (Appendix Table 7). All these results suggest that MSI2 might be a prognostic factor with a tumorigenic role in aggressive MCL.

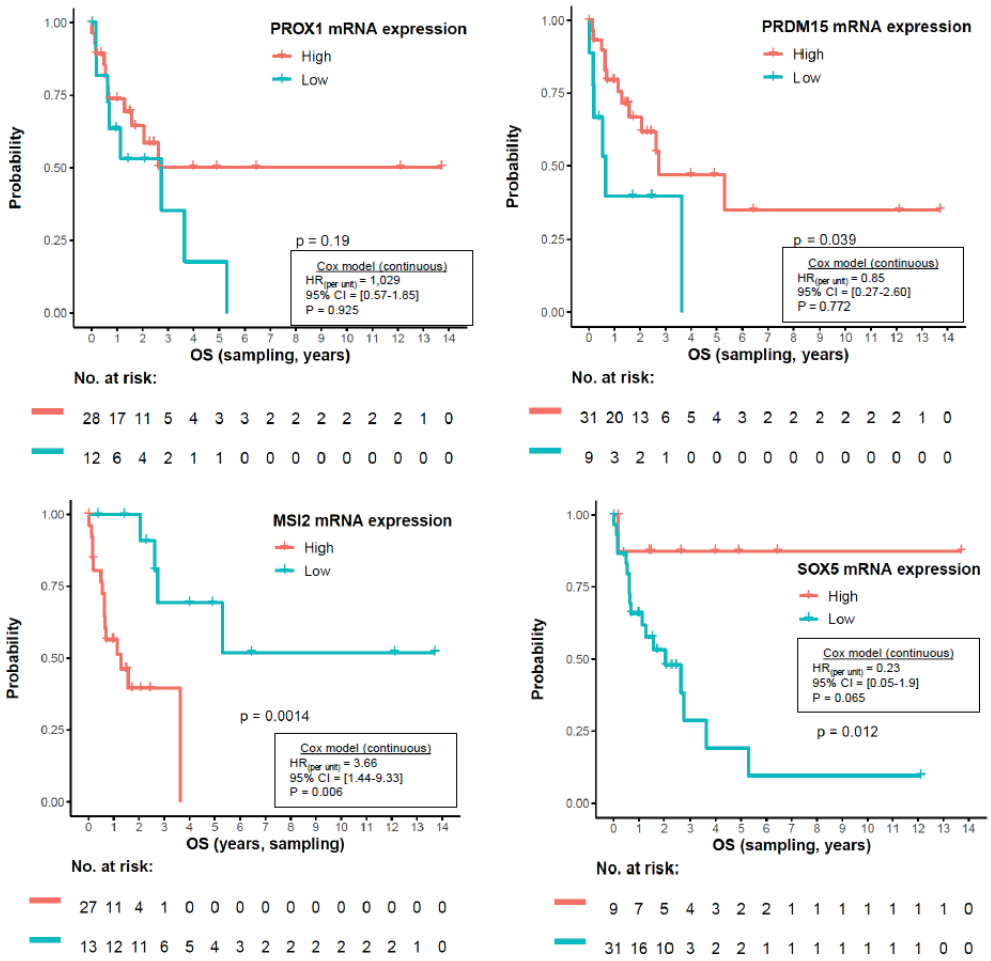

Figure 36. Clinical impact of SOX11 target genes related to stem cell functions in MCL patients. Kaplan-Meier curves showing the association of *PROX1*, *PRDM15*, *MSI2* or *SOX5* mRNA expression and overall survival (OS, in years) calculated from date of sampling in 40 MCL primary cases (GSE79196). High and low values were defined by maximally selected rank statistics (cutoff = 4.48, 5.794, 8.45 and 4.731, respectively). The P-value of log-rank test (p), the risk table (No. at risk), the hazard ratio (HR) with 95% confidence interval (CI) and Cox regression P value (P) are shown.

2.3 SOX11 upregulates MSI2 gene by direct binding to its promoter in MCL

In order to validate the *MSI2* direct regulation by SOX11 found previously by ChIP-chip and ChIP-qPCR (Vegliante et al., 2013), we examined MSI2 levels in our SOX11 knockout and overexpression MCL cell line models and observed a decrease and an increase, respectively, compared to their control cells (Figure 37A). RNA-seq data also confirmed the differences in *MSI2* expression (Figure 37B). Besides, MSI2 protein and

mRNA levels were recovered upon SOX11 ectopic overexpression in Z138-SOX11KO cell line (Z138-SOX11KO SOX11+) (Figure 37C and D, respectively), demonstrating the implication of SOX11 in the upregulation of MSI2 in MCL cells.

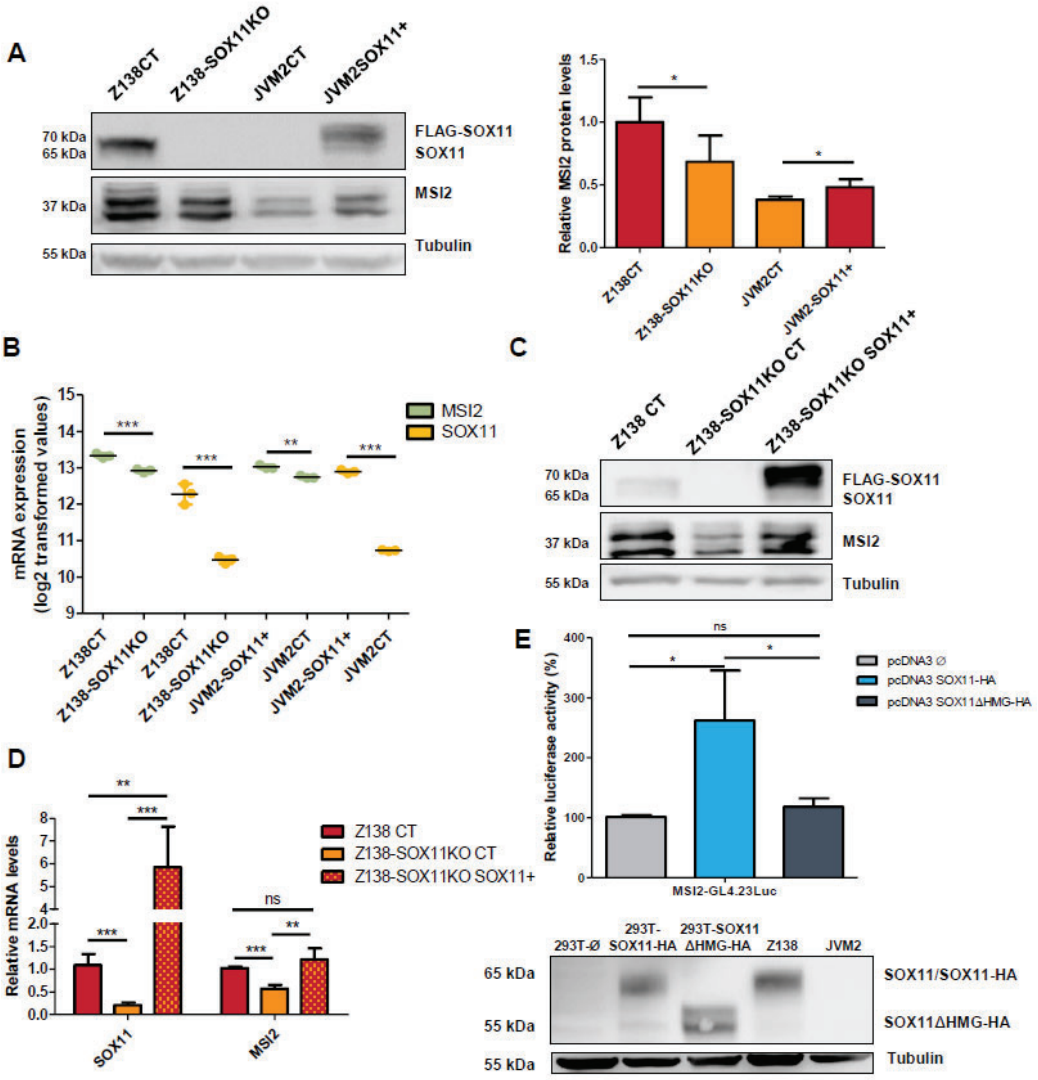

Figure 37. Direct modulation of MSI2 levels by SOX11 expression in MCL. (A) (Left) MSI2 and SOX11 levels in Z138-SOX11KO, Z138CT, JVM2CT and JVM2-SOX11+ MCL cell lines. Tubulin was used as loading control. **(Right)** Quantification of MSI2 levels normalized with tubulin and relative to Z138CT in 5 independent experiments. **(B)** *MSI2* and *SOX11* expression (log_2-transformed values) in Z138CT, Z138-SOX11KO, JVM2CT and JVM2-SOX11+ MCL cell lines, using RNA-seq data. **(C-D)** SOX11 and MSI2 protein **(C)** and mRNA **(D)** levels in Z138 WT, -SOX11KO CT and -SOX11KO SOX11+ (overexpression FLAG-tagged SOX11 protein) MCL cell lines. Tubulin was used as loading control for western blot, and *GUSB* to normalize mRNA expression in qRT-PCR. mRNA levels are relative to Z138CT and are represented as the

mean ± standard deviation of 3 independent experiments. **(E) (Top)** Luciferase assay in transient co-transfections of *MSI2* promoter region-GL4.23 Luc with SOX11 full-length (pcDNA3 SOX11-HA) or the truncated protein (pcDNA3 SOX11ΔHMG-HA) in HEK-293T cell line. Results are shown as fold induction percentage referred to empty vector (pcDNA3ϕ) in 3 independent experiments. **(Bottom)** SOX11 levels in HEK-293T pcDNA3ϕ, SOX11-HA and SOX11ΔHMG-HA cells after 48 h of transfection, and in Z138 and JVM2. Tubulin was used as loading control. The significance of differences was determined by unpaired two-tailed Student t-test: * P-value <0.05, ** P-value <0.01, *** P-value < 0.001, ns = not significant.

To corroborate that MSI2 expression changes were due to a direct binding of SOX11 to *MSI2*, we performed luciferase assays in 293T cells. Luciferase activity was observed only when the *MSI2* promoter cloned in front of a minimal luciferase reporter was transiently co-transfected with a vector expressing SOX11-HA full-length protein, but not with SOX11 lacking the HMG domain (SOX11ΔHMG-HA) (Figure 37E).

Taken together, these results indicate that SOX11 directly activates *MSI2* transcription through binding to its promoter.

2.4 MSI2 intronic superenhancers associate with MSI2 upregulation and SOX11 expression in MCL

To have a more comprehensive understanding of the mechanisms underlying MSI2 upregulation, we analyzed the epigenetic profile of the *MSI2* locus using multiple data generated in two SOX11+ and three SOX11- MCL primary samples, Z138 (SOX11+) and JVM2 (SOX11-) MCL cell lines, and naïve (NBC) and memory B-cells (MBC), including chromatin states, ATAC-seq, DNA methylation and RNA-seq data. *MSI2* promoter showed open chromatin and active histone marks in normal B cells as well as in both MCL subtypes (Figure 38A, black dashed rectangle). Besides, some intronic regions of *MSI2* locus had marks of weak enhancer in normal B cells (Figure 38A, chromatin states). Intriguingly, these regions were remodeled to a strong enhancer state exclusively in SOX11+/cMCL primary cases and cell line, but not in SOX11-/nnMCLs (Figure 38A-B). The strong enhancer regions present in SOX11+/cMCL subtype were also associated to higher chromatin accessibility, lower DNA methylation and increased mRNA expression, compared to SOX11-/nnMCLs and normal B cells (Figure 38A,

ATAC-seq, DNA methylation and RNA-seq negative strand). In fact, we observed four ATAC-seq peaks SOX11+/cMCL-specific inside *MSI2* intron 6 (Figure 38A, red rectangles).

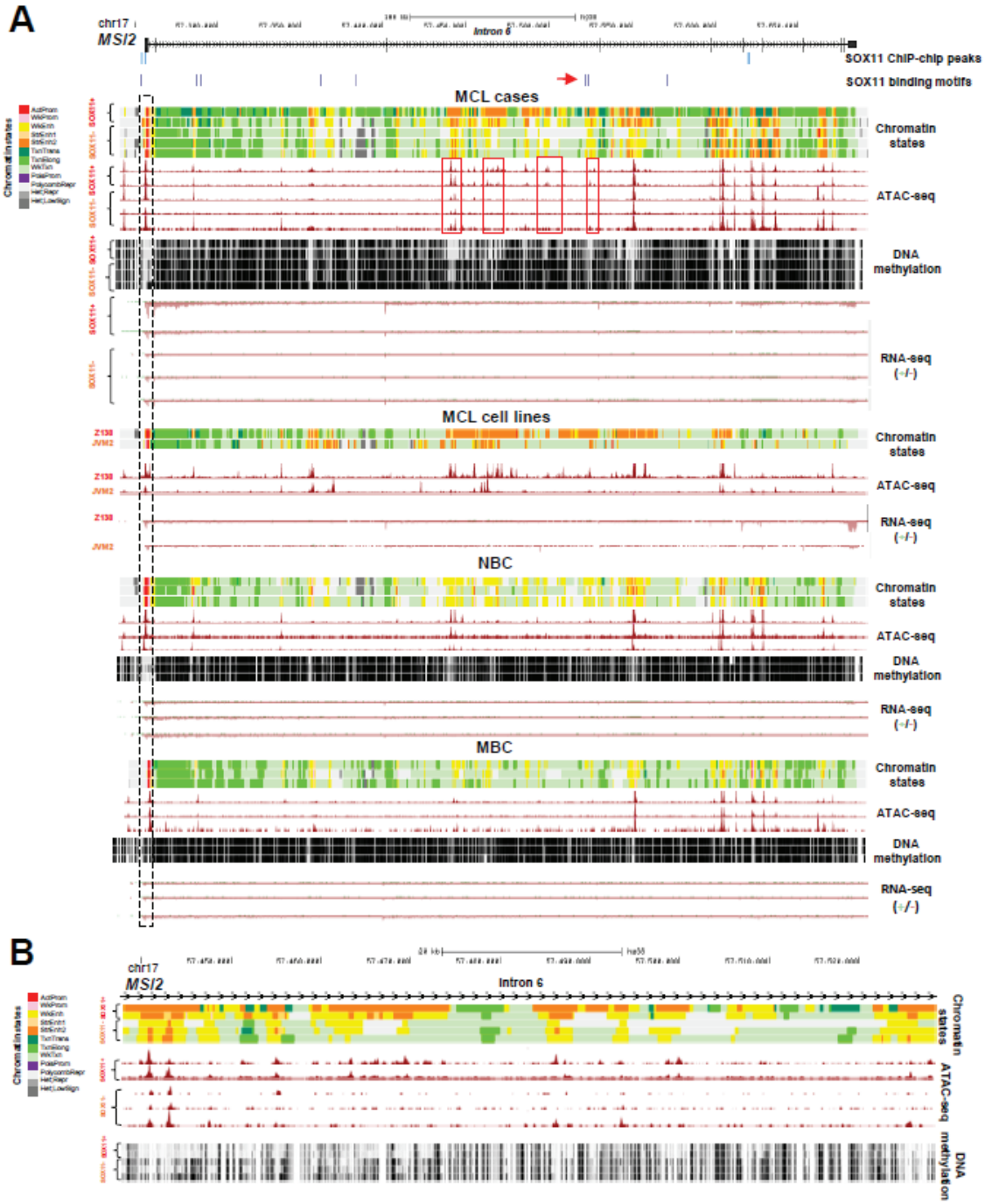

Figure 38. *MSI2* upregulation is associated with *MSI2* intronic superenhancers in SOX11+/cMCLs. (A) Multiple epigenetic layers of *MSI2* gene region (GRCh38/hg38 version,

chr17:57,240,242-57,691,985) and gene expression in MCL primary cases (2 SOX11+ and 3 SOX11-), MCL cell lines (Z138 and JVM2), naïve (NBC) and memory B-cells (MBC), generated in the BLUEPRINT consortium. Data includes different histone modification marks (H3K4me3, H3K27ac, H3K4me1, H3K36me3, H3K9me3, H3K27me3) by ChIP-seq, used to generate the chromatin states, chromatin accessibility by ATAC-seq, DNA methylation by whole-genome bisulfite sequencing and gene expression by RNA-seq. SOX11 binding motifs were obtained with PWMScan, using SOX11 human motif from Hocomoco v11 Human TF Collection, and two of the motifs found are highlighted with a red arrow. SOX11 binding regions (SOX11 ChIP-chip peaks) were obtained by SOX11-specific ChIP-chip experiment in MCL cell lines (GSE35021). Chromatin states indicated by different colors (upper-left legend), ATAC-seq (signal from 0 to 40), DNA methylation (signal from 0 to 1) and RNA-seq (signal for positive strand from 0 to 5 and for negative strand from -5 to 0) are shown. Promoter region is underlined with a black dashed rectangle. Specific SOX11+ MCL ATAC-seq peaks are highlighted with red rectangles. **(B)** Maximization of region chr17:57,438,165-57,527,952 (GRCh38/hg38 version) showing enhancer regions, ATAC-seq peaks (signal from 0 to 40) and DNA methylation (signal from 0 to 1) on *MSI2* intron 6 in 2 SOX11+ and 3 SOX11- MCL cases. Chromatin states are indicated by different colors (legend).

To further investigate the *MSI2* regulation by SOX11, we first explored the possibility that SOX11 could bind to these strong enhancer regions by searching for SOX11 consensus binding sites and SOX11 specific ChIP-chip peaks, previously obtained in MCL cell lines (Vegliante et al., 2013). We found a SOX11 binding motif in the promoter region, near to several peaks obtained by ChIP-chip (Figure 38A, SOX11 ChIP-chip peaks and SOX11 binding motifs). Although we could not detect SOX11 ChIP-chip peaks in the intron 6-7 region due to the absence of probes in the ChIP microarray, we observed some SOX11 binding motifs in these regions (Figure 38A, red arrow).

Secondly, we carried out FIMO analysis in SOX11+/cMCL-specific ATAC-seq peaks by using SOX family binding motifs (Appendix Table 8). We identified several matches to SOX factors, including SOX13, SOX12 or SOX2, in specific peaks, especially in ATAC-seq peak 4 (Appendix Table 9), in which we also observed SOX11 binding motifs (Figure 38A, red arrow).

These data support that *MSI2* expression may be regulated by epigenetic remodeling and suggest that SOX11 may play a role in this process.

2.5 MSI2 downregulation changes the gene expression profile of MCL cell lines

MSI2 is an RBP with a validated oncogenic function in several tumors, required for the maintenance of LSCs and the initiation of myeloid leukemias (Kharas et al., 2010; Ito et al., 2010; S. M. Park et al., 2015; S. Wang et al., 2015; Taggart et al., 2016). To elucidate the role of MSI2 in MCL, we first silenced MSI2 in Z138 MCL cell line. Three shRNA (sh2MSI2, sh4MSI2 and sh5MSI2) achieved efficient MSI2 silencing, showing reduced MSI2 protein levels compared to control cell lines (shCT), transduced with scramble-shRNA lentiviral particles (Figure 39A).

Then, we analyzed the gene expression profile of MSI2-knockdown and control cell lines by RNA-seq. We initially explored the intra- and inter-group variation by principal component analysis (PCA). The PCA showed that the gene expression of MSI2-knockdown samples differed from control samples (Figure 39B). However, the second principal component divided in two clusters the Z138shMSI2 samples, displaying differences between Z138sh2MSI2 and all other knockdown samples. This result forced us to discard the Z138sh2MSI2 samples for further analysis. We next performed differential expression analysis and found 277 upregulated and 124 downregulated genes in MSI2-knockdown compared to control cells (Figure 39C-D, Appendix Table 10).

Functional annotation analysis showed that genes downregulated upon MSI2 knockdown (upregulated by MSI2) were involved in cell cycle, DNA damage response, cancer and developmental pathways (Wnt and Notch signaling pathways), and pluripotency of stem cells (Figure 40A). On the other hand, genes upregulated upon MSI2 knockdown (downregulated by MSI2) were mainly related to cell death processes and mitochondrial activity. In agreement with these results, GSEA showed that the gene expression profile of MSI2-silenced cell lines (Z138MSI2KD) was enriched in apoptosis-related pathways, and genes downregulated in HSCs, while MSI2 control cells (Z138CT) in genes upregulated in HSCs (Figure 40B, Appendix Table 11).

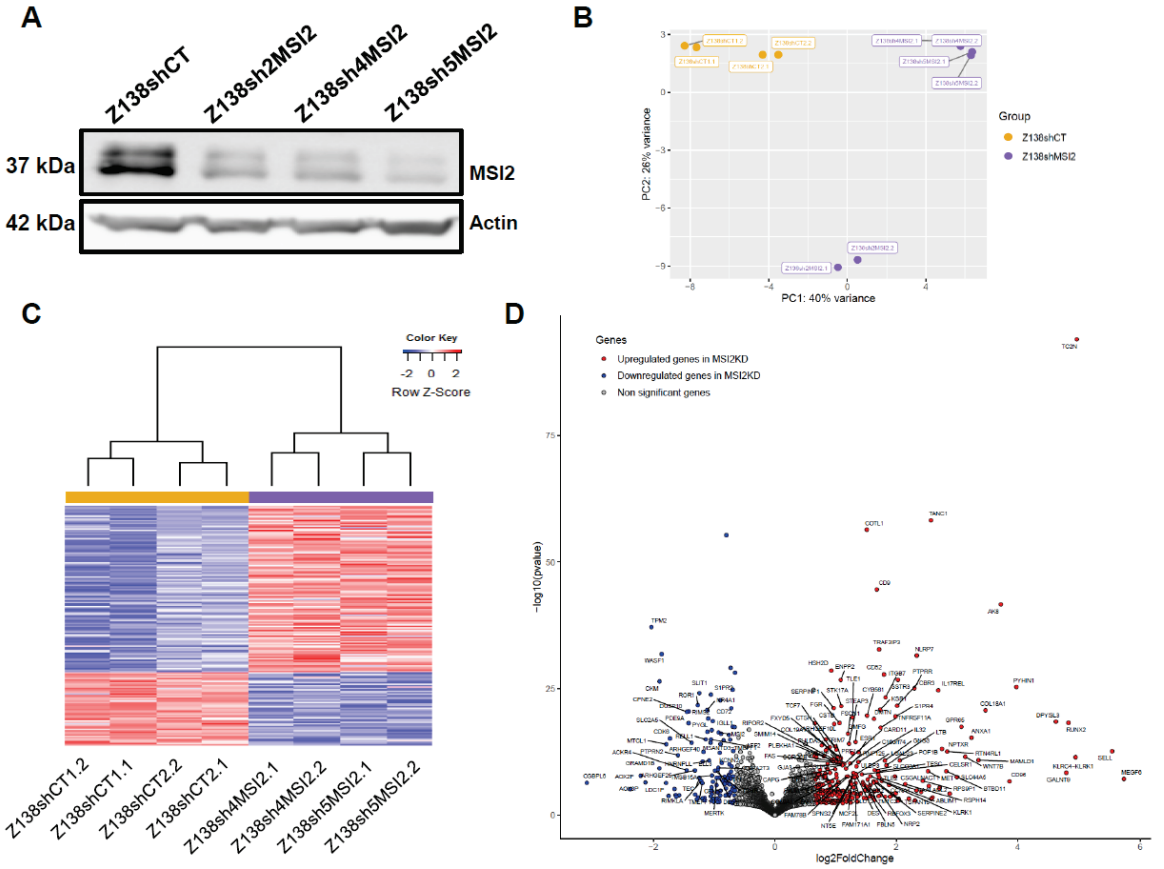

Figure 39. Genes differentially expressed upon MSI2 knockdown in Z138 MCL cell line. (A) MSI2 levels in Z138 MSI2-knockdown (sh2MSI2, sh4MSI2 and sh5MSI2) and control (shCT) MCL cell lines. Actin was used as a loading control. **(B)** Unsupervised principal component analysis (PCA) of gene expression data obtained by RNA-seq (n = 16,948 genes) from Z138shCT and Z138shMSI2 samples. **(C)** Scaled expression (Z-score) of 401 differentially expressed genes (277 upregulated and 124 downregulated genes; Appendix Table 10) in Z138shCT compared to sh4MSI2 and sh5MSI2 Z138 cell lines, obtained by RNA-seq. Samples are shown in columns (shCT in yellow and shMSI2 in purple) and genes in rows. Genes with an adjusted P-value <0.1 and absolute log2-transformed fold change >0.65 were considered. **(D)** Volcano plot showing genes differentially expressed after MSI2 knockdown in Z138 MCL cell line obtained by RNA-seq. The graph shows on the y-axis -log (P-value) and on the x-axis the log_2-transformed fold change. Genes upregulated and downregulated in Z138MSI2KD vs Z138CT with an adjusted P-value <0.1 and log_2-transformed fold change >0.65 or <-0.65 are colored in red and blue, respectively, and genes with an adjusted P-value <0.00005 and absolute log_2-transformed fold change >0.9 are labeled with their Gene Symbol.

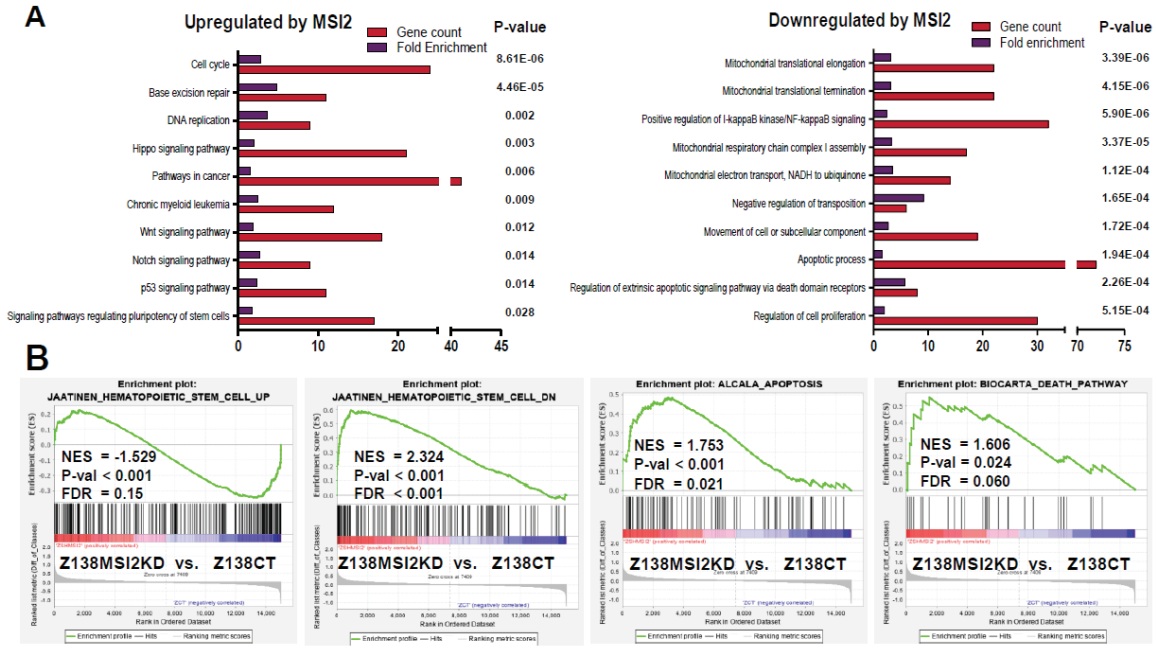

Figure 40. Dysregulated pathways upon MSI2 knockdown in Z138 MCL cell line (A) Functional annotation analysis obtained by DAVID Software of genes significant upregulated **(left)** and downregulated **(right)** by MSI2 according to an adjusted P-value <0.2 in the comparison of Z138CT vs Z138MSI2KD. The most significant terms, gene count, fold enrichment and P-value are indicated. **(B)** GSEA on RNA-seq data from Z138MSI2KD vs. Z138CT cell lines using gene sets related to HSCs and apoptosis. NES, P-val and FDR are shown.

2.6 MSI2 silencing decreases self-renewal, chemoresistance and survival of MCL tumoral cells

To analyze whether MSI2-mediated gene expression would be translated into functional effects, we generated a new MSI2-knockdown model by lentiviral transduction of Granta-519 MCL cell line with two shRNAs (sh4MSI2 and sh5MSI2). Silencing efficiency was higher in Z138 than in Granta-519 cells, and sh5MSI2 significantly reduced MSI2 protein levels three times more than sh4MSI2 (Figure 41A).

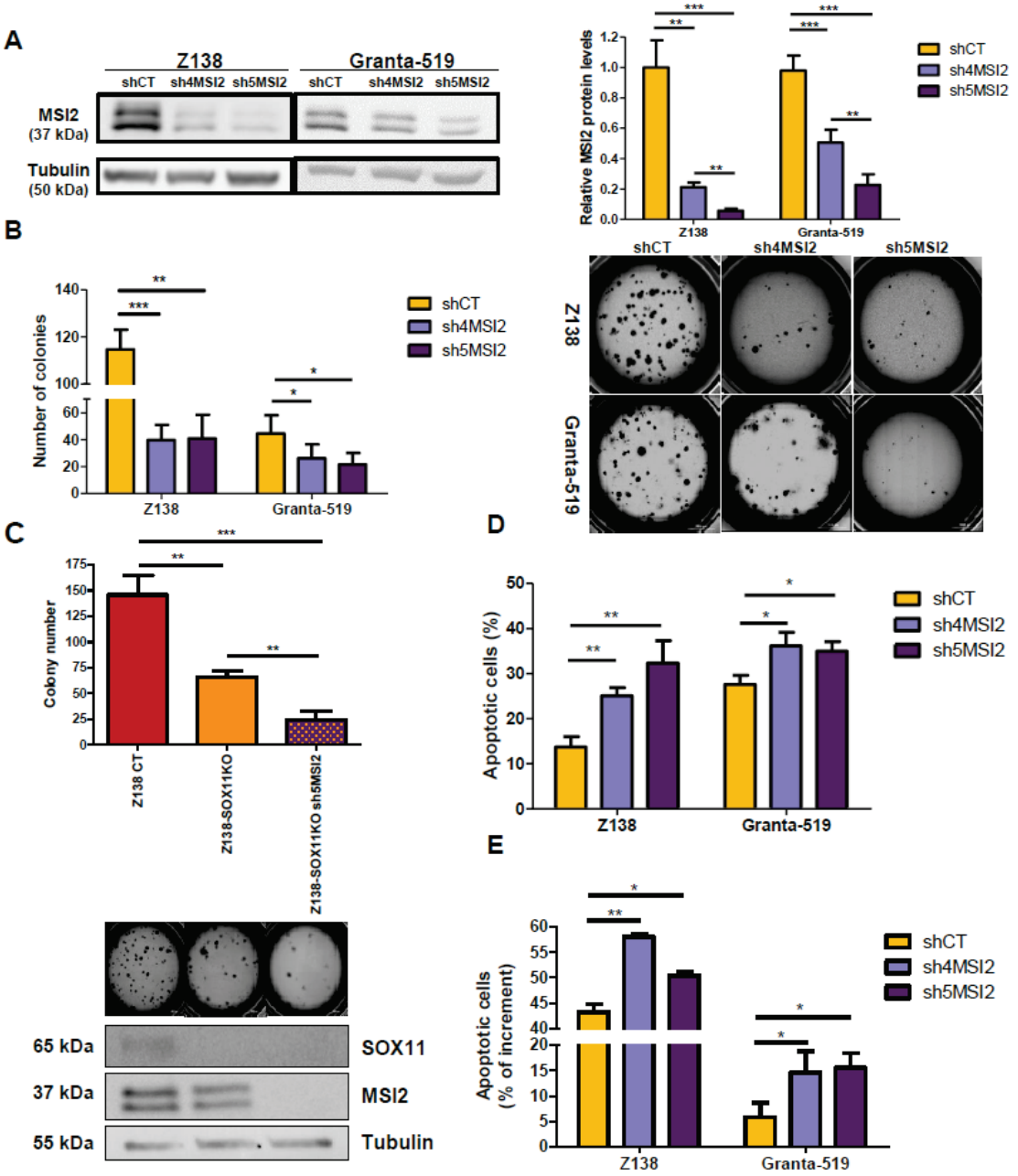

Figure 41. Functional effects upon MSI2 knockdown on self-renewal, cell survival and doxorubicin chemoresistance in MCL cell lines. (A) (Left) MSI2 levels in MSI2-knockdown (sh4MSI2 and sh5MSI2) and control (shCT) Z138 and Granta-519 MCL cell lines. Tubulin was used as a loading control. **(Right)** Quantification of MSI2 levels normalized with tubulin and relative to Z138 or Granta-519 shCT, respectively. **(B-C)** Number of colonies counted after 2 weeks of Z138 and Granta-519 shCT and shMSI2 **(B) (Left)**, and Z138 CT, SOX11KO and SOX11KO sh5MSI2 **(C) (Top)** cells growing in methylcellulose (1 colony >50 cells)**. (B) (Right) (C) (Mid)** Bright field images of colony assay were obtained using Cytation 5 Imaging Reader with 4X objective lens. To create the full picture 88 images were stitched together. **(C) (Bottom)**

SOX11 and MSI2 levels in Z138 CT, SOX11KO and SOX11KO sh5MSI2 cells. Tubulin was used as a loading control. **(D)** Annexin V+ population (in %) for shCT and shMSI2 Z138 and Granta-519 cells. **(E)** Apoptosis increment (doxorubicin Annexin V+ cells % – basal Annexin V+ cells %) after 24 hours of doxorubicin treatment in Z138 and Granta-519 shCT and shMSI2 cells (0.05 μM and 3 μM for Z138 and Granta-519 cell lines, respectively). Results of figures A, B, C, D and E are represented as the mean ± standard deviation of at least 3 independent experiments. The significance of difference was determined by unpaired two-tailed Student t-test: *P-value <0.05, ** P-value <0.01, *** P-value<0.001.

We analyzed the clonogenic growth of our MSI2-knockdown and control MCL models. MSI2-silenced cells formed lower number of colonies than control cells, with a reduction of >60% and >40% in Z138 and Granta-519 cells, respectively (Figure 41B). Interestingly, SOX11 knockout in Z138 cell line also reduced significantly colony growth compared to control cells (Figure 41C). These results suggest that SOX11 might be regulating MCL cell self-renewal through MSI2 modulation. However, depletion of MSI2 by shRNA silencing in SOX11KO showed a significant higher decrease in the number of colonies formed compared to SOX11KO alone in Z138 MCL cell line (Figure 41C). Additionally, MSI2 silencing induced apoptosis of MCL cells, with >2-fold and ~1.3-fold increase in Z138 and Granta-519 MSI2-knockdown cells (Figure 41D). MSI2 knockdown also intensified the chemosensitivity of MCL cells, as the shMSI2 cells exhibited a greater increase in apoptosis after doxorubicin treatment (relative to basal apoptosis) than the shCT cells (Figure 41E).

We also observed upregulation of several caspases (*CASP1*, *CASP10* and *CASP8*), genes related to mitochondrial apoptosis (*BAX* and *BLK*) and to extrinsic apoptosis (*FAS* and *PRF1*) in MSI2-knockdown MCL cells (Figure 42A-B). In parallel, there were an increased percentage of cleaved Caspase3+ cells and higher FAS levels in MSI2-knockdown compared to control MCL cells (Figure 42C-D, respectively). These results may explain the high increase in apoptosis and the chemosensitivity observed upon MSI2 knockdown in MCL cells.

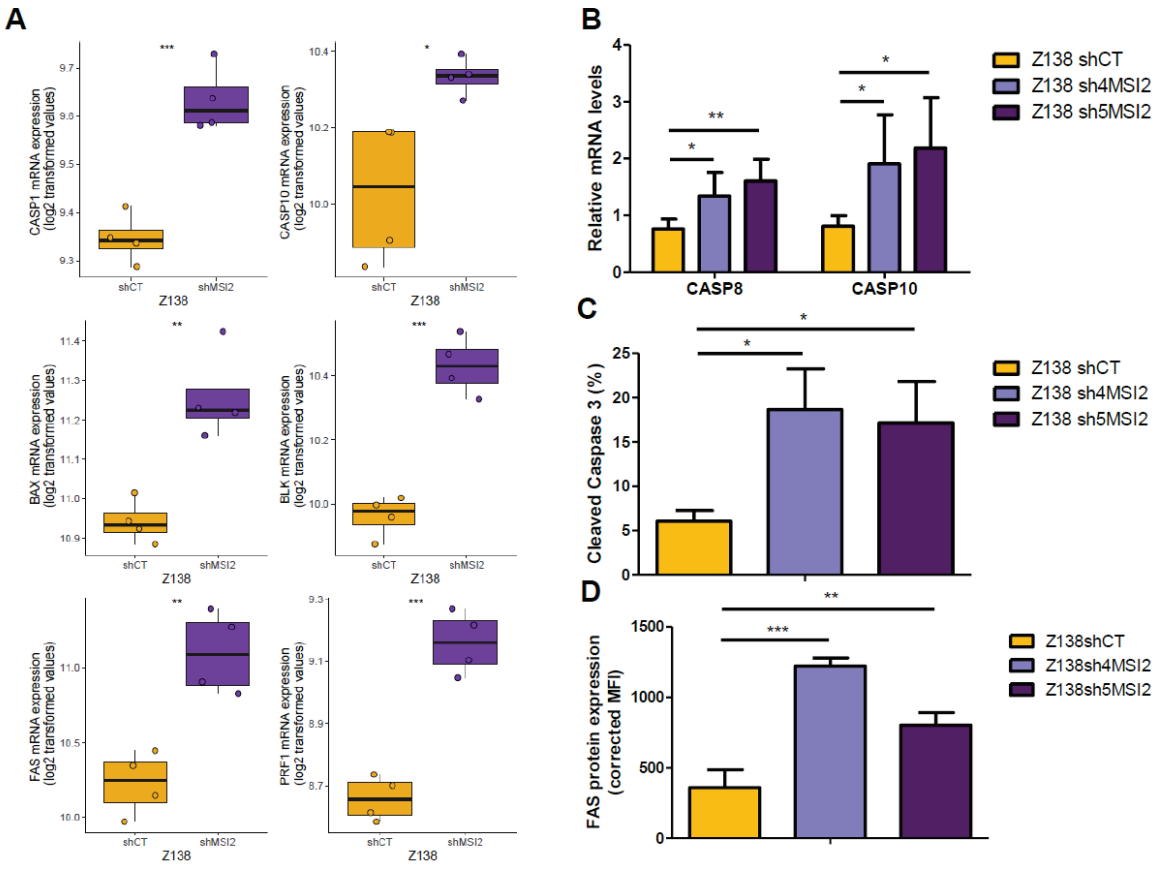

Figure 42. Apoptosis induced upon MSI2 knockdown is produced through upregulation of FAS and caspase cascade activation. (A) Expression (in $\log_2$ transformed values) of *CASP1*, *CASP10*, *BAX*, *BLK*, *FAS* and *PRF1* in Z138 shCT and shMSI2 cells, obtained by RNA-seq. **(B)** *CASP8* and *CASP10* expression, normalized to *GUSB* endogenous control, in Z138 shCT, sh4 and sh5MSI2 cells, obtained by qRT-PCR. The mRNA levels are relative to Z138 shCT. **(C-D)** Cleaved Caspase3 positive cells (in percentage) **(C)** and FAS levels **(D)** (corrected mean fluorescence intensity (MFI FAS – MFI isotype)) in Z138 shCT, sh4 and sh5MSI2 cells. The significance of difference was determined by unpaired two-tailed Student t-test in at least 3 independent experiments: *P-value <0.05, **P-value <0.01, ***P-value <0.001.

Interestingly, ectopic overexpression of MSI2 in Z138 MSI2-knockdown cells (Figure 43A) rescued them from apoptosis (Figure 43B), decreasing the percentage of cleaved Caspase3+ cells and FAS expression to equal levels observed in Z138CT cells (Figure 43C-D).

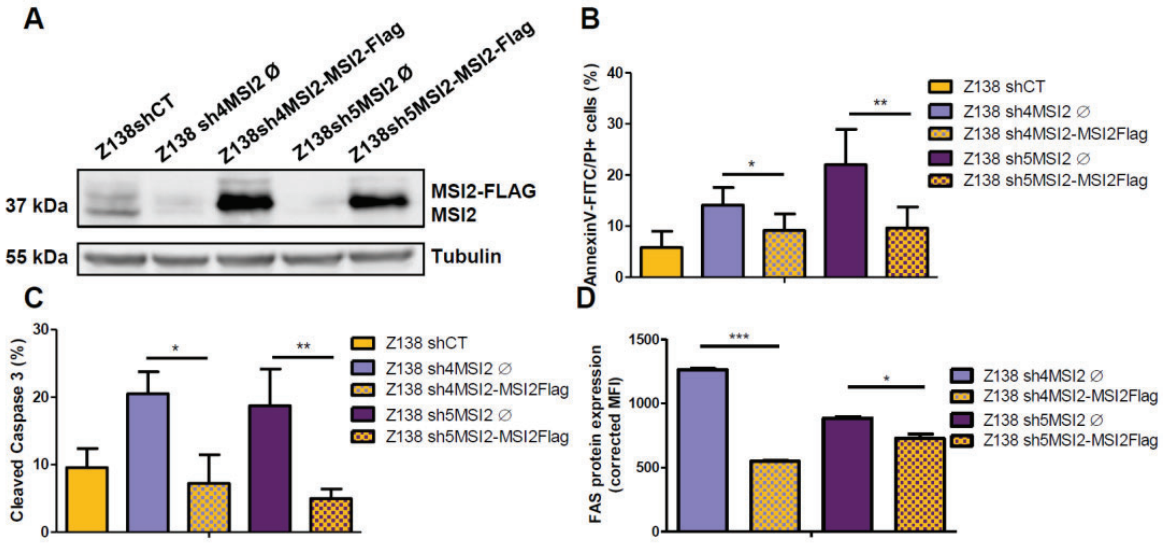

Figure 43. Apoptosis upon MSI2 knockdown is rescued after MSI2 overexpression in MCL cell lines. (A) MSI2-FLAG tagged and MSI2 endogenous levels in Z138 shCT, sh4MSI2 and sh5MSI2 cells transduced with EF1A empty plasmid (Ø) or EF1A plasmid expressing MSI2-FLAG tagged protein (MSI2-Flag). Tubulin was used as a loading control. **(B-D)** Apoptotic cells (AnnexinV-FITC/PI positive cells, in percentage) **(B)**, cleaved Caspase3 positive cells (in percentage) **(C)**, and FAS levels (corrected mean fluorescence intensity (MFI FAS – MFI isotype)) **(D)** in Z138 shCT cells, and in Z138 sh4MSI2 and sh5MSI2 cells transduced with EF1A empty plasmid (Ø) or EF1A plasmid expressing MSI2-FLAG (MSI2-Flag) tagged protein, obtained by flow cytometry. The significance of difference was determined by unpaired two-tailed Student t-test in at least 3 independent experiments: *P-value <0.05, **P-value <0.01, *** P-value <0.001.

Despite the changes observed in the expression of genes related to cell cycle and DNA damage response of MSI2-silenced cells, we did not find significant differences in proliferation or cell cycle, neither by EdU-PI staining or activation of proteins involved in cell cycle checkpoints in MSI2-knockdown compared to control cell lines (Figure 44A-B). However, we detected a general tendency of MSI2-silenced cells towards accumulating cells in G_0-G_1 phase (Figure 44A). Additionally, we found a slight increase in the protein levels of p21 in the Z138sh5MSI2 cell line compared to control cells (Figure 44B).

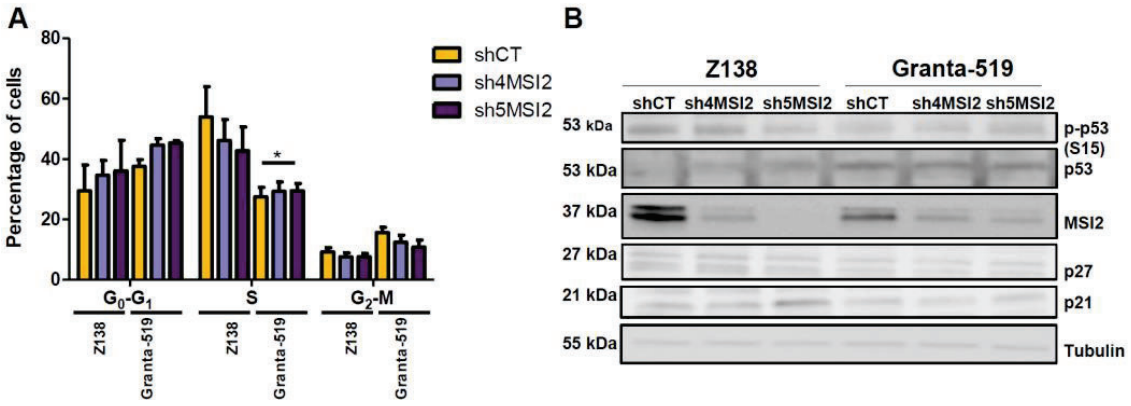

Figure 44. Effects of MSI2 knockdown in the cell cycle of MCL cells. **(A)** Cells in G_0-G_1, S and G_2-M phases of the cell cycle (in %) in Z138 and Granta-519 MSI2 knockdown (sh4MSI2 and sh5MSI2) and control cells (shCT) in at least 3 independent experiments. The significance of difference was determined by unpaired two-tailed Student t-test: *P-value <0.05. **(B)** Detection of phospho-p53 (S15), p53, MSI2, p27 and p21 protein levels in Z138 and Granta MSI2-knockdown and control cell lines. Tubulin was used as a loading control.

Our results showed that changes in the expression of signatures or pathways related to stem cells or apoptosis were translating into functional changes. In summary, MSI2 mediates self-renewal through increased colony growth, and enhances tumor survival and chemoresistance in MCL cells. Altogether, the results suggest that MSI2 is a tumorigenic factor in MCL.

2.7 Specific MSI2 inhibition with Ro 08-2750 small molecule significantly reduces survival and self-renewal of MCL

The possibility that MSI2 may act as a MCL tumorigenic factor led us to search for a MSI2 inhibitor able to overcome the phenotype caused by MSI2 in MCL. Ro 08-2750 is a small molecule that binds to MSI2 RNA-binding site impairing its RNA-binding activity, which in turns inhibit leukemogenesis in myeloid leukemia, and cell survival and proliferation in CLL (Minuesa et al., 2019; Palacios et al., 2021). In order to inhibit the MSI2 tumorigenic function in MCL, we tested Ro 08-2750 small molecule in MCL cell lines and primary cases.

We initially explored the MSI2 levels in three SOX11+ high-expressing, one SOX11+ low-expressing, and two SOX11- MCL or lymphoblastic cell lines. The three

SOX11+ high-expressing MCL cell lines showed high levels of MSI2, while HBL-2, JVM13 and JVM2 SOX11- or low-expressing cell lines had remarkably low levels (Figure 45A). We next examined the viability of these cell lines after Ro 08-2750 treatment at increasing concentrations. Z138, JeKo-1 and Granta-519 MSI2 high-expressing cell lines showed an impairment in viability after Ro 08-2750 treatment, with a half-effective concentration (EC50) of 5.9, 8.4 and 7.3 µM, respectively (Figure 45B). On the other hand, HBL-2, JVM13 and JVM2 MSI2 low-expressing cell lines presented higher EC50 (9.9, 13.8 and 31.2 µM, respectively). Indeed, we found a qualitative inverse correlation between Ro 08-2750 cytotoxicity, measured by the logEC50, and the MSI2 levels in MCL and lymphoblastic cell lines (Figure 45C). Moreover, treatment with Ro 08-2750 at 5 µM increased the apoptosis of MSI2 high-expressing MCL cell lines but not JVM2 MSI2 low-expressing (Figure 45D). These results suggest that Ro 08-2750-associated viability and apoptosis effects are produced by MSI2 inhibition, as cells with low MSI2 levels remain unaffected.

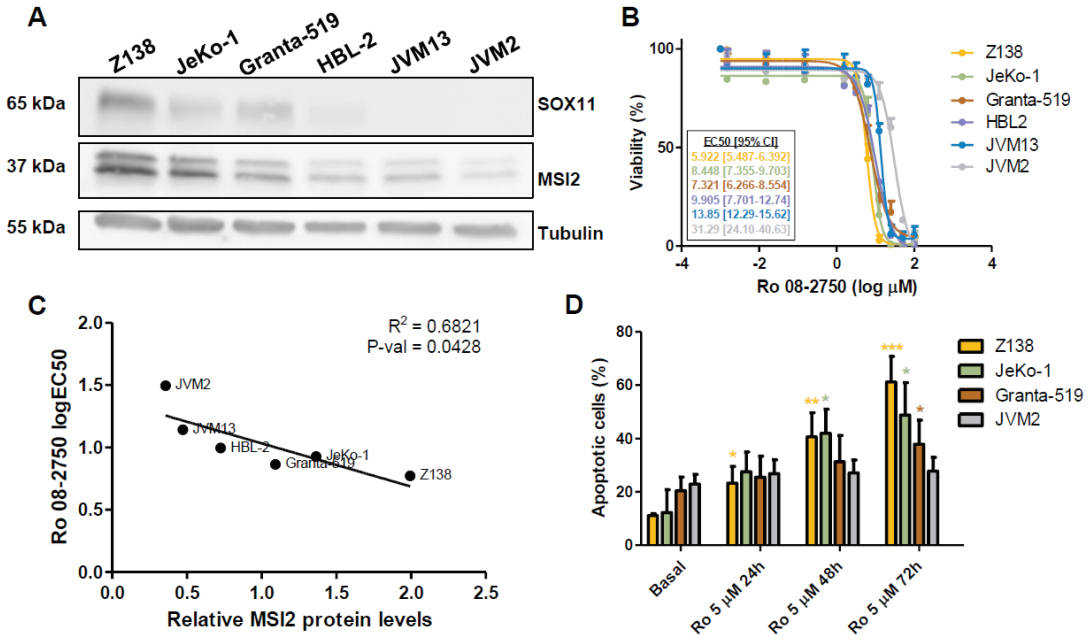

Figure 45. Ro 08-2750 MSI2 inhibitor induces cytotoxicity and apoptosis of MCL cell lines. **(A)** SOX11 and MSI2 levels in Z138, JeKo-1, Granta-519, HBL-2, JVM13 and JVM2 MCL and lymphoblastic cell lines. Tubulin was used as a loading control. **(B)** Cytotoxicity of Ro 08-2750 in Z138, JeKo-1, Granta-519, HBL-2, JVM13 and JVM2 MCL and lymphoblastic cell lines by MTT assay. Data is represented as percentage of viability at different Ro 08-2750 concentrations (in log

µM), relative to untreated cells. EC50 and confidence intervals (mean of 2 independent experiments) for each cell line are shown. **(C)** Qualitative correlation between Ro cytotoxicity levels, measured by the associated logEC50, and relative MSI2 protein levels obtained by western blot (normalized with tubulin) in MCL and lymphoblastic cell lines. Graph shows Pearson coefficient of determination (R^2) and p value (P-val). **(D)** Annexin V+ cells (in %) in Z138, JeKo-1 and Granta-519 SOX11+/MSI2^{High}, and JVM2 SOX11-/MSI2^{Low} MCL cell lines after 24h, 48h and 72h of Ro treatment at 5 µM or without treatment (basal). Statistical significance is determined by unpaired two-tailed Student t-test comparing to basal apoptosis in at least 3 independent experiments (asterisks comparisons: Z138 in yellow, JeKo-1 in green, Granta-519 in brown and JVM2 in grey). *P-value <0.05, ** P-value <0.01, *** P-value <0.001.

Then, we analyzed the colony growth of Z138 and Granta-519 cells after Ro 08-2750 treatment. MCL cells treated with increasing concentrations of Ro 08-2750 showed lower number of colonies than untreated cells (cultured with the excipient, DMSO), with a reduction of >30%, >50% and ~70-100% at 0.1 µM, 1 µM and 5 µM, respectively (Figure 46A). To demonstrate that the impairment in colony formation was not due to an increase in apoptosis, we treated Z138 cells at the lowest Ro 08-2750 dose at which we observed significant differences in colony growth, and measured the apoptosis. Z138 cells treated at 1 µM did not show increased apoptosis over time (Figure 46B).

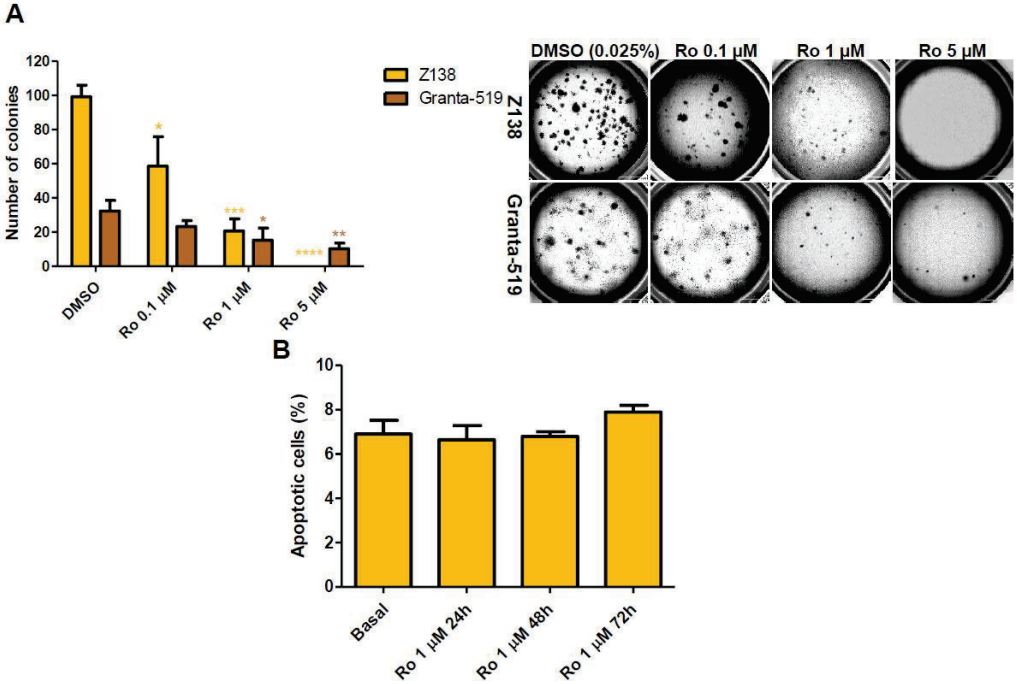

Figure 46. MSI2 inhibition with Ro 08-2750 affects the colony growth of MCL cell lines. (A) (Left) Colony formation assays (number of colonies) in Z138 and Granta-519 cell lines treated at

different concentrations of Ro 08-2750 drug (0.1 µM, 1 µM and 5 µM) or with 0.025% of DMSO, used as control. Results are represented as the mean ± standard deviation of at least 3 independent experiments. Statistical significance is determined by unpaired two-tailed Student t-test compared to DMSO (asterisk comparisons: Z138 in yellow, Granta-519 in brown). **(Right)** Bright field images of Z138 and Granta-519 colonies growing in methylcellulose medium, treated at different concentrations of Ro drug (0.1 µM, 1 µM and 5 µM) or with 0.025% of DMSO, obtained using Cytation 5 Imaging Reader with 4X objective lens. **(B)** Annexin V+ cells (in %) in Z138 MCL cell line after 24h, 48h and 72h of Ro treatment at 1 µM. *P-value <0.05, ** P-value <0.01, *** P-value <0.001, **** P-value < 0.0001.

Next, we tested the ALDH activity, widely used as a CSC marker, in MCL primary samples expressing high and low levels of *MSI2* (Figure 47A). ALDH activity was significantly higher in MSI2^{High} than in MSI2^{Low} cases (3-fold increase) (Figure 47B). Moreover, MSI2 inhibition with increasing concentrations of Ro 08-2750 treatment gradually reduced the ALDH activity towards minimal values, mainly in MSI2^{High} group (Figure 47C-D).

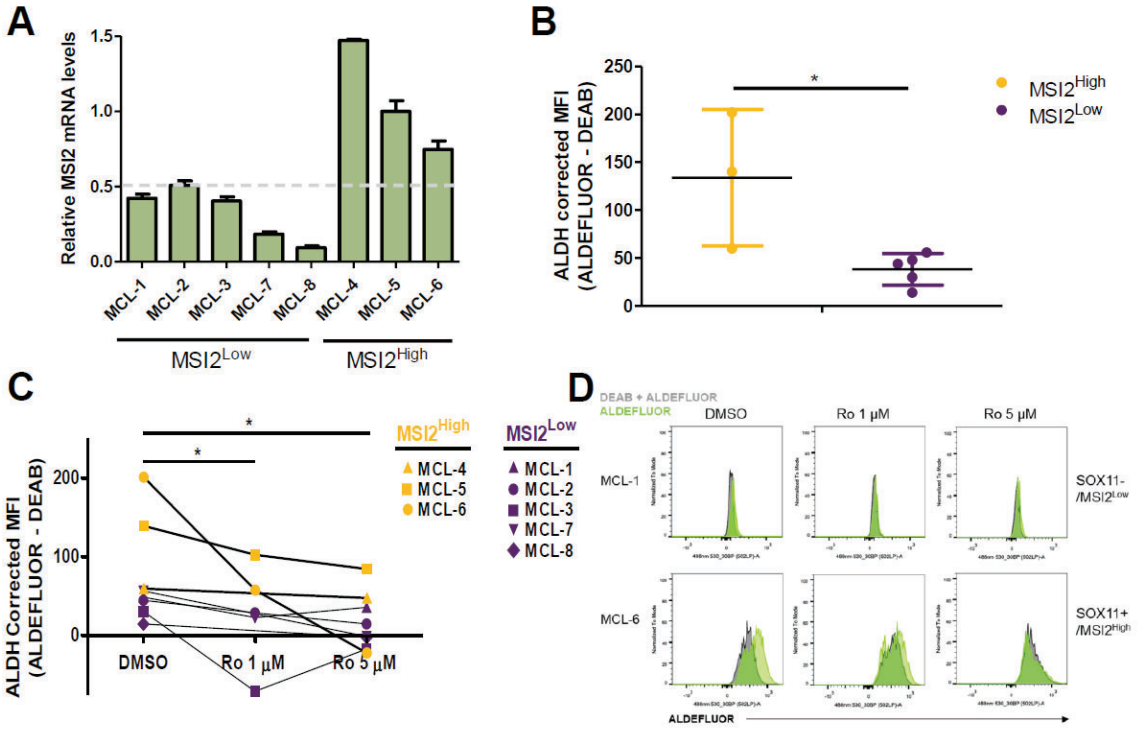

Figure 47. MSI2 inhibition with Ro 08-2750 treatment reduced ALDH activity of MCL primary cases. (A) *MSI2* expression, normalized to *GUSB* endogenous control, in MCL leukemic primary cases (N = 8). The mRNA levels are relative to MCL-5 case. A cutoff at 0.51 (grey line) in relative *MSI2* expression was established in order to separate cases with *MSI2* high and low

expression. **(B)** ALDH activity quantified as corrected mean fluorescence intensity (MFI ALDEFLUOR – MFI ALDEFLUOR+DEAB) in $MSI2^{High}$ (N=3) and $MSI2^{Low}$ (N=5) MCL primary leukemic cases, measured by ALDEFLUOR assay. Results are represented as the mean ± standard deviation of all the cases in each group. The significance of difference was determined by unpaired two-tailed Student t-test. **(C)** ALDH activity quantified as corrected mean fluorescence intensity (MFI ALDEFLUOR – MFI ALDEFLUOR+DEAB) in $MSI2^{Low}$ (N=5) and $MSI2^{High}$ (N=3) MCL primary leukemic cases, after 24 hours of treatment with 1 and 5 µM of Ro or 0.05% of DMSO. The significance of difference was determined by paired one-tailed Student t-test. **(D)** Histograms of ALDEFLUOR (in green) and ALDEFLUOR+DEAB (in grey) samples in representative $MSI2^{Low}$ (MCL-1) and $MSI2^{High}$ (MCL-6) MCL primary cases treated with 1 and 5 µM of Ro or 0.05% of DMSO. *P-value <0.05.

Finally, to globally assess the transcriptomic effects of Ro 08-2750, we performed RNA-seq in Z138 MCL cells treated with Ro 08-2750 at 20 µM or with 0.1% DMSO (excipient) for 4 hours. Differential expression analysis found 394 upregulated and 400 downregulated genes upon Ro 08-2750 treatment in Z138 cells (Appendix Table 12). GSEA showed that Z138 MSI2 knockdown cells were enriched for upregulated genes after Ro 08-2750 treatment, while Z138 control cells for downregulated genes (Figure 48A). Furthermore, approximately 10% of genes differentially expressed following Z138 MSI2 knockdown overlapped with ~5% of genes differentially expressed after Ro 08-2750 treatment in Z138 cells (Figure 48B). Although few genes overlapped between both lists, we identified pathways related to apoptosis in common, downregulated by MSI2 and upregulated by Ro 08-2750, and others related to developmental pathways (Wnt and Notch signaling pathways) upregulated by MSI2 and downregulated by Ro 08-2750 (Figure 40A, Appendix Table 13).

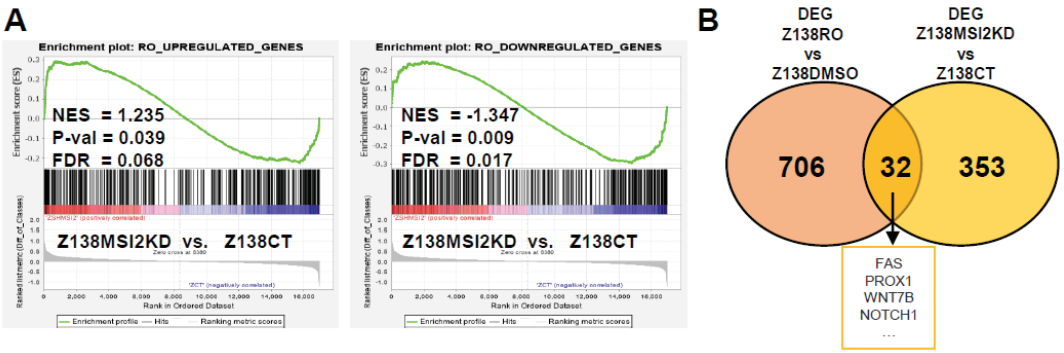

Figure 48. Ro 08-2750 treatment showed overlapping transcriptomic effects with MSI2 knockdown in Z138 MCL cell line. (A) GSEA in RNA-seq data comparing Z138MSI2KD vs. Z138CT cell lines using up- and downregulated gene sets in Z138 cell line following Ro 08-2750 treatment at 20 µM, in comparison with Z138 treated with 0.1% DMSO, obtained by differential expression analysis on RNA-seq data (Appendix Table 12). NES, P-val and FDR are shown. **(B)** Overlap between differentially expressed genes upon MSI2 knockdown (adjusted P-value <0.1 and log2-transformed fold change >0.65) (Appendix Table 10) and upon MSI2 inhibition with Ro 08-2750 at 20 µM for 4 hours (adjusted P-value<0.1 and log2-transformed fold change >0.65) (Appendix Table 12), both obtained by RNA-seq on Z138 MCL cell line.

Overall, these data support that Ro 08-2750 drug specifically inhibits MSI2 function, inducing toxicity and reducing self-renewal in MCL cell lines and primary cases, and inhibiting part of the specific genetic program of MSI2.

2.8 MSI2 binds *CDK6* and *NOTCH1* mRNAs and post-transcriptionally regulates their expression in MCL cell lines

MSI2 protein exerts its function through mRNAs binding to activate or block their translation to protein (Hattori et al., 2017; S. M. Park et al., 2015; Okabe et al., 2001). To find which genes MSI2 may regulate to achieve self-renewal and tumorigenicity features in MCL, we searched for genes directly regulated by MSI2 RBP in LT-HSCs (Nguyen et al., 2020) (MSI2 target genes in LT-HSCs) involved in stemness features (GO stem cell-related genes, Appendix Table 6) and differentially expressed genes between Z138 MSI2 knockdown and control cells (DEG Z138MSI2KD vs Z138CT, Appendix Table 10). Unexpectedly, only *CDK6*, *MSI2* and *NOTCH1* stem cell-related genes were identified as possible MSI2-direct targets in MCL.

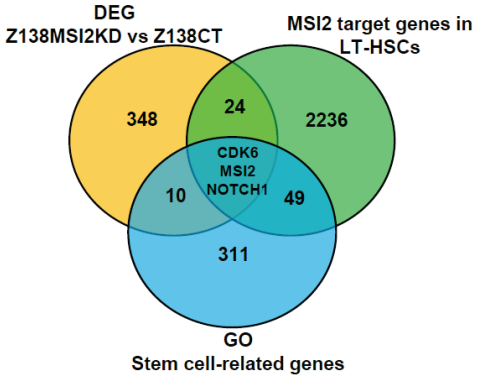

Figure 49. MSI2 candidate target genes related to stemness in MCL. Overlapp between differentially expressed genes after MSI2 knockdown in Z138 MCL cell line (yellow circle, Appendix Table 10; 385 genes), previously published direct target mRNAs of MSI2 in LT-HSCs, found by HyperTRIBE (green circle, 2312 genes) and gene ontology established stem cell-related genes (blue circle, 373 genes; Appendix Table 6).

To validate our MSI2 target candidates in MCL, we performed RNA immunoprecipitation in Z138 MCL cell line by using a MSI2 specific antibody that effectively immunoprecipitated MSI2 (Figure 50A, MSI2 IP). We obtained a significant enrichment of *CDK6* and *NOTCH1* mRNAs in MSI2 immunoprecipitation (MSI2 RIP) compared to IgG control immunoprecipitation fraction (IgG RIP) (Figure 50B).

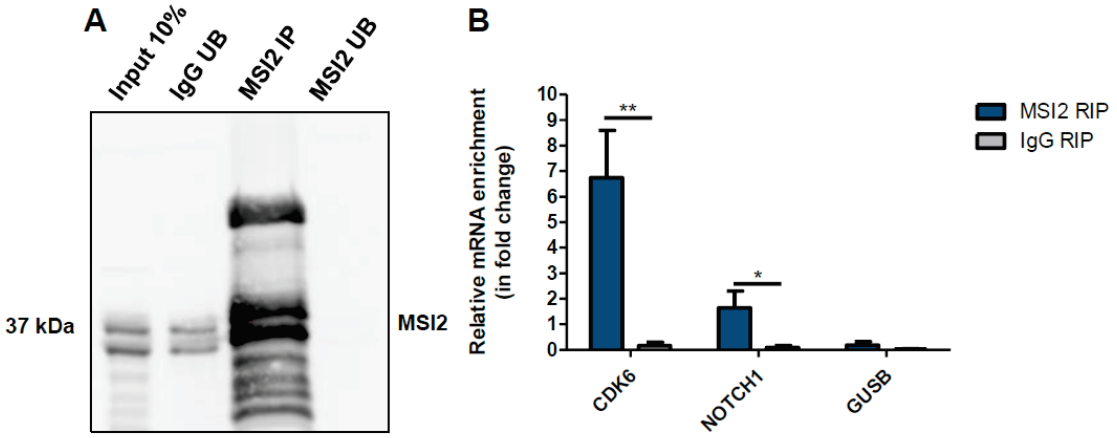

Figure 50. MSI2 binds to *CDK6* and *NOTCH1* mRNAs in MCL cell lines. (A) MSI2-pulldowns from lysates of Z138 MCL cell line (MSI2 IP), immunoprecipitated with a specific MSI2 antibody. The protein fraction unbound to MSI2 antibody (MSI2 UB) is shown. IgG was used as control for RNA immunprecipitation showing MSI2 protein in the unbound fraction (IgG UB). Input sample is the protein fraction before antibody addition (10% of total lysate) **(B)** *CDK6* and *NOTCH1* mRNA levels in MSI2 and IgG RIPs (RNA eluted fractions from MSI2- (MSI2 IP) and IgG-pulldowns (IgG IP), respectively), displayed as fold change relative to their input fraction in 3

independent experiments, obtained by qRT-PCR. *GUSB* mRNA enrichment was used as negative control. The significance of difference was determined by unpaired two-tailed Student t-test: * P-value <0.05, ** P-value <0.01.

In agreement with the *CDK6* and *NOTCH1* mRNA binding by MSI2, CDK6 and NOTCH1 mRNA and protein levels decreased after MSI2 silencing in Z138 MCL cell line (Figure 51A and B, respectively). MSI2 inhibition with Ro 08-2750 treatment also induced significantly lower levels of CDK6 and NOTCH1 proteins at 24 hours but not at 4 hours in Z138 MCL cell line, compared to untreated cells (DMSO) (Figure 51C). Altogether, these results suggest that MSI2 RBP may bind to *CDK6* and *NOTCH1* mRNAs inducing their translation in MCL.

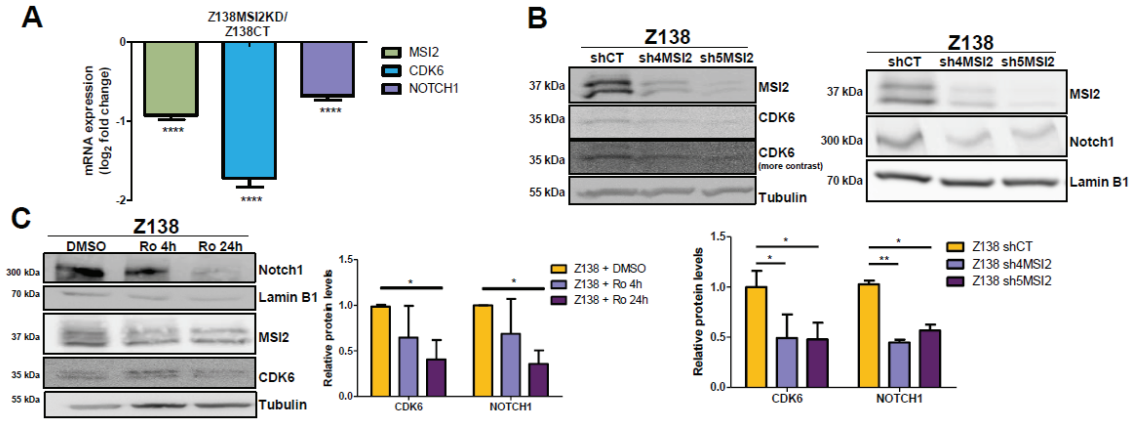

Figure 51. CDK6 and NOTCH1 decrease upon MSI2 knockdown or inhibition with Ro 08-2750 small molecule. (A) *MSI2*, *CDK6* and *NOTCH1* expression in $\log_2$ fold change between Z138MSI2KD and Z138CT MCL cell lines, from RNA-seq data (4 samples per group). Statistical significance is determined by Wald test: **** P-value <0.0001. **(B) (Top)** CDK6 **(left)**, NOTCH1 **(right)** and MSI2 levels in Z138shCT, sh4MSI2 and sh5MSI2 cell lines. Tubulin and lamin B1 were used as loading controls. **(Bottom)** Quantification of CDK6 and NOTCH1 protein levels normalized with tubulin or lamin B1 and relative to Z138shCT, in 3 independent western blot experiments. **(C) (Left)** MSI2, NOTCH1 and CDK6 levels in Z138 cell line after Ro 20 µM treatment for 4 or 24 hours or cultured with DMSO 0.1% solvent for 24 hours. Tubulin and lamin B1 were used as loading controls. **(Right)** Quantification of CDK6 and NOTCH1 protein levels normalized with tubulin and lamin B1, respectively, and relative to Z138 treated with DMSO 0.1% in 3 independent experiments. The significance of difference was determined by unpaired two-tailed Student t-test: * P-value <0.05, ** P-value <0.01.

However, we did not observe a correlation between *MSI2* and *NOTCH1* or *CDK6* expression in MCL primary cases (Figure 52A). Additionally, SOX11+/MSI2^{High} MCLs

did not show higher expression of *NOTCH1* and *CDK6* compared to SOX11-/MSI2^{Low} primary samples (Figure 52B).

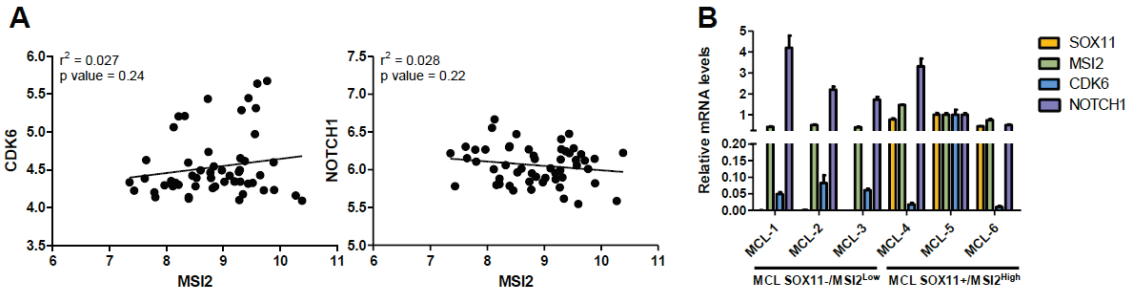

Figure 52. *CDK6*, *NOTCH1* and *MSI2* levels in MCL primary cases. (A) Correlations between *CDK6* **(Left)** and *NOTCH1* **(Right)** with *MSI2* mRNA levels. R^2 and the p value for pearson correlation is shown. **(B)** *SOX11*, *MSI2*, *CDK6* and *NOTCH1* expression, normalized with *GUSB* endogenous control, in MCL peripheral blood primary cases (3 SOX11-/MSI2^{Low} and 3 SOX11+/MSI2^{High}). The mRNA levels are relative to MCL-5 case.

2.9 MSI2 knockdown delays tumor growth in MCL xenograft mouse model

To investigate the potential tumorigenic role of MSI2 in MCL in vivo, we generated MSI2 knockdown- and control-luciferase+ (MSI2KD-Luc+ and MSI2CT-Luc+, respectively) mice models through intravenous injection of Z138sh5MSI2- and Z138shCT-luciferase+ cells into NSG mice. MSI2 depletion resulted in a significantly lower tumor growth over time compared to MSI2 control mice, captured by luciferase bioimage (LBI) signal every week (Figure 53).

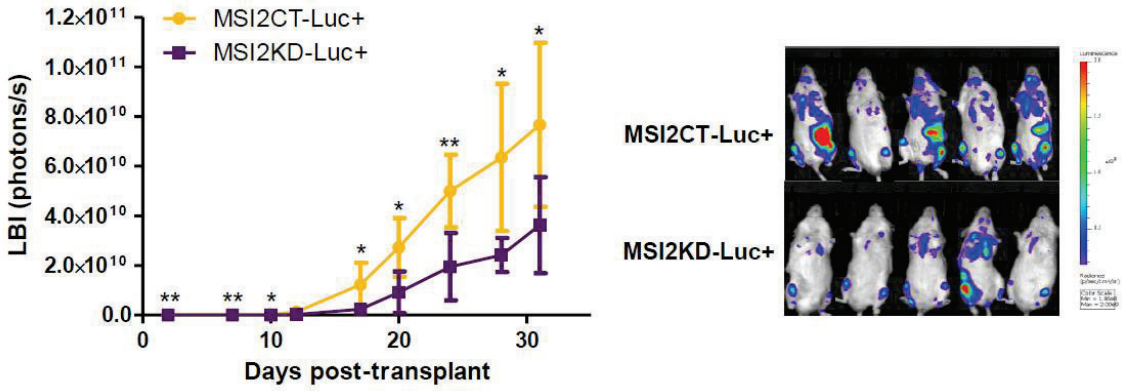

Figure 53. MSI2 knockdown delays tumor growth in MCL xenograft mouse model. (Left) NSG mice intravenously injected with 10x10^6 Z138shCT (n=5, MSI2CT-Luc+) or Z138sh5MSI2 (n=5, MSI2KD-Luc+) cells expressing the GFP and luciferase enzyme were imaged twice per week for 5 weeks. LBI signal (photons/s) shows the tumor growth at indicated days' post-tumor

transplant. LBI signal at mice ovaries was subtracted from the total signal for the two last points (day 28 and 31) to minimize the differences between males and females. **(Right)** Pictures showing the LBI signal in MSI2CT-Luc+ and MSI2KD-Luc+ MCL xenograft mice at day 31 post-transplant (luminescence signal from 1.00e8 to 2.00e9). The significance of difference was determined by unpaired two-tailed Student t-test: * P-value <0.05, ** P-value <0.01.

After 35 days, we euthanized the mice and processed their lymphoid organs. MSI2 knockdown mice showed lower percentage of MCL cells in spleen and bone marrow compartments compared to control mice (Figure 54A), confirmed by lower spleen weight (Figure 54B). However, no differences in peripheral blood were obtained (Figure 54A). In spite of collecting LBI signal around submandibular lymph nodes (Figure 53), we did not find MCL cells in processed lymph nodes (data not shown).

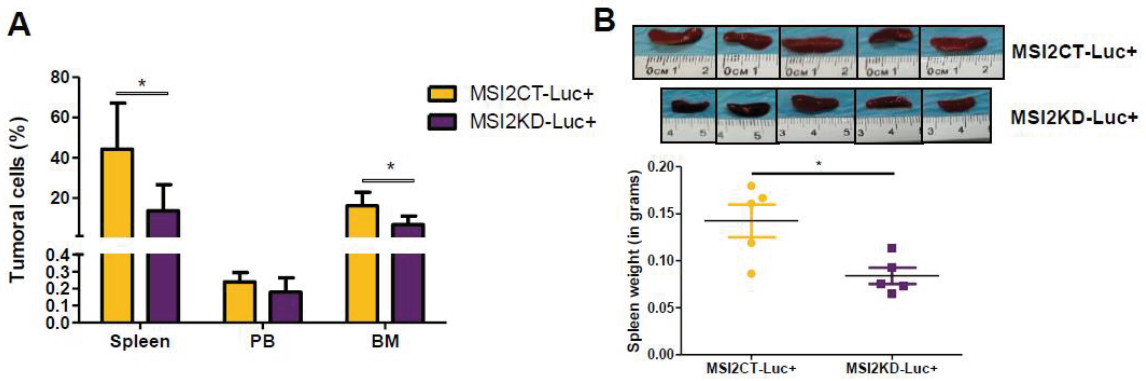

Figure 54. MSI2 depletion reduces the MCL engraftment in spleen and bone marrow of NSG mice. (A) MCL tumoral cells (in %) in different mice organs (spleen; peripheral blood, PB; bone marrow, BM), comparing MSI2CT-Luc+ and MSI2KD-Luc+ xenograft mice, analyzed using GFP fluorescence by flow cytometry. **(B) (Top)** Illustrative images of spleen engraftment in MSI2CT-Luc+ and MSI2KD-Luc+ MCL xenograft mice models. **(Bottom)** Spleen weight (in grams) in MSI2CT-Luc+ and MSI2KD-Luc+ xenograft mice models. The significance of difference was determined by unpaired two-tailed Student t-test: * P-value <0.05.

These results suggest that MSI2 promotes tumorigenic growth and increases the tumor engraftment in spleen and bone marrow of MCL xenograft mouse model.

We also tested the efficacy of Ro 08-2750 treatment in MSI2CT-Luc+ MCL xenograft mice to determine whether MSI2 inhibition might affect tumor growth in vivo. Mice were treated with Ro 08-2750 at 13.75 mg/kg or DMSO excipient by intraperitoneal injection every 3 days and were monitored for tumor growth (Figure 55A). The treatment

was not well tolerated by mice, as they exhibited symptoms of lethargy immediately after injection and acute weight loss (Figure 55B). In fact, two of the mice treated with Ro 08-2750 died at days 9 and 12. We observed decreased LBI signal in the Ro 08-2750 treated group, but probably due to poor absorption of luciferin (luciferase substrate), as mice showed damage in the digestive system resulting from treatment with Ro 08-2750 (Figure 56A). We euthanized these mice at day 12 post-injection due to endpoint criteria (>10% of weight loss).

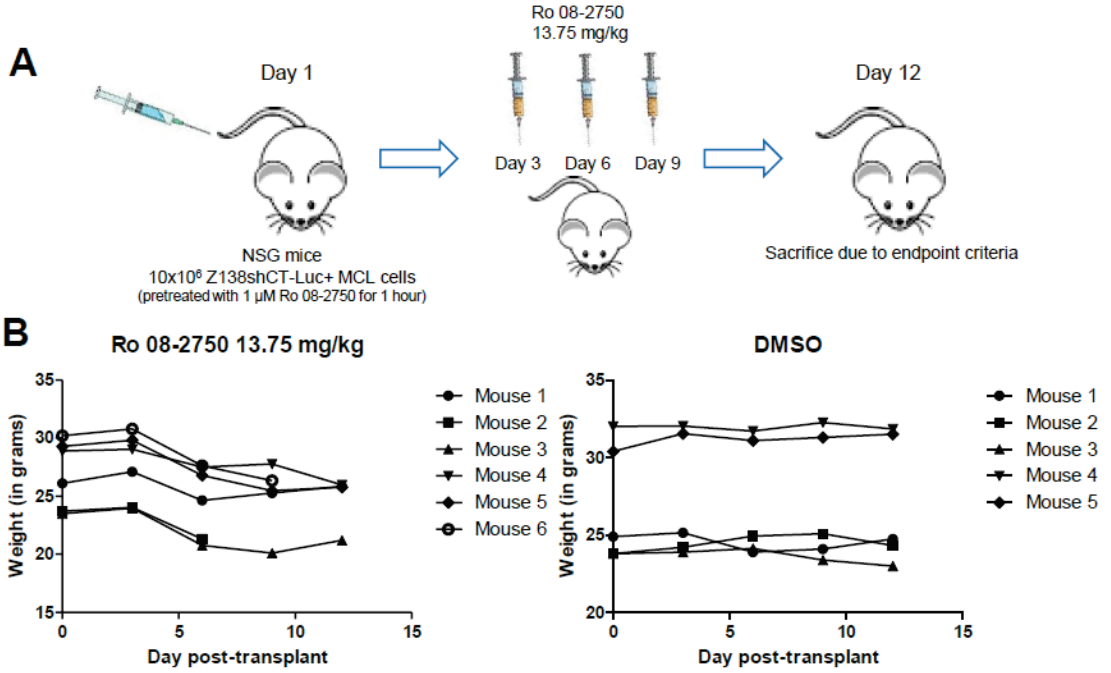

Figure 55. Ro 08-2750 treatment assay (13.75 mg/kg) in MCL xenograft mice models. (A) Schematic representation of the assay in NSG mice, showing Ro 08-2750 doses at indicated days. Only 3 doses could be administered due to toxicity signs. **(B)** Weight monitoring of MCL mice models treated with Ro 08-2750 at 13.75 mg/kg or with DMSO excipient during the assay.

Next, we analyzed the total number of MCL cells engrafted in bone marrow, but we did not find differences between mice treated with Ro 08-2750 or with DMSO. Ro 08-2750 treated mice had MCL cells in bone marrow, confirming that the negative signal in 3 of 4 mice at day 12 post-injection might be consequence of poor luciferin absorption and not by the absence of tumor cell engraftment (Figure 56B).

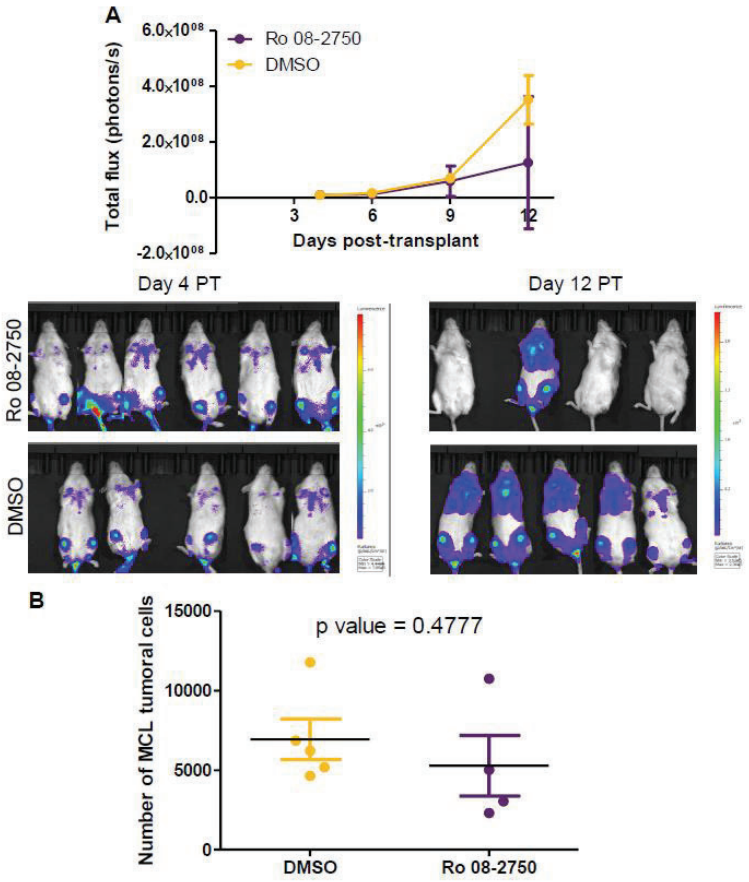

Figure 56. MCL tumor growth in NSG mice treated with Ro 08-2750 at 13.75 mg/kg or DMSO (A) (Top) LBI signal (photons/s) shows tumor growth at indicated days' post-tumor transplant in 6 MSI2CT-Luc+ mice treated with Ro 08-2750 at 13.75 mg/kg and in 5 MSI2CT-Luc+ mice treated with DMSO excipient. Two Ro treated mice died at days 9 and 12 post-trasplant. **(Bottom)** Pictures showing the LBI signal in MSI2CT-Luc+ Ro or DMSO treated MCL xenograft mice at days 4 and 12 post-transplant (PT). **(B)** Total number of MCL tumoral cells in bone marrow compartment of Ro 08-2750 and DMSO treated mice (GFP positive cells). The significance of difference was determined by unpaired two-tailed Student t-test.

To reduce Ro 08-2750 toxicity, we performed another in vivo inhibitory experiment halving Ro 08-2750 doses (7 mg/kg) (Figure 57A). However, the results obtained in this assay were similar to those obtained using 13.75 mg/kg of Ro 08-2750, showing slight weight loss in mice treated with Ro 08-2750 or DMSO (Figure 57B), toxicity symptoms in Ro 08-2750 treated mice, and no differences in tumor growth (Figure 58A), tumor engraftment (Figure 59A) and spleen weight (Figure 59B) between Ro 08-2750 and DMSO treated MSI2CT-Luc+ MCL xenograft mice.

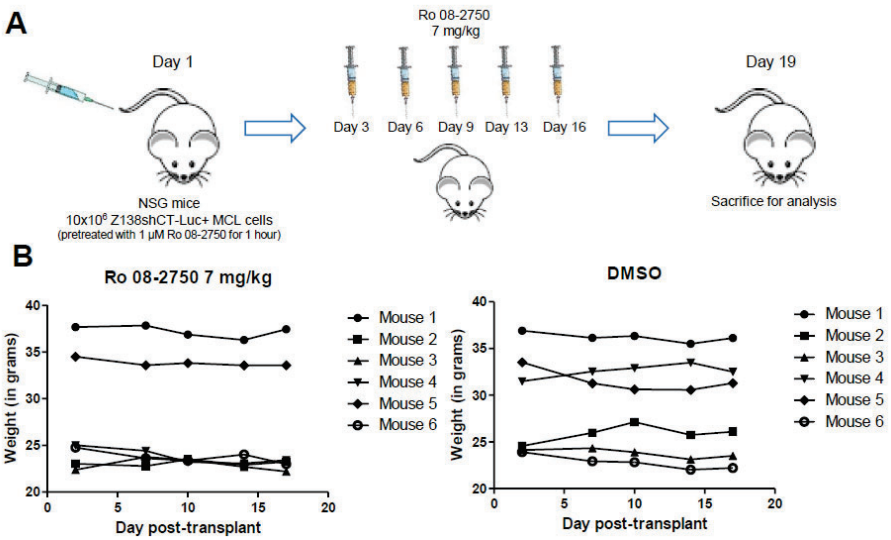

Figure 57. Ro 08-2750 treatment assay (7 mg/kg) in MCL xenograft mice models. (A) Schematic representation of the assay in NSG Z138shC-LUC+ xenotransplanted mice, showing Ro 08-2750 doses at indicated days. **(B)** Weight size monitored in MCL mice models treated with Ro 08-2750 at 7 mg/kg or with DMSO excipient during the assay.

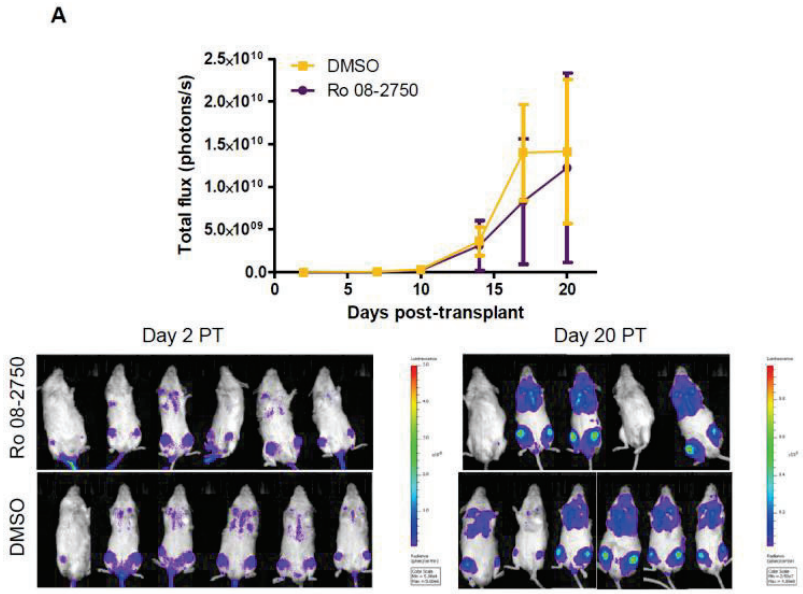

Figure 58. MCL tumor growth in NSG xenotransplanted mice treated with Ro 08-2750 at 7 mg/kg or DMSO. (Top) LBI signal (photons/s) shows tumor growth at indicated days' post-tumor transplant in 6 MSI2CT-Luc+ mice treated with Ro 08-2750 at 13.75 mg/kg and in 6 MSI2CT-Luc+ mice treated with DMSO excipient. One of the Ro treated mice died at day 7 post-transplant. **(Bottom)** Pictures showing the LBI signal in MSI2CT-Luc+ Ro or DMSO treated MCL xenograft mice at days 4 and 12 post-transplant (PT).

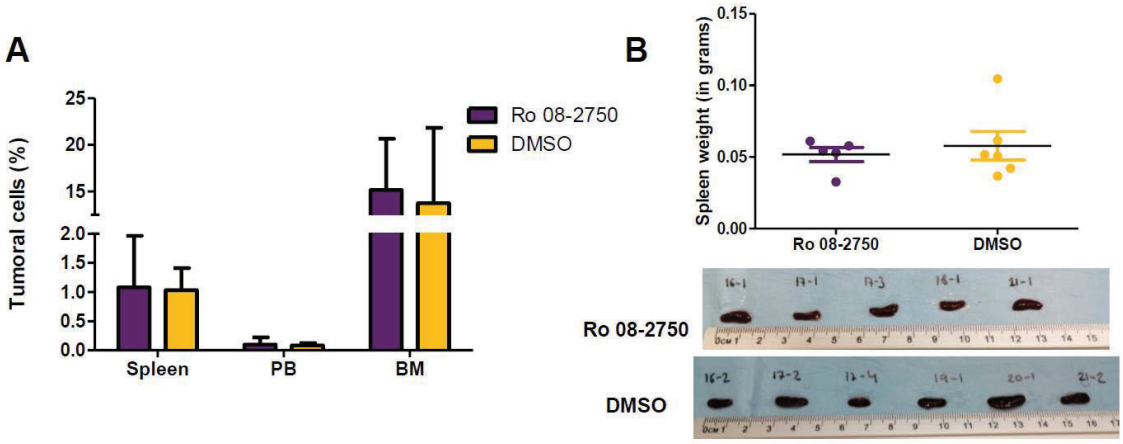

Figure 59. Engraftment of MCL cells in the spleen, peripheral blood and bone marrow of xenotransplanted NSG mice treated with Ro 08-2750 at 7 mg/kg or DMSO. (A) MCL tumoral cells (in %) in different mice organs (spleen; peripheral blood, PB; bone marrow, BM), comparing MSI2CT-Luc+ xenograft mice treated with Ro 08-2750 at 7 mg/kg or DMSO, analyzed using GFP fluorescence by flow cytometry. **(B) (Top)** Spleen weight (in grams) **(Bottom)** and illustrative images of spleen engraftment in MSI2CT-Luc+ xenograft mice treated with Ro 08-2750 at 7 mg/kg or DMSO.

The high toxicity observed in our NSG mice models using Ro 08-2750 treatment suggest that other compounds should be explored to follow up MSI2-specific inhibitory experiments in vivo and to demonstrate that MSI2 could represent a new target therapy for MCL patients with relapse.

STUDY 2

SOX11 and Epstein–Barr virus may substitute each other in the pathogenesis of Burkitt Lymphoma

Manuscript under preparation

1. INTRODUCTION

BL is a highly proliferative B cell neoplasm that originates from germinal center B cells. Traditionally, three clinical variants are distinguished: eBL, sBL and immunodeficiency-related BL. eBL is usually positive for EBV infection and presents with jaw or facial bone involvement. sBL involves abdomen, head and neck lymph nodes, and in some cases, bone marrow. Moreover, sBL is less commonly positive for EBV infection. Interestingly, several studies have revealed important genetic and molecular differences depending on the clinical variant and the EBV status of BL patients. For example, eBL acquires the t(8;14) mostly by SHM, while sBL by CSR mechanism. In addition, eBL shows increased expression of *AICDA* and higher mutational burden but lower mutations in driver genes, compared to sBL. These results suggest differences in the B cell of origin or in the acquired mechanisms driving oncogenesis in both subtypes of BLs.

Intriguingly, approximately 25-50% of the BL patients show SOX11 overexpression. SOX11 expression associates with the age of BL patients at diagnosis, showing expression predominantly in pediatric cases. Moreover, *SOX11* is found in the transcriptional molecular signature used to classify BL. Although SOX11 has an impact role in MCL prognosis, no association between SOX11 expression and survival have been found in BL. Several in vitro and in vivo studies have shown the oncogenic role of SOX11 in the pathogenesis of MCL by blocking B-cell differentiation, activating BCR signaling, and promoting angiogenesis and a protective tumor microenvironment with immune evasive mechanisms. However, the contribution of SOX11 to BL pathogenesis and clinical evolution remains unknown.

In order to understand the clinical relevance of SOX11 in BL, we investigated the association of SOX11 expression with different clinical and pathological variables, including EBV infection, *MYC-IG* break and mutational status of recurrently mutated genes in pediatric and adult BL primary cases. In addition, to shed light on the role of SOX11 in the development of BL, we analyzed the changes in gene expression profile

and performed functional analysis upon SOX11 overexpression and knockout in BL cell lines.

2. RESULTS

2.1 SOX11 expression is exclusive of EBV- BL patients

To understand the clinical relevance of SOX11 in BL, we first investigated the association of *SOX11* expression with molecular and clinical features in BL patients. Interestingly, using RNA-seq and clinical data from 117 pediatric BLs (Grande et al., 2019), we observed a significant higher expression of *SOX11* in EBV- and in sporadic cases than in EBV+ and endemic BL primary cases (Figure 60A-B, respectively). Association between EBV status and *SOX11* expression in BL was validated in an independent series of pediatric and adult sBL cases (Richter et al., 2022; Burkhardt et al., 2022), with SOX11 IHC data. This analysis showed a statistically significant association between SOX11 positivity and EBV negativity, as all EBV+ BL patients were negative for SOX11 (17/17); while out of 164 EBV- cases, 91 were SOX11- (55%) and 73 SOX11+ (45%) (Fisher's exact test, p value < 0.0001) (Figure 60C). These results suggest that SOX11 may be exclusively expressed in EBV- BL patients. However, 3 patients with eBL which are EBV-, showed high expression of *SOX11 (*Figure 60C, red circle), suggesting that *SOX11* expression is significantly associated but not exclusive of sBL.

Recently, using a newly high-sensitive methodology to detect EBV infection (RNAscope for *EBNA1* mRNA), Mundo and coworkers detected traces of EBV infection in previously classified conventional EBV- BL cases (Mundo et al., 2020). Using this technology, capable of detecting single molecules and preserving tissue morphology on tissue sections, we found positive traces of EBV in 57% (4/7) of the conventional SOX11-/EBER- cases tested, while 1 of the conventional SOX11+/EBER- sBL cases tested resulted negative for EBV traces, reinforcing that SOX11 and EBV positivity are mutually exclusive in BL.

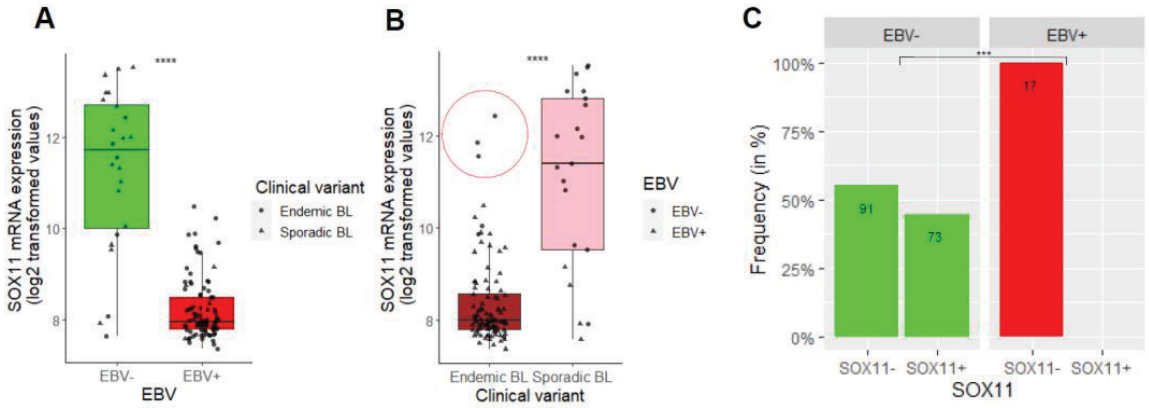

Figure 60. SOX11 is expressed exclussively in EBV- BL cases, suggesting a mutual exclussion in BL primary cases. (A-B) *SOX11* expression (log_2 transformed values) according to EBV status (EBV- and EBV+) **(A)** and clinical variant (eBL and sBL) **(B)** in 117 pediatric BL primary cases. Red circle highlights high *SOX11* expression in 3 eBL/EBV+ cases. Wilcoxon text was performed to test differences between groups. **(C)** Frequency of SOX11+ and SOX11- patients (by immunohistochemistry) in an independent series of pediatric and adult sBLs (n=181), according to EBV status. Fisher test was performed to test differences between group frequencies. *** P-value <0.001, **** P-value <0.0001.

2.2 *IG-MYC* translocation is predominantly generated by CSR in EBV-/SOX11+ BL

The *IG-MYC* break is one of the first hits in BL pathogenesis. This translocation can involve *IGH*, *IGL* or *IGK* chains, and can be acquired by SHM or CSR mechanisms (López et al., 2022). In order to explore the association of SOX11 with different *IG* partner and mechanism of *IG-MYC* translocation, we analyzed in detail the *IG-MYC* breakpoints in EBV+, EBV-/SOX11- and EBV-/SOX11+ BL cases, using processed WGS data, and SOX11 expression by IHC or RNA-seq data (SOX11 cut-off of 10.5 log_2 transformed values) from the ICGC (López et al., 2019) and BLGSP (Grande et al., 2019) BL cases. We observed that around 60% of the EBV-/SOX11- BL cases carried an *IGH-MYC* translocation, and in lower proportion, an *IGL-MYC* or an *IGK-MYC* translocation, showing significant differences compared to EBV-/SOX11+ BL cases (96% of cases with an *IGH-MYC* translocation), but not to EBV+ (81% of cases with an *IGH-MYC* translocation). However, we did not find significant differences within *IG* chain partners in the *IG-MYC* translocation comparing EBV-/SOX11+ and EBV+ BL cases (Figure 61A left).

In addition, we observed that 87.5% of the EBV-/SOX11+ (21/24), 41% of the EBV-/SOX11- (7/17), and 35% of the EBV+ (24/68) BL cases had the breakpoint located in the switch region of the *IGH* gene, while 12.5% of the EBV-/SOX11+ (3/24), 53% of the EBV-/SOX11- (9/17), and 59% of the EBV+ (40/68) BL cases had the breakpoint located in the V(D)J variable region of *IGH* or *IGL* as a result of SHM process (Figure 61A right). Only one case EBV+ seems to acquire the translocation by VDJ recombination process, while in a small subset of patients (3 EBV+ and 1 EBV-/SOX11-) it is not possible to discriminate between SHM or VDJ recombination. These results suggest that the *IG-MYC* translocation is predominantly generated by CSR in EBV-/SOX11+ BL cases, in EBV-/SOX11- cases is indistinctly generated by CSR or SHM mechanisms, and in EBV+ BLs is predominantly generated by SHM.

Besides, we observed lower *AICDA* and *BCL6* expression in EBV-/SOX11+ compared to EBV-/SOX11- and EBV+ BLs, although statistical significance was not achieved between EBV-/SOX11+ and EBV-/SOX11- cases (Figure 61B).

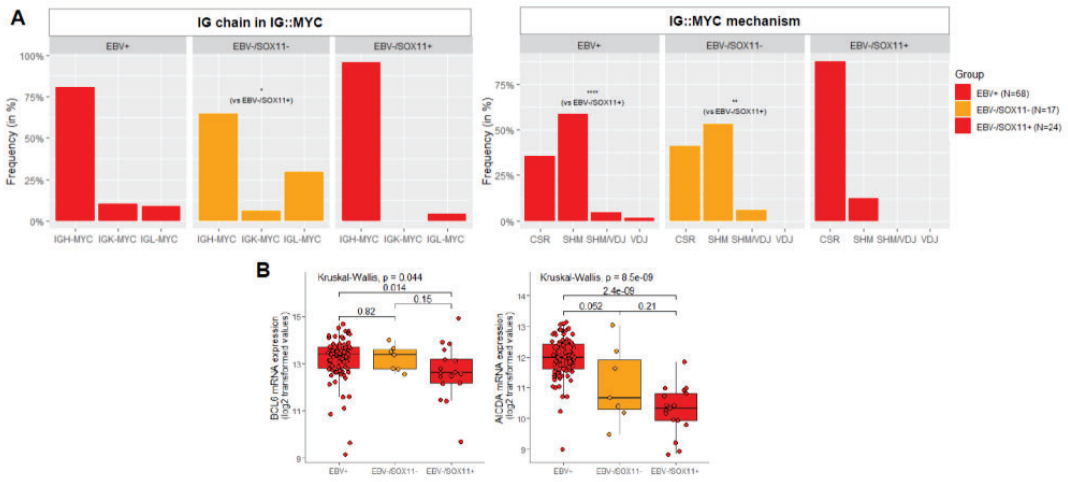

Figure 61. *IG-MYC* translocation in BL primary cases according to SOX11 expression levels. **(A) (left)** Frequency of *IGH-MYC*, *IGK-MYC* and *IGL-MYC* translocations, and **(right)** frequency of translocations acquired by CSR, SHM, SHM/VDJ or VDJ processes, in EBV+ (n=68), EBV-/SOX11- (n=17) and EBV-/SOX11+ (n=24) BLs. Fisher test was performed to evaluate differences between group frequencies. **(B)** *AICDA* and *BCL6* mRNA expression (log_2 transformed values) in EBV+ (n=93), EBV-/SOX11- (n=7) and EBV-/SOX11+ (n=17) BL cases. To test differences Kruskall-wallis was performed, and to evaluate pairwise differences, Wilcoxon test was used. * P-value <0.05, ** P-value <0.01, **** P-value <0.0001.

2.3 Mutational landscape of EBV+, EBV-/SOX11+ and EBV-/SOX11- BL primary cases

Several genes are recurrently mutated in BL, promoting oncogenic mechanisms in tumor cells (Schmitz et al., 2014; Roschewski et al., 2022). Here, we used previously published and processed WGS, and *SOX11* expression data (obtained by RNA-seq, cut-off of 10.5 log_2 transformed values) from 117 pediatric endemic and sporadic BL patients from the BLGSP (Grande et al., 2019), processed WGS data and SOX11 IHC of 24 pediatric sBL cases from the ICGC (López et al., 2019), and target mutational data of BL associated genes combined with SOX11 IHC of two different series with 91 pediatric and adults (Richter et al., 2022), and 51 (Burkhardt et al., 2022) pediatric sBL cases. We identified 19 coding genes mutated in more than 5% of the total BL cases (Figure 62). Several of these recurrently mutated genes are involved in BCR signaling, proliferation, SWI/SNF complex, sphingosine-1-phosphate pathway and epigenetic regulation, among other pathways.

To investigate a possible association between SOX11 expression and a specific mutational pattern in BL, we compared the frequencies of mutated genes in EBV+, EBV-/SOX11- and EBV-/SOX11+ BLs. We observed significant differences in the frequency of *CCND3*, *DDX3X*, *FOXO1*, *ID3*, *P2RY8*, *RFX7*, *SMARCA4* and *TP53* mutations between these groups of patients (Figure 62 left panel, q value <0.1). *CCND3*, *FOXO1*, *P2RY8* and *TP53* mutations seemed to be influenced by EBV, as pairwise comparisons showed that EBV-/SOX11- and EBV-/SOX11+ BLs share a higher frequency of mutations in *CCND3*, *P2RY8* and *TP53* genes, and lower in *FOXO1* gene than EBV+ BLs (q value <0.1) (Table 7). However, other differences cannot be attributed to the EBV status. For instance, EBV+ BL cases showed significantly more mutations in *DDX3X* and fewer in *RFX7* (62.11% and 2.11%, respectively) compared to EBV-/SOX11+ (35.29% and 16.18%, respectively; q value = 0.001 and 0.003), but not to EBV-/SOX11- (44.83% and 3.45%, respectively). In addition, EBV-/SOX11+ had a significantly higher frequency of mutations in *SMARCA4* and *ID3* (44.12% and 80.95%, respectively)

compared to EBV-/SOX11- (17.24% and 63.29%, respectively; q value = 0.057 in both comparisons) and EBV+ BLs (9.47% and 34.55%, respectively; q values < 0.0001).

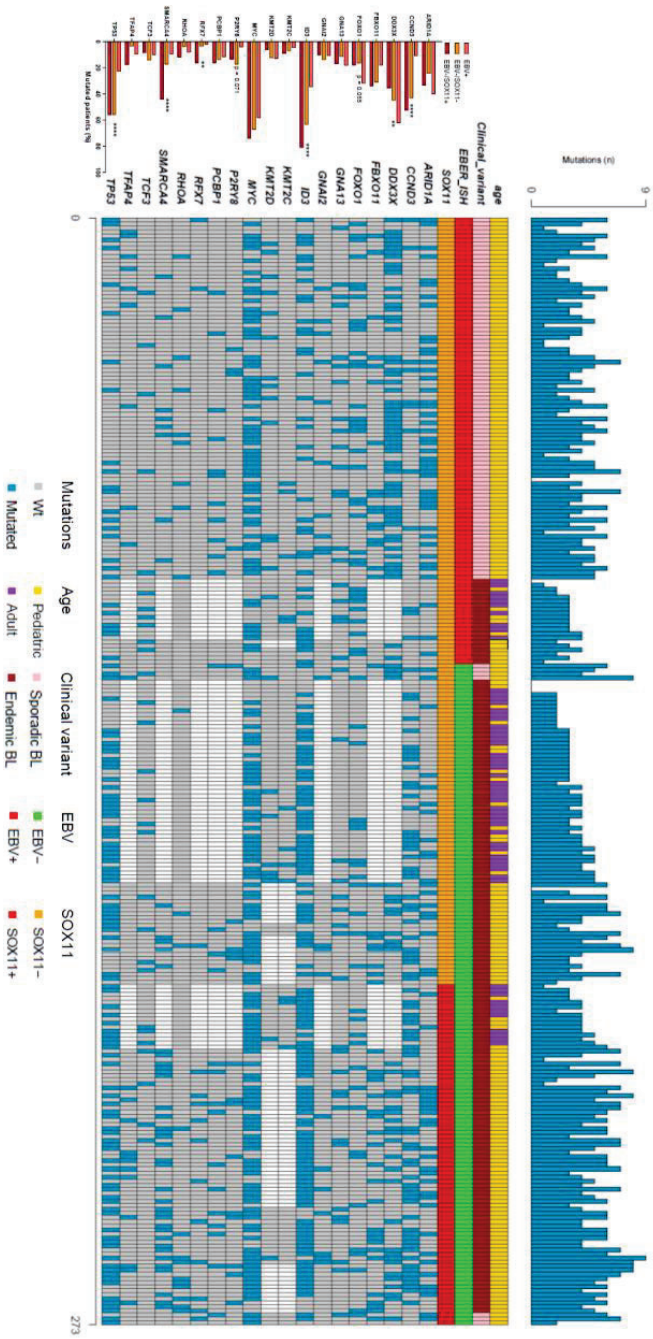

Figure 62. Mutational profile of BL primary cases according to EBV status and SOX11 expression. (Right) Mutational analysis in recurrently mutated driver genes of 273 BL primary cases. Mutations, EBV and SOX11 status, age (pediatric or adult) and clinical variant are shown. **(Left)** Frequencies of mutated cases in EBV+, EBV-/SOX11- and EBV-/SOX11+ for each gene are shown. Fisher's exact test with FDR correction was performed to evaluate differences in the frequencies between groups. **** P-value <0.0001, ** P-value <0.01.

Table 7. Frequency of BL patients with mutations in BL recurrently mutated genes, comparing EBV+, EBV-/SOX11- and EBV-/SOX11+ groups. P-values and q-values adjusted with FDR obtained with Fisher test are shown to test differences between groups. Significant q values (< 0.1) are highlighted in red.

Genes	EBV+ (% Mutated)	EBV- /SOX11- (% Mutated)	EBV- /SOX11+ (% Mutated)	q value EBV+ vs EBV- /SOX11-	q value EBV+ vs EBV- /SOX11+	q value EBV- /SOX11- vs EBV- /SOX11+
TP53	22.73	55.70	55.95	1.64E-05	5.46E-06	1.00E+00
SMARCA4	9.47	17.24	44.12	3.58E-01	1.42E-06	5.69E-02
RFX7	2.11	3.45	16.18	5.54E-01	2.62E-03	2.70E-01
P2RY8	4.21	17.24	13.24	5.09E-02	4.36E-02	9.58E-01
ID3	34.55	63.29	80.95	3.09E-04	5.95E-10	5.69E-02
FOXO1	31.82	16.46	17.86	3.64E-02	3.62E-02	9.58E-01
DDX3X	62.11	44.83	35.29	1.76E-01	1.38E-03	7.90E-01
CCND3	10.91	43.04	52.38	5.83E-06	1.25E-09	5.46E-01

In summary, we identified a specific mutational profile in EBV-/SOX11+ and EBV-/SOX11- BL patients, demonstrating that both EBV infection and SOX11 expression capture a distinguished mutational pattern in BL.

2.4 Transcriptional regulation of *SOX11* in BL

In MCL, the promoter region of *SOX11* contacts in a DNA 3D loop with a distal enhancer region (Queirós et al., 2016; Vilarrasa-Blasi et al., 2022). We analyzed the chromatin landscape of *SOX11* promoter and distal enhancer regions in one SOX11+ (BL2) and one SOX11- (DG75) BL cell lines. Then, we compared them with the chromatin landscape of SOX11+ and SOX11- MCLs, as well as normal B cells, obtained from BLUEPRINT consortium (Queirós et al., 2016; Beekman, Chapaprieta, et al., 2018; Vilarrasa-Blasi et al., 2021). We observed chromatin activating marks in the promoter region of *SOX11* in SOX11+ MCLs and in both BL cell lines, independently of SOX11 status (Figure 63, left panel). In addition, BL cell lines have strong and weak enhancer chromatin states in the same distal enhancer region found in SOX11+ MCLs. However, BL cells showed a similar chromatin remodeling to that found in germinal center b cells

(GCBC), with strong enhancer states in ATAC-seq peaks 2 and 3 (in blue), but absence of histone marks in the peak 1 (in blue), which is considered the specific strong enhancer peak in SOX11+ MCLs.

Thus, a different mechanism that the one observed in MCL may be regulating SOX11 expression in BL cells.

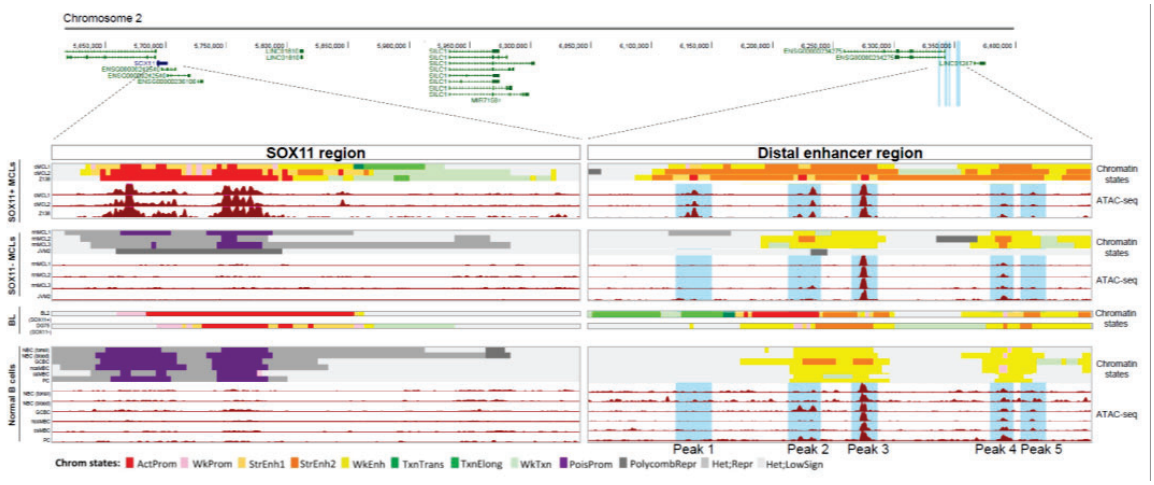

Figure 63. Chromatin landscape in *SOX11* promoter, exon and and distal enhancer regions. Chromatin states and chromatin accessibility (by ATAC-seq) in SOX11 (GRCh38/hg38 version, chr2: 5,689,354-5,710,132) and distal enhancer (GRCh38/hg38 version, chr2: 6,332,588-6,356,265) regions in SOX11+ MCLs (cMCL1 and cMCL2 primary cases and Z138 cell line), SOX11- MCLs (nnMCL1, nnMCL2 and nnMCL3 primary cases and JVM2 cell line), BL cell lines (BL2, SOX11+; DG75, SOX11-) and normal B cells (naïve B cells of tonsil and blood [NBC], germinal center B cells [GCBC], non-class-switched and class-switched memory B cells [ncsMBC, csMBC], and plasma cells [PC]), data generated in the BLUEPRINT consortium. Data includes different histone modification marks (H3K4me3, H3K27ac, H3K4me1, H3K36me3, H3K9me3, H3K27me3) by ChIP-seq, used to generate the chromatin states (bottom legend) and chromatin accessibility by ATAC-seq (signal from 0 to 40). ATAC-seq peaks in distal enhancer region are highlighted with blue.

2.5 Oncogenic pathways regulated by SOX11 in BL cell lines

In order to identify oncogenic pathways regulated by SOX11 in BL cells, we first generated a stable transfected BL cell line ectopically overexpressing SOX11 fused to the hormone binding domain of the estrogen receptor (ER-SOX11) in DG75 SOX11- BL cell line (Figure 64A). We used the 4-Hydroxytamoxifen (4-OHT) inducible system, that

allowed ER-SOX11 fusion protein to enter into the nucleus when DG75 ER-SOX11 cells were treated with 4-OHT (Figure 64B), enabling its transcriptional function. We found that our system was slightly leaky, as we detected SOX11 protein in the nucleus in DG75 ER-SOX11 cells non-treated with 4-OHT (Figure 64B). For this reason, we decided to analyze differential gene expression profile, comparing DG75 ER-SOX11 cells with control DG75 ER cells, both treated with 4-OHT for 8 or 24 hours.

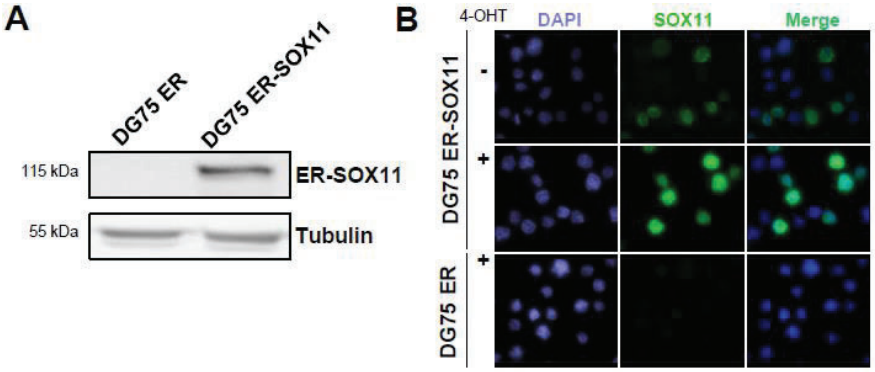

Figure 64. ER-SOX11 protein overexpression using the 4-OHT inducible system in stable transfected DG75 cell line. (A) Western blot experiment showing the levels of ER-SOX11 protein in DG75 ER-SOX11 BL cell line after 24h of 4-OHT treatment, DG75-ER was used as negative SOX11 expressing cell line and tubulin as loading control. **(B)** Immunofluorescence experiments showing the nuclear localization of the SOX11 protein in DG75 ER-SOX11 cells, DG75 ER cell line was used as SOX11 negative control, induced with 4-OHT for 24h. DAPI mark the cellular nucleus, and merge of the two immunofluorescences images (DAPI and SOX11) was done.

PCA showed that the variability between samples was significantly higher due to SOX11 overexpression (85% of the variance, PC1) than by time of induction (8 or 24 hours) (4% of the variance, PC2) (Figure 65A). Indeed, more than 65% of differential expressed genes upon SOX11 expression at 8h overlapped with the ones at 24h of induction (Figure 65B), suggesting similar changes in gene regulation at both hours.

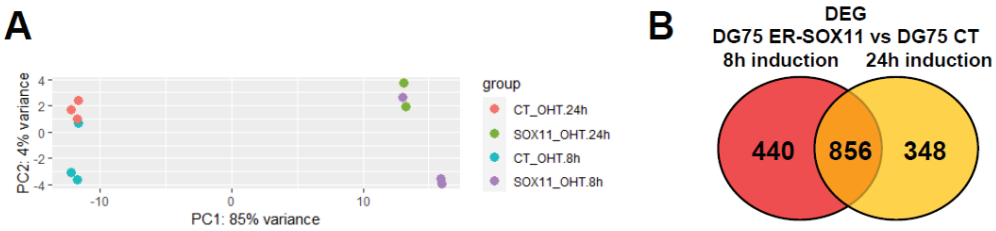

Figure 65. Different time points of 4-OHT exposition do not impact gene expression in DG75-ER-SOX11 BL cell line. (A) Principal component analysis on RNA-seq data from DG75-ER-

SOX11 and -CT BL cell lines upon 4-OHT induction for 8h and 24h. Principal components 1 and 2 are shown. **(B)** Overlap between differential expressed genes after 8h (in red, 1296 genes) and 24h (in yellow, 1204 genes) of SOX11 induction in DG75 ER-SOX11 BL cell line compared to DG75 CT.

For this reason, we grouped the samples from the two time points together to identify SOX11-specific gene expression profile in DG75 BL cell line. We found 866 upregulated and 828 downregulated genes in 4-OHT treated DG75 ER-SOX11 compared to control cell lines (Figure 66A-B and Appendix Table 14). By pathway enrichment analysis, we found that upregulated genes in DG75 ER-SOX11 were enriched in angiogenesis, integrins and G-protein signaling pathways, whereas downregulated genes were enriched in genes related to cadherin and Wnt, among others regulatory signaling pathways (Figure 66C).

In parallel, we generated a second SOX11+ BL cell line model, by lentiviral transduction of another SOX11- BL cell line (Ramos) using a lentiviral vector to constitutively overexpress FLAG-SOX11 protein (Ramos-SOX11) (Figure 67A). RNA-seq gene expression profiling experiments showed that 75 genes were upregulated and 11 downregulated genes, in Ramos-SOX11 compared to Ramos-CT (transduced cells with empty vector) (Figure 67B and Appendix Table 15).

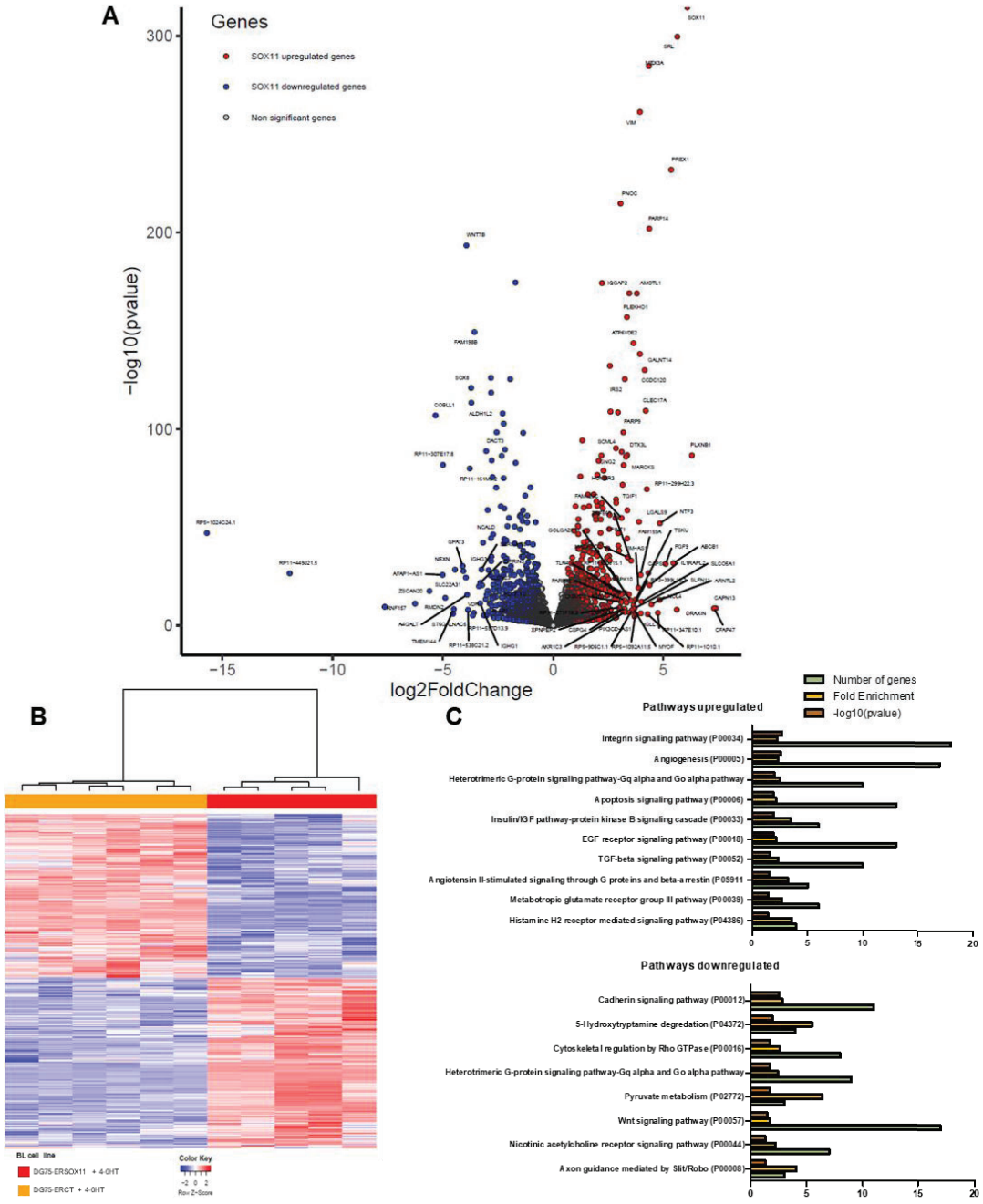

Figure 66. Gene expression analysis upon SOX11 overexpression in DG75-ER-SOX11 BL cell line. (A) Genes differentially expressed after SOX11 induction in DG75 ER-SOX11 compared to DG75 ER BL cell lines obtained by RNA-seq. The graph shows on the y-axis -log (P-value) and on the x-axis the log2-transformed fold change. Genes upregulated and downregulated in DG75 ER-SOX11 vs DG75 CT with an adjusted P-value <0.1 and log2-transformed fold change >0.65 or <-0.65 are colored in red and blue, respectively, and genes with an adjusted P-value < 0.00005 and absolute log2-transformed fold change >3 are labeled with their Gene Symbol. **(B)** Heatmap illustrating the scaled expression (Z-score) of 1694 differential expressed genes (866 upregulated

and 828 downregulated genes; Supplementary Table 1) in DG75-ERSOX11 compared to DG75 CT cell lines induced with 4-OHT for 8 and 24h, obtained by RNA-seq. Genes with an adjusted P-value <0.1 and absolute log2-transformed fold change >0.65 were considered. **(C)** Panther pathway enrichment analysis using differential expressed genes upregulated **(Top)** and downregulated **(Bottom)** between DG75-ER-SOX11 and DG75-ER after 4-OHT induction. Number of genes, fold enrichment and –log10(p value) for each pathway are shown. Only pathways with a p value <0.05 were considered.

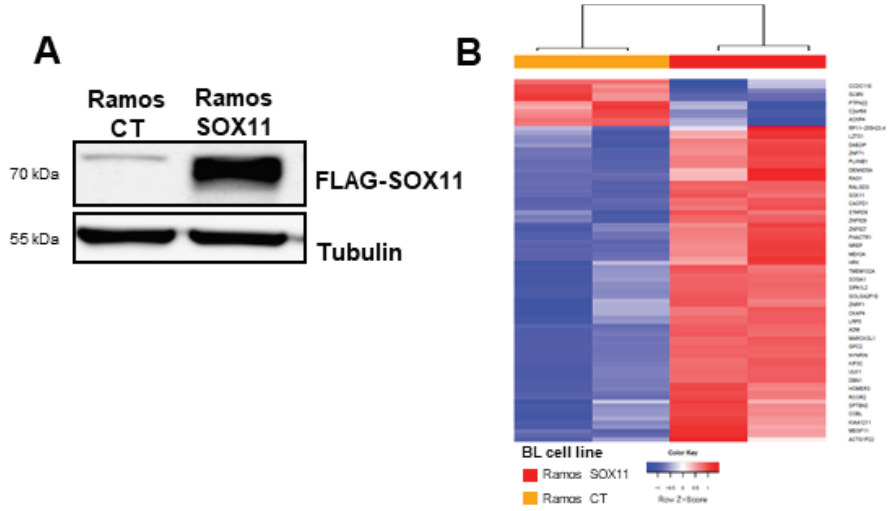

Figure 67. Gene expression analysis upon SOX11 overexpression in Ramos-SOX11 BL cell line. (A) Western blot experiments showing the constitutive overexpression of SOX11 FLAG-tagged protein in Ramos SOX11+ compared to the SOX11- control Ramos-CT BL cell lines. Tubulin was used as a loading control**. (B)** Heatmap showing scaled expression (Row Z-score) of 75 upregulated and 11 downregulated genes upon SOX11 overexpression in Ramos cell line, obtained by RNA-seq. Genes with an adjusted P-value <0.15 and absolute log2-transformed fold change >0.5 were considered.

GSEA using the gene expression profile of DG75 ER-SOX11 and Ramos-SOX11, compared to their respective controls, and all the curated gene sets (C2) from the Molecular Signatures Database (https://www.gsea-msigdb.org/gsea/msigdb/), showed that 8 gene sets found enriched in the SOX11+ BL cells overlapped between DG75 ER-SOX11 and Ramos-SOX11 cell lines (Figure 68A and Appendix Table 16). HUMMEL_BURKITTS_LYMPHOMA_UP signature (Appendix Table 16), that includes genes found upregulated in the BL molecular signature (Hummel et al., 2006) was one of the most statistically significant enriched gene sets. In fact, using the BL molecular signature DG75 ER-SOX11 and DG75 ER samples clustered separately

(Figure 68B), suggesting that this signature could be used to separate SOX11+ than SOX11- BL cell lines.

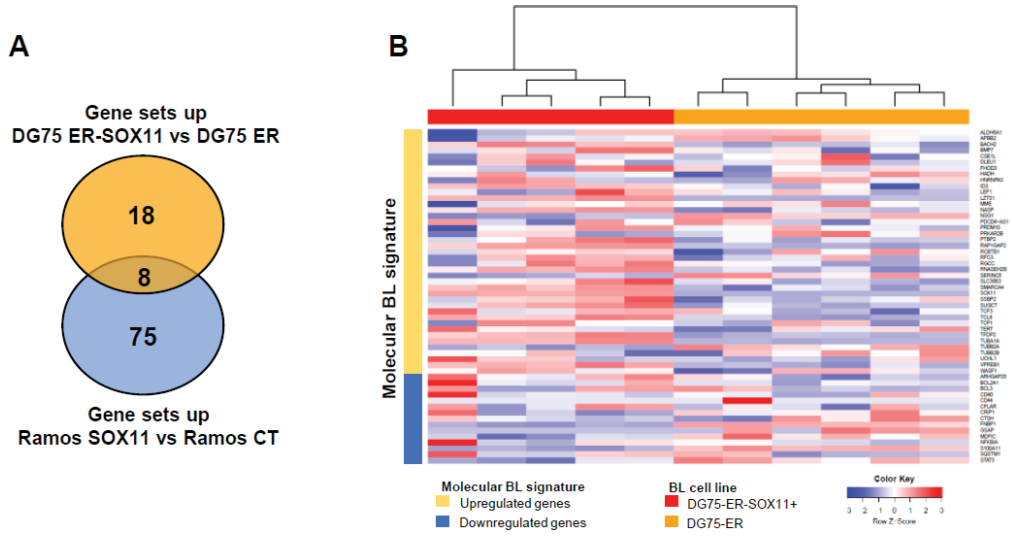

Figure 68. Signaling pathways regulated by SOX11 in BL cell lines. (A) Overlap of enriched gene sets from C2 curated database (GSEA) in DG75 ER-SOX11 compared to DG75 CT (in orange, 26 gene sets), and Ramos-SOX11 compared to Ramos CT (in blue, 83 gene sets). **(B)** Scaled expression of genes (row z-score) from the molecular BL signature (56/58 genes found in RNA-seq data) in DG75 ER-SOX11 and DG75 CT RNA-seq data. Genes usually upregulated in the molecular BL signature are shown in yellow and genes downregulated in blue (left).

2.6 SOX11-related BL signature

To identify a SOX11-specific BL signature, we overlapped differential expressed genes in DG75 (Appendix Table 14) and Ramos (Appendix Table 15) upon SOX11 overexpression obtaining 46 genes commonly regulated by SOX11 in BL cell lines (Figure 69 and Appendix Table 17).

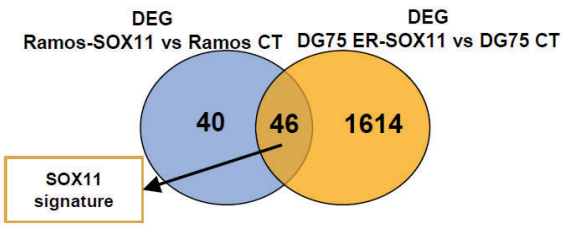

Figure 69. The SOX11 signature in BL. (A) Overlap of differential expressed genes between Ramos-SOX11 vs Ramos-CT (in blue, 86 genes, adjusted P-value <0.15 and absolute log_2-

transformed fold change >0.5) and DG75 ER-SOX11 vs DG75 CT (in orange, 1660 genes, adjusted P-value <0.1 and absolute log_2-transformed fold change >0.65).

Next, we knocked out SOX11 using the CRISPR-Cas9 gene editing system in the SOX11+ BL2 cell line (BL2-SOX11KO). Five different clones showed efficient SOX11 knock out, compared to other five control clones (Figure 70A). We performed RNA-seq in 2 of the clones and performed clustering analysis using the SOX11-specific BL signature (Appendix Table 17). Gene expression clustering analysis showed that BL2-SOX11KO clones clustered together in a separate group than the BL2 CT clones, suggesting that BL2 CT cell lines shared SOX11-specific signature lost in BL2-SOX11KO clones (Figure 70B).

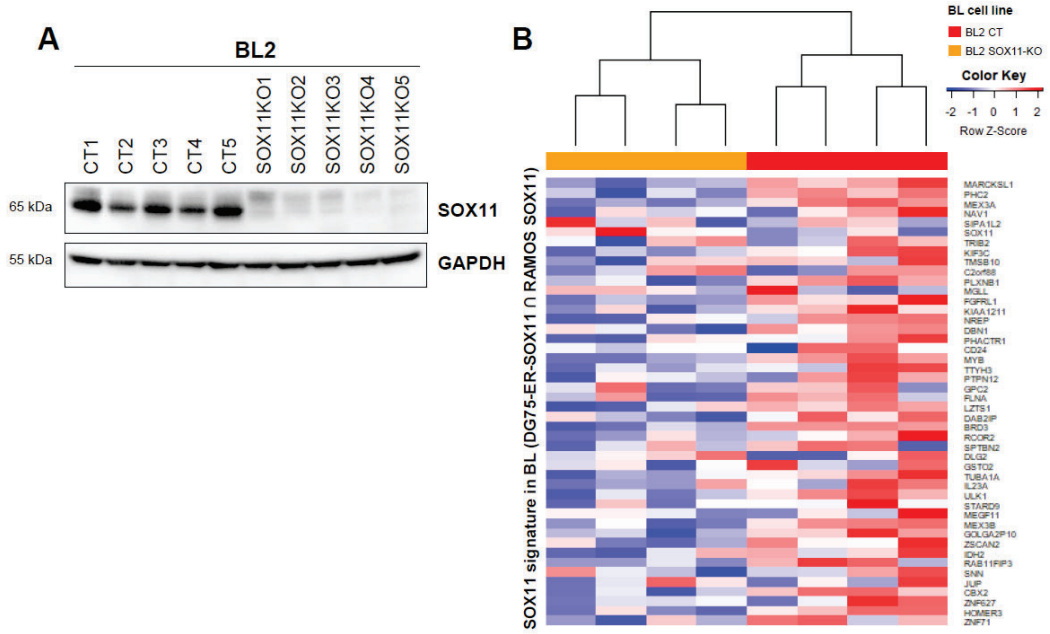

Figure 70. Loss of the SOX11-specific BL signature in BL2-SOX11KO cell lines. (A) SOX11 protein levels in BL2-SOX11KO and control SOX11+ BL2-CT clones. GAPDH was used as a loading control. **(B)** Row scaled expression (Z-score) of genes from the SOX11-specific BL signature (differentially expressed genes overlapping between DG75 ER-SOX11 and Ramos-SOX11) in RNA-seq data of BL2 CT and BL2-SOX11KO samples.

Interestingly, we performed k-means clustering analysis in two series of BL primary cases (117 pediatric (BLGSP) and 44 mBL adult (GSE4475), with available RNA-seq and gene expression microarray data, respectively) using the SOX11-specific BL signature (found in BL cell lines, Appendix Table 17). We observed that BL cases

clustered separately according to SOX11 high and low expression levels (Figure 71A). Moreover, most of the genes included in the SOX11-specific BL signature significantly correlated between them and with SOX11 expression, in both BL series (Figure 71B).

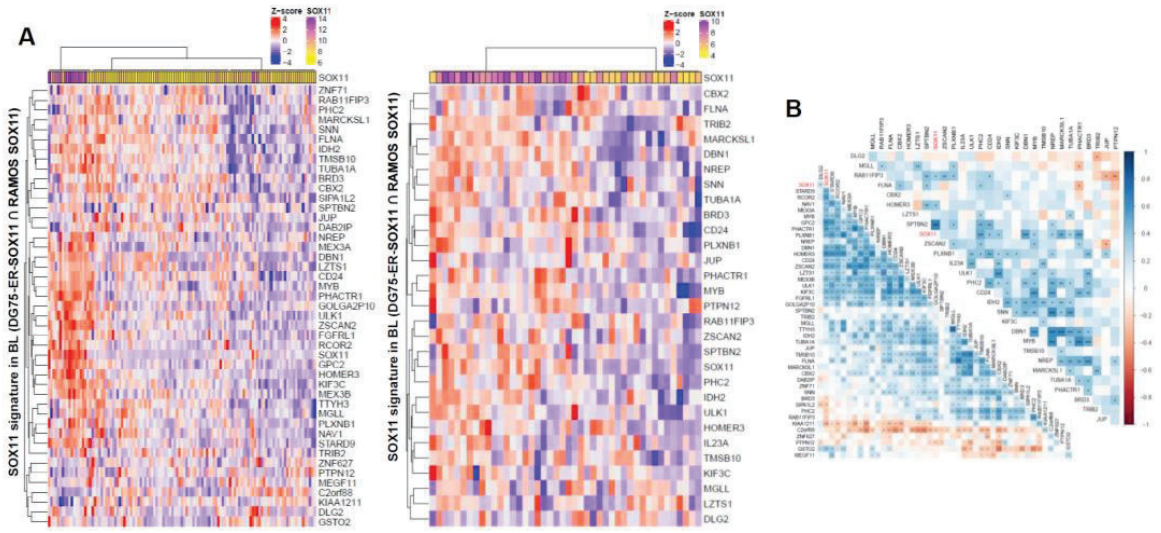

Figure 71. SOX11-specific BL signature in BL primary cases according to *SOX11* expression. **(A)** Row scaled expression (Z-score) of genes from the SOX11-specific BL signature (differentially expressed genes overlapping between DG75 ER-SOX11 and Ramos-SOX11) in RNA-seq data of 117 pediatric endemic and sporadic BL primary cases **(left)**, and in microarray data of 45 sporadic molecular BL primary cases **(right)**. K-means clustering was performed to separate samples in k=3 **(left)** and k=2 **(right)** groups. SOX11 expression is shown in top panel in each heatmap. **(B)** Correlation plots between the genes of the SOX11-specific BL signature in RNA-seq data of 117 pediatric endemic and sporadic BLs **(left)**, and in microarray data of 45 sporadic molecular BL primary cases **(right)**. Blue and red showed positive and negative pearson correlation coefficients, respectively. P-values from pearson correlation are shown: * <0.05, ** <0.01, *** <0.001.

These results suggest that the SOX11-specific BL signature found in transduced cell lines is also reproduced in BL primary cases, and that the genes included in this signature might be directly or indirectly regulated by SOX11 in BL cells.

2.7 Comparison between SOX11 functional role in MCL and BL

SOX11 is a transcription factor that directly regulates transcription of genes involved in MCL oncogenic pathways (Beekman, Amador, et al., 2018). Interestingly, GSEA showed that genes upregulated in cMCL/SOX11+ vs nnMCL/SOX11- primary

cases (Appendix Table 5), and genes upregulated in Z138CT vs Z138-SOX11KO MCL cell lines (Figure 37A), were enriched in 4-OHT-treated DG75 ER-SOX11 and in Ramos-SOX11 cells compared to their respective control cell lines, DG75 ER and Ramos-CT (Figure 72A)

In order to identify common direct SOX11-target genes in MCL and BL cells, we overlapped the differential expressed genes upon SOX11 overexpression in DG75 ER-SOX11 (Appendix Table 14) and SOX11 KO in Z138 MCL cell lines (Z138-SOX11KO), and SOX11-direct target genes in MCL (SOX11 target genes), identified by ChIP-chip in Z138 MCL cell line (Vegliante et al., 2013) (Figure 34A). We observed that around 11% (185/1660 genes) of the differentially expressed genes in DG75 ER-SOX11 BL cell line overlapped with those differentially expressed in Z138 SOX11+ MCL cell line (Figure 72B, top). Furthermore, 22 of the 185 commonly dysregulated genes between SOX11+ and SOX11- cell lines in both lymphomas overlapped with genes directly regulated by SOX11 in MCL. The 297 common genes (red circle, Figure 72B, top) between DG75 BL and Z138 MCL cell lines were involved in oxidative stress, heterotrimeric G proteins, chemokines and cytokines, integrins, angiogenesis and PDGF signaling pathways (Figure 72B, bottom).

Then, we decided to validate selected genes (*PLXNB1*, *CD24* and *MEX3A*) found differentially expressed according to SOX11 expression in both lymphomas, MCL and BL (red circle, Figure 72B, top). By qRT-PCR, we observed that *PLXNB1*, *CD24* and *MEX3A* showed increased expression upon SOX11 overexpression in BL and MCL (DG75 ER-SOX11, Ramos-SOX11, JVM2-SOX11+), and decreased expression after SOX11-KO (BL2-SOX11KO and Z138-SOX11KO), compared to respective control cells (Figure 72C left and right, respectively). Moreover, MEX3A and CD24 proteins increased in SOX11-overexpressing and/or decreased in SOX11-KO BL and MCL cells (Figure 72D-E, respectively).

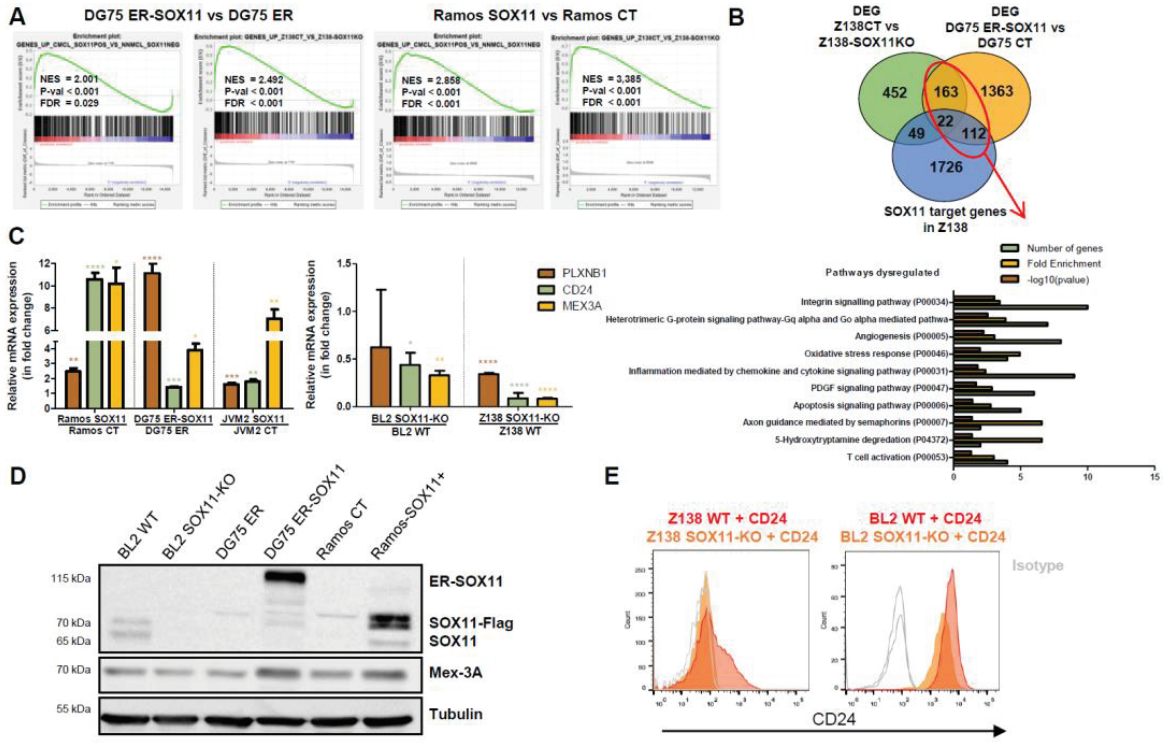

Figure 72. SOX11 shares similar transcriptional roles in MCL and BL. (A) Enrichment of SOX11-upregulated genes sets in MCL primary cases (upregulated in cMCL/SOX11+ vs nnMCL/SOX11-; GENES_UP_CMCL_SOX11POS_VS_NNMCL_SOX11NEG) and Z138 MCL cell lines (upregulated in Z138CT vs Z138-SOX11KO MCL cell lines; GENES_UP_Z138CT_VS_Z138-SOX11KO), in DG75 ER-SOX11 compared to DG75-ER and in Ramos-SOX11 vs Ramos-CT cell lines. NES, P-value (P-val) and FDR are shown. **(B) (Top)** Overlap between differentially expressed genes in 4-OHT induced DG75 ER-SOX11 BL cell line (in yellow, 1660 genes), upon SOX11 KO in Z138 MCL cell line (in green, 686 genes), and SOX11 target genes in MCL found by ChIP on chip in Z138 cell line (in blue, 1909 genes). **(Bottom)** Pathway enrichment analysis on common genes between differentially expressed genes in DG75-ER-SOX11 BL cells, and upon SOX11 KO in Z138 MCL cells and SOX11 targets genes obtained by ChIP on chip in Z138 MCL cells (red circle). Number of genes, fold enrichment and –log10(p value) for each pathway are shown. **(C)** *PLXNB1*, *CD24* and *MEX3A* relative mRNA expression (normalized to *GUSB* endogenous control) in BL and MCL SOX11-overexpressing cell lines (left, Ramos-SOX11, DG75 ER-SOX11 and JVM2-SOX11), and in SOX11-KO BL and MCL cell lines (right, BL2-SOX11KO and Z138-SOX11KO). Data is shown as mean ± standard deviation of the fold change between SOX11-overexpressing or SOX11-KO and control cells values, obtained in 3 independent experiments. Statistical significance was obtained by unpaired two-tailed Student t-test. **(D)** Western blot experiments showing MEX3A and SOX11 protein levels (ER-SOX11, SOX11-FLAG or endogenous SOX11) in BL2 SOX11-KO, DG75 ER-SOX11, and Ramos SOX11 and their control cell lines BL2 WT, DG75 ER and Ramos CT. Tubulin was used as a loading

control. **(E)** Histograms showing CD24 protein levels analyzed by flow cytometry experiments in Z138 and BL2 SOX11-KO MCL and BL cell line models and their respective controls. CD24 staining is shown in red for SOX11+ cells and in orange for SOX11- cells, whereas isotype controls are shown in grey.

SOX11 promotes the migration and transmigration of MCL cells towards stromal cells through the activation of *CXCR4* and *FAK* expression (Balsas et al., 2017). In BL cells, SOX11 overexpression showed dysregulation of genes involved in chemokines and integrin-related signaling pathways, suggesting that SOX11 could be involved in similar migration-related pathways to those in MCL cells. Thus, we explored in our RNA-seq gene expression profile data the regulation of chemokine receptors and/or integrin of our SOX11-overexpressing BL cell line models, compared to its control cell lines. We observed that *CXCR5*, *CCR7* and *ITGB7* were significantly upregulated in 4-OHT treated DG75 ER-SOX11 compared to DG75 ER control cells (Figure 73A). CXCR5 is the chemokine receptor of CXCL13 cytokine. However, we did not observe a significant higher tumor cell migration towards CXCL13 or adhesion to SNKT stromal cells comparing SOX11+ and SOX11- BL cell line models (data not shown). VCAM-1 is one of the glycoproteins that interact with integrin α4β7 (ITGA4 and ITGB7). Interestingly, we observed a significant higher adhesion of SOX11+ cells to VCAM-1 than SOX11- BL cells (Figure 73B).

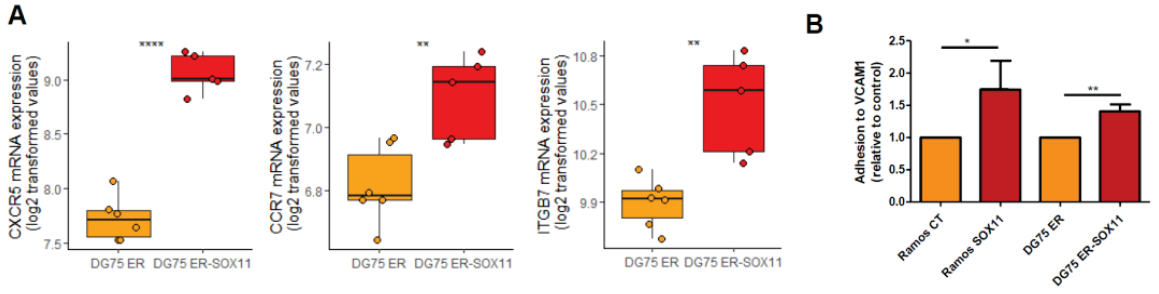

Figure 73. SOX11+ BL cells have more adhesion to VCAM-1. (A) *CXCR5*, *CCR7* and *ITGB7* expression (log_2 transformed values) in DG75 ER and DG75 ER-SOX11, obtained by RNA-seq. **(B)** Relative adhesion to VCAM-1 measured as the ratio of fluorescence emission of calcein-labeled cells between those that have been attached to untreated microplate wells precoated with VCAM-1 and those attached in an unspecific way (VCAM-1 adhesion/inespecific cell adhesion in BSA 0.5%). Statistical significance was obtained by unpaired two-tailed Student t-test. * P-value <0.05, ** P-value < 0.01, **** P-value < 0.0001.

Kuo and coworkers generated an Eμ-SOX11 transgenic mice and observed that in vivo, SOX11 induces the activation of the BCR pathway in MCL-like tumor cells (Kuo et al., 2018). Our in vitro experiments did not show significant differences in BCR-mediated downstream pathway activation, between SOX11+ and SOX11- BL cell line models stimulated with IgM (data not shown).

Overall, our results demonstrate that, although SOX11 regulates genes involved in similar signaling pathway in BL and MCL, some of the already demonstrated oncogenic functions of SOX11 in MCL, as tumor cell migration or activation of the BCR signaling pathway, are not recapitulated in BL cell lines. On the other hand, upregulation of ITGB7 and increased adhesion to VCAM-1 in SOX11+ compared to SOX11- BL cells, suggest that SOX11 promotes cell adhesion mediated by integrin's in BL.

DISCUSSION

Activation of oncogenes and inhibition of tumor suppressor genes are key events in the development of many types of tumors. This may be achieved by different mechanisms, such as gene mutations (Campbell et al., 2020) and gene expression changes caused by epigenetic dysregulation or dysregulation of RNA stability, processing and translation, among others (White & Sharrocks, 2010). These mechanisms can lead to the abnormal activation of oncogenes or inhibition of tumor suppressor genes, ultimately resulting in uncontrolled cell growth, resistance to therapies, and tumor progression. The characterization of these mechanisms is essential to understand the oncogenic mechanisms of tumors.

Chromosomal translocations that occur in B cell lymphomas are a well-known example of oncogene activation (Küppers & Dalla-Favera, 2001). These translocations involve the fusion of *IG* genes with a proto-oncogene, leading to the constitutive activation of an oncogene. Although these translocations are a well-known cause of oncogene activation in B cells, they are not sufficient on their own to induce tumorigenesis (Schüler et al., 2009; Müller et al., 1995). B cell lymphomas require additional oncogenic mechanisms to become fully transformed and malignant (Shaffer et al., 2012). Thus, the understanding of the secondary oncogenic mechanisms that drive tumor development is crucial to develop effective treatments for cancer.

My thesis' aims were to unravel the mechanisms involved in the aberrant overactivation of specific oncogenes and to characterize their functional role in aggressive B cell lymphomas, contributing to understand the molecular basis of lymphomagenesis and ultimately improve patient's outcomes.

SOX11 is a transcription factor expressed in progenitors and embryonic stem cells that regulates proliferation and cell fate (Vegliante et al., 2011; Larson et al., 2010; Yu et al., 2020; Haslinger et al., 2009), along with other SOX factors (Bergsland et al., 2011). Additionally, SOX11 is upregulated in some undifferentiated tumor cells with CSC features, enhancing CSC properties and promoting drug resistance in tumor cells (Tirosh et al., 2016; Oliemuller et al., 2017; Tsang et al., 2021). SOX11 is aberrantly overexpressed in MCL, BL and ALL lymphoid neoplasms (Beekman, Amador, et al.,

2018). In MCL, SOX11 acts as an oncogene (Vegliante et al., 2013; Palomero et al., 2014, 2016; Balsas et al., 2017; Kuo et al., 2018; Balsas et al., 2021), and is predominantly overexpressed in the aggressive cMCL and negative or very weakly expressed in the nnMCL subtype. Furthermore, SOX11 overexpression is significantly associated with a worse prognosis in patients with MCL (Fernàndez et al., 2010).

Several studies have found evidences of CSC in MCL (Medina et al., 2014; Jung et al., 2011; Kim et al., 2015; Z. Chen et al., 2010), which may explain the recurrent relapses and poor responses to first line treatment in patients with cMCL. Since SOX11 is involved in progenitor's cell fate and contributes to enhance stemness-properties in some tumors, in **Study 1**, I investigated whether SOX11 could promote stem cell-like properties through the activation of stem cell-related genes in MCL. To achieve this main objective, I analyzed SOX11-target genes involved in stemness that might function as prognostic biomarkers and possible targets for new therapeutic strategies in aggressive MCLs.

In **Study 1**, we observed that the gene expression profile of SOX11+ MCL primary cases and cell lines showed a significant enrichment in hematopoietic and leukemic stem cell-related gene signatures, indicating that SOX11 might be involved in the regulation of stemness features in MCL. Several gene signature have been previously used as prognostic markers in MCL, including the proliferation signature, the L-MCL16 assay and a Cyclin D1-dependent transcriptional signature (Rosenwald et al., 2003; Clot et al., 2018; Demajo et al., 2021). In this study, we analyzed whether a SOX11-specific stem cell-related gene signature correlated with patients' overall survival in MCLs. However, the analyses did not show evidence for survival prediction using this signature within SOX11+ MCLs, suggesting that the prediction value observed was not independent of SOX11 expression.

Reanalysis of previously published ChIP-chip experiments in MCL cell lines revealed that SOX11 is directly regulating only *MSI2*, *PROX1*, *PRDM15*, and *SOX5* genes, within all stem cell-related genes differentially expressed between SOX11+ and SOX11- MCL primary cases. Gene expression profiling upon SOX11 knockout and

SOX11 ectopically overexpression reinforced these results, showing a significant downregulation and upregulation, respectively, of those genes in MCL cell lines.

Interestingly, MSI2 and PROX1 are involved in the regulation of mouse HSCs maintenance and commitment, but in opposite ways (Hope et al., 2010). MSI2 is highly expressed in HSCs, and its knockdown affects HSC repopulation, whereas its overexpression prevents differentiation, both in vitro and in vivo (Kharas et al., 2010; Hope et al., 2010; De Andrés-Aguayo et al., 2011). Specifically, MSI2 conditional ablation in mice models affects HSC quiescence and balancing between self-renewal and commitment, through dysregulation of the TGF-β signaling pathway (S.-M. Park et al., 2014). In addition, it has been described a CD133+ CSC population in MCL primary cells that exhibits high expression of MSI2 (Medina et al., 2014). Conversely, PROX1 acts as an antagonist of the HSC maintenance, as its downregulation promotes an enhanced expansion of the HSC compartment (Hope et al., 2010), and it is considered a tumor suppressor (Hope & Sauvageau, 2011). Despite having opposite roles in HSC function, both genes are upregulated in SOX11+ compared to SOX11- MCLs.

PRDM15 is a member of the PRDM family of transcription factors involved in cell identity and fate determination (Leszczyński et al., 2020). Moreover, it was recently described that PRDM15 promotes B cell lymphomagenesis through regulation of PI3K/AKT/mTOR signaling and glycolysis (Mzoughi et al., 2020). Finally, SOX5 is a SOXD transcription factor that plays a role in the activation of adult neural stem cells (L. Li et al., 2022) and is considered a tumor suppressor in brain stem cells (Kurtsdotter et al., 2017).

In MCL patients, only high levels of *MSI2* were significantly associated with lower survival rates, independently of other high-risk factors, including *TP53* and *CDKN2A* alterations, SOX11 expression and CNA. MSI2 is also overexpressed in other hematological malignancies, and has been linked to shorter survival in several diseases, such as chronic myeloid leukemia (CML), AML, myelodysplastic syndromes (MDS), CLL and B-ALL (Ito et al., 2010; Kharas et al., 2010; Byers et al., 2011; S. M. Park et al., 2015; Taggart et al., 2016; Palacios et al., 2021; Mu et al., 2013). In addition, MSI2 is

upregulated during the progression of CML; its levels are higher during aggressive blast crisis compared to the slow growing chronic phase of the disease (Ito et al., 2010; Kharas et al., 2010). Taken together, these results suggest that MSI2 could be considered as a prognostic biomarker in hematologic neoplasms, including MCL. Nonetheless, the number of patients in our study is limited, and a larger cohort of patients is needed to confirm its value as a prognostic biomarker in MCL.

The mechanism underlying MSI2 overexpression has not been thoroughly studied yet. Some studies suggest that HOXA9, MEIS1 and the fusion protein NUP98/HOXA13 can bind to the MSI2 promoter, increasing MSI2 expression (Ito et al., 2010; G. G. Wang et al., 2006; Di Giacomo et al., 2014). However, these three proteins are not expressed in all the tumors in which MSI2 is involved. Conversely, Palacios and colleagues have proposed that proliferative stimulus may increase MSI2 expression in CLL primary samples (Palacios et al., 2021).

In this study, we have demonstrated that SOX11 directly regulates MSI2 in MCL. SOX11 knockout and overexpression in MCL cell lines reduced and increased, respectively, the levels of MSI2 in MCL cells. Furthermore, rescue of SOX11 in SOX11-KO MCL cell line models increased MSI2 expression, reaching similar levels as Z138WT MCL cell line. Previously, SOX11-specific ChIP-chip experiments showed an enrichment of *MSI2* promoter regions in SOX11+ MCL cell lines (Vegliante et al., 2013). Now, we have demonstrated, through luciferase assays, that SOX11 directly activates MSI2 transcription by binding to its promoter, as only 293T adherent cells expressing SOX11-full length but not SOX11-ΔHMG (lacking the HMG domain), cotransfected with the promoter of *MSI2* in front of the luciferin gene, presented luciferase activity. These results suggest that SOX11 directly activates MSI2 transcription in MCL. Nevertheless, MSI2 is expressed in most SOX11- MCL cells, at low levels, and the modulation of MSI2 levels by SOX11 in SOX11-overexpressing and -knockout MCL cells is moderated. Taken together, these observations suggest that other factors might collaborate with SOX11 in the transcriptional regulation of MSI2 in MCL.

SOX11 knockout reduced colony growth while decreasing MSI2 levels in MCL cells, suggesting that SOX11 is involved in stemness features mainly through MSI2 transcriptional regulation. However, the impairment in colony formation was greater upon MSI2 silencing in SOX11-KO cells, indicating that MSI2 shows SOX11-independent effects on colony growth, and supporting that other factors might also contribute to MSI2 function on the regulation of self-renewal in MCL. Thus, further studies are needed to fully understand the regulation of MSI2 in MCL.

The analysis of the *MSI2* epigenetic landscape revealed that both naïve and memory B cells, which are considered the cells of origin of cMCL and nnMCL, respectively (Queirós et al., 2016; Navarro et al., 2012), showed low expression of MSI2 associated to active *MSI2* promoter and weak intronic enhancers, characterized by poor accessibility and hypermethylation. Interestingly, the *MSI2* locus exhibited chromatin remodeling towards strong enhancer states, increased accessibility, and hypomethylation in these regions in SOX11+ MCLs, but not in the SOX11-. These findings suggest that epigenetic changes may be modulating MSI2 overexpression in this tumor. However, additional experiments are needed to demonstrate the direct implication of these super-enhancers in the upregulation of MSI2 in aggressive MCLs. For instance, the silencing or activation of MSI2 enhancer regions through CRISPR interference (Fulco et al., 2016) or small activating RNAs (Ghanbarian et al., 2021) would confirm this hypothesis.

Although only the expression of *SOX11*, *SOX4* and *SOX12* has been confirmed in MCL (Wasik et al., 2013), SOX family factor binding motifs, including the SOX11 motif, were found in ATAC-seq peaks, which are localized in the intronic enhancer regions of *MSI2* and are specific to SOX11+ MCLs. Considering that SOX family factors act sequentially in the same progenitor cells genes to control differentiation and cell fate (Bergsland et al., 2011), it is not surprising to find multiple binding motifs for several SOX factors in *MSI2* enhancer regions. It was recently described that SOX2 and SOX11 may act as pioneer transcription factors inducing chromatin remodelation (Dodonova et al., 2020). The presence of SOX11 binding motifs around intronic enhancer regions modified in SOX11+ MCLs may indicate a role of this transcription factor in the

chromatin remodeling of these regions. Nevertheless, further studies confirming the binding of SOX11 to *MSI2* enhancer regions, and the chromatin remodeling of *MSI2* enhancer regions upon SOX11 overexpression in SOX11- MCL cell lines, could help to confirm this hypothesis.

MSI2 expression has been associated to gene expression changes and increased tumorigenesis in several solid (Kudinov et al., 2016; Fang et al., 2017; S. Wang et al., 2015) and hematological malignancies (Kharas et al., 2010; Ito et al., 2010; S. M. Park et al., 2015; Taggart et al., 2016; Palacios et al., 2021). Previous studies have demonstrated that MSI2 knockdown impairs blast crisis in in vitro and in vivo CML models, promoting differentiation and reduced clonogenic growth of leukemic cells (Ito et al., 2010). Kharas et al reported that MSI2 knockdown decreased proliferation and increased apoptosis and differentiation of AML and CML cell lines, associated to decreased expression of Wnt, Ras-MAPK and Myc signaling pathways (Kharas et al., 2010). In addition, depletion of MSI2 in Lin-Sca-1+c-Kit+ cells (LSK) with the MLL-AF9 translocation, characteristic of mixed-lineage leukemia's (MLL), reduced clonogenic growth in vitro and leukemic infiltration in vivo (S. M. Park et al., 2015), whereas LSK normal cells with deletion of MSI2 showed enrichment in hematopoietic self-renewal downregulated gene signatures (S.-M. Park et al., 2014).

On the other hand, the overexpression of MSI2 together with BCR-ABL translocation in mice promoted increased tumor burden and the presence of tumor immature populations, resembling blastic phases of CML (Kharas et al., 2010). MSI2 knockdown and overexpression have also functional effects in MDS. Deletion of MSI2 in vivo impairs MDS-like disease, whereas overexpression drives MDS transformation, maintaining stem and progenitor cells (Taggart et al., 2016). A recent study by Palacios et al. shed light on the role of MSI2 in B cell neoplasms (Palacios et al., 2021). The authors reported high MSI2 levels in the proliferative fraction of CLL primary cells ($CXCR4^{dim}CD5^{bright}$). In addition, they demonstrated that MSI2 downregulation in CLL and BL cell lines induced apoptosis by activating caspase 3 and cell cycle arrest and activating p27 and p53.

Based on all these findings, we investigated the effect of MSI2 silencing in MCL cell lines. Our results showed that MSI2 silencing in MCL cell lines upregulated genes related to cell death and mitochondrial activity, and downregulated HSC-related gene signatures and genes of the Wnt and Notch signaling pathways, which are also very important pathways for HSCs (Reya et al., 2003; Duncan et al., 2005). These findings are consistent with previously described studies on CLL, myeloid malignancies, and LSK cells (Palacios et al., 2021; Kharas et al., 2010; S.-M. Park et al., 2014). Moreover, dysregulation of gene signatures related to mitochondria has been observed in mice intestinal epithelium following MSI1 and MSI2 induction (N. Li et al., 2015), and upon MSI2 deletion in HSCs mouse cells (S.-M. Park et al., 2014).

Besides, MSI2-knockdown MCL cells exhibited reduced clonogenic growth and increased apoptosis, consistent with previously described observations in CML, AML, MLL and CLL cells (H. Zhang et al., 2014; Ito et al., 2010; Kharas et al., 2010; S. M. Park et al., 2015; Palacios et al., 2021). Notably, MSI2 silencing induced apoptosis through upregulation of caspases and genes related to mitochondrial and extrinsic apoptosis in MCL, particularly by inducing FAS and activating caspase 3, as seen in CLL cells (Palacios et al., 2021). This effect is reversed by MSI2 rescue in MSI2-knockdown MCL cells. MSI2 silencing also increased sensitivity to chemotherapy in MCL cells, similar to what has been observed in AML cells (Han et al., 2015). Furthermore, MCL primary samples with high MSI2 levels displayed an increased ALDH+ cell population compared to $MSI2^{Low}$ MCL primary cases, linking MSI2 with stemness properties in MCL.

Although MSI2 knockdown in CLL (Palacios et al., 2021) and in CML cells (H. Zhang et al., 2014) induced cell cycle arrest through upregulation of p27, p53, and p21, we did not observe significant differences in cell cycle arrest or induction of cell cycle inhibitors in our MSI2-knockdown MCL cells. However, we observed a not-significant tendency to increased G_0-G_1 cell populations and p21 levels in sh5MSI2 compared to control MCL cell lines. One possible explanation for the proliferative function discrepancy of MSI2 between CLL and MCL could be the presence of multiple alterations

affecting proliferation and cell growth in MCL (reviewed in (Beà & Amador, 2017)), which might mask the effects of MSI2 suppression in this lymphoma. In summary, our findings suggest that MSI2 is necessary for survival and maintenance of self-renewal and chemoresistance phenotypes in MCL, enhancing CSC properties.

Minuesa and colleagues described a new small molecule, Ro 08-2750, capable of inhibiting MSI2 activity in myeloid leukemias both in vitro and in vivo (Minuesa et al., 2019). Ro 08-2750 binds specifically to MSI2 RNA-binding motif, competing with RNA binding and inhibiting MSI2 function. Our study showed an inverse correlation between MSI2 levels and cell viability upon Ro 08-2750 treatment, highlighting the specificity of this drug for MSI2 inhibition in MCL cell lines. Besides, induction of apoptosis and reduction of colony growth was specifically observed only in Ro 08-2750-treated MCL cells with high levels of MSI2. Similarly, Ro treatment induced apoptosis and cell cycle arrest in AML, CML and CLL cells, and promoted differentiation while decreasing colony formation in myeloid leukemia cells (Minuesa et al., 2019; Palacios et al., 2021). Furthermore, the ALDH+ cell population was eliminated after Ro 08-2750 treatment in MCL primary samples, particularly in cases with high MSI2 expression. Taken together, all these results suggest that Ro 08-2750 may induce apoptosis and decreased self-renewal in MCL cells by inhibiting MSI2 function.

MSI2 is an RBP that mediates its function by regulating the translation of oncogenic targets (Kharas et al., 2010; S. M. Park et al., 2015). Minuesa and colleagues have reported that CML and AML cells treated with Ro 08-2750 shared similar gene expression profiles with MSI2 knockdown CML and AML cells, showing reduced levels of MSI2 target genes, including SMAD3 and C-MYC (Minuesa et al., 2019). In our study, we have shown that Ro 08-2750 inhibition dysregulated part of the MSI2-specific transcriptional program in MCL cell lines, including apoptotic and Wnt and Notch developmental pathways. However, we found few genes commonly deregulated by Ro 08-2750 treatment and MSI2-knockdown. The discrepancy could be due to off-target effects of Ro 08-2750 treatment, although NGF, a described protein inhibited by this small molecule (Arkin & Wells, 2004), is not expressed in MCL cells. We compared 4 and 24

hours of Ro 08-2750 treatment, and observed a significant increase of CDK6 and NOTCH1 protein levels only at 24 but not at 4 hours. Since RNA-seq experiments were performed on MCL cells treated with Ro 08-2750 for 4h, an insufficient exposition to this drug could be a plausible explanation for the differences observed on gene expression profile between functional inhibition with Ro 08-2750 and knockdown of MSI2 in MCL.

It has been reported that MSI family proteins can increase Notch signaling through inhibition of the *NUMB* antagonist (Imai et al., 2001; Ito et al., 2010). Interestingly, we have demonstrated that MSI2 directly binds to the mRNA of essential stemness genes *NOTCH1* and *CDK6* (N. Liu et al., 2013; Stier et al., 2002; Scheicher et al., 2015; Laurenti et al., 2015) , and regulates their translation in MCL. Interestingly, MSI2 knockdown and functional inhibition with Ro 08-2750 decreased NOTCH1 and CDK6 protein levels, demonstrating the involvement of MSI2 in the post-transcriptional regulation of these two proteins. However, we did not detect differences in the expression of these two genes in MCL primary cases according to *MSI2* expression. *NOTCH1* is mutated in around 5-14% of MCL patients (Kridel et al., 2012; Beà et al., 2013), and some of these mutations lead to higher NOTCH1 levels after stimulation with DLL4 Notch ligand in MCL cell lines (Silkenstedt et al., 2019). Moreover, cell cycle regulators are widely mutated in MCL patients. Thus, levels of NOTCH1 and CDK6 may be regulated by other factors in MCL primary samples, masking the direct effects of MSI2 on these two mRNAs observed in our MCL transduced cell lines.

In myeloid leukemias, MSI2 induces tumorigenic growth and engraftment in lymphoid organs (Kharas et al., 2010; S. M. Park et al., 2015; Ito et al., 2010; Taggart et al., 2016). Along similar lines, MSI2 knockdown severely reduced tumor growth and tumor engraftment into bone marrow and spleen in MSI2KD compared to MSI2CT xenotransplanted MCL NSG mice models. Despite two different publications described no toxic effects upon Ro 08-2750 treatment in mice and showed decreased tumor burden (Minuesa et al., 2019; Palacios et al., 2021), we were unable to reproduce these experiments, due to a very high toxicity in our MCL NSG mice models.

It is worth mentioning that two months before the publication of our study, a new publication emerged, describing the role of MSI2 in B cell lymphomas, including MCL (Erazo et al., 2022). In this study, Erazo and colleagues identified MSI2 as a driver gene promoting resistance to protein arginine methyltransferase 5 (PRMT5) inhibition, and showed cooperation between MSI2 and PRMT5 to promote increased c-MYC and BCL2 expression. They proposed strategies of drug combination, targeting at the same time both PRMT5 and MSI2 or BCL2 to inhibit the PRMT5/MSI2/c-MYC/BCL2 axis. The authors showed that higher expression of MSI2 correlated with shorter DLBCL patient's survival and with relapse in MCL and DLBCL cases, linking MSI2 with chemoresistance. In line with our study in MCL, Erazo et al. also reported a decreased viability of cells upon MSI2 knockdown in MCL and DLBCL cell lines, and a reduction on tumor growth of MSI2-depleted cells in subcutaneous MCL xenotransplanted mice models. However, in contrast to our cell cycle in vitro results, they observed decreased proliferation, characterized by lower Ki-67, in MSI2-knockdown compared to control subcutaneous MCL xenotransplanted mice models.

The authors also performed in vitro inhibitory experiments with Ro 08-2750 in MCL and DLBCL cell lines, showing effects in cell viability similar to those described in our study. In line with our observations after MSI2 knockdown, Erazo and collaborators did not observe cell cycle arrest after MSI2 inhibition with Ro 08-2750 small molecule. Regarding gene expression analysis, we detected more transcriptional changes upon Ro 08-2750 treatment, probably because we used a higher Ro 08-2750 concentration than Erazo et al. In addition, common pathways, including p53, apoptosis and TNF were upregulated after treatment, in both studies. Although Erazo and colleagues reported the direct regulation of BCL2 and MYC by MSI2, we did not find significant differences in the expression of these two genes between MSI2-knockdown and -control samples; only *MYCN* appear downregulated upon MSI2 depletion. However, we did not analyze the effects in BCL2 and MYC protein levels. In summary, our study agrees with most of the results reported by Erazo et al., which contribute to highlight the oncogenic role of MSI2

in MCL, demonstrating its correlation with relapse and resistance to targeted therapies in aggressive MCLs.

Overall, our **Study 1** findings suggest that MSI2 upregulation in MCL is partially regulated by SOX11 binding to its promoter and associates with active intronic super-enhancers. MSI2 upregulation may contribute to the maintenance of stem cell properties in MCL cells by promoting the translation of stemness-related genes and inhibiting the translation of pro-apoptotic factors, that would provide tumor cells with self-renewal capabilities, higher cell survival, and chemoresistance. Those changes on phenotype may be reverted through MSI2 functional inhibition by silencing with shRNA or Ro 08-2750 treatment (Figure 74). Therefore, our results open a new perspective for treatment, highlighting MSI2 oncogene as a potential therapeutic target to inhibit drug resistance and relapse in aggressive MCLs.

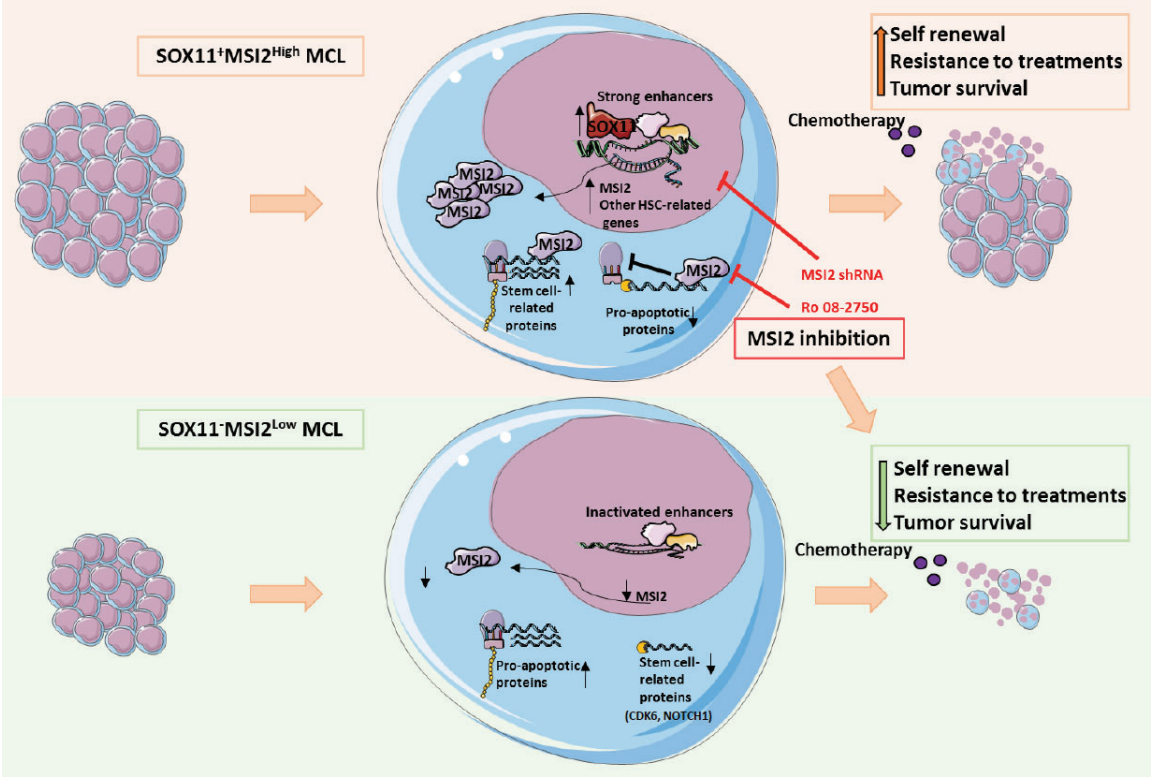

Figure 74. Hypothetical model underlying the mechanism of aberrant expression and oncogenic function of MSI2 in MCL. Hematopoietic and leukemic stem cell-related gene signatures are enriched and MSI2 is upregulated in SOX11+ MCL cases (upper panel) compared to SOX11- MCL primary cases and cell lines (lower panel). SOX11 binds to *MSI2* promoter,

activating its expression in aggressive MCLs. Additionally, MSI2 upregulation is associated with activated *MSI2* intronic enhancers in MCL. MSI2 RBP regulates developmental and cell death pathways, activating translation of stem cell-related proteins (CDK6 and NOTCH1) and inducing downregulation of pro-apoptotic transcripts in MCL. MSI2 expression increases in vitro clonogenic growth, cell survival and resistance to chemotherapy in MCL, and in vivo tumorigenic growth in MCL xenograft mice models. MSI2 functional inhibition by silencing with shRNAs or Ro 08-2750 treatment can reverse stemness phenotypes in MCL, restoring the expression of pro-apoptotic proteins, downregulating stem cell-related transcripts, increasing apoptosis, drug sensitivity and decreasing colony formation.

The t(8;14) leading MYC overexpression in BL is not enough to drive BL pathogenesis (Sung et al., 2005). EBV infection is a crucial event in BL development, particularly in endemic BL. Interestingly, EBV- and EBV+ BLs exhibit distinct clinical and molecular characteristics (López et al., 2022). On the other hand, SOX11 is expressed in a broad range of BLs (Dictor et al., 2009; Mozos et al., 2009), with a higher frequency in pediatric patients (Richter et al., 2022). Several studies have described oncogenic functions of SOX11 in MCL (reviewed in (Beekman, Amador, et al., 2018)). However, the functional role of SOX11 in BL remains unknown. In the **Study 2** of my thesis, we have investigated the possible oncogenic role of SOX11 in BL. In this study, we evaluated the relationship between SOX11 and several clinical and molecular features in BL patients and explored its transcriptional and functional involvement in this malignancy.

Our **Study 2** has revealed an unexpected negative association between SOX11 and EBV infection. Remarkably, in our series of BL patients, SOX11 expression and EBV infection were mutually exclusive. Although we observed a tendency of lower expression of SOX11 in eBL, mutual exclusion was not observed in eBL cases. Recent studies have detected traces of EBV infection in conventional EBV- BL cases using highly sensitive techniques (Mundo et al., 2020, 2017), suggesting that the viral genome may be progressively lost from a tumor that was initially clonally infected (Hänel et al., 2001; Mundo et al., 2020). Thus, EBV infection likely occurs early in the pathogenesis of BL, providing a selective advantage to tumor cells, but secondary oncogenic mechanisms can result in the gradual virus loss, known as "hit-and-run" mechanism. Using this sensitive approach, we identified traces of EBV infection in some conventional EBV-/SOX11- BL

cases, but not in the SOX11+ cases analyzed. These results support our hypothesis of a mutual exclusion between SOX11 and EBV, and suggest that the proportion of cases with initial EBV infection may be higher than previously estimated in the group of SOX11- BL cases studied. Unfortunately, the low number of cases analyzed by this methodology represents a limitation for our hypothetic conclusions. Nonetheless, our observations suggest a molecular dichotomy that implies a potential role for both EBV and SOX11 in BL transformation.

The pathognomonic *IG-MYC* translocation is considered the genetic hallmark of BL. This translocation frequently involves the *IGH* gene, although *IGK* and *IGL* can also be rearranged, and is mostly acquired by the action of AICDA enzyme during CSR and SHM processes (López et al., 2022). Interestingly, we found differences in the *IG* partner between EBV-/SOX11+ and EBV-/SOX11- BLs, as EBV-/SOX11- BLs showed a significant lower proportion of *IGH* translocations and more of *IG* light chains compared to EBV-/SOX11+ cases. It has been described that EBV+ BLs mainly acquire the translocation during SHM, whereas the EBV- BLs acquire it through CSR (Grande et al., 2019; López et al., 2019; Thomas et al., 2022). In our study, we have shown that most of the EBV-/SOX11+ BLs acquired the *IG-MYC* translocation during the CSR process. Nevertheless, this predominance towards CSR was not observed in the EBV-/SOX11- BLs, which show predominantly SHM-mediated translocations, a pattern similar to EBV+ BLs. Commonly, BL shows a mature B cell phenotype, and its cell of origin has been postulated to be a germinal center B cell. However, in the WHO classification, a more immature phenotype of precursor B cells has been also listed in some BL cases (Swerdlow et al., 2017). Recently, Wagener and collaborators reported that these cases could be distinguished from classical BL due to differences in the *IG-MYC* translocation architecture, since they showed translocations acquired during VDJ recombination, a process mediated by RAG1 and RAG2 (Wagener et al., 2018). In agreement, we observed at least one BL case following this pattern.

In MCL, the *IG-CCND1* translocation usually involves an *IGH* partner and it is mainly acquired during VDJ recombination, independently of the SOX11 status (Nadeu

et al., 2020). Our group has described that SOX11 directly activates PAX5 and inhibits BCL6, blocking B-cell maturation and the entrance of tumor cells into the germinal center, explaining the differences observed in the B cell of origin between cMCL (naïve-like B cell) and nnMCL (germinal center experienced, memory-like B cell) (Vegliante et al., 2013; Palomero et al., 2016). We have observed that SOX11+ BLs have lower expression of the germinal center transcription factor *BCL6* and *AICDA*, than EBV+ BL primary cases, following Palomero et al. results that show a decreased in BCL6 and AICDA mRNA and protein levels upon SOX11 overexpression in BL cell lines (Palomero et al., 2016). In addition, higher AICDA expression in EBV+ compared to EBV- BLs has been previously reported (Grande et al., 2019). Nevertheless, no differences between *AICDA* and *BCL6* levels were found between EBV-/SOX11- and EBV+ BL cases, suggesting that the differences observed in the levels of both genes could be mediated by SOX11 expression rather than EBV status in BLs.

A recent study has suggested that CSR occurs earlier than SHM mechanism in B cell differentiation, taking place outside the germinal center. *BCL6* and *AICDA* are expressed at lower levels during isotype switching, but both are progressively upregulated latter, increasing during germinal center reaction and SHM process (Roco et al., 2019). We have seen less expression of *BCL6* and *AICDA*, and predominance of CSR-mediated *IG-MYC* translocations in SOX11+ BL cases, raising the possibility that SOX11+ BL cases might arise from an earlier stage at germinal center B cell differentiation process than SOX11- or EBV+ BLs. The repression of BCL6 expression by SOX11, which consequently blocks entrance into the germinal center in MCL, raises doubts regarding the development of SOX11+ B-cell lymphomas from germinal center B cells. One possible explanation is that due to lower SOX11 expression levels in BL than in MCL cases (Mozos et al., 2009), this factor would play a lighter role in BL than in MCL. We hypothesize that even if the translocation occurs before the germinal center reaction in SOX11+ BLs, the low levels of SOX11 in BL cells would not be enough to block their entry into germinal center, as would happen for MCL cells with superior levels of SOX11.

Interestingly, it has been published that EBV+ BLs harbor higher mutational rates in the V(D)J *IG* regions than EBV- BL cases, suggesting antigen selection (Bellan et al., 2005). It would be worthwhile to investigate whether SOX11+ BL cases exhibit lower rates of *IGHV* somatic mutations than SOX11- BLs, as in MCL (Navarro et al., 2012). Those analyses would provide additional insight into the origin and evolution of SOX11+ BLs.

It is believed than in EBV+ BLs, virus infection induces hyperactivation of AICDA, promoting aberrant SHM and increased mutational burden (Grande et al., 2019). However, several evidences suggest that EBV+ BL cells harbor fewer driver gene mutations than EBV- (Abate et al., 2015; Kaymaz et al., 2017; Grande et al., 2019; López et al., 2019; Richter et al., 2022; Thomas et al., 2022), indicating that EBV infection may relieve the pressure towards selection of mutagenic mechanism. Indeed, EBV infection can immortalize B cells, promoting uncontrolled cell proliferation (Mrozek-Gorska et al., 2019), and contributing to B cell lymphomagenesis through the function of its encoded proteins (Fish et al., 2014; Lam & Sugden, 2003).

In this study, we have observed that EBV-/SOX11+ BLs displayed a distinctive mutational landscape, with more mutations in *SMARCA4* and *ID3*, compared to EBV-/SOX11- and EBV+ cases. In addition, EBV+ BLs exhibited more mutations in *DDX3X* and fewer in *RFX7* compared to SOX11+ but not to SOX11- BLs. These findings suggest that EBV+ and SOX11+ cases might have different oncogenic mechanisms leading to BL pathogenesis. For instance, loss-of-function mutations in *DDX3X*, found predominantly in EBV+ BLs, might alleviate proteotoxic stress caused by MYC overactivation in MYC-driven lymphomas (Gong et al., 2021). In addition, the concomitant SOX11 expression in BL cases with *SMARCA4* mutations is also observed in MCL patients (Nadeu et al., 2020), and mutations in both genes are simultaneously found in the rare Coffin-Siris congenital syndrome (Iwamoto et al., 2021). Although the relationship between SOX11 and SMARCA4 in lymphomas is unknown, recent studies suggest that SOX11 may regulate the transcription of some SWI/SNF core components, including SMARCA4, in neuroblastoma (Decaesteker et al., 2023). Moreover, recent findings from our group

indicate that SOX11 interacts with SMARCA4 and other proteins of the SWI/SNF complex to regulate gene transcription. Nevertheless, the role of this interaction in the context of *SMARCA4* mutations is not yet well understood.

Thomas et al recently described how BL can be categorized into three genetic subgroups, namely IC-BL, DGG-BL and Q53-BL, based on their mutational landscape and gene expression profile (Thomas et al., 2022). Interestingly, we observed that SOX11 is significantly upregulated in the IC-BL compared to DGG-BL subgroup. This study has reported that IC-BLs showed a significant higher frequency of *ID3* and *CCND3* mutations, whereas DGG-BLs of *DDX3X*, *GNA13* and *GNAI2* mutations, corroborating some of our findings in SOX11+ and SOX11- BLs. However, the high prevalence of EBV+ BL cases in DGG-BL compared to IC-BL could be biasing these results, given the molecular dichotomy observed between SOX11 and EBV.

In conclusion, in the **Study 2** of my thesis, I have observed that EBV and SOX11 are mutually exclusive in BL, and that SOX11+ BLs mainly exhibit *IG-MYC* translocations acquired during CSR, rather than SHM, as seen in SOX11- and EBV+ BL cases. In addition, we have observed lower levels of *BCL6* and *AICDA* in SOX11+ BLs, alongside a distinct mutational landscape characterized by a higher frequency of *SMARCA4*, *ID3* and *RFX7* mutations, and a lower frequency of mutations in *DDX3X* gene, compared to EBV+ and SOX11- BLs (Figure 75). Overall, we hypothesize that BL transformation could take place at different stages during germinal center differentiation and by distinct pathogenic mechanisms in SOX11+ vs. SOX11- and EBV+ BLs.

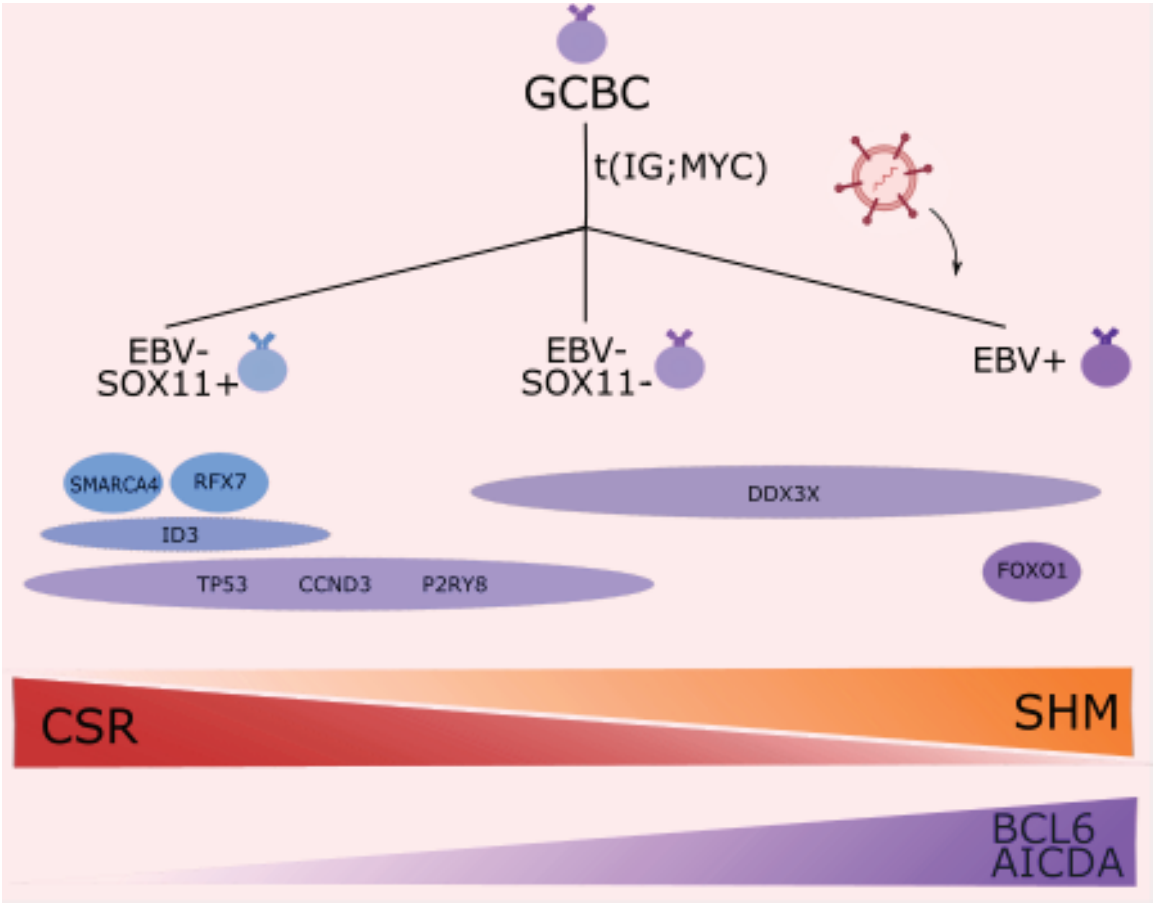

Figure 75. Model of the molecular dichotomy between EBV and SOX11 in BL. SOX11 positive expression is exclusive of EBV- BLs. In addition, the *IG-MYC* translocation is mainly acquired by CSR in EBV-/SOX11+ BLs, and by SHM in the EBV-/SOX11- and EBV+ BLs. *BCL6* and *AICDA* expression are significantly lower in EBV-/SOX11+ than in EBV-/SOX11- or EBV+ BL cases. Finally, the three BL subgroups show different mutational landscapes, with higher prevalence of *SMARCA4*, *RFX7* and *ID3* and lower of *DDX3X* mutations in SOX11+ compared to SOX11- BLs, and higher prevalence of *TP53*, *CCND3* and *P2RY8* mutations, and lower of *FOXO1* in EBV- compared to EBV+ BLs.

The regulation of SOX11 has been extensively investigated in MCL. Previous studies suggested an epigenetic mechanism as the cause of its aberrant overexpression in MCL (Gustavsson et al., 2010; Vegliante et al., 2011; Wasik et al., 2013). More recently, Queirós and collaborators have explored the chromatin states and 3D structure around *SOX11* landscape in MCL (Queirós et al., 2016). They discovered that the *SOX11* promoter contacts with a distal enhancer region in a DNA 3D loop, which may contribute to the activation of SOX11 transcription in MCL (Queirós et al., 2016; Vilarrasa-Blasi et

al., 2022). Other study has suggested that SOX11 could be regulated by CCND1 and STAT3 (Mohanty et al., 2019). However, their results are controversial, as reported by Vilarrasa-Blasi and colleagues (Vilarrasa-Blasi et al., 2022).

However, in BL we observed that SOX11+ and SOX11- BL cell lines exhibit a similar chromatin landscape in the *SOX11* distal enhancer region comparable to the one observed in normal germinal center B cells, which are thought to be the cell of origin of BL and do not express SOX11. We also did not observe enhancer-specific histone marks in the accessible peak 1, discovered by Vilarrasa-Blasi and colleagues in MCL, suggesting that this peak is not associated to SOX11 expression in BLs (Vilarrasa-Blasi et al., 2022). Taken together, these results suggest that the *SOX11* distal enhancer found in MCL is not the primary driver for SOX11 transcription in BL. Thus, a distinct mechanism might regulate SOX11 in BL compared to MCL. Further studies are needed to clarify the regulation of SOX11 in BL. For instance, it would be interesting to investigate whether the DNA 3D loop observed in MCL is also present in SOX11+ BL cell lines and primary samples. In addition, chromatin accessibility studies in BL cell lines and cases could be informative in revealing differences between MCL and BL. A reverse-chip of the *SOX11* promoter and distal enhancer regions in BL cell lines could provide additional insights into the regulation of SOX11. Finally, it is important to note that our analysis is based on the chromatin states of only one SOX11+ and one SOX11- BL cell line. A more extensive analysis of additional cell lines and primary cases would provide robust results.

To investigate whether SOX11 has an oncogenic role in BL as observed in MCL, we generated stable transduced BL cell line models ectopically overexpressing SOX11 or with SOX11 knockout. Our results showed differential expressed genes related to G-proteins, integrins and angiogenesis. We observed that this SOX11-specific BL signature was consistently reproduced in other BL cell lines and in primary cases. Intriguingly, one of the molecular BL signatures, which includes SOX11 as one of the genes (Hummel et al., 2006), was enriched in SOX11+ BL cell lines. Furthermore, SOX11 overexpression in BL cells recapitulated part of the SOX11 transcriptional program found in MCL,

overlapping with some of the SOX11-dependent regulated pathways validated in MCL (Beekman, Amador, et al., 2018).

Our findings also revealed that SOX11-specific regulated pathways in BL and MCL share common genes, such as PLXNB1 and CD24, which regulate tumor cell migration (Ye et al., 2010; Altevogt et al., 2021), and MEX3A, an RBP involved in the chemoresistance of colon CSCs (Álvarez-Varela et al., 2022). These genes were validated by qRT-PCR and western blot experiments as upregulated and downregulated upon SOX11 ectopic overexpression and knockout, respectively, in both BL and MCL cells. Thus, our results suggest that SOX11 regulates a similar transcriptional program in BL and MCL, controlling similar pathways in both lymphomas.

In MCL, SOX11 regulates tumor cell migration and invasion through the activation of the G protein CXCR4 and FAK, promoting invasion and homing, as well as increasing angiogenesis via PDGFA activation (Balsas et al., 2017; Palomero et al., 2014). In BL, we observed that SOX11 increases the expression of *CXCR5*, *CCR7*, and *ITGB7*, but not *CXCR4* or *PDGFA*. CXCR5 and CCR7 are the chemokine receptors of CXCL13 and CCL19/CCL21 cytokines, respectively, which mediate B cell homing to the lymph nodes and Peyer's Patches compartments (Okada et al., 2002). Integrin α4β7, which is composed by *ITGA4* and *ITGB7*, regulates lymphocyte binding to mucosal tissues, enabling their homing to the Peyer's Patches (Berlin et al., 1993).

Interestingly, one of the main tumor localizations in sBL are the Peyer's Patches, and a subset of sBL may originate from germinal center B cells expressing IgA, which are predominantly found in Peyer's Patches mucosal tissue (López et al., 2019). However, we did not find differences in the migration of BL cells towards CXCL13 cytokine or SNKT bone marrow stromal cells, independently of SOX11 expression. By contrast, SOX11-overexpressing BL cells showed a higher adhesion to VCAM-1, one of the glycoproteins expressed by endothelial cells, that interact with α4β7 promoting the B cell homing into the Peyer's Patches (Ruegg et al., 1992).

All these results suggest that SOX11 may be involved in the homing of BL cells to the Peyer's Patches. However, further experiments and analysis are needed to identify the functional role of SOX11 in BL homing. Anatomic site analysis of tumors in BL primary cases in relation to SOX11 expression would help to demonstrate our hypothesis. Finally, SOX11 activates the BCR pathway in MCL (Kuo et al., 2018). However, we did not find differences in BCR activation between SOX11+ and SOX11- BL cells.

In conclusion, the second part of the **Study 2** has shown that the previously described *SOX11* distal enhancer regions associated to SOX11 expression in MCL are not observed in BL cases. We observe that there are similarities in the transcriptional program regulated by SOX11 in BL and MCL. However, we did not reproduce in BL cells the already demonstrated oncogenic mechanism regulated by SOX11 in MCL (Figure 76). The molecular dichotomy observed between SOX11 and EBV suggests that both EBV and SOX11 may play a major role in early stages for tumorigenic transformation of a mature B cell into a BL. However, the limited functional effects observed in our SOX11 BL cell line models suggest that SOX11 might not have a key role in the maintenance of BL in later stages. However, further studies are needed to validate our last hypothesis.

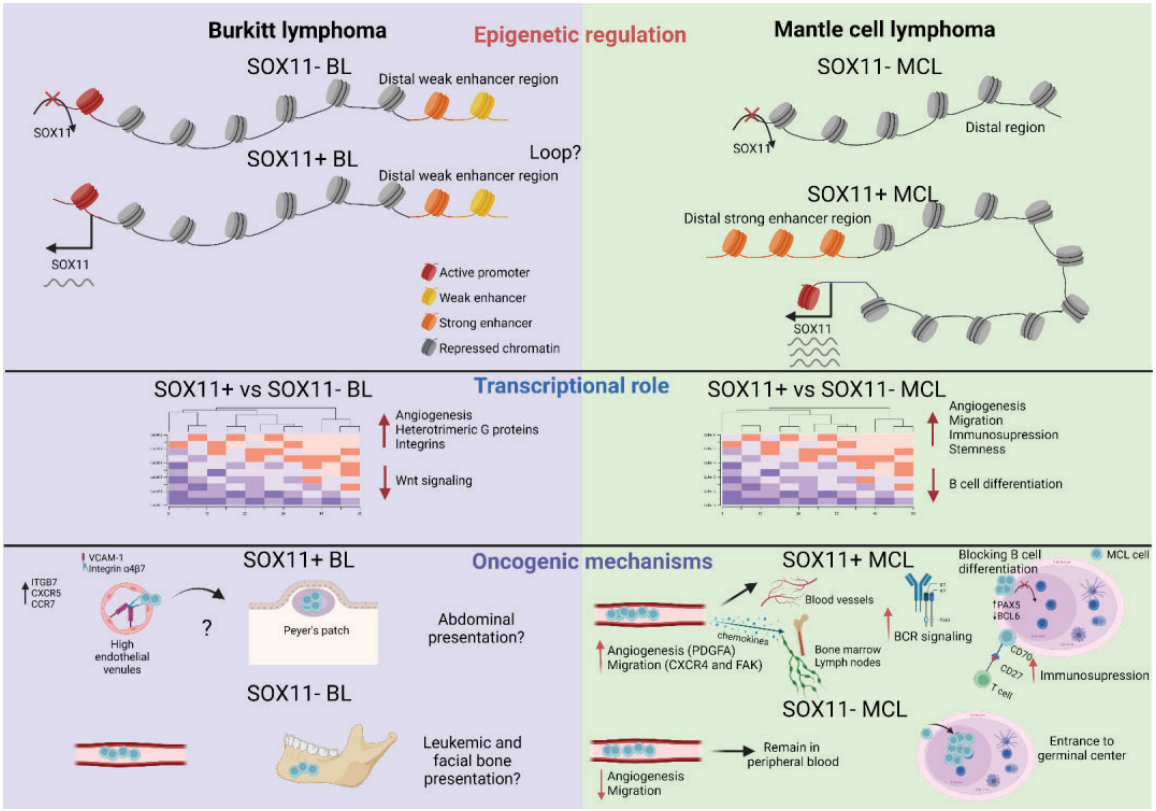

Figure 76. Hypothetical model showing similarities and differences between the SOX11 epigenetic regulation, and the transcriptional and oncogenic role of SOX11 in BL and MCL. In MCL, a *SOX11* distal enhancer region is associated with SOX11 overexpression. This distal enhancer interacts with the *SOX11* active promoter in a 3D DNA loop. Active histone marks are present in the *SOX11* promoter, and also weak and strong enhancers of distal enhancer regions, in both SOX11+ and SOX11- BLs. However, 3D loop experiments would be needed to analyze if exists another active super-enhancer in contact with the *SOX11* promoter in BL. SOX11 regulates similar transcriptional programs in BL and MCL, including angiogenesis, migration, and Wnt pathways. However, demonstrated oncogenic pathways regulated by SOX11 in MCL, as migration, BCR signaling, and B cell differentiation, were not reproduced in BL cells. Instead, a significant higher expression of *ITGB7*, *CCR7*, and greater adhesion to VCAM-1 in SOX11+ compared to SOX11- BL cell lines suggested a key role of SOX11 regulating tumor cell homing into the Peyer's patches, which may be linked to the abdominal presentation observed in sBL.

Overall, in this thesis I have investigated the role of two oncogenes, MSI2 and SOX11, in two different lymphomas, MCL and BL, respectively. I have unraveled the mechanisms involved in the upregulation of MSI2 in MCL, and MSI2 oncogenic contribution promoting stemness properties and tumorigenesis in MCL, highlighting MSI2 as a new possible target for therapeutic interventions to overcome drug resistance in aggressive MCL. Moreover, I have provided insights into the functional role of SOX11 in BL, showing a possible dichotomy between EBV and SOX11, with different cell of origins and pathogenic mechanisms in the early stages of BL transformation. Our findings have improved our understanding of the molecular mechanisms underlying these lymphomas and might guide the development of more effective therapies in the future.

CONCLUSIONS

1. Stem cells-related gene signatures are enriched in SOX11+ MCLs compared to SOX11- MCLs. Knockout of SOX11 in MCL cells impairs colony growth. These results suggest that SOX11 may promote stem cell-like properties through activation of stem cell-related genes in MCL.

2. MSI2 is a stem cell-related gene upregulated in SOX11+ MCLs compared to SOX11- MCLs. MSI2 upregulation is associated with poor overall survival in MCL patients, independently of other high-risk factors in MCL, indicating that MSI2 could be considered a prognostic biomarker in MCL.

3. SOX11 directly activates the transcription of MSI2 in MCL through its binding to *MSI2* promoter region.

4. Specific chromatin remodeling in the intronic regions of MSI2 with stronger, hypomethylated, and more accessible enhancers, are associated with increased MSI2 expression in SOX11+ MCLs but not in SOX11- MCLs or their normal B cell counterparts. These finding suggest that epigenetic mechanisms may control MSI2 expression.

5. Functional inhibition of MSI2 by knockdown or Ro 08-2750 treatment results in the dysregulation of stem cells- and apoptosis-related genes, leading to a decrease in self-renewal, tumor cell survival, and chemoresistance in MCL in vitro. Conversely, MSI2 overexpression rescues tumor cell survival by downregulating FAS and inactivating caspase 3.

6. MSI2 knockdown reduces tumor growth and dissemination of MCL cells into the bone marrow and spleen of immunosuppressed xenograft MCL mouse models, suggesting that MSI2 is tumorigenic and could be a good therapeutic target for aggressive MCL.

7. SOX11 expression and EBV infection are mutually exclusive in BL, suggesting a potential role for both, EBV and SOX11, in the early transformation of BLs.

8. SOX11+ BLs mainly acquire the *IG-MYC* translocation through CSR, rather than SHM, and have lower levels of *BCL6* and *AICDA* than SOX11- and EBV+ BLs, indicating that they might be originated from a germinal center B cell in an early stage of differentiation.

9. SOX11+ BL patients have higher number of mutations in *ID3*, *SMARCA4* and *RFX7*, and fewer in *DDX3X* genes, compared to SOX11- and EBV+ BLs, suggesting a divergence in the BL pathogenic mechanisms.

10. SOX11+ and SOX11- BL cell lines show similar chromatin landscape in both *SOX11* promoter and distal enhancer regions, contrary to epigenetic chromatin differences observed between SOX11+ and SOX11- MCLs, indicating that the mechanism leading to SOX11 upregulation in BL differs from the ones observed in MCL.

11. A SOX11-specific gene BL signature, discovered through the overlap of gene expression profiles upon SOX11 ectopic overexpression in two BL cell lines, can discriminate between BL primary cases with low and high expression of SOX11, highlighting the presence of a SOX11-specific transcriptional program in BL cells.

12. SOX11 overexpression in BL cell lines activates integrin, angiogenesis, and G protein pathway gene programs, mimicking some of the gene signatures found in SOX11+ MCL cell lines and primary cases.

13. SOX11+ BL cell lines did not display increased migration or BCR activation, as observed in MCL. However, they showed greater adhesion to VCAM-1, potentially through integrin α4β7, suggesting that SOX11 might play a role in the invasion of BL cells into Peyer's patches.

REFERENCES

Abate, F., Ambrosio, M. R., Mundo, L., Laginestra, M. A., Fuligni, F., Rossi, M., Zairis, S., Gazaneo, S., De Falco, G., Lazzi, S., Bellan, C., Rocca, B. J., Amato, T., Marasco, E., Etebari, M., Ogwang, M., Calbi, V., Ndede, I., Patel, K., … Rabadan, R. (2015). Distinct Viral and Mutational Spectrum of Endemic Burkitt Lymphoma. *PLOS Pathogens*, *11*(10), e1005158. https://doi.org/10.1371/JOURNAL.PPAT.1005158

Adam, P., Schiefer, A. I., Prill, S., Henopp, T., Quintanilla-Martínez, L., Bösmüller, H. C., Chott, A., & Fend, F. (2012). Incidence of preclinical manifestations of mantle cell lymphoma and mantle cell lymphoma in situ in reactive lymphoid tissues. *Modern Pathology : An Official Journal of the United States and Canadian Academy of Pathology, Inc*, *25*(12), 1629–1636. https://doi.org/10.1038/MODPATHOL.2012.117

Afgan, E., Baker, D., Batut, B., Van Den Beek, M., Bouvier, D., Ech, M., Chilton, J., Clements, D., Coraor, N., Grüning, B. A., Guerler, A., Hillman-Jackson, J., Hiltemann, S., Jalili, V., Rasche, H., Soranzo, N., Goecks, J., Taylor, J., Nekrutenko, A., & Blankenberg, D. (2018). The Galaxy platform for accessible, reproducible and collaborative biomedical analyses: 2018 update. *Nucleic Acids Research*, *46*(W1), W537–W544. https://doi.org/10.1093/NAR/GKY379

Aggarwal, P., Vaites, L. P., Kim, J. K., Mellert, H., Gurung, B., Nakagawa, H., Herlyn, M., Hua, X., Rustgi, A. K., McMahon, S. B., & Diehl, J. A. (2010). Nuclear cyclin D1/CDK4 kinase regulates CUL4 expression and triggers neoplastic growth via activation of the PRMT5 methyltransferase. *Cancer Cell*, *18*(4), 329–340. https://doi.org/10.1016/J.CCR.2010.08.012

Akkaya, M., Kwak, K., & Pierce, S. K. (2020). B cell memory: building two walls of protection against pathogens. *Nature Reviews. Immunology*, *20*(4), 229. https://doi.org/10.1038/S41577-019-0244-2

Alaggio, R., Amador, C., Anagnostopoulos, I., Attygalle, A. D., Araujo, I. B. de O., Berti, E., Bhagat, G., Borges, A. M., Boyer, D., Calaminici, M., Chadburn, A., Chan, J. K. C., Cheuk, W., Chng, W. J., Choi, J. K., Chuang, S. S., Coupland, S. E., Czader, M., Dave, S. S., … Xiao, W. (2022). The 5th edition of the World Health Organization Classification of Haematolymphoid Tumours: Lymphoid Neoplasms. *Leukemia 2022 36:7*, *36*(7), 1720–1748. https://doi.org/10.1038/s41375-022-01620-2

Albero, R., Enjuanes, A., Demajo, S., Castellano, G., Pinyol, M., García, N., Capdevila, C., Clot, G., Suárez-Cisneros, H., Shimada, M., Karube, K., López-Guerra, M., Colomer, D., Beà, S., Martin-Subero, J. I., Campo, E., & Jares, P. (2018). Cyclin D1 overexpression induces global transcriptional downregulation in lymphoid neoplasms. *The Journal of Clinical Investigation*, *128*(9), 4132–4147. https://doi.org/10.1172/JCI96520

Alizadeh, A. A., Elsen, M. B., Davis, R. E., Ma, C. L., Lossos, I. S., Rosenwald, A., Boldrick, J. C., Sabet, H., Tran, T., Yu, X., Powell, J. I., Yang, L., Marü, G. E., Moore, T., Hudson, J., Lu, L., Lewis, D. B., Tibshirani, R., Sherlock, G., … Staudt, L. M. (2000). Distinct types of diffuse large B-cell lymphoma identified by gene expression profiling. *Nature*, *403*(6769), 503–511. https://doi.org/10.1038/35000501

Altevogt, P., Sammar, M., Hüser, L., & Kristiansen, G. (2021). Novel insights into the function of CD24: A driving force in cancer. *International Journal of Cancer*, *148*(3), 546–559. https://doi.org/10.1002/IJC.33249

Álvarez-Varela, A., Novellasdemunt, L., Barriga, F. M., Hernando-Momblona, X., Cañellas-Socias, A., Cano-Crespo, S., Sevillano, M., Cortina, C., Stork, D., Morral, C., Turon, G., Slebe, F., Jiménez-Gracia, L., Caratù, G., Jung, P., Stassi, G., Heyn, H., Tauriello, D. V. F., Mateo, L., … Batlle, E. (2022). Mex3a marks drug-tolerant persister colorectal cancer cells that mediate relapse after chemotherapy. *Nature Cancer*, *3*(9), 1052–1070. https://doi.org/10.1038/S43018-022-00402-0

Aly, R. M., & Ghazy, H. F. (2015). Prognostic significance of MSI2 predicts unfavorable outcome in adult B-acute lymphoblastic leukemia. *International Journal of Laboratory Hematology*, *37*(2), 272–278. https://doi.org/10.1111/ijlh.12284

Angelopoulou, M. K., Siakantariz, M. P., Vassilakopoulos, T. P., Kontopidou, F. N., Rassidakis, G. Z.,

Dimopoulou, M. N., Kittas, C., & Pangalis, G. A. (2002). The splenic form of mantle cell lymphoma. *European Journal of Haematology*, *68*(1), 12–21. https://doi.org/10.1034/J.1600-0609.2002.00551.X

Arkin, M. M. R., & Wells, J. A. (2004). Small-molecule inhibitors of protein–protein interactions: progressing towards the dream. *Nature Reviews Drug Discovery 2004 3:4*, *3*(4), 301–317. https://doi.org/10.1038/NRD1343

Armitage, J. O., Gascoyne, R. D., Lunning, M. A., & Cavalli, F. (2017). Non-Hodgkin lymphoma. *The Lancet*, *390*(10091), 298–310. https://doi.org/10.1016/S0140-6736(16)32407-2

Aukema, S. M., Hoster, E., Rosenwald, A., Canoni, D., Delfau-Larue, M. H., Rymkiewicz, G., Thorns, C., Hartmann, S., Kluin-Nelemans, H., Hermine, O., Dreyling, M., & Klapper, W. (2018). Expression of TP53 is associated with the outcome of MCL independent of MIPI and Ki-67 in trials of the European MCL Network. *Blood*, *131*(4), 417–420. https://doi.org/10.1182/BLOOD-2017-07-797019

Avilion, A. A., Nicolis, S. K., Pevny, L. H., Perez, L., Vivian, N., & Lovell-Badge, R. (2003). Multipotent cell lineages in early mouse development depend on SOX2 function. *Genes & Development*, *17*(1), 126–140. https://doi.org/10.1101/GAD.224503

Balsas, P., Palomero, J., Eguileor, Á., Rodríguez, M. L., Vegliante, M. C., Planas-Rigol, E., Sureda-Gómez, M., Cid, M. C., Campo, E., & Amador, V. (2017). SOX11 promotes tumor protective microenvironment interactions through CXCR4 and FAK regulation in mantle cell lymphoma. *Blood*, *130*(4), 501–513. https://doi.org/10.1182/blood-2017-04-776740

Balsas, P., Veloza, L., Clot, G., Sureda-Gómez, M., Rodriguez, M.-L., Masaoutis, C., Frigola, G., Navarro, A., Beà, S., Nadeu, F., Gine, E., López-Guillermo, A., Martinez, A., Ribera-Cortada, I., Engel, P., Quintanilla-Martinez, L., Klapper, W., Campo, E., & Amador, V. (2021). SOX11, CD70 and Treg cells configure the tumor immune microenvironment of aggressive mantle cell lymphoma. *Blood*, *138*(22), 2202–2215. https://doi.org/10.1182/BLOOD.2020010527

Bannister, A. J., & Kouzarides, T. (2011). Regulation of chromatin by histone modifications. *Cell Research 2011 21:3*, *21*(3), 381–395. https://doi.org/10.1038/cr.2011.22

Basso, K., & Dalla-Favera, R. (2012). Roles of BCL6 in normal and transformed germinal center B cells. *Immunological Reviews*, *247*(1), 172–183. https://doi.org/10.1111/J.1600-065X.2012.01112.X

Beà, S., & Amador, V. (2017). Role of SOX11 and Genetic Events Cooperating with Cyclin D1 in Mantle Cell Lymphoma. *Current Oncology Reports*, *19*(6), 1–10. https://doi.org/10.1007/S11912-017-0598-1/METRICS

Beà, S., Ribas, M., Hernández, J. M., Bosch, F., Pinyol, M., Hernandez, L., Garcia, J. L., Flores, T., Gonzalez, M., López-Guillermo, A., Piris, M. A., Cardesa, A., Montserrat, E., Miró, R., & Campo, E. (1999). Increased Number of Chromosomal Imbalances and High-Level DNA Amplifications in Mantle Cell Lymphoma Are Associated With Blastoid Variants. *Blood*, *93*(12), 4365–4374. https://doi.org/10.1182/BLOOD.V93.12.4365

Beà, S., Salaverria, I., Armengol, L., Pinyol, M., Fernández, V., Hartmann, E. M., Jares, P., Amador, V., Hernández, L., Navarro, A., Ott, G., Rosenwald, A., Estivill, X., & Campo, E. (2009). Uniparental disomies, homozygous deletions, amplifications, and target genes in mantle cell lymphoma revealed by integrative high-resolution whole-genome profiling. *Blood*, *113*(13), 3059–3069. https://doi.org/10.1182/BLOOD-2008-07-170183

Beà, S., Valdés-Mas, R., Navarro, A., Salaverria, I., Martín-Garcia, D., Jares, P., Giné, E., Pinyol, M., Royo, C., Nadeu, F., Conde, L., Juan, M., Clot, G., Vizán, P., Di Croce, L., Puente, D. A., López-Guerra, M., Moros, A., Roue, G., … Campo, E. (2013). Landscape of somatic mutations and clonal evolution in mantle cell lymphoma. *Proceedings of the National Academy of Sciences of the United States of America*, *110*(45), 18250–18255. https://doi.org/10.1073/PNAS.1314608110

Beekman, R., Amador, V., & Campo, E. (2018). SOX11, a key oncogenic factor in mantle cell lymphoma. *Current Opinion in Hematology*, *25*(4), 299–306. https://doi.org/10.1097/MOH.0000000000000434

Beekman, R., Chapaprieta, V., Russiñol, N., Vilarrasa-Blasi, R., Verdaguer-Dot, N., Martens, J. H. A., Duran-Ferrer, M., Kulis, M., Serra, F., Javierre, B. M., Wingett, S. W., Clot, G., Queirós, A. C., Castellano, G., Blanc, J., Gut, M., Merkel, A., Heath, S., Vlasova, A., … Martin-Subero, J. I. (2018). The reference epigenome and regulatory chromatin landscape of chronic lymphocytic leukemia. *Nature Medicine*, *24*(6), 868. https://doi.org/10.1038/S41591-018-0028-4

Bellan, C., Lazzi, S., Hummel, M., Palummo, N., De Santi, M., Amato, T., Nyagol, J., Sabattini, E., Lazure, T., Pileri, S. A., Raphael, M., Stein, H., Tosi, P., & Leoncini, L. (2005). Immunoglobulin gene analysis reveals 2 distinct cells of origin for EBV-positive and EBV-negative Burkitt lymphomas. *Blood*, *106*(3), 1031–1036. https://doi.org/10.1182/blood-2005-01-0168

Beltran, E., Fresquet, V., Martinez-Useros, J., Richter-Larrea, J. A., Sagardoy, A., Sesma, I., Almada, L. L., Montes-Moreno, S., Siebert, R., Gesk, S., Calasanz, M. J., Malumbres, R., Rieger, M., Prosper, F., Lossos, I. S., Piris, M. A., Fernandez-Zapico, M. E., & Martinez-Climent, J. A. (2011). A cyclin-D1 interaction with BAX underlies its oncogenic role and potential as a therapeutic target in mantle cell lymphoma. *Proceedings of the National Academy of Sciences of the United States of America*, *108*(30), 12461–12466. https://doi.org/10.1073/PNAS.1018941108/-/DCSUPPLEMENTAL/PNAS.201018941SI.PDF

Bergsland, M., Ramsköld, D., Zaouter, C., Klum, S., Sandberg, R., & Muhr, J. (2011). Sequentially acting Sox transcription factors in neural lineage development. *Genes & Development*, *25*(23), 2453–2464. https://doi.org/10.1101/GAD.176008.111

Bergsland, M., Werme, M., Malewicz, M., Perlmann, T., & Muhr, J. (2006). The establishment of neuronal properties is controlled by Sox4 and Sox11. *Genes and Development*, *20*(24), 3475–3486. https://doi.org/10.1101/gad.403406

Berlin, C., Berg, E. L., Briskin, M. J., Andrew, D. P., Kilshaw, P. J., Holzmann, B., Weissman, I. L., Hamann, A., & Butcher, E. C. (1993). α4β7 integrin mediates lymphocyte binding to the mucosal vascular addressin MAdCAM-1. *Cell*, *74*(1), 185–195. https://doi.org/10.1016/0092-8674(93)90305-A

Bernard, P., & Harley, V. R. (2010). Acquisition of SOX transcription factor specificity through protein-protein interaction, modulation of Wnt signalling and post-translational modification. *The International Journal of Biochemistry & Cell Biology*, *42*(3), 400–410. https://doi.org/10.1016/J.BIOCEL.2009.10.017

Bevington, S., & Boyes, J. (2013). Transcription-coupled eviction of histones H2A/H2B governs V(D)J recombination. *The EMBO Journal*, *32*(10), 1381–1392. https://doi.org/10.1038/EMBOJ.2013.42

Bhattaram, P., Penzo-Méndez, A., Kato, K., Bandyopadhyay, K., Gadi, A., Taketo, M. M., & Lefebvre, V. (2014). SOXC proteins amplify canonical WNT signaling to secure nonchondrocytic fates in skeletogenesis. *The Journal of Cell Biology*, *207*(5), 657–671. https://doi.org/10.1083/JCB.201405098

Bhattaram, P., Penzo-Méndez, A., Sock, E., Colmenares, C., Kaneko, K. J., Vassilev, A., DePamphilis, M. L., Wegner, M., & Lefebvre, V. (2010). Organogenesis relies on SoxC transcription factors for the survival of neural and mesenchymal progenitors. *Nature Communications*, *1*(1). https://doi.org/10.1038/NCOMMS1008

Bienvenu, F., Jirawatnotai, S., Elias, J. E., Meyer, C. A., Mizeracka, K., Marson, A., Frampton, G. M., Cole, M. F., Odom, D. T., Odajima, J., Geng, Y., Zagozdzon, A., Jecrois, M., Young, R. A., Liu, X. S., Cepko, C. L., Gygi, S. P., & Sicinski, P. (2010). Transcriptional role of cyclin D1 in development revealed by a genetic-proteomic screen. *Nature*, *463*(7279), 374–378. https://doi.org/10.1038/NATURE08684

Bonilla, F. A., & Oettgen, H. C. (2010). Adaptive immunity. *Journal of Allergy and Clinical Immunology*, *125*(2 SUPPL. 2), S33–S40. https://doi.org/10.1016/j.jaci.2009.09.017

Bossen, C., Murre, C. S., Chang, A. N., Mansson, R., Rodewald, H. R., & Murre, C. (2015). Brg1 activates enhancer repertoires to establish B cell identity and modulate cell growth. *Nature Immunology*, *16*(7),

775. https://doi.org/10.1038/NI.3170

Boyer, L. A., Tong, I. L., Cole, M. F., Johnstone, S. E., Levine, S. S., Zucker, J. P., Guenther, M. G., Kumar, R. M., Murray, H. L., Jenner, R. G., Gifford, D. K., Melton, D. A., Jaenisch, R., & Young, R. A. (2005). Core transcriptional regulatory circuitry in human embryonic stem cells. *Cell*, *122*(6), 947–956. https://doi.org/10.1016/J.CELL.2005.08.020

Brennan, D. J., Ek, S., Doyle, E., Drew, T., Foley, M., Flannelly, G., O'Connor, D. P., Gallagher, W. M., Kilpinen, S., Kallioniemi, O. P., Jirstrom, K., O'Herlihy, C., & Borrebaeck, C. A. K. (2009). The transcription factor Sox11 is a prognostic factor for improved recurrence-free survival in epithelial ovarian cancer. *European Journal of Cancer*, *45*(8), 1510–1517. https://doi.org/10.1016/J.EJCA.2009.01.028

Brennan, S. K., Meade, B., Wang, Q., Merchant, A. A., Kowalski, J., & Matsui, W. (2010). Mantle cell lymphoma activation enhances bortezomib sensitivity. *Blood*, *116*(20), 4185–4191. https://doi.org/10.1182/blood-2010-02-268375

Burger, J. A., Ghia, P., Rosenwald, A., & Caligaris-Cappio, F. (2009). The microenvironment in mature B-cell malignancies: a target for new treatment strategies. *Blood*, *114*(16), 3367. https://doi.org/10.1182/BLOOD-2009-06-225326

Burger, J. A., & Kipps, T. J. (2009). Chemokine Receptors and Stromal Cells in the Homing and Homeostasis of Chronic Lymphocytic Leukemia B Cells. *Https://Doi-Org.Sire.Ub.Edu/10.1080/10428190290011921*, *43*(3), 461–466. https://doi.org/10.1080/10428190290011921

Burkhardt, B., Michgehl, U., Rohde, J., Erdmann, T., Berning, P., Reutter, K., Rohde, M., Borkhardt, A., Burmeister, T., Dave, S., Tzankov, A., Dugas, M., Sandmann, S., Fend, F., Finger, J., Mueller, S., Gökbuget, N., Haferlach, T., Kern, W., … Lenz, G. (2022). Clinical relevance of molecular characteristics in Burkitt lymphoma differs according to age. *Nature Communications*, *13*(1). https://doi.org/10.1038/S41467-022-31355-8

Burkhardt, B., Oschlies, I., Klapper, W., Zimmermann, M., Woessmann, W., Meinhardt, A., Landmann, E., Attarbaschi, A., Niggli, F., Schrappe, M., & Reiter, A. (2011). Non-Hodgkin's lymphoma in adolescents: experiences in 378 adolescent NHL patients treated according to pediatric NHL-BFM protocols. *Leukemia*, *25*(1), 153–160. https://doi.org/10.1038/LEU.2010.245

Burkitt, D. (1958). A sarcoma involving the jaws in African children. *The British Journal of Surgery*, *46*(197), 218–223. https://doi.org/10.1002/BJS.18004619704

Byers, R. J., Currie, T., Tholouli, E., Rodig, S. J., & Kutok, J. L. (2011). MSI2 protein expression predicts unfavorable outcome in acute myeloid leukemia. *Blood*, *118*(10), 2857–2867. https://doi.org/10.1182/blood-2011-04-346767

Bylund, M., Andersson, E., Novitch, B. G., & Muhr, J. (2003). Vertebrate neurogenesis is counteracted by Sox1-3 activity. *Nature Neuroscience*, *6*(11), 1162–1168. https://doi.org/10.1038/NN1131

Cacciatore, M., Guarnotta, C., Calvaruso, M., Sangaletti, S., Florena, A. M., Franco, V., Colombo, M. P., & Tripodo, C. (2012). Microenvironment-Centred Dynamics in Aggressive B-Cell Lymphomas. *Advances in Hematology*, *2012*, 12. https://doi.org/10.1155/2012/138079

Camacho, E., Hernández, L., Hernández, S., Tort, F., Bellosillo, B., Beà, S., Bosch, F., Montserrat, E., Cardesa, A., Fernández, P. L., & Campo, E. (2002). ATM gene inactivation in mantle cell lymphoma mainly occurs by truncating mutations and missense mutations involving the phosphatidylinositol-3 kinase domain and is associated with increasing numbers of chromosomal imbalances. *Blood*, *99*(1), 238–244. https://doi.org/10.1182/BLOOD.V99.1.238

Campbell, P. J., Getz, G., Korbel, J. O., Stuart, J. M., Jennings, J. L., Stein, L. D., Perry, M. D., Nahal-Bose, H. K., Ouellette, B. F. F., Li, C. H., Rheinbay, E., Nielsen, G. P., Sgroi, D. C., Wu, C. L., Faquin, W. C., Deshpande, V., Boutros, P. C., Lazar, A. J., Hoadley, K. A., … Zhang, J. (2020). Pan-cancer

analysis of whole genomes. *Nature 2020 578:7793*, *578*(7793), 82–93. https://doi.org/10.1038/s41586-020-1969-6

Campo, E., Jaffe, E. S., Cook, J. R., Quintanilla-Martinez, L., Swerdlow, S. H., Anderson, K. C., Brousset, P., Cerroni, L., de Leval, L., Dirnhofer, S., Dogan, A., Feldman, A. L., Fend, F., Friedberg, J. W., Gaulard, P., Ghia, P., Horwitz, S. M., King, R. L., Salles, G., … Zelenetz, A. D. (2022). The International Consensus Classification of Mature Lymphoid Neoplasms: a report from the Clinical Advisory Committee. *Blood*, *140*(11), 1229–1253. https://doi.org/10.1182/BLOOD.2022015851

Carbone, A., Vaccher, E., & Gloghini, A. (2022). Hematologic cancers in individuals infected by HIV. *Blood*, *139*(7), 995–1012. https://doi.org/10.1182/BLOOD.2020005469

Carlesso, N., Aster, J. C., Sklar, J., & Scadden, D. T. (1999). Notch1-Induced Delay of Human Hematopoietic Progenitor Cell Differentiation Is Associated With Altered Cell Cycle Kinetics. *Blood*, *93*(3), 838–848. https://doi.org/10.1182/BLOOD.V93.3.838

Carmeliet, P., & Jain, R. K. (2011). Molecular mechanisms and clinical applications of angiogenesis. *Nature 2011 473:7347*, *473*(7347), 298–307. https://doi.org/10.1038/NATURE10144

Caron, G., Le Gallou, S., Lamy, T., Tarte, K., & Fest, T. (2009). CXCR4 Expression Functionally Discriminates Centroblasts versus Centrocytes within Human Germinal Center B Cells. *The Journal of Immunology*, *182*(12), 7595–7602. https://doi.org/10.4049/JIMMUNOL.0804272

Carvajal-Cuenca, A., Sua, L. F., Silva, N. M., Pittaluga, S., Royo, C., Song, J. Y., Sargent, R. L., Espinet, B., Climent, F., Jacobs, S. A., Delabie, J., Naresh, K. N., Bagg, A., Brousset, P., Warnke, R. A., Serrano, S., Harris, N. L., Swerdlow, S. H., Jaffe, E. S., & Campo, E. (2012). In situ mantle cell lymphoma: clinical implications of an incidental finding with indolent clinical behavior. *Haematologica*, *97*(2), 270. https://doi.org/10.3324/HAEMATOL.2011.052621

Cedar, H., & Bergman, Y. (2011). Epigenetics of haematopoietic cell development. *Nature Reviews Immunology 2011 11:7*, *11*(7), 478–488. https://doi.org/10.1038/NRI2991

Cerutti, A., & Rescigno, M. (2008). The Biology of Intestinal Immunoglobulin A Responses. *Immunity*, *28*(6), 740–750. https://doi.org/10.1016/J.IMMUNI.2008.05.001

Chaplin, D. D. (2010). Overview of the immune response. *The Journal of Allergy and Clinical Immunology*, *125*(2 Suppl 2). https://doi.org/10.1016/J.JACI.2009.12.980

Chen, Y. H., Gao, J., Fan, G., & Peterson, L. C. (2009). Nuclear expression of sox11 is highly associated with mantle cell lymphoma but is independent of t(11;14)(q13;q32) in non-mantle cell B-cell neoplasms. *Modern Pathology 2010 23:1*, *23*(1), 105–112. https://doi.org/10.1038/modpathol.2009.140

Chen, Z., Ayala, P., Wang, M., Fayad, L., Katz, R. L., Romaguera, J., Caraway, N., Neelapu, S. S., Kwak, L. W., Simmons, P. J., & McCarty, N. (2010). Prospective isolation of clonogenic mantle cell lymphoma-initiating cells. *Stem Cell Research*, *5*(3), 212–225. https://doi.org/10.1016/j.scr.2010.07.003

Cheung, K. J. J., Horsman, D. E., & Gascoyne, R. D. (2009). The significance of TP53 in lymphoid malignancies: mutation prevalence, regulation, prognostic impact and potential as a therapeutic target. *British Journal of Haematology*, *146*(3), 257–269. https://doi.org/10.1111/J.1365-2141.2009.07739.X

Cheung, M., Abu-Elmagd, M., Clevers, H., & Scotting, P. J. (2000). Roles of Sox4 in central nervous system development. *Molecular Brain Research*, *79*(1–2), 180–191. https://doi.org/10.1016/S0169-328X(00)00109-1

Clot, G., Jares, P., Giné, E., Navarro, A., Royo, C., Pinyol, M., Martín-Garcia, D., Demajo, S., Espinet, B., Salar, A., Ferrer, A., Muntañola, A., Aymerich, M., Rauert-Wunderlich, H., Jaffe, E. S., Connors, J. M., Gascoyne, R. D., Delabie, J., López-Guillermo, A., … Campo, E. (2018). A gene signature that distinguishes conventional and leukemic nonnodal mantle cell lymphoma helps predict outcome. *Blood*, *132*(4), 413–422. https://doi.org/10.1182/BLOOD-2018-03-838136

Cobaleda, C., Schebesta, A., Delogu, A., & Busslinger, M. (2007). Pax5: the guardian of B cell identity and function. *Nature Immunology*, *8*(5), 463–470. https://doi.org/10.1038/NI1454

Colomer, D., & Campo, E. (2014). Unlocking new therapeutic targets and resistance mechanisms in mantle cell lymphoma. *Cancer Cell*, *25*(1), 7–9. https://doi.org/10.1016/j.ccr.2013.12.011

Conrotto, P., Andréasson, U., Kuci, V., Borrebaeck, C. A. K., & Ek, S. (2011). Knock-down of SOX11 induces autotaxin-dependent increase in proliferation in vitro and more aggressive tumors in vivo. *Molecular Oncology*, *5*(6), 527–537. https://doi.org/10.1016/J.MOLONC.2011.08.001

Coronel, L., Riege, K., Schwab, K., Förste, S., Häckes, D., Semerau, L., Bernhart, S. H., Siebert, R., Hoffmann, S., & Fischer, M. (2021). Transcription factor RFX7 governs a tumor suppressor network in response to p53 and stress. *Nucleic Acids Research*, *49*(13), 7437–7456. https://doi.org/10.1093/NAR/GKAB575

Croci, G. A., Hoster, E., Beà, S., Clot, G., Enjuanes, A., Scott, D. W., Cabeçadas, J., Veloza, L., Campo, E., Clasen-Linde, E., Goswami, R. S., Helgeland, L., Pileri, S., Rymkiewicz, G., Reinke, S., Dreyling, M., & Klapper, W. (2020). Reproducibility of histologic prognostic parameters for mantle cell lymphoma: cytology, Ki67, p53 and SOX11. *Virchows Archiv*, *477*(2), 259–267. https://doi.org/10.1007/S00428-020-02750-7/FIGURES/8

Dalla-Favera, R., & Gaidano, G. (2001). *Cancer* (H. S. and R. S. DeVita VT (ed.)). Lippincott Williams and Wilkins.

Dave, S. S., Fu, K., Wright, G. W., Lam, L. T., Kluin, P., Boerma, E.-J., Greiner, T. C., Weisenburger, D. D., Rosenwald, A., Ott, G., Müller-Hermelink, H.-K., Gascoyne, R. D., Delabie, J., Rimsza, L. M., Braziel, R. M., Grogan, T. M., Campo, E., Jaffe, E. S., Dave, B. J., … Staudt, L. M. (2006). Molecular diagnosis of Burkitt's lymphoma. *The New England Journal of Medicine*, *354*(23), 2431–2442. https://doi.org/10.1056/NEJMOA055759

De-Thé, G., Geser, A., Day, N. E., Tukei, P. M., Williams, E. M., Beri, D. P., Smith, P. G., Dean, A. G., Bornkamm, G. W., Feorino, P., & Henle, W. (1978). Epidemiological evidence for causal relationship between Epstein-Barr virus and Burkitt's lymphoma from Ugandan prospective study. *Nature 1978 274:5673*, *274*(5673), 756–761. https://doi.org/10.1038/274756A0

De Andrés-Aguayo, L., Varas, F., Kallin, E. M., Infante, J. F., Wurst, W., Floss, T., & Graf, T. (2011). Musashi 2 is a regulator of the HSC compartment identified by a retroviral insertion screen and knockout mice. *Blood*, *118*(3), 554–564. https://doi.org/10.1182/blood-2010-12-322081

De Bont, J. M., Kros, J. M., Passier, M. M. C. J., Reddingius, R. E., Sillevis Smitt, P. A. E., Luider, T. M., Den Boer, M. L., & Pieters, R. (2008). Differential expression and prognostic significance of SOX genes in pediatric medulloblastoma and ependymoma identified by microarray analysis. *Neuro-Oncology*, *10*(5), 648–660. https://doi.org/10.1215/15228517-2008-032

De Falco, G., Ambrosio, M. R., Fuligni, F., Onnis, A., Bellan, C., Rocca, B. J., Navari, M., Etebari, M., Mundo, L., Gazaneo, S., Facchetti, F., Pileri, S. A., Leoncini, L., & Piccaluga, P. P. (2015). Burkitt lymphoma beyond MYC translocation: N-MYC and DNA methyltransferases dysregulation. *BMC Cancer*, *15*(1). https://doi.org/10.1186/S12885-015-1661-7

De Silva, N. S., & Klein, U. (2015). Dynamics of B cells in germinal centres. *Nature Reviews. Immunology*, *15*(3), 137. https://doi.org/10.1038/NRI3804

Decaesteker, B., Louwagie, A., Loontiens, S., De Vloed, F., Bekaert, S. L., Roels, J., Vanhauwaert, S., De Brouwer, S., Sanders, E., Berezovskaya, A., Denecker, G., D'haene, E., Van Haver, S., Van Loocke, W., Van Dorpe, J., Creytens, D., Van Roy, N., Pieters, T., Van Neste, C., … Speleman, F. (2023). SOX11 regulates SWI/SNF complex components as member of the adrenergic neuroblastoma core regulatory circuitry. *Nature Communications*, *14*(1), 1267. https://doi.org/10.1038/S41467-023-36735-2

Deffenbacher, K. E., Iqbal, J., Sanger, W., Shen, Y., Lachel, C., Liu, Z., Liu, Y., Lim, M. S., Perkins, S. L.,

Fu, K., Smith, L., Lynch, J., Staudt, L. M., Rimsza, L. M., Jaffe, E., Rosenwald, A., Ott, G. K., Delabie, J., Campo, E., … Chan, W. C. (2012). Molecular distinctions between pediatric and adult mature B-cell non-Hodgkin lymphomas identified through genomic profiling. *Blood*, *119*(16), 3757–3766. https://doi.org/10.1182/BLOOD-2011-05-349662

Delfau-Larue, M. H., Klapper, W., Berger, F., Jardin, F., Briere, J., Salles, G., Casasnovas, O., Feugier, P., Haioun, C., Ribrag, V., Thieblemont, C., Unterhalt, M., Dreyling, M., Macintyre, E., Pott, C., Hermine, O., & Hoster, E. (2015). High-dose cytarabine does not overcome the adverse prognostic value of CDKN2A and TP53 deletions in mantle cell lymphoma. *Blood*, *126*(5), 604–611. https://doi.org/10.1182/BLOOD-2015-02-628792

Demajo, S., Albero, R., Clot, G., Castellano, G., Navarro, A., Capdevila, C., Enjuanes, A., Nadeu, F., Gine, E., Pinyol, M., Jaffe, E. S., Ott, G., Staudt, L. M., Rosenwald, A., Scott, D. W., Rimsza, L. M., Lopez-Guillermo, A., Bea, S., Campo, E., & Jares, P. (2021). A Cyclin D1-Dependent Transcriptional Program Predicts Clinical Outcome in Mantle Cell Lymphoma. *Clinical Cancer Research : An Official Journal of the American Association for Cancer Research*, *27*(1), 213–225. https://doi.org/10.1158/1078-0432.CCR-20-2868

Dengler, H. S., Baracho, G. V., Omori, S. A., Bruckner, S., Arden, K. C., Castrillon, D. H., DePinho, R. A., & Rickert, R. C. (2008). Distinct roles for Foxo1 at multiple stages of B cell differentiation. *Nature Immunology*, *9*(12), 1388. https://doi.org/10.1038/NI.1667

Di Giacomo, D., Pierini, V., Barba, G., Ceccarelli, V., Vecchini, A., & Mecucci, C. (2014). Blast crisis Ph+ chronic myeloid leukemia with NUP98/HOXA13 up-regulating MSI2. *Molecular Cytogenetics*, *7*(1), 1–7. https://doi.org/10.1186/1755-8166-7-42

Dictor, M., Ek, S., Sundberg, M., Warenholt, J., György, C., Sernbo, S., Gustavsson, E., Abu-Alsoud, W., Wadström, T., & Borrebaeck, C. (2009). Strong lymphoid nuclear expression of SOX11 transcription factor defines lymphoblastic neoplasms, mantle cell lymphoma and Burkitt's lymphoma. *Haematologica*, *94*(11), 1563–1568. https://doi.org/10.3324/haematol.2009.008474

Dobner, T., Wolf, I., Emrich, T., & Lipp, M. (1992). Differentiation-specific expression of a novel G protein-coupled receptor from Burkitt's lymphoma. *European Journal of Immunology*, *22*(11), 2795–2799. https://doi.org/10.1002/EJI.1830221107

Dodonova, S. O., Zhu, F., Dienemann, C., Taipale, J., & Cramer, P. (2020). Nucleosome-bound SOX2 and SOX11 structures elucidate pioneer factor function. *Nature*, *580*(7805), 669–672. https://doi.org/10.1038/s41586-020-2195-y

Dreyfuss, G., Kim, V. N., & Kataoka, N. (2002). Messenger-RNA-binding proteins and the messages they carry. *Nature Reviews Molecular Cell Biology 2002 3:3*, *3*(3), 195–205. https://doi.org/10.1038/NRM760

Dreyling, M., Aurer, I., Cortelazzo, S., Hermine, O., Hess, G., Jerkeman, M., Le Gouill, S., Ribrag, V., Trněný, M., Visco, C., Walewski, J., Zaja, F., & Zinzani, P. L. (2018). Treatment for patients with relapsed/refractory mantle cell lymphoma: European-based recommendations. *Leukemia and Lymphoma*, *59*(8), 1814–1828. https://doi.org/10.1080/10428194.2017.1403602/SUPPL_FILE/ILAL_A_1403602_SM9356.ZIP

Dreyling, M., Ferrero, S., & Hermine, O. (2014). How to manage mantle cell lymphoma. *Leukemia 2014 28:11*, *28*(11), 2117–2130. https://doi.org/10.1038/LEU.2014.171

Dreyling, M., Lenz, G., Hoster, E., Van Hoof, A., Gisselbrecht, C., Schmits, R., Metzner, B., Truemper, L., Reiser, M., Steinhauer, H., Boiron, J. M., Boogaerts, M. A., Aldaoud, A., Silingardi, V., Kluin-Nelemans, H. C., Hasford, J., Parwaresch, R., Unterhalt, M., & Hiddemann, W. (2005). Early consolidation by myeloablative radiochemotherapy followed by autologous stem cell transplantation in first remission significantly prolongs progression-free survival in mantle-cell lymphoma: results of a prospective randomized trial of the European. *Blood*, *105*(7), 2677–2684. https://doi.org/10.1182/BLOOD-2004-10-3883

Drillenburg, P., & Pals, S. T. (2000). Cell adhesion receptors in lymphoma dissemination. *Blood*, *95*(6), 1900–1910. https://doi.org/10.1182/BLOOD.V95.6.1900

Duncan, A. W., Rattis, F. M., DiMascio, L. N., Congdon, K. L., Pazianos, G., Zhao, C., Yoon, K., Cook, J. M., Willert, K., Gaiano, N., & Reya, T. (2005). Integration of Notch and Wnt signaling in hematopoietic stem cell maintenance. *Nature Immunology*, *6*(3), 314–322. https://doi.org/10.1038/NI1164

Ek, S., Dictor, M., Jerkeman, M., Jirström, K., & Borrebaeck, C. A. K. (2008). Nuclear expression of the non B-cell lineage Sox11 transcription factor identifies mantle cell lymphoma. *Blood*, *111*(2), 800–805. https://doi.org/10.1182/BLOOD-2007-06-093401

Elcheva, I. A., Wood, T., Chiarolanzio, K., Chim, B., Wong, M., Singh, V., Gowda, C. P., Lu, Q., Hafner, M., Dovat, S., Liu, Z., Muljo, S. A., & Spiegelman, V. S. (2020). RNA-binding protein IGF2BP1 maintains leukemia stem cell properties by regulating HOXB4, MYB, and ALDH1A1. *Leukemia*, *34*(5), 1354–1363. https://doi.org/10.1038/S41375-019-0656-9

Enjuanes, A., Albero, R., Clot, G., Navarro, A., Beà, S., Pinyol, M., Martín-Subero, J. I., Klapper, W., Staudt, L. M., Jaffe, E. S., Rimsza, L., Braziel, R. M., Delabie, J., Cook, J. R., Tubbs, R. R., Gascoyne, R., Connors, J. M., Weisenburger, D. D., Greiner, T. C., … Jares, P. (2013). Genome-wide methylation analyses identify a subset of mantle cell lymphoma with a high number of methylated CpGs and aggressive clinicopathological features. *International Journal of Cancer*, *133*(12), 2852. https://doi.org/10.1002/IJC.28321

Erazo, T., Evans, C. M., Zakheim, D., Chu, K. L., Refermat, A. Y., Asgari, Z., Yang, X., Da Silva Ferreira, M., Mehta, S., Russo, M. V., Knezevic, A., Zhang, X. P., Chen, Z., Fennell, M., Garippa, R., Seshan, V., de Stanchina, E., Barbash, O., Batlevi, C. L., … Kharas, M. G. (2022). TP53 mutations and RNA-binding protein MUSASHI-2 drive resistance to PRMT5-targeted therapy in B-cell lymphoma. *Nature Communications*, *13*(1). https://doi.org/10.1038/S41467-022-33137-8

Ernst, J., & Kellis, M. (2012). ChromHMM: automating chromatin-state discovery and characterization. *Nature Methods*, *9*(3), 215–216. https://doi.org/10.1038/NMETH.1906

Ernst, J., & Kellis, M. (2017). Chromatin-state discovery and genome annotation with ChromHMM. *Nature Protocols*, *12*(12), 2478–2492. https://doi.org/10.1038/nprot.2017.124

Ernst, J., Kheradpour, P., Mikkelsen, T. S., Shoresh, N., Ward, L. D., Epstein, C. B., Zhang, X., Wang, L., Issner, R., Coyne, M., Ku, M., Durham, T., Kellis, M., & Bernstein, B. E. (2011). Mapping and analysis of chromatin state dynamics in nine human cell types. *Nature 2011 473:7345*, *473*(7345), 43–49. https://doi.org/10.1038/NATURE09906

Esteller, M. (2008). Epigenetics in Cancer. *Https://Doi-Org.Sire.Ub.Edu/10.1056/NEJMra072067*, *358*(11), 1148–1159. https://doi.org/10.1056/NEJMRA072067

Fang, T., Lv, H., Wu, F., Wang, C., Li, T., Lv, G., Tang, L., Guo, L., Tang, S., Cao, D., Wu, M., Yang, W., & Wang, H. (2017). Musashi 2 contributes to the stemness and chemoresistance of liver cancer stem cells via LIN28A activation. *Cancer Letters*, *384*, 50–59. https://doi.org/10.1016/J.CANLET.2016.10.007

Feng, W., Khan, M. A., Bellvis, P., Zhu, Z., Bernhardt, O., Herold-Mende, C., & Liu, H. K. (2013). The chromatin remodeler CHD7 regulates adult neurogenesis via activation of soxc transcription factors. *Cell Stem Cell*, *13*(1), 62–72. https://doi.org/10.1016/j.stem.2013.05.002

Fernàndez, V., Salamero, O., Espinet, B., Solé, F., Royo, C., Navarro, A., Camacho, F., Beà, S., Hartmann, E., Amador, V., Hernández, L., Agostinelli, C., Sargent, R. L., Rozman, M., Aymerich, M., Colomer, D., Villamor, N., Swerdlow, S. H., Pileri, S. A., … Campo, E. (2010). Genomic and gene expression profiling defines indolent forms of mantle cell lymphoma. *Cancer Research*, *70*(4), 1408–1418. https://doi.org/10.1158/0008-5472.CAN-09-3419

Fischer, U., Yang, J. J., Ikawa, T., Hein, D., Vicente-Dueñas, C., Borkhardt, A., & Sánchez-García, I. (2020).

Cell Fate Decisions: The Role of Transcription Factors in Early B-cell Development and Leukemia. *Blood Cancer Discovery*, *1*(3), 224–233. https://doi.org/10.1158/2643-3230.BCD-20-0011

Fish, K., Chen, J., & Longnecker, R. (2014). Epstein-Barr virus latent membrane protein 2A enhances MYC-driven cell cycle progression in a mouse model of B lymphoma. *Blood*, *123*(4), 530–540. https://doi.org/10.1182/BLOOD-2013-07-517649

Fornes, O., Castro-Mondragon, J. A., Khan, A., Van Der Lee, R., Zhang, X., Richmond, P. A., Modi, B. P., Correard, S., Gheorghe, M., Baranašić, D., Santana-Garcia, W., Tan, G., Chèneby, J., Ballester, B., Parcy, F., Sandelin, A., Lenhard, B., Wasserman, W. W., & Mathelier, A. (2020). JASPAR 2020: update of the open-access database of transcription factor binding profiles. *Nucleic Acids Research*, *48*(D1), D87–D92. https://doi.org/10.1093/NAR/GKZ1001

Fulco, C. P., Munschauer, M., Anyoha, R., Munson, G., Grossman, S. R., Perez, E. M., Kane, M., Cleary, B., Lander, E. S., & Engreitz, J. M. (2016). Systematic mapping of functional enhancer-promoter connections with CRISPR interference. *Science (New York, N.Y.)*, *354*(6313), 769. https://doi.org/10.1126/SCIENCE.AAG2445

Gaidano, G., Pasqualucci, L., Capello, D., Berra, E., Deambrogi, C., Rossi, D., Larocca, L. M., Gloghini, A., Carbone, A., & Dalla-Favera, R. (2003). Aberrant somatic hypermutation in multiple subtypes of AIDS-associated non-Hodgkin lymphoma. *Blood*, *102*(5), 1833–1841. https://doi.org/10.1182/BLOOD-2002-11-3606

Gebauer, F., Schwarzl, T., Valcárcel, J., & Hentze, M. W. (2020). RNA-binding proteins in human genetic disease. *Nature Reviews Genetics 2020 22:3*, *22*(3), 185–198. https://doi.org/10.1038/S41576-020-00302-Y

Ghanbarian, H., Aghamiri, S., Eftekhary, M., Wagner, N., & Wagner, K. D. (2021). Small Activating RNAs: Towards the Development of New Therapeutic Agents and Clinical Treatments. *Cells*, *10*(3), 1–13. https://doi.org/10.3390/CELLS10030591

Gianni, A. M., Magni, M., Martelli, M., Di Nicola, M., Carlo-Stella, C., Pilotti, S., Rambaldi, A., Cortelazzo, S., Patti, C., Parvis, G., Benedetti, F., Capria, S., Corradini, P., Tarella, C., & Barbui, T. (2003). Long-term remission in mantle cell lymphoma following high-dose sequential chemotherapy and in vivo rituximab-purged stem cell autografting (R-HDS regimen). *Blood*, *102*(2), 749–755. https://doi.org/10.1182/BLOOD-2002-08-2476

Giulino-Roth, L., Wang, K., MacDonald, T. Y., Mathew, S., Tam, Y., Cronin, M. T., Palmer, G., Lucena-Silva, N., Pedrosa, F., Pedrosa, M., Teruya-Feldstein, J., Bhagat, G., Alobeid, B., Leoncini, L., Bellan, C., Rogena, E., Pinkney, K. A., Rubin, M. A., Ribeiro, R. C., … Cesarman, E. (2012). Targeted genomic sequencing of pediatric Burkitt lymphoma identifies recurrent alterations in antiapoptotic and chromatin-remodeling genes. *Blood*, *120*(26), 5181–5184. https://doi.org/10.1182/BLOOD-2012-06-437624

Gong, C., Krupka, J. A., Gao, J., Grigoropoulos, N. F., Giotopoulos, G., Asby, R., Screen, M., Usheva, Z., Cucco, F., Barrans, S., Painter, D., Zaini, N. B. M., Haupl, B., Bornelöv, S., Ruiz De Los Mozos, I., Meng, W., Zhou, P., Blain, A. E., Forde, S., … Hodson, D. J. (2021). Sequential inverse dysregulation of the RNA helicases DDX3X and DDX3Y facilitates MYC-driven lymphomagenesis. *Molecular Cell*, *81*(19), 4059-4075.e11. https://doi.org/10.1016/J.MOLCEL.2021.07.041

Grande, B. M., Gerhard, D. S., Jiang, A., Griner, N. B., Abramson, J. S., Alexander, T. B., Allen, H., Ayers, L. W., Bethony, J. M., Bhatia, K., Bowen, J., Casper, C., Choi, J. K., Culibrk, L., Davidsen, T. M., Dyer, M. A., Gastier-Foster, J. M., Gesuwan, P., Greiner, T. C., … Staudt, L. M. (2019). Genome-wide discovery of somatic coding and noncoding mutations in pediatric endemic and sporadic Burkitt lymphoma. *Blood*, *133*(12), 1313–1324. https://doi.org/10.1182/BLOOD-2018-09-871418

Greaves, M. F. (1986). Differentiation-linked leukemogenesis in lymphocytes. *Science (New York, N.Y.)*, *234*(4777), 697–704. https://doi.org/10.1126/SCIENCE.3535067

Grønbæk, K., Nedergaard, T., Andersen, M. K., Thor Straten, P., Guldberg, P., Møller, P., Zeuthen, J., Ebbe Hansen, N., Hou-Jensen, K., & Ralfkiaer, E. (1998). Concurrent disruption of cell cycle associated genes in mantle cell lymphoma: a genotypic and phenotypic study of cyclin D1, p16, p15, p53 and pRb. *Leukemia*, *12*(8), 1266–1271. https://doi.org/10.1038/SJ.LEU.2401090

Grønbaek, K., Worm, J., Ralfkiaer, E., Ahrenkiel, V., Hokland, P., & Guldberg, P. (2002). ATM mutations are associated with inactivation of the ARF-TP53 tumor suppressor pathway in diffuse large B-cell lymphoma. *Blood*, *100*(4), 1430–1437. https://doi.org/10.1182/BLOOD-2002-02-0382

Guo, M., Price, M. J., Patterson, D. G., Barwick, B. G., Haines, R. R., Kania, A. K., Bradley, J. E., Randall, T. D., Boss, J. M., & Scharer, C. D. (2018). EZH2 represses the B cell transcriptional program and regulates antibody secreting cell metabolism and antibody production. *Journal of Immunology (Baltimore, Md. : 1950)*, *200*(3), 1039. https://doi.org/10.4049/JIMMUNOL.1701470

Gustavsson, E., Sernbo, S., Andersson, E., Brennan, D. J., Dictor, M., Jerkeman, M., Borrebaeck, C. A. K., & Ek, S. (2010). SOX11 expression correlates to promoter methylation and regulates tumor growth in hematopoietic malignancies. *Molecular Cancer*, *9*(1), 1–12. https://doi.org/10.1186/1476-4598-9-187/FIGURES/6

Han, Y., Ye, A., Zhang, Y., Cai, Z., Wang, W., Sun, L., Jiang, S., Wu, J., Yu, K., & Zhang, S. (2015). Musashi-2 Silencing Exerts Potent Activity against Acute Myeloid Leukemia and Enhances Chemosensitivity to Daunorubicin. *PLOS ONE*, *10*(8), e0136484. https://doi.org/10.1371/JOURNAL.PONE.0136484

Hanahan, D. (2022). Hallmarks of Cancer: New Dimensions. *Cancer Discovery*, *12*(1), 31–46. https://doi.org/10.1158/2159-8290.CD-21-1059

Hanahan, D., & Weinberg, R. A. (2000). The Hallmarks of Cancer. *Cell*, *100*(1), 57–70. https://doi.org/10.1016/S0092-8674(00)81683-9

Hanahan, D., & Weinberg, R. A. (2011). Hallmarks of cancer: the next generation. *Cell*, *144*(5), 646–674. https://doi.org/10.1016/J.CELL.2011.02.013

Hänel, P., Hummel, M., Anagnostopoulos, I., & Stein, H. (2001). Analysis of single EBER-positive and negative tumour cells in EBV-harbouring B-cell non-Hodgkin lymphomas. *The Journal of Pathology*, *195*(3), 355–360. https://doi.org/10.1002/PATH.954

Hartmann, E. M., Be, S., Navarro, A., Trapp, V., Campo, E., Ott, G., & Rosenwald, A. (2012). Increased tumor cell proliferation in mantle cell lymphoma is associated with elevated insulin-like growth factor 2 mRNA-binding protein 3 expression. *Modern Pathology : An Official Journal of the United States and Canadian Academy of Pathology, Inc*, *25*(9), 1227–1235. https://doi.org/10.1038/MODPATHOL.2012.84

Hartmann, E. M., Campo, E., Wright, G., Lenz, G., Salaverria, I., Jares, P., Xiao, W., Braziel, R. M., Rimsza, L. M., Chan, W. C., Weisenburger, D. D., Delabie, J., Jaffe, E. S., Gascoyne, R. D., Dave, S. S., Mueller-Hermelink, H. K., Staudt, L. M., Ott, G., Beà, S., & Rosenwald, A. (2010). Pathway discovery in mantle cell lymphoma by integrated analysis of high-resolution gene expression and copy number profiling. *Blood*, *116*(6), 953–961. https://doi.org/10.1182/BLOOD-2010-01-263806

Haslinger, A., Schwarz, T. J., Covic, M., & Chichung Lie, D. (2009). Expression of Sox11 in adult neurogenic niches suggests a stage-specific role in adult neurogenesis. *European Journal of Neuroscience*, *29*(11), 2103–2114. https://doi.org/10.1111/j.1460-9568.2009.06768.x

Hattori, A., McSkimming, D., Kannan, N., & Ito, T. (2017). RNA binding protein MSI2 positively regulates FLT3 expression in myeloid leukemia. *Leukemia Research*, *54*, 47–54. https://doi.org/10.1016/J.LEUKRES.2017.01.015

Heigwer, F., Kerr, G., & Boutros, M. (2014). E-CRISP: fast CRISPR target site identification. *Nature Methods*, *11*(2), 122–123. https://doi.org/10.1038/nmeth.2812

Hernández, L., Beà, S., Pinyol, M., Ott, G., Katzenberger, T., Rosenwald, A., Bosch, F., López-Guillermo,

A., Delabie, J., Colomer, D., Montserrat, E., & Campo, E. (2005). CDK4 and MDM2 gene alterations mainly occur in highly proliferative and aggressive mantle cell lymphomas with wild-type INK4a/ARF locus. *Cancer Research*, *65*(6), 2199–2206. https://doi.org/10.1158/0008-5472.CAN-04-1526

Hoffman, B., & Liebermann, D. A. (2008). Apoptotic signaling by c-MYC. *Oncogene*, *27*(50), 6462–6472. https://doi.org/10.1038/ONC.2008.312

Hope, K. J., Cellot, S., Ting, S. B., MacRae, T., Mayotte, N., Iscove, N. N., & Sauvageau, G. (2010). An RNAi Screen Identifies Msi2 and Prox1 as Having Opposite Roles in the Regulation of Hematopoietic Stem Cell Activity. *Cell Stem Cell*, *7*(1), 101–113. https://doi.org/10.1016/J.STEM.2010.06.007

Hope, K. J., & Sauvageau, G. (2011). Roles for MSI2 and PROX1 in hematopoietic stem cell activity. *Current Opinion in Hematology*, *18*(4), 203–207. https://doi.org/10.1097/MOH.0B013E328347888A

Hoster, E., Dreyling, M., Klapper, W., Gisselbrecht, C., Van Hoof, A., Kluin-Nelemans, H. C., Pfreundschuh, M., Reiser, M., Metzner, B., Einsele, H., Peter, N., Jung, W., Wörmann, B., Ludwig, W. D., Dührsen, U., Eimermacher, H., Wandt, H., Hasford, J., Hiddemann, W., & Unterhalt, M. (2008). A new prognostic index (MIPI) for patients with advanced-stage mantle cell lymphoma. *Blood*, *111*(2), 558–565. https://doi.org/10.1182/BLOOD-2007-06-095331

Hoster, E., Klapper, W., Hermine, O., Kluin-Nelemans, H. C., Walewski, J., Van Hoof, A., Trneny, M., Geisler, C. H., Raimondo, F. Di, Szymczyk, M., Stilgenbauer, S., Thieblemont, C., Hallek, M., Forstpointner, R., Pott, C., Ribrag, V., Doorduijn, J., Hiddemann, W., Dreyling, M. H., & Unterhalt, M. (2014). Confirmation of the mantle-cell lymphoma International Prognostic Index in randomized trials of the European Mantle-Cell Lymphoma Network. *Journal of Clinical Oncology : Official Journal of the American Society of Clinical Oncology*, *32*(13), 1338–1346. https://doi.org/10.1200/JCO.2013.52.2466

Hoster, E., Rosenwald, A., Berger, F., Bernd, H. W., Hartmann, S., Loddenkemper, C., Barth, T. F. E., Brousse, N., Pileri, S., Rymkiewicz, G., Kodet, R., Stilgenbauer, S., Forstpointner, R., Thieblemont, C., Hallek, M., Coiffier, B., Vehling-Kaiser, U., Bouabdallah, Ŕ., Kanz, L., … Klapper, W. (2016). Prognostic Value of Ki-67 Index, Cytology, and Growth Pattern in Mantle-Cell Lymphoma: Results From Randomized Trials of the European Mantle Cell Lymphoma Network. *Journal of Clinical Oncology : Official Journal of the American Society of Clinical Oncology*, *34*(12), 1386–1394. https://doi.org/10.1200/JCO.2015.63.8387

Hou, L., Srivastava, Y., & Jauch, R. (2017). Molecular basis for the genome engagement by Sox proteins. *Seminars in Cell & Developmental Biology*, *63*, 2–12. https://doi.org/10.1016/J.SEMCDB.2016.08.005

Hu, Z., Medeiros, L. J., Chen, Z., Chen, W., Li, S., Konoplev, S. N., Lu, X., Pham, L. V., Young, K. H., Wang, W., & Hu, S. (2017). Mantle Cell Lymphoma With MYC Rearrangement: A Report of 17 Patients. *The American Journal of Surgical Pathology*, *41*(2), 216–224. https://doi.org/10.1097/PAS.0000000000000758

Hummel, M., Bentink, S., Berger, H., Klapper, W., Wessendorf, S., Barth, T. F. E., Bernd, H.-W., Cogliatti, S. B., Dierlamm, J., Feller, A. C., Hansmann, M.-L., Haralambieva, E., Harder, L., Hasenclever, D., Kühn, M., Lenze, D., Lichter, P., Martin-Subero, J. I., Möller, P., … Siebert, R. (2006). A Biologic Definition of Burkitt's Lymphoma from Transcriptional and Genomic Profiling. *New England Journal of Medicine*, *354*(23), 2419–2430. https://doi.org/10.1056/nejmoa055351

Iaccarino, I., Hancock, D., Evan, G., & Downward, J. (2003). c-Myc induces cytochrome c release in Rat1 fibroblasts by increasing outer mitochondrial membrane permeability in a Bid-dependent manner. *Cell Death and Differentiation*, *10*(5), 599–608. https://doi.org/10.1038/SJ.CDD.4401211

Imai, T., Tokunaga, A., Yoshida, T., Hashimoto, M., Mikoshiba, K., Weinmaster, G., Nakafuku, M., & Okano, H. (2001). The neural RNA-binding protein Musashi1 translationally regulates mammalian numb gene expression by interacting with its mRNA. *Molecular and Cellular Biology*, *21*(12), 3888–3900. https://doi.org/10.1128/MCB.21.12.3888-3900.2001

Irizarry, R. A., Hobbs, B., Collin, F., Beazer-Barclay, Y. D., Antonellis, K. J., Scherf, U., & Speed, T. P. (2003). Exploration, normalization, and summaries of high density oligonucleotide array probe level data. *Biostatistics (Oxford, England)*, *4*(2), 249–264. https://doi.org/10.1093/biostatistics/4.2.249

Ito, T., Kwon, H. Y., Zimdahl, B., Congdon, K. L., Blum, J., Lento, W. E., Zhao, C., Lagoo, A., Gerrard, G., Foroni, L., Goldman, J., Goh, H., Kim, S.-H., Kim, D.-W., Chuah, C., Oehler, V. G., Radich, J. P., Jordan, C. T., & Reya, T. (2010). Regulation of myeloid leukaemia by the cell-fate determinant Musashi. *Nature*, *466*(7307), 765–768. https://doi.org/10.1038/nature09171

Iwamoto, O., Koga, C., Matsumoto, H., Terasaki, S., Kusukawa, J., & Kameyama, T. (2021). Coffin-Siris Syndrome. *Asian Journal of Oral and Maxillofacial Surgery*, *15*(3), 205–207. https://doi.org/10.1016/S0915-6992(03)80044-4

Jaffe, E. S., Harris, N. L., Stein, H., & Isaacson, P. G. (2008). Classification of lymphoid neoplasms: the microscope as a tool for disease discovery. *Blood*, *112*(12), 4384–4399. https://doi.org/10.1182/BLOOD-2008-07-077982

Jain, P., Kanagal-Shamanna, R., Zhang, S., Ahmed, M., Ghorab, A., Zhang, L., Ok, C. Y., Li, S., Hagemeister, F., Zeng, D., Gong, T., Chen, W., Badillo, M., Nomie, K., Fayad, L., Medeiros, L. J., Neelapu, S., Fowler, N., Romaguera, J., … Wang, M. L. (2018). Long-term outcomes and mutation profiling of patients with mantle cell lymphoma (MCL) who discontinued ibrutinib. *British Journal of Haematology*, *183*(4), 578–587. https://doi.org/10.1111/BJH.15567

Jain, P., & Wang, M. L. (2022). Mantle cell lymphoma in 2022-A comprehensive update on molecular pathogenesis, risk stratification, clinical approach, and current and novel treatments. *American Journal of Hematology*, *97*(5), 638–656. https://doi.org/10.1002/AJH.26523

Jares, P., Colomer, D., & Campo, E. (2007). Genetic and molecular pathogenesis of mantle cell lymphoma: perspectives for new targeted therapeutics. *Nature Reviews Cancer 2007 7:10*, *7*(10), 750–762. https://doi.org/10.1038/NRC2230

Jiang, Y., Soong, T. D., Wang, L., Melnick, A. M., & Elemento, O. (2012). Genome-Wide Detection of Genes Targeted by Non-Ig Somatic Hypermutation in Lymphoma. *PLOS ONE*, *7*(7), e40332. https://doi.org/10.1371/JOURNAL.PONE.0040332

Jirawatnotai, S., Hu, Y., Livingston, D. M., & Sicinski, P. (2012). Proteomic identification of a direct role for cyclin d1 in DNA damage repair. *Cancer Research*, *72*(17), 4289–4293. https://doi.org/10.1158/0008-5472.CAN-11-3549

Johnston, W. T., Mutalima, N., Sun, D., Emmanuel, B., Bhatia, K., Aka, P., Wu, X., Borgstein, E., Liomba, G. N., Kamiza, S., Mkandawire, N., Batumba, M., Carpenter, L. M., Jaffe, H., Molyneux, E. M., Goedert, J. J., Soppet, D., Newton, R., & Mbulaiteye, S. M. (2014). Relationship between Plasmodium falciparum malaria prevalence, genetic diversity and endemic Burkitt lymphoma in Malawi. *Scientific Reports*, *4*. https://doi.org/10.1038/SREP03741

Jung, H. J., Chen, Z., & McCarty, N. (2011). Stem-like tumor cells confer drug resistant properties to mantle cell lymphoma. *Leukemia and Lymphoma*, *52*(6), 1066–1079. https://doi.org/10.3109/10428194.2011.562570

Kawano, Y., Kobune, M., Yamaguchi, M., Nakamura, K., Ito, Y., Sasaki, K., Takahashi, S., Nakamura, T., Chiba, H., Sato, T., Matsunaga, T., Azuma, H., Ikebuchi, K., Ikeda, H., Kato, J., Niitsu, Y., & Hamada, H. (2003). Ex vivo expansion of human umbilical cord hematopoietic progenitor cells using a coculture system with human telomerase catalytic subunit (hTERT)-transfected human stromal cells. *Blood*, *101*(2), 532–540. https://doi.org/10.1182/BLOOD-2002-04-1268

Kaymaz, Y., Oduor, C. I., Yu, H., Otieno, J. A., Ong'echa, J. M., Moormann, A. M., & Bailey, J. A. (2017). Comprehensive Transcriptome and Mutational Profiling of Endemic Burkitt Lymphoma Reveals EBV Type-Specific Differences. *Molecular Cancer Research : MCR*, *15*(5), 563–576. https://doi.org/10.1158/1541-7786.MCR-16-0305

Kelly, G. L., Stylianou, J., Rasaiyaah, J., Wei, W., Thomas, W., Croom-Carter, D., Kohler, C., Spang, R., Woodman, C., Kellam, P., Rickinson, A. B., & Bell, A. I. (2013). Different patterns of Epstein-Barr virus latency in endemic Burkitt lymphoma (BL) lead to distinct variants within the BL-associated gene expression signature. *Journal of Virology*, *87*(5), 2882–2894. https://doi.org/10.1128/JVI.03003-12

Keramari, M., Razavi, J., Ingman, K. A., Patsch, C., Edenhofer, F., Ward, C. M., & Kimber, S. J. (2010). Sox2 is essential for formation of trophectoderm in the preimplantation embryo. *PloS One*, *5*(11), e13952. https://doi.org/10.1371/JOURNAL.PONE.0013952

Kharas, M. G., Lengner, C. J., Al-Shahrour, F., Bullinger, L., Ball, B., Zaidi, S., Morgan, K., Tam, W., Paktinat, M., Okabe, R., Gozo, M., Einhorn, W., Lane, S. W., Scholl, C., Fröhling, S., Fleming, M., Ebert, B. L., Gilliland, D. G., Jaenisch, R., & Daley, G. Q. (2010). Musashi-2 regulates normal hematopoiesis and promotes aggressive myeloid leukemia. *Nature Medicine*, *16*(8), 903–908. https://doi.org/10.1038/nm.2187

Kim, S. M., Lee, S. T., Ryu, K. J., Kim, H. J., Kim, S. H., Ko, Y. H., Kim, W. S., & Kim, S. J. (2015). A subset of CD45+/CD19-cells in bone marrow may be associated with clinical outcomes of patients with mantle cell lymphoma. *Leukemia and Lymphoma*, *56*(11), 3052–3057. https://doi.org/10.3109/10428194.2015.1025391

Klein, U., & Dalla-Favera, R. (2008). Germinal centres: role in B-cell physiology and malignancy. *Nature Reviews Immunology 2008 8:1*, *8*(1), 22–33. https://doi.org/10.1038/NRI2217

Klein, U., Klein, G., Ehlin-Henriksson, B., Rajewsky, K., & Kuppers, R. (1995). Burkitt's lymphoma is a malignancy of mature B cells expressing somatically mutated V region genes. *Molecular Medicine*, *1*(5), 495. https://doi.org/10.1007/bf03401587

Klemm, S. L., Shipony, Z., & Greenleaf, W. J. (2019). Chromatin accessibility and the regulatory epigenome. *Nature Reviews Genetics 2018 20:4*, *20*(4), 207–220. https://doi.org/10.1038/S41576-018-0089-8

Klumb, C. E., Furtado, D. R., De Resende, L. M. M., Carriço, M. K., Coelho, A. M., De Meis, E., Maia, R. C., & Rumjanek, F. D. (2003). DNA sequence profile of TP53 gene mutations in childhood B-cell non-Hodgkin's lymphomas: prognostic implications. *European Journal of Haematology*, *71*(2), 81–90. https://doi.org/10.1034/J.1600-0609.2003.00094.X

Kouzarides, T. (2007). Chromatin Modifications and Their Function. *Cell*, *128*(4), 693–705. https://doi.org/10.1016/j.cell.2007.02.005

Kreso, A., & Dick, J. E. (2014). Evolution of the cancer stem cell model. *Cell Stem Cell*, *14*(3), 275–291. https://doi.org/10.1016/J.STEM.2014.02.006

Kridel, R., Meissner, B., Rogic, S., Boyle, M., Telenius, A., Woolcock, B., Gunawardana, J., Jenkins, C., Cochrane, C., Ben-Neriah, S., Tan, K., Morin, R. D., Opat, S., Sehn, L. H., Connors, J. M., Marra, M. A., Weng, A. P., Steidl, C., & Gascoyne, R. D. (2012). Whole transcriptome sequencing reveals recurrent NOTCH1 mutations in mantle cell lymphoma. *Blood*, *119*(9), 1963–1971. https://doi.org/10.1182/BLOOD-2011-11-391474

Kubo, H., Shimizu, M., Taya, Y., Kawamoto, T., Michida, M., Kaneko, E., Igarashi, A., Nishimura, M., Segoshi, K., Shimazu, Y., Tsuji, K., Aoba, T., & Kato, Y. (2009). Identification of mesenchymal stem cell (MSC)-transcription factors by microarray and knockdown analyses, and signature molecule-marked MSC in bone marrow by immunohistochemistry. *Genes to Cells*, *14*(3), 407–424. https://doi.org/10.1111/j.1365-2443.2009.01281.x

Kudinov, A. E., Deneka, A., Nikonova, A. S., Beck, T. N., Ahn, Y.-H., Liu, X., Martinez, C. F., Schultz, F. A., Reynolds, S., Yang, D.-H., Cai, K. Q., Yaghmour, K. M., Baker, K. A., Egleston, B. L., Nicolas, E., Chikwem, A., Andrianov, G., Singh, S., Borghaei, H., … Boumber, Y. (2016). Musashi-2 (MSI2) supports TGF-β signaling and inhibits claudins to promote non-small cell lung cancer (NSCLC) metastasis. *Proceedings of the National Academy of Sciences*, *113*(25), 6955–6960.

https://doi.org/10.1073/PNAS.1513616113

Kulakovskiy, I. V, Vorontsov, I. E., Yevshin, I. S., Sharipov, R. N., Fedorova, A. D., Rumynskiy, E. I., Medvedeva, Y. A., Magana-Mora, A., Bajic, V. B., Papatsenko, D. A., Kolpakov, F. A., & Makeev, V. J. (2018). HOCOMOCO: towards a complete collection of transcription factor binding models for human and mouse via large-scale ChIP-Seq analysis. *Nucleic Acids Research*, *46*(D1), D252–D259. https://doi.org/10.1093/NAR/GKX1106

Kuo, P. Y., Jatiani, S. S., Rahman, A. H., Edwards, D., Jiang, Z., Ahr, K., Perumal, D., Leshchenko, V. V., Brody, J., Shaknovich, R., Hilda Ye, B., & Parekh, S. (2018). SOX11 augments BCR signaling to drive MCL-like tumor development. *Blood*, *131*(20), 2247–2255. https://doi.org/10.1182/BLOOD-2018-02-832535

Kuo, P. Y., Leshchenko, W., Fazzari, M. J., Perumal, D., Gellen, T., He, T., Iqbal, J., Baumgartner-Wennerholm, S., Nygren, L., Zhang, F., Zhang, W., Suh, K. S., Goy, A., Yang, D. T., Chan, W. C., Kahl, B. S., Verma, A. K., Gascoyne, R. D., Kimby, E., … Parekh, S. (2015). High-resolution chromatin immunoprecipitation (ChIP) sequencing reveals novel binding targets and prognostic role for SOX11 in mantle cell lymphoma. *Oncogene*, *34*(10), 1231–1240. https://doi.org/10.1038/ONC.2014.44

Küppers, R., & Dalla-Favera, R. (2001). Mechanisms of chromosomal translocations in B cell lymphomas. *Oncogene*, *20*(40), 5580–5594. https://doi.org/10.1038/SJ.ONC.1204640

Küppers, R., Klein, U., Hansmann, M.-L., & Rajewsky, K. (1999). Cellular origin of human B-cell lymphomas. *The New England Journal of Medicine*, *341*(20), 1520–1529. https://doi.org/10.1056/NEJM199911113412007

Kurtova, A. V., Tamayo, A. T., Ford, R. J., & Burger, J. A. (2009). Mantle cell lymphoma cells express high levels of CXCR4, CXCR5, and VLA-4 (CD49d): importance for interactions with the stromal microenvironment and specific targeting. *Blood*, *113*(19), 4604. https://doi.org/10.1182/BLOOD-2008-10-185827

Kurtsdotter, I., Topcic, D., Karlén, A., Singla, B., Hagey, D. W., Bergsland, M., Siesjö, P., Nistér, M., Carlson, J. W., Lefebvre, V., Persson, O., Holmberg, J., & Muhr, J. (2017). SOX5/6/21 Prevent Oncogene-Driven Transformation of Brain Stem Cells. *Cancer Research*, *77*(18), 4985–4997. https://doi.org/10.1158/0008-5472.CAN-17-0704

Lam, N., & Sugden, B. (2003). CD40 and its viral mimic, LMP1: similar means to different ends. *Cellular Signalling*, *15*(1), 9–16. https://doi.org/10.1016/S0898-6568(02)00083-9

Larson, B. L., Ylostalo, J., Lee, R. H., Gregory, C., & Prockop, D. J. (2010). Sox11 is expressed in early progenitor human multipotent stromal cells and decreases with extensive expansion of the cells. *Tissue Engineering - Part A*, *16*(11), 3385–3394. https://doi.org/10.1089/ten.tea.2010.0085

Laurenti, E., Frelin, C., Xie, S., Ferrari, R., Dunant, C. F., Zandi, S., Neumann, A., Plumb, I., Doulatov, S., Chen, J., April, C., Fan, J. B., Iscove, N., & Dick, J. E. (2015). CDK6 Levels Regulate Quiescence Exit in Human Hematopoietic Stem Cells. *Cell Stem Cell*, *16*(3), 302–313. https://doi.org/10.1016/J.STEM.2015.01.017

Lefebvre, V., Dumitriu, B., Penzo-Méndez, A., Han, Y., & Pallavi, B. (2007). Control of cell fate and differentiation by Sry-related high-mobility-group box (Sox) transcription factors. *The International Journal of Biochemistry & Cell Biology*, *39*(12), 2195–2214. https://doi.org/10.1016/J.BIOCEL.2007.05.019

Lenz, G., Dreyling, M., Hoster, E., Wörmann, B., Dührsen, U., Metzner, B., Eimermacher, H., Neubauer, A., Wandt, H., Steinhauer, H., Martin, S., Heidemann, E., Aldaoud, A., Parwaresch, R., Hasford, J., Unterhalt, M., & Hiddemann, W. (2005). Immunochemotherapy with rituximab and cyclophosphamide, doxorubicin, vincristine, and prednisone significantly improves response and time to treatment failure, but not long-term outcome in patients with previously untreated mantle cell

lymphoma: results of a prospective randomized trial of the German Low Grade Lymphoma Study Group (GLSG). *Journal of Clinical Oncology : Official Journal of the American Society of Clinical Oncology*, *23*(9), 1984–1992. https://doi.org/10.1200/JCO.2005.08.133

Lenze, D., Leoncini, L., Hummel, M., Volinia, S., Liu, C. G., Amato, T., De Falco, G., Githanga, J., Horn, H., Nyagol, J., Ott, G., Palatini, J., Pfreundschuh, M., Rogena, E., Rosenwald, A., Siebert, R., Croce, C. M., & Stein, H. (2011). The different epidemiologic subtypes of Burkitt lymphoma share a homogenous micro RNA profile distinct from diffuse large B-cell lymphoma. *Leukemia*, *25*(12), 1869–1876. https://doi.org/10.1038/LEU.2011.156

Leszczyński, P., Śmiech, M., Parvanov, E., Watanabe, C., Mizutani, K. I., & Taniguchi, H. (2020). Emerging Roles of PRDM Factors in Stem Cells and Neuronal System: Cofactor Dependent Regulation of PRDM3/16 and FOG1/2 (Novel PRDM Factors). *Cells*, *9*(12). https://doi.org/10.3390/CELLS9122603

Leucci, E., Onnis, A., Cocco, M., De Falco, G., Imperatore, F., Giuseppina, A., Costanzo, V., Cerino, G., Mannucci, S., Cantisani, R., Nyagol, J., Mwanda, W., Iriso, R., Owang, M., Schurfeld, K., Bellan, C., Lazzi, S., & Leoncini, L. (2010). B-cell differentiation in EBV-positive Burkitt lymphoma is impaired at posttranscriptional level by miRNA-altered expression. *International Journal of Cancer*, *126*(6), 1316–1326. https://doi.org/10.1002/IJC.24655

Li, E. (2002). Chromatin modification and epigenetic reprogramming in mammalian development. *Nature Reviews Genetics 2002 3:9*, *3*(9), 662–673. https://doi.org/10.1038/NRG887

Li, L., Medina-Mené Ndez, C., García-Corzo, L., Có Rdoba-Beldad, C. M., Quiroga, A. C., Calleja Barca, E., Zinchuk, V., Muñ Oz-Ló Pez, S., Rodríguez-Martín, P., Ciorraga, M., Colmena, I. S., Ferná Ndez, S., Vicario, C., Nicolis, S. K., Ronique Lefebvre, V., Mira, H., & Morales, A. V. (2022). *SoxD genes are required for adult neural stem cell activation In brief SoxD genes are required for adult neural stem cell activation*. https://doi.org/10.1016/j.celrep.2022.110313

Li, N., Yousefi, M., Nakauka-Ddamba, A., Gregory, B. D., Yu, Z., & Correspondence, C. J. L. (2015). *The Msi Family of RNA-Binding Proteins Function Redundantly as Intestinal Oncoproteins Accession Numbers GSE74321 GSE54598*. https://doi.org/10.1016/j.celrep.2015.11.022

Li, Z., Van Calcar, S., Qu, C., Cavenee, W. K., Zhang, M. Q., & Ren, B. (2003). A global transcriptional regulatory role for c-Myc in Burkitt's lymphoma cells. *Proceedings of the National Academy of Sciences of the United States of America*, *100*(14), 8164–8169. https://doi.org/10.1073/PNAS.1332764100/SUPPL_FILE/2764SUPPDATASETFIG4.XLS

Littlewood, T. D., Hancock, D. C., Danielian, P. S., Parker, M. G., & Evan, G. I. (1995). A modified oestrogen receptor ligand-binding domain as an improved switch for the regulation of heterologous proteins. *Nucleic Acids Research*, *23*(10), 1686–1690. https://academic.oup.com/nar/article/23/10/1686/2400381

Liu, N., Zhang, J., & Ji, C. (2013). The emerging roles of Notch signaling in leukemia and stem cells. *Biomarker Research*, *1*(1), 1–7. https://doi.org/10.1186/2050-7771-1-23

Liu, Y., Zhou, X., & Wang, X. (2021). Targeting the tumor microenvironment in B-cell lymphoma: challenges and opportunities. *Journal of Hematology & Oncology 2021 14:1*, *14*(1), 1–17. https://doi.org/10.1186/S13045-021-01134-X

Loo, S. K., Suzina, S. S., Musa, M., & Wong, K. K. (2018). DNMT1 is associated with cell cycle and DNA replication gene sets in diffuse large B-cell lymphoma. *Pathology, Research and Practice*, *214*(1), 134–143. https://doi.org/10.1016/J.PRP.2017.10.005

López, C., Burkhardt, B., Chan, J. K. C., Leoncini, L., Mbulaiteye, S. M., Ogwang, M. D., Orem, J., Rochford, R., Roschewski, M., & Siebert, R. (2022). Burkitt lymphoma. *Nature Reviews. Disease Primers*, *8*(1). https://doi.org/10.1038/S41572-022-00404-3

López, C., Kleinheinz, K., Aukema, S. M., Rohde, M., Bernhart, S. H., Hübschmann, D., Wagener, R., Toprak, U. H., Raimondi, F., Kreuz, M., Waszak, S. M., Huang, Z., Sieverling, L., Paramasivam, N.,

Seufert, J., Sungalee, S., Russell, R. B., Bausinger, J., Kretzmer, H., … Siebert, R. (2019). Genomic and transcriptomic changes complement each other in the pathogenesis of sporadic Burkitt lymphoma. *Nature Communications*, *10*(1). https://doi.org/10.1038/S41467-019-08578-3

Love, C., Sun, Z., Jima, D., Li, G., Zhang, J., Miles, R., Richards, K. L., Dunphy, C. H., Choi, W. L., Srivastava, G., Lugar, P. L., Rizzieri, D. A., Lagoo, A. S., Bernal-Mizrachi, L., Mann, K. P., Flowers, C. R., Naresh, K. N., Evens, A. M., Chadburn, A., … Dave, S. S. (2012). The genetic landscape of mutations in Burkitt lymphoma. *Nature Genetics*, *44*(12), 1321–1325. https://doi.org/10.1038/NG.2468

Luanpitpong, S., Poohadsuan, J., Samart, P., Kiratipaiboon, C., Rojanasakul, Y., & Issaragrisil, S. (2018). Reactive oxygen species mediate cancer stem-like cells and determine bortezomib sensitivity via Mcl-1 and Zeb-1 in mantle cell lymphoma. *Biochimica et Biophysica Acta - Molecular Basis of Disease*, *1864*(11), 3739–3753. https://doi.org/10.1016/j.bbadis.2018.09.010

Lunning, M. A., & Green, M. R. (2015). Mutation of chromatin modifiers; an emerging hallmark of germinal center B-cell lymphomas. *Blood Cancer Journal 2015 5:10*, *5*(10), e361–e361. https://doi.org/10.1038/bcj.2015.89

Ma, I., & Allan, A. L. (2011). The Role of Human Aldehyde Dehydrogenase in Normal and Cancer Stem Cells. *Stem Cell Reviews and Reports*, *7*(2), 292–306. https://doi.org/10.1007/S12015-010-9208-4/FIGURES/2

Mallampati, S., Sun, B., Lu, Y., Ma, H., Gong, Y., Wang, D., Lee, J. S., Lin, K., & Sun, X. (2014). Integrated genetic approaches identify the molecular mechanisms of Sox4 in early B-cell development: intricate roles for RAG1/2 and CK1ε. *Blood*, *123*(26), 4064–4076. https://doi.org/10.1182/BLOOD-2013-12-543801

Mani, S. A., Guo, W., Liao, M. J., Eaton, E. N., Ayyanan, A., Zhou, A. Y., Brooks, M., Reinhard, F., Zhang, C. C., Shipitsin, M., Campbell, L. L., Polyak, K., Brisken, C., Yang, J., & Weinberg, R. A. (2008). The epithelial-mesenchymal transition generates cells with properties of stem cells. *Cell*, *133*(4), 704–715. https://doi.org/10.1016/J.CELL.2008.03.027

Martín-Garcia, D., Navarro, A., Valdés-Mas, R., Clot, G., Gutiérrez-Abril, J., Prieto, M., Ribera-Cortada, I., Woroniecka, R., Rymkiewicz, G., Bens, S., De Leval, L., Rosenwald, A., Ferry, J. A., Hsi, E. D., Fu, K., Delabie, J., Weisenburger, D., De Jong, D., Climent, F., … Bea, S. (2019). CCND2 and CCND3 hijack immunoglobulin light-chain enhancers in cyclin D1- mantle cell lymphoma. *Blood*, *133*(9), 940–951. https://doi.org/10.1182/BLOOD-2018-07-862151

Martin, P., Chadburn, A., Christos, P., Weil, K., Furman, R. R., Ruan, J., Elstrom, R., Niesvizky, R., Ely, S., Diliberto, M., Melnick, A., Knowles, D. M., Chen-Kiang, S., Coleman, M., & Leonard, J. P. (2009). Outcome of deferred initial therapy in mantle-cell lymphoma. *Journal of Clinical Oncology : Official Journal of the American Society of Clinical Oncology*, *27*(8), 1209–1213. https://doi.org/10.1200/JCO.2008.19.6121

McCall, M. N., Bolstad, B. M., & Irizarry, R. A. (2010). Frozen robust multiarray analysis (fRMA). *Biostatistics*, *11*(2), 242–253. https://doi.org/10.1093/BIOSTATISTICS/KXP059

Medina, D. J., Abass-Shereef, J., Walton, K., Goodell, L., Aviv, H., Strair, R. K., & Budak-Alpdogan, T. (2014). Cobblestone-area forming cells derived from patients with mantle cell lymphoma are enriched for CD133+ tumor-initiating cells. *PLoS ONE*, *9*(4). https://doi.org/10.1371/journal.pone.0091042

Melchers, F. (2015). Checkpoints that control B cell development. *The Journal of Clinical Investigation*, *125*(6), 2203–2210. https://doi.org/10.1172/JCI78083

Minuesa, G., Albanese, S. K., Xie, W., Kazansky, Y., Worroll, D., Chow, A., Schurer, A., Park, S.-M., Rotsides, C. Z., Taggart, J., Rizzi, A., Naden, L. N., Chou, T., Gourkanti, S., Cappel, D., Passarelli, M. C., Fairchild, L., Adura, C., Glickman, J. F., … Kharas, M. G. (2019). Small-molecule targeting of MUSASHI RNA-binding activity in acute myeloid leukemia. *Nature Communications 2019 10:1*,

10(1), 1–15. https://doi.org/10.1038/s41467-019-10523-3

Mlynarczyk, C., Fontán, L., & Melnick, A. (2019). Germinal center-derived lymphomas: The darkest side of humoral immunity. *Immunological Reviews*, *288*(1), 214–239. https://doi.org/10.1111/IMR.12755

Mohanty, A., Sandoval, N., Phan, A., Nguyen, T. V., Chen, R. W., Budde, E., Mei, M., Popplewell, L., Pham, L. V., Kwak, L. W., Weisenburger, D. D., Rosen, S. T., Chan, W. C., Müschen, M., & Ngo, V. N. (2019). Regulation of SOX11 expression through CCND1 and STAT3 in mantle cell lymphoma. *Blood*, *133*(4), 306–318. https://doi.org/10.1182/BLOOD-2018-05-851667

Molyneux, E. M., Rochford, R., Griffin, B., Newton, R., Jackson, G., Menon, G., Harrison, C. J., Israels, T., & Bailey, S. (2012). Burkitt's lymphoma. *The Lancet*, *379*(9822), 1234–1244. https://doi.org/10.1016/S0140-6736(11)61177-X

Mozos, A., Royo, C., Hartmann, E., De Jong, D., Baró, C., Valera, A., Fu, K., Weisenburger, D. D., Delabie, J., Chuang, S. S., Jaffe, E. S., Ruiz-Marcellan, C., Dave, S., Rimsza, L., Braziel, R., Gascoyne, R. D., Solé, F., López-Guillermo, A., Colomer, D., … Campo, E. (2009). SOX11 expression is highly specific for mantle cell lymphoma and identifies the cyclin D1-negative subtype. *Haematologica*, *94*(11), 1555–1562. https://doi.org/10.3324/haematol.2009.010264

Mrozek-Gorska, P., Buschle, A., Pich, D., Schwarzmayr, T., Fechtner, R., Scialdone, A., & Hammerschmidt, W. (2019). Epstein–Barr virus reprograms human B lymphocytes immediately in the prelatent phase of infection. *Proceedings of the National Academy of Sciences of the United States of America*, *116*(32), 16046–16055. https://doi.org/10.1073/PNAS.1901314116/-/DCSUPPLEMENTAL

Mu, Q., Wang, Y., Chen, B., Qian, W., Meng, H., Tong, H., Chen, F., Ma, Q., Ni, W., Chen, S., & Jin, J. (2013). High expression of Musashi-2 indicates poor prognosis in adult B-cell acute lymphoblastic leukemia. *Leukemia Research*, *37*(8), 922–927. https://doi.org/10.1016/j.leukres.2013.05.012

Müller, J. R., Janz, S., Goedert, J. J., Potter, M., & Rabkin, C. S. (1995). Persistence of immunoglobulin heavy chain/c-myc recombination-positive lymphocyte clones in the blood of human immunodeficiency virus-infected homosexual men. *Proceedings of the National Academy of Sciences of the United States of America*, *92*(14), 6577. https://doi.org/10.1073/PNAS.92.14.6577

Mundo, L., Ambrosio, M. R., Picciolini, M., Bello, G. Lo, Gazaneo, S., Del Porro, L., Lazzi, S., Navari, M., Onyango, N., Granai, M., Bellan, C., Falco, G. De, Gibellini, D., Piccaluga, P. P., & Leoncini, L. (2017). Unveiling Another Missing Piece in EBV-Driven Lymphomagenesis: EBV-Encoded MicroRNAs Expression in EBER-Negative Burkitt Lymphoma Cases. *Frontiers in Microbiology*, *8*(MAR). https://doi.org/10.3389/FMICB.2017.00229

Mundo, L., Del Porro, L., Granai, M., Siciliano, M. C., Mancini, V., Santi, R., Marcar, L., Vrzalikova, K., Vergoni, F., Di Stefano, G., Schiavoni, G., Segreto, G., Onyango, N., Nyagol, J. A., Amato, T., Bellan, C., Anagnostopoulos, I., Falini, B., Leoncini, L., … Lazzi, S. (2020). Frequent traces of EBV infection in Hodgkin and non-Hodgkin lymphomas classified as EBV-negative by routine methods: expanding the landscape of EBV-related lymphomas. *Modern Pathology : An Official Journal of the United States and Canadian Academy of Pathology, Inc*, *33*(12), 2407–2421. https://doi.org/10.1038/S41379-020-0575-3

Mzoughi, S., Fong, J. Y., Papadopoli, D., Koh, C. M., Hulea, L., Pigini, P., Di Tullio, F., Andreacchio, G., Hoppe, M. M., Wollmann, H., Low, D., Caldez, M. J., Peng, Y., Torre, D., Zhao, J. N., Uchenunu, O., Varano, G., Motofeanu, C. M., Lakshmanan, M., … Guccione, E. (2020). PRDM15 is a key regulator of metabolism critical to sustain B-cell lymphomagenesis. *Nature Communications 2020 11:1*, *11*(1), 1–14. https://doi.org/10.1038/s41467-020-17064-0

Nadeu, F., Martin-Garcia, D., Clot, G., Díaz-Navarro, A., Duran-Ferrer, M., Navarro, A., Vilarrasa-Blasi, R., Kulis, M., Royo, R., Gutiérrez-Abril, J., Valdés-Mas, R., López, C., Chapaprieta, V., Puiggros, M., Castellano, G., Costa, D., Aymerich, M., Jares, P., Espinet, B., … Campo, E. (2020). Genomic and epigenomic insights into the origin, pathogenesis, and clinical behavior of mantle cell lymphoma subtypes. *Blood*, *136*(12), 1419–1432. https://doi.org/10.1182/BLOOD.2020005289

Nagasawa, T. (2006). Microenvironmental niches in the bone marrow required for B-cell development. *Nature Reviews Immunology 2006 6:2*, *6*(2), 107–116. https://doi.org/10.1038/NRI1780

Nakashima, M. O., Durkin, L., Bodo, J., Lin, J., Quintanilla-Martinez, L., Fu, K., & Hsi, E. D. (2014). Utility and diagnostic pitfalls of SOX11 monoclonal antibodies in mantle cell lymphoma and other lymphoproliferative disorders. *Applied Immunohistochemistry & Molecular Morphology : AIMM*, *22*(10), 720–727. https://doi.org/10.1097/PAI.0000000000000067

Natkunam, Y., Vainer, G., Chen, J., Zhao, S., Marinelli, R. J., Hammer, A. S., Hamilton-Dutoit, S., Pikarsky, E., Amir, G., Levy, R., Yisraeli, J. K., & Lossos, I. S. (2007). Expression of the RNA-binding protein VICKZ in normal hematopoietic tissues and neoplasms. *Haematologica*, *92*(2). https://doi.org/10.3324/HAEMATOL.10724

Navarro, A., Beà, S., Jares, P., & Campo, E. (2020). Molecular Pathogenesis of Mantle Cell Lymphoma. *Hematology/Oncology Clinics of North America*, *34*(5), 795–807. https://doi.org/10.1016/J.HOC.2020.05.002

Navarro, A., Clot, G., Martínez-Trillos, A., Pinyol, M., Jares, P., González-Farré, B., Martínez, D., Trim, N., Fernández, V., Villamor, N., Colomer, D., Costa, D., Salaverria, I., Martín-Garcia, D., Erber, W., López, C., Jayne, S., Siebert, R., Dyer, M. J. S., … Beà, S. (2017). Improved classification of leukemic B-cell lymphoproliferative disorders using a transcriptional and genetic classifier. *Haematologica*, *102*(9), 360–363. https://doi.org/10.3324/haematol.2016.160374

Navarro, A., Clot, G., Royo, C., Jares, P., Hadzidimitriou, A., Agathangelidis, A., Bikos, V., Darzentas, N., Papadaki, T., Salaverria, I., Pinyol, M., Puig, X., Palomero, J., Vegliante, M. C., Amador, V., Martinez-Trillos, A., Stefancikova, L., Wiestner, A., Wilson, W., … Campo, E. (2012). Molecular subsets of mantle cell lymphoma defined by the IGHV mutational status and SOX11 expression have distinct biologic and clinical features. *Cancer Research*, *72*(20), 5307–5316. https://doi.org/10.1158/0008-5472.CAN-12-1615

Nguyen, D. T. T., Lu, Y., Chu, K. L., Yang, X., Park, S. M., Choo, Z. N., Chin, C. R., Prieto, C., Schurer, A., Barin, E., Savino, A. M., Gourkanti, S., Patel, P., Vu, L. P., Leslie, C. S., & Kharas, M. G. (2020). HyperTRIBE uncovers increased MUSASHI-2 RNA binding activity and differential regulation in leukemic stem cells. *Nature Communications*, *11*(1), 2026. https://doi.org/10.1038/s41467-020-15814-8

Nordström, L., Andréasson, U., Jerkeman, M., Dictor, M., Borrebaeck, C., & Ek, S. (2012). Expanded clinical and experimental use of SOX11 - using a monoclonal antibody. *BMC Cancer*, *12*(1), 1–11. https://doi.org/10.1186/1471-2407-12-269/TABLES/3

Nordström, L., Sernbo, S., Eden, P., Grønbæk, K., Kolstad, A., Räty, R., Karjalainen, M. L., Geisler, C., Ralfkiær, E., Sundström, C., Laurell, A., Delabie, J., Ehinger, M., Jerkeman, M., & Ek, S. (2014). SOX11 and TP53 add prognostic information to MIPI in a homogenously treated cohort of mantle cell lymphoma – a Nordic Lymphoma Group study. *British Journal of Haematology*, *166*(1), 98–108. https://doi.org/10.1111/BJH.12854

Nygren, L., Wennerholm, S. B., Klimkowska, M., Christensson, B., Kimby, E., & Sander, B. (2012). Prognostic role of SOX11 in a population-based cohort of mantle cell lymphoma. *Blood*, *119*(18), 4215–4223. https://doi.org/10.1182/BLOOD-2011-12-400580

O'Geen, H., Echipare, L., & Farnham, P. J. (2011). Using ChIP-Seq Technology to Generate High-Resolution Profiles of Histone Modifications. *Methods in Molecular Biology (Clifton, N.J.)*, *791*, 265. https://doi.org/10.1007/978-1-61779-316-5_20

Ogden, C. A., Pound, J. D., Batth, B. K., Owens, S., Johannessen, I., Wood, K., & Gregory, C. D. (2005). Enhanced apoptotic cell clearance capacity and B cell survival factor production by IL-10-activated macrophages: implications for Burkitt's lymphoma. *Journal of Immunology (Baltimore, Md. : 1950)*, *174*(5), 3015–3023. https://doi.org/10.4049/JIMMUNOL.174.5.3015

Okabe, M., Imai, T., Kurusu, M., Hiromi, Y., & Okano, H. (2001). Translational repression determines a neuronal potential in Drosophila asymmetric cell division. *Nature*, *411*(6833), 94–98. https://doi.org/10.1038/35075094

Okada, T., Ngo, V. N., Ekland, E. H., Förster, R., Lipp, M., Littman, D. R., & Cyster, J. G. (2002). Chemokine requirements for b cell entry to lymph nodes and Peyer's patches. *Journal of Experimental Medicine*, *196*(1), 65–75. https://doi.org/10.1084/JEM.20020201/VIDEO-2

Okazaki, I. M., Kinoshita, K., Muramatsu, M., Yoshikawa, K., & Honjo, T. (2002). The AID enzyme induces class switch recombination in fibroblasts. *Nature*, *416*(6878), 340–345. https://doi.org/10.1038/NATURE727

Okosun, J., Bödör, C., Wang, J., Araf, S., Yang, C. Y., Pan, C., Boller, S., Cittaro, D., Bozek, M., Iqbal, S., Matthews, J., Wrench, D., Marzec, J., Tawana, K., Popov, N., O'riain, C., O'shea, D., Carlotti, E., Davies, A., … Fitzgibbon, J. (2014). Integrated genomic analysis identifies recurrent mutations and evolution patterns driving the initiation and progression of follicular lymphoma. *Nature Genetics*, *46*(2), 176–181. https://doi.org/10.1038/NG.2856

Oliemuller, E., Kogata, N., Bland, P., Kriplani, D., Daley, F., Haider, S., Shah, V., Sawyer, E. J., & Howard, B. A. (2017). SOX11 promotes invasive growth and ductal carcinoma in situ progression. *Journal of Pathology*, *243*(2), 193–207. https://doi.org/10.1002/path.4939

Oliemuller, E., Newman, R., Tsang, S. M., Foo, S., Muirhead, G., Noor, F., Haider, S., Aurrekoetxea-Rodríguez, I., Vivanco, M. D. M., & Howard, B. A. (2020). Sox11 promotes epithelial/mesenchymal hybrid state and alters tropism of invasive breast cancer cells. *ELife*, *9*, 1–29. https://doi.org/10.7554/ELIFE.58374

Orkin, S. H. (1995). Hematopoiesis: how does it happen? *Current Opinion in Cell Biology*, *7*(6), 870–877. https://doi.org/10.1016/0955-0674(95)80072-7

Orkin, S. H. (2000). Diversification of haematopoietic stem cells to specific lineages. *Nature Reviews. Genetics*, *1*(1), 57–64. https://doi.org/10.1038/35049577

Orkin, S. H., & Zon, L. I. (2008). Hematopoiesis: An Evolving Paradigm for Stem Cell Biology. *Cell*, *132*(4), 631–644. https://doi.org/10.1016/J.CELL.2008.01.025

Palacios, F., Yan, X. J., Ferrer, G., Chen, S. S., Vergani, S., Yang, X., Gardner, J., Barrientos, J. C., Rock, P., Burack, R., Kolitz, J. E., Allen, S. L., Kharas, M. G., Abdel-Wahab, O., Rai, K. R., & Chiorazzi, N. (2021). Musashi 2 influences chronic lymphocytic leukemia cell survival and growth making it a potential therapeutic target. *Leukemia*, 1–16. https://doi.org/10.1038/s41375-020-01115-y

Palomero, J., Vegliante, M. C., Eguileor, A., Rodr'guez, M. L., Balsas, P., Mart'nez, D., Campo, E., & Amador, V. (2016). SOX11 defines two different subtypes of mantle cell lymphoma through transcriptional regulation of BCL6. *Leukemia*, *30*(7), 1580–1599. https://doi.org/10.1038/leu.2015.355

Palomero, J., Vegliante, M. C., Rodríguez, M. L., Eguileor, Á., Castellano, G., Planas-Rigol, E., Jares, P., Ribera-Cortada, I., Cid, M. C., Campo, E., & Amador, V. (2014). SOX11 promotes tumor angiogenesis through transcriptional regulation of PDGFA in mantle cell lymphoma. *Blood*, *124*(14), 2235–2247. https://doi.org/10.1182/blood-2014-04-569566

Park, S.-M., Deering, R. P., Lu, Y., Tivnan, P., Lianoglou, S., Al-Shahrour, F., Ebert, B. L., Hacohen, N., Leslie, C., Daley, G. Q., Lengner, C. J., & Kharas, M. G. (2014). Musashi-2 controls cell fate, lineage bias, and TGF-β signaling in HSCs. *Journal of Experimental Medicine*, *211*(1), 71–87. https://doi.org/10.1084/JEM.20130736

Park, S. M., Gönen, M., Vu, L., Minuesa, G., Tivnan, P., Barlowe, T. S., Taggart, J., Lu, Y., Deering, R. P., Hacohen, N., Figueroa, M. E., Paietta, E., Fernandez, H. F., Tallman, M. S., Melnick, A., Levine, R., Leslie, C., Lengner, C. J., & Kharas, M. G. (2015). Musashi2 sustains the mixed-lineage leukemia'driven stem cell regulatory program. *Journal of Clinical Investigation*, *125*(3), 1286–1298. https://doi.org/10.1172/JCI78440

Pasqualucci, L., Khiabanian, H., Fangazio, M., Vasishtha, M., Messina, M., Holmes, A. B., Ouillette, P., Trifonov, V., Rossi, D., Tabbò, F., Ponzoni, M., Chadburn, A., Murty, V. V., Bhagat, G., Gaidano, G., Inghirami, G., Malek, S. N., Rabadan, R., & Dalla-Favera, R. (2014). Genetics of follicular lymphoma transformation. *Cell Reports*, *6*(1), 130–140. https://doi.org/10.1016/J.CELREP.2013.12.027

Pasqualucci, L., Neumeister, P., Goossens, T., Nanjangud, G., Chaganti, R. S. K., Küppers, R., & Dalla-Favera, R. (2001). Hypermutation of multiple proto-oncogenes in B-cell diffuse large-cell lymphomas. *Nature*, *412*(6844), 341–346. https://doi.org/10.1038/35085588

Perez-Amill, L., Suñe, G., Antoñana-Vildosola, A., Castella, M., Najjar, A., Bonet, J., Fernández-Fuentes, N., Inogés, S., López, A., Bueno, C., Juan, M., Urbano-Ispizua, A., & Martín-Antonio, B. (2021). Preclinical development of a humanized chimeric antigen receptor against B cell maturation antigen for multiple myeloma. *Haematologica*, *106*(1), 173–184. https://doi.org/10.3324/HAEMATOL.2019.228577

Petrakis, G., Veloza, L., Clot, G., Gine, E., Gonzalez-Farre, B., Navarro, A., Bea, S., Martínez, A., Lopez-Guillermo, A., Amador, V., Ribera-Cortada, I., & Campo, E. (2019). Increased tumour angiogenesis in SOX11-positive mantle cell lymphoma. *Histopathology*, *75*(5), 704–714. https://doi.org/10.1111/his.13935

Pham, L. V., Tamayo, A. T., Yoshimura, L. C., Lo, P., & Ford, R. J. (2003). Inhibition of constitutive NF-kappa B activation in mantle cell lymphoma B cells leads to induction of cell cycle arrest and apoptosis. *Journal of Immunology (Baltimore, Md. : 1950)*, *171*(1), 88–95. https://doi.org/10.4049/JIMMUNOL.171.1.88

Piccaluga, P. P., De Falco, G., Kustagi, M., Gazzola, A., Agostinelli, C., Tripodo, C., Leucci, E., Onnis, A., Astolfi, A., Sapienza, M. R., Bellan, C., Lazzi, S., Tumwine, L., Mawanda, M., Ogwang, M., Calbi, V., Formica, S., Califano, A., Pileri, S. A., & Leoncini, L. (2011). Gene expression analysis uncovers similarity and differences among Burkitt lymphoma subtypes. *Blood*, *117*(13), 3596–3608. https://doi.org/10.1182/blood-2010-08-301556

Pieper, K., Grimbacher, B., & Eibel, H. (2013). B-cell biology and development. *The Journal of Allergy and Clinical Immunology*, *131*(4), 959–971. https://doi.org/10.1016/J.JACI.2013.01.046

Pinyol, M., Bea, S., Plà, L., Ribrag, V., Bosq, J., Rosenwald, A., Campo, E., & Jares, P. (2007). Inactivation of RB1 in mantle-cell lymphoma detected by nonsense-mediated mRNA decay pathway inhibition and microarray analysis. *Blood*, *109*(12), 5422–5429. https://doi.org/10.1182/BLOOD-2006-11-057208

Pinyol, M., Hernandez, L., Cazorla, M., Balbín, M., Jares, P., Fernandez, P. L., Montserrat, E., Cardesa, A., Lopez-Otín, C., & Campo, E. (1997). Deletions and Loss of Expression of P16INK4a and P21Waf1 Genes Are Associated With Aggressive Variants of Mantle Cell Lymphomas. *Blood*, *89*(1), 272–280. https://doi.org/10.1182/BLOOD.V89.1.272

Potti, A., Ganti, A. K., Kargas, S., & Koch, M. (2002). Immunohistochemical detection of C-kit (CD117) and vascular endothelial growth factor (VEGF) overexpression in mantle cell lymphoma. *Anticancer Research*, *22*(5), 2899–2901. https://europepmc.org/article/med/12530014

Pouremamali, F., Vahedian, V., Hassani, N., Mirzaei, S., Pouremamali, A., Kazemzadeh, H., Faridvand, Y., Jafari-gharabaghlou, D., Nouri, M., & Maroufi, N. F. (2022). The role of SOX family in cancer stem cell maintenance: With a focus on SOX2. *Pathology, Research and Practice*, *231*. https://doi.org/10.1016/J.PRP.2022.153783

Prichard, M., Harris, T., Williams, M. E., & Densmore, J. J. (2009). Treatment strategies for relapsed and refractory aggressive non-Hodgkin's lymphoma. *Expert Opinion on Pharmacotherapy*, *10*(6), 983–995. https://doi.org/10.1517/14656560902895715

Prieto, C., & Kharas, M. G. (2020). RNA Regulators in Leukemia and Lymphoma. *Cold Spring Harbor Perspectives in Medicine*, *10*(5). https://doi.org/10.1101/CSHPERSPECT.A034967

Pui, J. C., Allman, D., Xu, L., DeRocco, S., Karnell, F. G., Bakkour, S., Lee, J. Y., Kadesch, T., Hardy, R.

R., Aster, J. C., & Pear, W. S. (1999). Notch1 expression in early lymphopoiesis influences B versus T lineage determination. *Immunity*, *11*(3), 299–308. https://doi.org/10.1016/S1074-7613(00)80105-3

Qu, Y., Zhou, C., Zhang, J., Cai, Q., Li, J., Du, T., Zhu, Z., Cui, X., & Liu, B. (2014). The metastasis suppressor SOX11 is an independent prognostic factor for improved survival in gastric cancer. *International Journal of Oncology*, *44*(5), 1512–1520. https://doi.org/10.3892/IJO.2014.2328

Queirós, A. C., Beekman, R., Vilarrasa-Blasi, R., Duran-Ferrer, M., Clot, G., Merkel, A., Raineri, E., Russiñol, N., Castellano, G., Beà, S., Navarro, A., Kulis, M., Verdaguer-Dot, N., Jares, P., Enjuanes, A., Calasanz, M. J., Bergmann, A., Vater, I., Salaverría, I., … Martín-Subero, J. I. (2016). Decoding the DNA Methylome of Mantle Cell Lymphoma in the Light of the Entire B Cell Lineage. *Cancer Cell*, *30*(5), 806–821. https://doi.org/10.1016/J.CCELL.2016.09.014

Raffeld, M., & Jaffe, E. S. (1991). bcl-1, t(ll;14), and Mantle Cell-Derived Lymphomas. *Blood*, *78*(2), 259–263. https://doi.org/10.1182/BLOOD.V78.2.259.259

Rahal, R., Frick, M., Romero, R., Korn, J. M., Kridel, R., Chan, F. C., Meissner, B., Bhang, H. E., Ruddy, D., Kauffmann, A., Farsidjani, A., Derti, A., Rakiec, D., Naylor, T., Pfister, E., Kovats, S., Kim, S., Dietze, K., Dörken, B., … Stegmeier, F. (2014). Pharmacological and genomic profiling identifies NF-κB-targeted treatment strategies for mantle cell lymphoma. *Nature Medicine*, *20*(1), 87–92. https://doi.org/10.1038/NM.3435

Reya, T., Duncan, A. W., Ailles, L., Domen, J., Scherer, D. C., Willert, K., Hintz, L., Nusse, R., & Weissman, I. L. (2003). A role for Wnt signalling in self-renewal of haematopoietic stem cells. *Nature*, *423*(6938), 409–414. https://doi.org/10.1038/NATURE01593

Ribera-Cortada, I., Martinez, D., Amador, V., Royo, C., Navarro, A., Beà, S., Gine, E., De Leval, L., Serrano, S., Wotherspoon, A., Colomer, D., Martinez, A., & Campo, E. (2015). Plasma cell and terminal B-cell differentiation in mantle cell lymphoma mainly occur in the SOX11-negative subtype. *Modern Pathology : An Official Journal of the United States and Canadian Academy of Pathology, Inc*, *28*(11), 1435–1447. https://doi.org/10.1038/MODPATHOL.2015.99

Richter, J., John, K., Staiger, A. M., Rosenwald, A., Kurz, K., Michgehl, U., Ott, G., Franzenburg, S., Kohler, C., Finger, J., Oschlies, I., Paul, U., Siebert, R., Spang, R., Burkhardt, B., & Klapper, W. (2022). Epstein–Barr virus status of sporadic Burkitt lymphoma is associated with patient age and mutational features. *British Journal of Haematology*, *196*(3), 681–689. https://doi.org/10.1111/BJH.17874

Richter, J., Schlesner, M., Hoffmann, S., Kreuz, M., Leich, E., Burkhardt, B., Rosolowski, M., Ammerpohl, O., Wagener, R., Bernhart, S. H., Lenze, D., Szczepanowski, M., Paulsen, M., Lipinski, S., Russell, R. B., Adam-Klages, S., Apic, G., Claviez, A., Hasenclever, D., … Siebert, R. (2012). Recurrent mutation of the ID3 gene in Burkitt lymphoma identified by integrated genome, exome and transcriptome sequencing. *Nature Genetics*, *44*(12), 1316–1320. https://doi.org/10.1038/NG.2469

Rinaldi, A., Kwee, I., Taborelli, M., Largo, C., Uccella, S., Martin, V., Poretti, G., Gaidano, G., Calabrese, G., Martinelli, G., Baldini, L., Pruneri, G., Capella, C., Zucca, E., Cotter, F. E., Cigudosa, J. C., Catapano, C. V., Tibiletti, M. G., & Bertoni, F. (2006). Genomic and expression profiling identifies the B-cell associated tyrosine kinase Syk as a possible therapeutic target in mantle cell lymphoma. *British Journal of Haematology*, *132*(3), 303–316. https://doi.org/10.1111/J.1365-2141.2005.05883.X

Robbiani, D. F., Deroubaix, S., Feldhahn, N., Oliveira, T. Y., Callen, E., Wang, Q., Jankovic, M., Silva, I. T., Rommel, P. C., Bosque, D., Eisenreich, T., Nussenzweig, A., & Nussenzweig, M. C. (2015). Plasmodium Infection Promotes Genomic Instability and AID-Dependent B Cell Lymphoma. *Cell*, *162*(4), 727–737. https://doi.org/10.1016/J.CELL.2015.07.019

Roco, J. A., Mesin, L., Binder, S. C., Meyer-Hermann, M., Victora, G. D., Correspondence, C. G. V., Nefzger, C., Gonzalez-Figueroa, P., Canete, P. F., Ellyard, J., Shen, Q., Robert, P. A., Cappello, J., Vohra, H., Zhang, Y., Nowosad, C. R., Schiepers, A., Corcoran, L. M., Toellner, K.-M., … Vinuesa, C. G. (2019). Class-Switch Recombination Occurs Infrequently in Germinal Centers Article Class-Switch Recombination Occurs Infrequently in Germinal Centers. *Immunity*, *51*, 337–350.

https://doi.org/10.1016/j.immuni.2019.07.001

Roschewski, M., Staudt, L. M., & Wilson, W. H. (2022). Burkitt's Lymphoma. *The New England Journal of Medicine*, *387*(12), 1111–1122. https://doi.org/10.1056/NEJMRA2025746

Rosenwald, A., Wright, G., Wiestner, A., Chan, W. C., Connors, J. M., Campo, E., Gascoyne, R. D., Grogan, T. M., Muller-Hermelink, H. K., Smeland, E. B., Chiorazzi, M., Giltnane, J. M., Hurt, E. M., Zhao, H., Averett, L., Henrickson, S., Yang, L., Powell, J., Wilson, W. H., … Staudt, L. M. (2003). The proliferation gene expression signature is a quantitative integrator of oncogenic events that predicts survival in mantle cell lymphoma. *Cancer Cell*, *3*(2), 185–197. https://doi.org/10.1016/S1535-6108(03)00028-X

Rosich, L., Montraveta, A., Xargay-Torrent, S., Lo´pez-Guerra, M., Rolda´n, J., Aymerich, M., Salaverria, I., Bea`, S., Campo, E., Pe´rez-Gala´n, P., Roue´, G., & Colomer, D. (2014). Dual PI3K/mTOR inhibition is required to effectively impair microenvironment survival signals in mantle cell lymphoma. *Oncotarget*, *5*(16), 6788–6800. https://doi.org/10.18632/ONCOTARGET.2253

Rossant, J., & Tam, P. P. L. (2009). Blastocyst lineage formation, early embryonic asymmetries and axis patterning in the mouse. *Development (Cambridge, England)*, *136*(5), 701–713. https://doi.org/10.1242/DEV.017178

Rothenberg, E. V. (2014). Transcriptional Control of Early T and B Cell Developmental Choices. *Https://Doi-Org.Sire.Ub.Edu/10.1146/Annurev-Immunol-032712-100024*, *32*, 283–321. https://doi.org/10.1146/ANNUREV-IMMUNOL-032712-100024

Royo, C., Navarro, A., Clot, G., Salaverria, I., Giné, E., Jares, P., Colomer, D., Wiestner, A., Wilson, W. H., Vegliante, M. C., Fernandez, V., Hartmann, E. M., Trim, N., Erber, W. N., Swerdlow, S. H., Klapper, W., Dyer, M. J. S., Vargas-Pabón, M., Ott, G., … Beà, S. (2012). Non-nodal type of mantle cell lymphoma is a specific biological and clinical subgroup of the disease. *Leukemia*, *26*(8), 1895–1898. https://doi.org/10.1038/leu.2012.72

Ruddell, A., Mezquita, P., Brandvold, K. A., Farr, A., & Iritani, B. M. (2003). B lymphocyte-specific c-Myc expression stimulates early and functional expansion of the vasculature and lymphatics during lymphomagenesis. *The American Journal of Pathology*, *163*(6), 2233–2245. https://doi.org/10.1016/S0002-9440(10)63581-X

Rudelius, M., Rosenfeldt, M. T., Leich, E., Rauert-Wunderlich, H., Solimando, A., Beilhack, A., Ott, G., & Rosenwald, A. (2018). Inhibition of focal adhesion kinase overcomes resistance of mantle cell lymphoma to ibrutinib in the bone marrow microenvironment. *Haematologica*, *103*(1), 116–125. https://doi.org/10.3324/HAEMATOL.2017.177162

Ruegg, C., Postigo, A. A., Sikorski, E. E., Butcher, E. C., Pytela, R., & Erle, D. J. (1992). Role of integrin alpha 4 beta 7/alpha 4 beta P in lymphocyte adherence to fibronectin and VCAM-1 and in homotypic cell clustering. *The Journal of Cell Biology*, *117*(1), 179–189. https://doi.org/10.1083/JCB.117.1.179

Saba, N. S., Liu, D., Herman, S. E. M., Underbayev, C., Tian, X., Behrend, D., Weniger, M. A., Skarzynski, M., Gyamfi, J., Fontan, L., Melnick, A., Grant, C., Roschewski, M., Navarro, A., Beà, S., Pittaluga, S., Dunleavy, K., Wilson, W. H., & Wiestner, A. (2016). Pathogenic role of B-cell receptor signaling and canonical NF-κB activation in mantle cell lymphoma. *Blood*, *128*(1), 82–92. https://doi.org/10.1182/BLOOD-2015-11-681460

Saha, A., & Robertson, E. S. (2011). Epstein-Barr virus-associated B-cell lymphomas: pathogenesis and clinical outcomes. *Clinical Cancer Research : An Official Journal of the American Association for Cancer Research*, *17*(10), 3056–3063. https://doi.org/10.1158/1078-0432.CCR-10-2578

Sandberg, M., Källström, M., & Muhr, J. (2005). Sox21 promotes the progression of vertebrate neurogenesis. *Nature Neuroscience 2005 8:8*, *8*(8), 995–1001. https://doi.org/10.1038/NN1493

Sander, B., Campo, E., & Hsi, E. D. (2022). Chronic lymphocytic leukaemia/small lymphocytic lymphoma and mantle cell lymphoma: from early lesions to transformation. *Virchows Archiv 2022 482:1*, *482*(1),

131–145. https://doi.org/10.1007/S00428-022-03460-Y

Sander, S., Calado, D. P., Srinivasan, L., Köchert, K., Zhang, B., Rosolowski, M., Rodig, S. J., Holzmann, K., Stilgenbauer, S., Siebert, R., Bullinger, L., & Rajewsky, K. (2012). Synergy between PI3K signaling and MYC in Burkitt lymphomagenesis. *Cancer Cell*, *22*(2), 167–179. https://doi.org/10.1016/J.CCR.2012.06.012

Sarkar, A., & Hochedlinger, K. (2013). The Sox Family of Transcription Factors: Versatile Regulators of Stem and Progenitor Cell Fate. *Cell Stem Cell*, *12*(1), 15–30. https://doi.org/10.1016/J.STEM.2012.12.007

Sarkozy, C., Terré, C., Jardin, F., Radford, I., Roche-Lestienne, C., Penther, D., Bastard, C., Rigaudeau, S., Pilorge, S., Morschhauser, F., Bouscary, D., Delarue, R., Farhat, H., Rousselot, P., Hermine, O., Tilly, H., Chevret, S., & Castaigne, S. (2014). Complex karyotype in mantle cell lymphoma is a strong prognostic factor for the time to treatment and overall survival, independent of the MCL international prognostic index. *Genes, Chromosomes & Cancer*, *53*(1), 106–116. https://doi.org/10.1002/GCC.22123

Satou, A., Asano, N., Nakazawa, A., Osumi, T., Tsurusawa, M., Ishiguro, A., Elsayed, A. A., Nakamura, N., Ohshima, K., Kinoshita, T., & Nakamura, S. (2015). Epstein-barr virus (EBV)-positive sporadic burkitt lymphoma: An age-related lymphoproliferative disorder? *American Journal of Surgical Pathology*, *39*(2), 227–235. https://doi.org/10.1097/PAS.0000000000000332

Scheicher, R., Hoelbl-Kovacic, A., Bellutti, F., Tigan, A.-S., Prchal-Murphy, M., Heller, G., Schneckenleithner, C., Salazar-Roa, M., Zöchbauer-Müller, S., Zuber, J., Malumbres, M., Kollmann, K., & Sexl, V. (2015). CDK6 as a key regulator of hematopoietic and leukemic stem cell activation. *Blood*, *125*(1), 90–101. https://doi.org/10.1182/BLOOD-2014-06-584417

Scheller, M., Huelsken, J., Rosenbauer, F., Taketo, M. M., Birchmeier, W., Tenen, D. G., & Leutz, A. (2006). Hematopoietic stem cell and multilineage defects generated by constitutive beta-catenin activation. *Nature Immunology*, *7*(10), 1037–1047. https://doi.org/10.1038/NI1387

Schilham, M. W., Oosterwegel, M. A., Moerer, P., Ya, J., De Boert, P. A. J., Van De Wetering, M., Verbeek, S., Lamers, W. H., Kruisbeek, A. M., Cumano, A., & Clevers, H. (1996). Defects in cardiac outflow tract formation and pro-B-lymphocyte expansion in mice lacking Sox-4. *Nature 1996 380:6576*, *380*(6576), 711–714. https://doi.org/10.1038/380711A0

Schmitz, R., Ceribelli, M., Pittaluga, S., Wright, G., & Staudt, L. M. (2014). Oncogenic Mechanisms in Burkitt Lymphoma. *Cold Spring Harbor Perspectives in Medicine*, *4*(2). https://doi.org/10.1101/CSHPERSPECT.A014282

Schmitz, R., Young, R. M., Ceribelli, M., Jhavar, S., Xiao, W., Zhang, M., Wright, G., Shaffer, A. L., Hodson, D. J., Buras, E., Liu, X., Powell, J., Yang, Y., Xu, W., Zhao, H., Kohlhammer, H., Rosenwald, A., Kluin, P., Müller-Hermelink, H. K., … Staudt, L. M. (2012). Burkitt lymphoma pathogenesis and therapeutic targets from structural and functional genomics. *Nature*, *490*(7418), 116–120. https://doi.org/10.1038/NATURE11378

Schroeder, H. W., & Cavacini, L. (2010). Structure and Function of Immunoglobulins. *The Journal of Allergy and Clinical Immunology*, *125*(2 0 2), S41. https://doi.org/10.1016/J.JACI.2009.09.046

Schüler, F., Dölken, L., Hirt, C., Kiefer, T., Berg, T., Fusch, G., Weitmann, K., Hoffmann, W., Fusch, C., Janz, S., Rabkin, C. S., & Dölken, G. (2009). Prevalence and frequency of circulating t(14;18)-MBR translocation carrying cells in healthy individuals. *International Journal of Cancer. Journal International Du Cancer*, *124*(4), 958. https://doi.org/10.1002/IJC.23958

Scott, D. W., & Gascoyne, R. D. (2014). The tumour microenvironment in B cell lymphomas. *Nature Reviews Cancer 2014 14:8*, *14*(8), 517–534. https://doi.org/10.1038/nrc3774

Seifert, M., Sellmann, L., Bloehdorn, J., Wein, F., Stilgenbauer, S., Dürig, J., & Küppers, R. (2012). Cellular origin and pathophysiology of chronic lymphocytic leukemia. *The Journal of Experimental Medicine*,

209(12), 2183. https://doi.org/10.1084/JEM.20120833

Shaffer, A. L., Rosenwald, A., & Staudt, L. M. (2002). Lymphoid Malignancies: the dark side of B-cell differentiation. *Nature Reviews Immunology 2002 2:12*, *2*(12), 920–933. https://doi.org/10.1038/NRI953

Shaffer, A. L., Young, R. M., & Staudt, L. M. (2012). Pathogenesis of human B cell lymphomas. *Annual Review of Immunology*, *30*, 565–610. https://doi.org/10.1146/ANNUREV-IMMUNOL-020711-075027

Shaknovich, R., Cerchietti, L., Tsikitas, L., Kormaksson, M., De, S., Figueroa, M. E., Ballon, G., Yang, S. N., Weinhold, N., Reimers, M., Clozel, T., Luttrop, K., Ekstrom, T. J., Frank, J., Vasanthakumar, A., Godley, L. A., Michor, F., Elemento, O., & Melnick, A. (2011). DNA methyltransferase 1 and DNA methylation patterning contribute to germinal center B-cell differentiation. *Blood*, *118*(13), 3559–3569. https://doi.org/10.1182/BLOOD-2011-06-357996

Shapiro-Shelef, M., & Calame, K. C. (2005). Regulation of plasma-cell development. *Nature Reviews Immunology 2005 5:3*, *5*(3), 230–242. https://doi.org/10.1038/NRI1572

Shepherd, J. H., Uray, I. P., Mazumdar, A., Tsimelzon, A., Savage, M., Hilsenbeck, S. G., & Brown, P. H. (2016). The SOX11 transcription factor is a critical regulator of basal-like breast cancer growth, invasion, and basal-like gene expression. *Oncotarget*, *7*(11), 13106–13121. https://doi.org/10.18632/ONCOTARGET.7437

Silkenstedt, E., Arenas, F., Colom-Sanmartí, B., Xargay-Torrent, S., Higashi, M., Giró, A., Rodriguez, V., Fuentes, P., Aulitzky, W. E., Van Der Kuip, H., Beà, S., Toribio, M. L., Campo, E., López-Guerra, M., & Colomer, D. (2019). Notch1 signaling in NOTCH1-mutated mantle cell lymphoma depends on Delta-Like ligand 4 and is a potential target for specific antibody therapy. *Journal of Experimental & Clinical Cancer Research : CR*, *38*(1). https://doi.org/10.1186/S13046-019-1458-7

Sinclair, A. H., Berta, P., Palmer, M. S., Hawkins, J. R., Griffiths, B. L., Smith, M. J., Foster, J. W., Frischauf, A. M., Lovell-Badge, R., & Goodfellow, P. N. (1990). A gene from the human sex-determining region encodes a protein with homology to a conserved DNA-binding motif. *Nature*, *346*(6281), 240–244. https://doi.org/10.1038/346240A0

Sinner, D., Kordich, J. J., Spence, J. R., Opoka, R., Rankin, S., Lin, S.-C. J., Jonatan, D., Zorn, A. M., & Wells, J. M. (2007). Sox17 and Sox4 differentially regulate beta-catenin/T-cell factor activity and proliferation of colon carcinoma cells. *Molecular and Cellular Biology*, *27*(22), 7802–7815. https://doi.org/10.1128/MCB.02179-06

Sock, E., Rettig, S. D., Enderich, J., Bösl, M. R., Tamm, E. R., & Wegner, M. (2004). Gene targeting reveals a widespread role for the high-mobility-group transcription factor Sox11 in tissue remodeling. *Molecular and Cellular Biology*, *24*(15), 6635–6644. https://doi.org/10.1128/MCB.24.15.6635-6644.2004

Springer, T. A. (1994). Traffic signals for lymphocyte recirculation and leukocyte emigration: the multistep paradigm. *Cell*, *76*(2), 301–314. https://doi.org/10.1016/0092-8674(94)90337-9

Srinivasan, L., Sasaki, Y., Calado, D. P., Zhang, B., Paik, J. H., DePinho, R. A., Kutok, J. L., Kearney, J. F., Otipoby, K. L., & Rajewsky, K. (2009). PI3 Kinase Signals BCR-Dependent Mature B Cell Survival. *Cell*, *139*(3), 573–586. https://doi.org/10.1016/j.cell.2009.08.041

Stein, J. V., & Nombela-Arrieta, C. (2005). Chemokine control of lymphocyte trafficking: a general overview. *Immunology*, *116*(1), 1–12. https://doi.org/10.1111/J.1365-2567.2005.02183.X

Stier, S., Cheng, T., Dombkowski, D., Carlesso, N., & Scadden, D. T. (2002). Notch1 activation increases hematopoietic stem cell self-renewal in vivo and favors lymphoid over myeloid lineage outcome. *Blood*, *99*(7), 2369–2378. https://doi.org/10.1182/BLOOD.V99.7.2369

Stolt, C. C., Schlierf, A., Lommes, P., Hillgärtner, S., Werner, T., Kosian, T., Sock, E., Kessaris, N.,

Richardson, W. D., Lefebvre, V., & Wegner, M. (2006). SoxD Proteins Influence Multiple Stages of Oligodendrocyte Development and Modulate SoxE Protein Function. *Developmental Cell*, *11*(5), 697–709. https://doi.org/10.1016/J.DEVCEL.2006.08.011

Sun, B., Mallampati, S., Gong, Y., Wang, D., Lefebvre, V., & Sun, X. (2013). Sox4 is required for the survival of pro-B cells. *Journal of Immunology (Baltimore, Md.: 1950)*, *190*(5), 2080–2089. https://doi.org/10.4049/JIMMUNOL.1202736

Sung, S. P., Joong, S. K., Tessarollo, L., Owens, J. D., Peng, L., Seong, S. H., Seung, T. C., Torrey, T. A., Cheung, W. C., Polakiewicz, R. D., McNeil, N., Ried, T., Mushinski, J. F., Morse, H. C., & Janz, S. (2005). Insertion of c-Myc into Igh induces B-cell and plasma-cell neoplasms in mice. *Cancer Research*, *65*(4), 1306–1315. https://doi.org/10.1158/0008-5472.CAN-04-0268

Swerdlow, S. H., Campo, E., Harris, N. L., Jaffe, E. S., Pileri, S. A., Stein, H., Thiele, J., & Vardiman, J. . (2017). WHO Classification of Tumours of Haematopoietic and Lymphoid Tissues. In *World Health Organization Calssification of Tumours of Haematopoietic and Lymphoid Tissue* (Vol. 4th). https://doi.org/10.1017/CBO9781107415324.004

Swerdlow, S. H., Campo, E., Pileri, S. A., Lee Harris, N., Stein, H., Siebert, R., Advani, R., Ghielmini, M., Salles, G. A., Zelenetz, A. D., & Jaffe, E. S. (2016). The 2016 revision of the World Health Organization classification of lymphoid neoplasms. *Blood*, *127*(20), 2375–2390. https://doi.org/10.1182/blood-2016-01-643569

Taggart, J., Ho, T. C., Amin, E., Xu, H., Barlowe, T. S., Perez, A. R., Durham, B. H., Tivnan, P., Okabe, R., Chow, A., Vu, L., Park, S. M., Prieto, C., Famulare, C., Patel, M., Lengner, C. J., Verma, A., Roboz, G., Guzman, M., … Kharas, M. G. (2016). MSI2 is required for maintaining activated myelodysplastic syndrome stem cells. *Nature Communications*, *7*, 10739. https://doi.org/10.1038/ncomms10739

Takahashi, K., & Yamanaka, S. (2006). Induction of pluripotent stem cells from mouse embryonic and adult fibroblast cultures by defined factors. *Cell*, *126*(4), 663–676. https://doi.org/10.1016/J.CELL.2006.07.024

Tanaka, S., & Baba, Y. (2020). B Cell Receptor Signaling. In J.-Y. Wang (Ed.), *B Cells in Immunity and Tolerance* (pp. 23–36). Springer Singapore. https://doi.org/10.1007/978-981-15-3532-1_2

Teshima, K., Nara, M., Watanabe, A., Ito, M., Ikeda, S., Hatano, Y., Oshima, K., Seto, M., Sawada, K., & Tagawa, H. (2014). Dysregulation of BMI1 and microRNA-16 collaborate to enhance an anti-apoptotic potential in the side population of refractory mantle cell lymphoma. *Oncogene*, *33*(17), 2191–2203. https://doi.org/10.1038/onc.2013.177

Thein, D. C., Thalhammer, J. M., Hartwig, A. C., Bryan Crenshaw, E., Lefebvre, V., Wegner, M., & Sock, E. (2010). The closely related transcription factors Sox4 and Sox11 function as survival factors during spinal cord development. *Journal of Neurochemistry*, *115*(1), 131–141. https://doi.org/10.1111/J.1471-4159.2010.06910.X

Thomas, N., Dreval, K., Gerhard, D. S., Hilton, L. K., Abramson, J. S., Barta, S. K., Bartlett, N. L., Bethony, J., Bhatia, K., Bowen, J., Bryan, A. C., Cesarman, E., Casper, C., Cruz, M., Dyer, M., Farinha, P., Gastier-Foster, J., Gerrie, A. S., Grande, B., … Morin, R. D. (2022). GENETIC SUBGROUPS INFORM ON PATHOBIOLOGY IN ADULT AND PEDIATRIC BURKITT LYMPHOMA. *Blood*. https://doi.org/10.1182/BLOOD.2022016534

Thomson, M., Liu, S. J., Zou, L. N., Smith, Z., Meissner, A., & Ramanathan, S. (2011). Pluripotency factors in embryonic stem cells regulate differentiation into germ layers. *Cell*, *145*(6), 875–889. https://doi.org/10.1016/J.CELL.2011.05.017

Tierney, R. J., Shannon-Lowe, C. D., Fitzsimmons, L., Bell, A. I., & Rowe, M. (2015). Unexpected patterns of Epstein–Barr virus transcription revealed by a High throughput PCR array for absolute quantification of viral mRNA. *Virology*, *474*, 117. https://doi.org/10.1016/J.VIROL.2014.10.030

Till, J. E., & McCulloch, E. A. (1961). A direct measurement of the radiation sensitivity of normal mouse

bone marrow cells. *Radiation Research*, *14*, 213–222. https://doi.org/10.2307/3570892

Tirosh, I., Venteicher, A. S., Hebert, C., Escalante, L. E., Patel, A. P., Yizhak, K., Fisher, J. M., Rodman, C., Mount, C., Filbin, M. G., Neftel, C., Desai, N., Nyman, J., Izar, B., Luo, C. C., Francis, J. M., Patel, A. A., Onozato, M. L., Riggi, N., … Suvà, M. L. (2016). Single-cell RNA-seq supports a developmental hierarchy in human oligodendroglioma. *Nature*, *539*(7628), 309–313. https://doi.org/10.1038/nature20123

Tort, F., Hernández, S., Beà, S., Camacho, E., Fernández, V., Esteller, M., Fraga, M. F., Burek, C., Rosenwald, A., Hernńdez, L., & Campo, E. (2005). Checkpoint kinase 1 (CHK1) protein and mRNA expression is downregulated in aggressive variants of human lymphoid neoplasms. *Leukemia*, *19*(1), 112–117. https://doi.org/10.1038/SJ.LEU.2403571

Tort, F., Hernàndez, S., Beà, S., Martínez, A., Esteller, M., Herman, J. G., Puig, X., Camacho, E., Sánchez, M., Nayach, I., Lopez-Guillermo, A., Fernández, P. L., Colomer, D., Hernàndez, L., & Campo, E. (2002). CHK2-decreased protein expression and infrequent genetic alterations mainly occur in aggressive types of non-Hodgkin lymphomas. *Blood*, *100*(13), 4602–4608. https://doi.org/10.1182/BLOOD-2002-04-1078

Tsang, S. M., Kim, H., Oliemuller, E., Newman, R., Boateng, N. A., Guppy, N., & Howard, B. A. (2021). Sox11 regulates mammary tumour-initiating and metastatic capacity in Brca1-deficient mouse mammary tumour cells. *Disease Models & Mechanisms*, *14*(5). https://doi.org/10.1242/DMM.046037

Tsurusaki, Y., Koshimizu, E., Ohashi, H., Phadke, S., Kou, I., Shiina, M., Suzuki, T., Okamoto, N., Imamura, S., Yamashita, M., Watanabe, S., Yoshiura, K. I., Kodera, H., Miyatake, S., Nakashima, M., Saitsu, H., Ogata, K., Ikegawa, S., Miyake, N., & Matsumoto, N. (2014). De novo SOX11 mutations cause Coffin-Siris syndrome. *Nature Communications*, *5*. https://doi.org/10.1038/NCOMMS5011

Van De Wetering, M., Oosterwegel, M., Van Norren, K., & Clevers, H. (1993). Sox-4, an Sry-like HMG box protein, is a transcriptional activator in lymphocytes. *The EMBO Journal*, *12*(10), 3847–3854. https://doi.org/10.1002/J.1460-2075.1993.TB06063.X

Vega, F., Davuluri, Y., Cho-Vega, J. H., Singh, R. R., Ma, S., Wang, R. Y., Multani, A. S., Drakos, E., Pham, L. V., Lee, Y. C. L., Shen, L., Ambrus, J., Medeiros, L. J., & Ford, R. J. (2010). Side population of a murine mantle cell lymphoma model contains tumour-initiating cells responsible for lymphoma maintenance and dissemination. *Journal of Cellular and Molecular Medicine*, *14*(6 B), 1532–1545. https://doi.org/10.1111/j.1582-4934.2009.00865.x

Vegliante, M. C., Palomero, J., Pérez-Galán, P., Roué, G., Castellano, G., Navarro, A., Clot, G., Moros, A., Suárez-Cisneros, H., Beà, S., Hernández, L., Enjuanes, A., Jares, P., Villamor, N., Colomer, D., Martín-Subero, J. I., Campo, E., & Amador, V. (2013). SOX11 regulates PAX5 expression and blocks terminal B-cell differentiation in aggressive mantle cell lymphoma. *Blood*, *121*(12), 2175–2185. https://doi.org/10.1182/blood-2012-06-438937

Vegliante, M. C., Royo, C., Palomero, J., Salaverria, I., Balint, B., Martín-Guerrero, I., Agirre, X., Lujambio, A., Richter, J., Xargay-Torrent, S., Bea, S., Hernandez, L., Enjuanes, A., Calasanz, M. J., Rosenwald, A., Ott, G., Roman-Gomez, J., Prosper, F., Esteller, M., … Amador, V. (2011). Epigenetic activation of SOX11 in Lymphoid Neoplasms by Histone modifications. *PLoS ONE*, *6*(6). https://doi.org/10.1371/journal.pone.0021382

Vereide, D. T., Seto, E., Chiu, Y. F., Hayes, M., Tagawa, T., Grundhoff, A., Hammerschmidt, W., & Sugden, B. (2014). Epstein-Barr virus maintains lymphomas via its miRNAs. *Oncogene*, *33*(10), 1258–1264. https://doi.org/10.1038/ONC.2013.71

Victora, G. D., Dominguez-Sola, D., Holmes, A. B., Deroubaix, S., Dalla-Favera, R., & Nussenzweig, M. C. (2012). Identification of human germinal center light and dark zone cells and their relationship to human B-cell lymphomas. *Blood*, *120*(11), 2240–2248. https://doi.org/10.1182/BLOOD-2012-03-415380

Victora, G. D., & Nussenzweig, M. C. (2022). Germinal Centers. *Annual Review of Immunology*, *40*, 413–442. https://doi.org/10.1146/ANNUREV-IMMUNOL-120419-022408

Vilarrasa-Blasi, R., Soler-Vila, P., Verdaguer-Dot, N., Russiñol, N., Di Stefano, M., Chapaprieta, V., Clot, G., Farabella, I., Cuscó, P., Kulis, M., Agirre, X., Prosper, F., Beekman, R., Beà, S., Colomer, D., Stunnenberg, H. G., Gut, I., Campo, E., Marti-Renom, M. A., & Martin-Subero, J. I. (2021). Dynamics of genome architecture and chromatin function during human B cell differentiation and neoplastic transformation. *Nature Communications*, *12*(1), 1–18. https://doi.org/10.1038/s41467-020-20849-y

Vilarrasa-Blasi, R., Verdaguer-Dot, N., Belver, L., Soler-Vila, P., Beekman, R., Chapaprieta, V., Kulis, M., Queirós, A. C., Parra, M., Calasanz, M. J., Agirre, X., Prosper, F., Beà, S., Colomer, D., Marti-Renom, M. A., Ferrando, A., Campo, E., & Martin-Subero, J. I. (2022). Insights into the mechanisms underlying aberrant SOX11 oncogene expression in mantle cell lymphoma. *Leukemia*, *36*(2), 583–587. https://doi.org/10.1038/S41375-021-01389-W

Vose, J. M. (2017). Mantle cell lymphoma: 2017 update on diagnosis, risk-stratification, and clinical management. *American Journal of Hematology*, *92*(8), 806–813. https://doi.org/10.1002/AJH.24797

Wagener, R., López, C., Kleinheinz, K., Bausinger, J., Aukema, S. M., Nagel, I., Toprak, U. H., Seufert, J., Altmüller, J., Thiele, H., Schneider, C., Kolarova, J., Park, J., Hübschmann, D., Murga Penas, E. M., Drexler, H. G., Attarbaschi, A., Hovland, R., Kjeldsen, E., … Siebert, R. (2018). IG- MYC + neoplasms with precursor B-cell phenotype are molecularly distinct from Burkitt lymphomas. *Blood*, *132*(21), 2280–2285. https://doi.org/10.1182/BLOOD-2018-03-842088

Wang, G. G., Pasillas, M. P., & Kamps, M. P. (2006). Persistent transactivation by meis1 replaces hox function in myeloid leukemogenesis models: evidence for co-occupancy of meis1-pbx and hox-pbx complexes on promoters of leukemia-associated genes. *Molecular and Cellular Biology*, *26*(10), 3902–3916. https://doi.org/10.1128/MCB.26.10.3902-3916.2006

Wang, L., Lawrence, M. S., Wan, Y., Stojanov, P., Sougnez, C., Stevenson, K., Werner, L., Sivachenko, A., DeLuca, D. S., Zhang, L., Zhang, W., Vartanov, A. R., Fernandes, S. M., Goldstein, N. R., Folco, E. G., Cibulskis, K., Tesar, B., Sievers, Q. L., Shefler, E., … Wu, C. J. (2011). SF3B1 and Other Novel Cancer Genes in Chronic Lymphocytic Leukemia. *The New England Journal of Medicine*, *365*(26), 2497. https://doi.org/10.1056/NEJMOA1109016

Wang, M. L., Rule, S., Martin, P., Goy, A., Auer, R., Kahl, B. S., Jurczak, W., Advani, R. H., Romaguera, J. E., Williams, M. E., Barrientos, J. C., Chmielowska, E., Radford, J., Stilgenbauer, S., Dreyling, M., Jedrzejczak, W. W., Johnson, P., Spurgeon, S. E., Li, L., … Blum, K. A. (2013). Targeting BTK with Ibrutinib in Relapsed or Refractory Mantle-Cell Lymphoma. *Http://Dx.Doi.Org/10.1056/NEJMoa1306220*, *369*(6), 507–516. https://doi.org/10.1056/NEJMOA1306220

Wang, S., Li, N., Yousefi, M., Nakauka-Ddamba, A., Li, F., Parada, K., Rao, S., Minuesa, G., Katz, Y., Gregory, B. D., Kharas, M. G., Yu, Z., & Lengner, C. J. (2015). Transformation of the intestinal epithelium by the MSI2 RNA-binding protein. *Nature Communications*, *6*(1), 1–15. https://doi.org/10.1038/ncomms7517

Wang, X., Asplund, A. C., Porwit, A., Flygare, J., Smith, C. I. E., Christensson, B., & Sander, B. (2008). The subcellular Sox11 distribution pattern identifies subsets of mantle cell lymphoma: correlation to overall survival. *British Journal of Haematology*, *143*(2), 248–252. https://doi.org/10.1111/J.1365-2141.2008.07329.X

Wang, X., Björklund, S., Wasik, A. M., Grandien, A., Andersson, P., Kimby, E., Dahlman-Wright, K., Zhao, C., Christensson, B., & Sander, B. (2010). Gene Expression Profiling and Chromatin Immunoprecipitation Identify DBN1, SETMAR and HIG2 as Direct Targets of SOX11 in Mantle Cell Lymphoma. *PLOS ONE*, *5*(11), e14085. https://doi.org/10.1371/JOURNAL.PONE.0014085

Wasik, A. M., Lord, M., Wang, X., Zong, F., Andersson, P., Kimby, E., Christensson, B., Karimi, M., & Sander, B. (2013). SOXC transcription factors in mantle cell lymphoma: the role of promoter

methylation in SOX11 expression. *Scientific Reports*, *3*. https://doi.org/10.1038/SREP01400

Wästerlid, T., Nordström, L., Freiburghaus, C., Pedersen, M., Nørgaard, P., Gang, A. O., Brown, P., Dictor, M., Jerkeman, M., & Ek, S. (2017). Frequency and clinical implications of SOX11 expression in Burkitt lymphoma. *Leukemia and Lymphoma*, *58*(7), 1760–1763. https://doi.org/10.1080/10428194.2016.1258701/SUPPL_FILE/ILAL_A_1258701_SM4151.DOC

Wegner, M. (2010). All purpose Sox: The many roles of Sox proteins in gene expression. *The International Journal of Biochemistry & Cell Biology*, *42*(3), 381–390. https://doi.org/10.1016/J.BIOCEL.2009.07.006

Weigle, B., Ebner, R., Temme, A., Schwind, S., Schmitz, M., Kiessling, A., Rieger, M. A., Schackert, G., Schackert, H. K., & Rieber, E. P. (2005). Highly specific overexpression of the transcription factor SOX11 in human malignant gliomas. *Oncology Reports*, *13*(1), 139–144. https://doi.org/10.3892/OR.13.1.139/HTML

White, R. J., & Sharrocks, A. D. (2010). Coordinated control of the gene expression machinery. *Trends in Genetics*, *26*(5), 214–220. https://doi.org/10.1016/J.TIG.2010.02.004

Willis, T. G., & Dyer, M. J. S. (2000). The role of immunoglobulin translocations in the pathogenesis of B-cell malignancies. *Blood*, *96*(3), 808–822. https://doi.org/10.1182/BLOOD.V96.3.808

Yang, W., Wang, Y., Yu, Z., Li, Z., An, G., Liu, W., Lv, R., Ma, L., Yi, S., & Qiu, L. (2017). SOX11 regulates the pro-apoptosis signal pathway and predicts a favorable prognosis of mantle cell lymphoma. *International Journal of Hematology*, *106*(2), 212–220. https://doi.org/10.1007/S12185-017-2236-Y

Ye, S., Hao, X., Zhou, T., Wu, M., Wei, J., Wang, Y., Zhou, L., Jiang, X., Ji, L., Chen, Y., You, L., Zhang, Y., Xu, G., Zhou, J., Ma, D., & Wang, S. (2010). Plexin-B1 silencing inhibits ovarian cancer cell migration and invasion. *BMC Cancer*, *10*. https://doi.org/10.1186/1471-2407-10-611

Young, R. M., Phelan, J. D., Wilson, W. H., & Staudt, L. M. (2019). Pathogenic B cell receptor signaling in lymphoid malignancies: new insights to improve treatment. *Immunological Reviews*, *291*(1), 190. https://doi.org/10.1111/IMR.12792

Yu, F., Wu, F., Li, F., Liao, X., Wang, Y., Li, X., Wang, C., Shi, Y., & Ye, L. (2020). Wnt7b-induced Sox11 functions enhance self-renewal and osteogenic commitment of bone marrow mesenchymal stem cells. *Stem Cells*, *38*(8), 1020–1033. https://doi.org/10.1002/stem.3192

Zaja, F., Federico, M., Vitolo, U., & Zinzani, P. L. (2014). Management of relapsed/refractory mantle cell lymphoma: A review of current therapeutic strategies. *Leukemia and Lymphoma*, *55*(5), 988–998. https://doi.org/10.3109/10428194.2013.825903/SUPPL_FILE/DISCLOSURE.ZIP

Zech, L., Haglund, U., Nilsson, K., & Klein, G. (1976). Characteristic chromosomal abnormalities in biopsies and lymphoid-cell lines from patients with Burkitt and non-Burkitt lymphomas. *International Journal of Cancer*, *17*(1), 47–56. https://doi.org/10.1002/IJC.2910170108

Zhang, H., Tan, S., Wang, J., Chen, S., Quan, J., Xian, J., Zhang, S. S., He, J., & Zhang, L. (2014). Musashi2 modulates K562 leukemic cell proliferation and apoptosis involving the MAPK pathway. *Experimental Cell Research*, *320*(1), 119–127. https://doi.org/10.1016/j.yexcr.2013.09.009

Zhang, J., Dominguez-Sola, D., Hussein, S., Lee, J. E., Holmes, A. B., Bansal, M., Vlasevska, S., Mo, T., Tang, H., Basso, K., Ge, K., Dalla-Favera, R., & Pasqualucci, L. (2015). Disruption of KMT2D perturbs germinal center B cell development and promotes lymphomagenesis. *Nature Medicine*, *21*(10), 1190–1198. https://doi.org/10.1038/NM.3940

Zhang, J., Jima, D., Moffitt, A. B., Liu, Q., Czader, M., Hsi, E. D., Fedoriw, Y., Dunphy, C. H., Richards, K. L., Gill, J. I., Sun, Z., Love, C., Scotland, P., Lock, E., Levy, S., Hsu, D. S., Dunson, D., & Dave, S. S. (2014). The genomic landscape of mantle cell lymphoma is related to the epigenetically determined chromatin state of normal B cells. *Blood*, *123*(19), 2988–2996. https://doi.org/10.1182/BLOOD-2013-07-517177

Zhao, S., Kanagal-Shamanna, R., Navsaria, L., Ok, C. Y., Zhang, S., Nomie, K., Han, G., Hao, D., Hill, H. A., Jiang, C., Yao, Y., Nastoupil, L., Westin, J., Fayad, L., Nair, R., Steiner, R., Ahmed, S., Samaniego, F., Iyer, S. P., … Jain, P. (2020). Efficacy of venetoclax in high risk relapsed mantle cell lymphoma (MCL) - outcomes and mutation profile from venetoclax resistant MCL patients. *American Journal of Hematology*, *95*(6), 623–629. https://doi.org/10.1002/AJH.25796

Zhao, S., Nichols, J., Smith, A. G., & Li, M. (2004). SoxB transcription factors specify neuroectodermal lineage choice in ES cells. *Molecular and Cellular Neurosciences*, *27*(3), 332–342. https://doi.org/10.1016/J.MCN.2004.08.002

Zhou, H. M., Zhang, J. G., Zhang, X., & Li, Q. (2021). Targeting cancer stem cells for reversing therapy resistance: mechanism, signaling, and prospective agents. *Signal Transduction and Targeted Therapy*, *6*(1), 1–17. https://doi.org/10.1038/s41392-020-00430-1

Zon, L. I. (2008). Intrinsic and extrinsic control of haematopoietic stem-cell self-renewal. *Nature 2008 453:7193*, *453*(7193), 306–313. https://doi.org/10.1038/NATURE07038

Zorn, A. M., Barish, G. D., Williams, B. O., Lavender, P., Klymkowsky, M. W., & Varmus, H. E. (1999). Regulation of Wnt Signaling by Sox Proteins: XSox17α/β and XSox3 Physically Interact with β-catenin. *Molecular Cell*, *4*(4), 487–498. https://doi.org/10.1016/S1097-2765(00)80200-2

Zvelebil, M., Oliemuller, E., Gao, Q., Wansbury, O., MacKay, A., Kendrick, H., Smalley, M. J., Reis-Filho, J. S., & Howard, B. A. (2013). Embryonic mammary signature subsets are activated in Brca1-/- and basal-like breast cancers. *Breast Cancer Research : BCR*, *15*(2), R25. https://doi.org/10.1186/BCR3403

APPENDIX

Appendix Table 1. Primers or Taqman probes used for cloning, sequencing or qRT-PCR.

Gene or region	Primers or Taqman probes
MSI2 luciferase region	Forward: 5'-TCCTTGATCAAAATTTGCATTG-3'
	Reverse: 5'-TATGCGAAAGTAAATGAAGCTGA-3'
SOX11 Sanger sequencing region	Forward: 5'-TGATGTTCGACCTGAGCTTG-3'
	Reverse: 5'-AGATGTCGTGACGCAAAGAAA-3'
CDK6	Forward: 5'-TCTCCCGGCACTTCTGAAAT-3'
	Reverse: 5'-ACACCAGGTAGAAGGACTGC-3'
NOTCH1	Forward: 5'-ACTGTACCGAGGATGTGGAC-3'
	Reverse: 5'-ACACTCGCAGTAGAAGGAGG-3'
MSI2	Forward: 5’-CCAAAGTTGCATTTCCTCGT-3’
	Reverse: 5’-ACAAAGCCAAACCCTCTGTG-3’
SOX11	Forward: 5’-GACCCAGACTGGTGCAAGAC-3’
	Reverse: 5’-GCTGTCCTTCAGCATTTTCC-3’
GUSB	Forward: 5’-CGTGGTTGGAGAGCTCATTT-3’
	Reverse: 5’-GAACGCTGCACTTTTTGGTT-3’
CASP8	hs01018151_m1
CASP10	hs01017899_m1
MEX3A	Forward: 5’-TCTACAAAGAGGCCGAGCTG-3’
	Reverse: 5’-CCCTCACCGGTGTCTTGATG-3’
PLXNB1	Forward: 5’-ACTGTGACACCATCTCCCAG-3’
	Reverse: 5’-AATGCTGCAGTGTGTTCAGG-3’
CD24	Forward: 5’-GCTCCTACCCACGCAGATTT-3’
	Reverse: 5’-GAGACCACGAAGAGACTGGC-3’

Appendix Table 2. MCL sample information and experimental conditions for RNA extraction, library amplification and RNA-seq.

Dataset	Case or samples	SOX11	RNA extraction	Library	Sequencing
MCL primary cases	M027	Neg.	TRIZOL	TruSeq Stranded Total RNA kit with Ribo-	75 bp paired-end
	M029	Pos.			
	M032	Pos.			

				Zero Gold	
	M248	Pos.			
	M399	Pos.			
	M397	Pos.			
	M432	Pos.			
	M435	Pos.			
	M395	Pos.			
	M244	Neg.			
	M003	Neg.			
	M076	Neg.			
Z138 SOX11 knock out	Z138-SOX11KO 1	Neg.	RNeasy Plus kit	TruSeq RNA Sample Prep Kit v2	50 bp single-end
	Z138-SOX11KO 2	Neg.			
	Z138-SOX11KO 3	Neg.			
	Z138 CT 1	Pos.			
	Z138 CT 2	Pos.			
	Z138 CT 3	Pos.			
JVM2 overexpressing SOX11	JVM2CT 1	Neg.	RNeasy Plus kit	TruSeq RNA Sample Prep Kit v2	50 bp single-end
	JVM2CT 2	Neg.			
	JVM2CT 3	Neg.			
	JVM2-SOX11+ 1	Pos.			
	JVM2-SOX11+ 2	Pos.			
	JVM2-SOX11+ 3	Pos.			
Z138 MSI2 silencing	Z138sh4MSI2 1	NR	RNeasy Plus kit	TruSeq RNA Sample Prep Kit v2	50 bp paired-end
	Z138sh4MSI2 2	NR			
	Z138sh5MSI2 1	NR			

	Z138sh5MSI2 2	NR			
	Z138shCT 1.1	NR			
	Z138shCT 1.2	NR			
	Z138shCT 2.1	NR			
	Z138shCT 2.2	NR			
Z138 MSI2 inhibition with Ro 08-2750	Z138 DMSO 1	NR	RNeasy Plus kit	TruSeq RNA Sample Prep Kit v2	50 bp paired-end
	Z138 DMSO 2	NR			
	Z138 DMSO 3	NR			
	Z138 RO 1	NR			
	Z138 RO 2	NR			
	Z138 RO 3	NR			
DG75 ER + 4-OHT 8h	DG75 ER 8h 1	Neg.	RNeasy Plus kit	TruSeq RNA Sample Prep Kit v2	50 bp paired-end
	DG75 ER 8h 2	Neg.			
	DG75 ER 8h 3	Neg.			
DG75 ER + 4-OHT 24h	DG75 ER 24h 1	Neg.	RNeasy Plus kit	TruSeq RNA Sample Prep Kit v2	50 bp paired-end
	DG75 ER 24h 2	Neg.			
	DG75 ER 24h 3	Neg.			
DG75 ER-SOX11 + 4-OHT 8h	DG75 ER-SOX11 8h 1	Pos.	RNeasy Plus kit	TruSeq RNA Sample Prep Kit v2	50 bp paired-end
	DG75 ER-SOX11 8h 2	Pos.			
	DG75 ER-SOX11 8h 3	Pos.			

DG75 ER-SOX11 + 4-OHT 24h	DG75 ER-SOX11 24h 1	Pos.	RNeasy Plus kit	TruSeq RNA Sample Prep Kit v2	50 bp paired-end
	DG75 ER-SOX11 24h 2	Pos.			
	DG75 ER-SOX11 24h 3	Pos.			
Ramos CT	Ramos CT1	Neg.	RNeasy Plus kit	TruSeq RNA Sample Prep Kit v2	50 bp paired-end
	Ramos CT2	Neg.			
Ramos SOX11	Ramos SOX11-1	Pos.	RNeasy Plus kit	TruSeq RNA Sample Prep Kit v2	50 bp paired-end
	Ramos SOX11-2	Pos.			
BL2 CT	BL2 CT1	Pos.	RNeasy Plus kit	TruSeq RNA Sample Prep Kit v2	50 bp paired-end
	BL2 CT2	Pos.			
	BL2 CT3	Pos.			
	BL2 CT4	Pos.			
BL2 SOX11-KO	BL2-SOX11KO1	Neg.	RNeasy Plus kit	TruSeq RNA Sample Prep Kit v2	50 bp paired-end
	BL2-SOX11KO2	Neg.			
	BL2-SOX11KO3	Neg.			
	BL2-SOX11KO4	Neg.			

Pos: Positive; Neg: Negative, NR: No relevant.

Appendix Table 3. Antibodies used for western blot, RNA immunoprecipitation, flow cytometry and immunofluroescence.

Protein	Company	Reference	Dilution	WB	RIP	FC	IF	IHC
SOX11	Cell Marque	MRQ-58	1/1000	X				X
SOX11	Abcam	ab170916	1/100				X	
MSI2	Abcam	ab76148	1/1000	X	X			
CDK6	Santa Cruz	sc-56282	1/200	X				
NOTCH1 (D1E11)	Cell Signaling	#3608	1/1000	X				
p-27 (KIP1)	BD Biosciences	554069	1/1000	X				
p-21 (WAF1)	Sigma-Aldrich	P1484	1/1000	X				
p-53	Cell signaling	9282	1/1000	X				

Phospho-p-53 (S15)	Cell signaling	9286	1/1000	X				
Alpha-Tubulin	Sigma-Aldrich	CP06	1/5000	X				
Beta-Actin	Sigma-Aldrich	a5441	1/5000	X				
Lamin B1	Abcam	ab65986	1/5000	X				
Anti-rabbit IgG (A488 conjugated)	Thermo scientific	A21206	1/400				X	
Anti-rabbit IgG (HRP conjugated)	DAKO	P0217	1/5000	X				
Anti-mouse IgG (HRP conjugated)	DAKO	P0260	1/5000	X				
Anti-rabbit IgG (HRP conjugated)	Cell signaling	#7074	1/1000	X				
Anti-mouse IgG (HRP conjugated)	Cell signaling	#7076	1/1000	X				
Mex-3A	Abcam	ab-79046	1/1000	X				
GAPDH	Santa Cruz	sc-137179	1/1000	X				
p-Syk (Y525/526)	Cell signaling	2710P	1/1000	X				
Normal rabbit IgG	Millipore	sc-2027			X			
Active Caspase-3 FITC	BD Biosciences	550480				X		
Fas FITC (CD95)	Thermo scientific	11-0959-42				X		
Mouse IgG1 kappa isotype FITC	Thermo scientific	11-4714-42				X		
CD24 PE	BD	555428				X		
IgG2a kappa isotype PE	eBioscience	12-4732-42				X		

WB: Western Blot, RIP: RNA immunoprecipitation, FC: Flow Cytometry, IF: immunofluorescence, IHC: immunohistochemistry.

Appendix Table 4. Stem cell-related gene sets used for GSEA in SOX11+ vs SOX11- MCLs.

Enriched in SOX11+ vs SOX11-						
NAME	**SIZE**	**ES**	**NES**	**NOM p-val**	**FDR q-val**	**FWER p-val**
BENPORATH_OCT4_TARGETS	270	0.510	1.610	0.002	0.035	0.018
BENPORATH_NOS_TARGETS	165	0.530	1.607	0.000	0.019	0.019
JAATINEN_HEMATOPOIETIC_STEM_CELL_UP	290	0.671	1.606	0.002	0.013	0.019
IVANOVA_HEMATOPOIESIS_STEM_CELL	176	0.536	1.583	0.002	0.015	0.032
GAL_LEUKEMIC_STEM_CELL_UP	129	0.488	1.582	0.000	0.012	0.032
BHATTACHARYA_EMBRYONIC_STEM_CELL	71	0.668	1.544	0.014	0.020	0.063
IVANOVA_HEMATOPOIESIS_STEM_CELL_LONG_TERM	203	0.461	1.481	0.010	0.044	0.147
HADDAD_B_LYMPHOCYTE_PROGENITOR	259	0.572	1.453	0.012	0.054	0.192
BENPORATH_NANOG_TARGETS	891	0.442	1.452	0.008	0.048	0.192
CONRAD_STEM_CELL	35	0.496	1.374	0.062	0.098	0.358
KEGG_HEDGEHOG_SIGNALING_PATHWAY	52	0.392	1.346	0.081	0.116	0.42
GAL_LEUKEMIC_STEM_CELL_DN	233	0.583	1.344	0.070	0.109	0.427
HADDAD_T_LYMPHOCYTE_AND_NK_PROGENITOR_DN	60	0.696	1.324	0.080	0.120	0.467
RAMALHO_STEMNESS_UP	68	0.472	1.231	0.119	0.214	0.646
LIANG_HEMATOPOIESIS_STEM_CELL_NUMBER_QTL	16	0.576	1.224	0.170	0.209	0.65
WONG_EMBRYONIC_STEM_CELL_CORE	323	0.536	1.205	0.266	0.219	0.674
RAMALHO_STEMNESS_DN	65	0.523	1.175	0.269	0.248	0.727
HOEBEKE_LYMPHOID_STEM_CELL_UP	87	0.454	1.154	0.206	0.265	0.757
EPPERT_CE_HSC_LSC	38	0.477	1.103	0.297	0.322	0.81
JAATINEN_HEMATOPOIETIC_STEM_CELL_DN	214	0.572	1.047	0.478	0.392	0.857
EPPERT_HSC_R	119	0.406	1.043	0.373	0.380	0.858
ENGELMANN_CANCER_PROGENITORS_UP	44	0.367	1.019	0.404	0.398	0.878
ENGELMANN_CANCER_PROGENITORS_DN	63	0.302	0.957	0.521	0.482	0.926
HOFFMANN_IMMATURE_TO_MATURE_B_LYMPHOCYTE_DN	29	0.385	0.845	0.670	0.675	0.978

Enriched in SOX11- VS SOX11+						
NAME	**SIZE**	**ES**	**NES**	**NOM p-val**	**FDR q-val**	**FWER p-val**
HOFFMANN_IMMATURE_TO_MATURE_B_LYMPHOCYTE_UP	21	-0.648	-1.341	0.110	0.185	0.449
BIOCARTA_IL3_PATHWAY	15	-0.542	-1.194	0.190	0.244	0.707
KEGG_HEMATOPOIETIC_CELL_LINEAGE	84	-0.313	-0.768	0.830	0.828	0.988

ES: enrichment score, NES: Normalized enrichment score

Appendix Table 5. Differentially expressed genes between SOX11+ and SOX11- leukemic MCL (GSE79196) with adjusted P-value <0.05 and absolute log2 fold change >0.7.

Genes upregulated in SOX11+ MCLs vs SOX11- MCLs							
SOX11	HDGFL3	ZNF711	NREP	PON2	FNBP1L	APBB2	CRIM1
FARP1	DBN1	ABCA6	FHL1	DCHS1	SATB1	MYO6	TCL1A
CNR1	GLUL	CRY1	FCGBP	KANK1	PLEKHG4B	IGF1R	NINL
MARCKSL1	GSDME	CDCA7	SERPINE2	RASSF6	DLL1	HRK	FMNL2
LAPTM4B	MEX3D	CNN3	PNMA2	RNGTT	PSD3	PPM1L	KAZN
SERPINF1	STMN1	SLC44A5	CTBP2	VANGL2	ATP11A	ITGB8	DIP2C
NSG1	SSBP3	PTPRG	ZWINT	BEX3	MSR1	TM6SF1	RGS12
LRRN1	TJP2	MGC70870	ROBO1	LRATD2	CLEC2B	LCK	TBC1D4
SYT17	CABLES1	TSPAN13	DNMT3A	PTPRK	SORL1	BEX2	CD24
BTBD3	SMARCA1	HMGB3	CHI3L2	CRNDE	LATS2	MYH10	ZBED3
B3GALNT1	BEX5	FBXO15	FAM169A	FADS3	PRKAR2B	CACHD1	TIAM1
PELI2	CTPS2	CYTH3	TSHZ2	UCHL1	SERPINB9P1	RETREG1	LGALS3BP
CECR2	ID2	PKD2	LINC00954	TNFRSF21	LRRC34	C11orf95	RTL6
COL1A2	LINC01102	GTF2IRD1	ARMCX2	SEPTIN11	HNRNPC	BCL7A	CDYL2
MYBL2	CMTM3	TRPC1	H2BW4P	MEX3B	AXIN2	ULK2	RELL1
SETMAR	FAM43A	CCDC191	PHLDB2	ZKSCAN7	PFN2	MFHAS1	JUP
TYMS	ACVR2B	CDK2AP1	TCL6	RIMKLB	LINC00888	ASAP2	SPRY2
PRDX2	RGCC	SPATS2L	LINC00865	PROX1	TFDP2	FGF9	H1-10
UHRF1	GSTA4	NUDT11	MAP3K20	INSR	GRIK3	DIPK1B	MGLL
BEX4	ADD2	PRF1	C14orf132	LOC101927811	CASP6	KIF21A	TUBB
TRIB2	MTCL1	SLC35G2	MIR181A2HG	TSPYL5	FUT4	PARD3	NOL4L
ZNF135	MEST	IGLJ3	LDLR	CAMK2N1	PHYHD1	HIP1	PDE9A
SERINC5	SPIN1	RBMS1	TRIQK	KCTD3	EPDR1	PEG10	PTPRN2
NET1	SLC12A7	RCN1	TMEM263	FEZ1	TNFSF8	PALLD	C12orf75
SCD	HOMER3	CHROMR	GSTP1	SPIN4	ZBTB8A	NAV1	DMXL2
LTBP1	POTEM	BAZ2B	SGCB	ZC3HAV1L	AMOTL1	ZNF667-AS1	KLHL6
IL13RA1	NFE2L3	CRIM1-DT	TANC2	PLXNB1	TCF7L2	KANK2	NEXMIF
RFLNB	ARHGAP6	PLXND1	TENM4	TTC39C	DLG5	N4BP2	ZNF667
YES1	EPHA4	PTP4A3	HMGN5	TESC	COL27A1	FAM171A1	ARHGAP44
MBOAT2	GPSM1	NAP1L3	TMEM237	ABRACL	PODXL	CORO2B	TIMP2
CCL4	SOBP	CEP41	LOC100506098	FAM161A	AASS	LHFPL2	PAG1
OLFM4	AGPAT4-IT1	PRICKLE1	AKAP7	MARK1	CYP2C8	NAP1L2	GRAMD2B
DTX1	MEGF6	DCAF12	LGALSL	TMEM44	ANKRD50	GEM	ARHGAP21
CLIC6	SYT11	TLR4	GOLIM4	DNAJC6	JAM2	LOC389906	TPM2

CRYM	ZMAT1	DCLK2	TNFSF4	RFTN1	SFMBT2	RASSF4	FZD6
P2RX1	TUBB2A	PLBD1	CLDN23	TET1	CARMIL1	GADD45A	HMGB3P1
L3MBTL4	CDC14B	MERTK	ANK2	CA2	APP	RMI2	SOCS6
KBTBD11	JAKMIP2	RNF130	ZNF704	CEBPD	MYO1E	CADM1	TNFRSF25
LOC101927432	NPTX2	TRO	KCNMB4	FSTL1	CCDC50	ALDH7A1	DNAJA4
SMARCA4	MYL6B	MAGED1	SCAMP5	NDFIP2	LINC01224	BUB1	CLIC4
SIRPA	MIR9-3HG	PLSCR1	KIAA1217	ITGA6	ZNF521	ZAP70	UBTD2
GAL3ST4	ZSCAN2	HIPK2	HS2ST1	EGLN3	TUBA1A	CXADR	SLC30A4
HIVEP3	IGF2BP2	CYB561	NUF2	WNK3	BCL6	COL18A1	MSI2
ECT2	ARMH1	CKB	RNFT2	TSPAN14	ZNF185	GINS1	TRIM36
TTC8	KHDRBS3	MAMLD1	SLC16A14	TIMELESS	DPY19L1	CACNB3	TSPAN6
TTK	FZD2	SBK1	HEG1	PLA2G2D	PAM	CPNE8	MYBPC2
PSAT1	DTX3	STAU2	TIA1	KDM5B	SLC39A8	MYO15B	GAS2
SATB2	MDK	ZC3H12C	ZNF184	RTN4	KLHL42	DAB2IP	BIVM
BCR	BFSP2	MLLT11	SMYD2	CCDC14	APH1B	IL23A	BAMBI
SMAD2	PRDM15	TCEAL8	CAMSAP2	LINC00965	ATP2B4	OCA2	CCNB1
OGFRL1	CENPW	ZNF471	SNX29P2	ANXA5	WDR41	PAWR	PRKCI
C15orf61	ZNF92	IDH2	CENPF	CEP128	SH3PXD2A	LGR4	PKP4
CLIP2	QPCT	MCF2L	ZNF532	C20orf194	GPRC5C	GDF11	MCM2
ZNF101	RCC2	ZNF496	ATP6V1D	ZNRF1	PADI4	CD5	PALD1
PLK4	KIT	YEATS2	BRCA1	PHC1	PTOV1	MORC4	PXYLP1
ZNF738	KLHL14	HACD1	PLCG1	CBX1	STARD9	ZNF542P	SLC7A11
STMP1	PAK1	MMP11	TUBA1B	PDE3B	LPIN1	TUG1	POU3F3
ST14	MAP4K4	FAM81A	LEPROTL1	DOCK6	ZNF43	ATP6V0E2	PCDHB14
AGAP1	CYSTM1	SEPHS1	CENPJ	HES6	NBEA	LOC100506990	COMMD4
HNRNPA0	CCDC69	PIWIL4	OPTN	NR2F6	ZNF260	TRERF1	FRK
IFT81	PNMA1	RHOU	GUCY1B1	RAB15	LOC105379426	FANCI	UBE2E3
TST	C18orf54	DPCD	ZNF610	HENMT1	MGC12916	ZNF827	MARCKS
LMO7	NOSIP	PHC2	MID2	MAGED2	KIAA1958	TUBA1C	CDC45
CD9	CHL1	SVIL	MYADM	TUBB2B	LRP6	BTNL9	DDAH1
ATL1	GNAQ	PHEX	MYBL1	ARSD	PXDN	BIK	KLRC4
CDKN1C	CTTNBP2NL	TOX2	BDH2	KANSL1L	CHDH	ARHGAP32	CD38
RHOB	KIF5C	SPATA7	LOC729732	PGM2L1	MVB12B	RIMS3	STK39
CENPU	KIAA0895L	ZNF117	ALDH2	GINS2	CHML	ZMYND8	MAGI2
ARMCX1	ZNF232	RHOBTB1	ACVR2A	CYP2R1	MECOM	SSX2IP	NNT-AS1
PAFAH1B3	ADGRD1	PFKP	PBLD	C1orf198	BAIAP2L1	RAB3IP	JAG1
SH3BP4	NSUN7	MAP1B	ANKRD36BP2	SLC16A4	IL17RB	DPYSL2	RGS1

CERS6	TMEM255A	SOX4	MYB	AGPAT4	HS3ST3B1	HMCES	SCCPDH
KCNK9	FBLN2	CPXM1	ARHGEF40	MYO10	ZNF608	BAIAP3	TSC22D1
MSRB2	DACT1	GPR137B	ABCA9	GABARAPL1	PLXNA1	ZNF618	GM2A
KCNH8	INSM1	DTL	VEZT	GOLGA2P10	SLC25A27	C12orf49	TEAD2
TUNAR	EPCAM	CKS2	LDOC1	PHGDH	TUBB3	PCTP	ARHGEF4
ZNF254	PTPRS	ABR	ABHD17C	BLMH	BLVRA	CKS1B	PNMA6A
RIC8B	MELK	RPL39L	TTC7B	CDK2	FBXL16	SDK1	KCTD15
PLCXD2	RRBP1	E2F3	ZSCAN9	CASD1	TCEAL9		

Genes downregulated in SOX11+ MCLs vs SOX11- MCLs

CARD11	NFKBIE	ELOVL5	ZNF540	FAM13A-AS1	PER3	COPA	GNMT
ZC3H12D	THAP6	C11orf1	WNT16	CBX5	GRK5	MXD1	ZFP36
SPRYD7	CD70	SMAGP	ERCC6L2	NPAT	RHOF	ABCD3	MCM9
PSMG1	EEF1D	DBF4	HVCN1	FXYD5	INAFM2	KDM6A	CXCR3
MOB3A	PEA15	ASXL1	VAV3	PNP	CAPN14	EED	B4GALT1
CDC40	CFL2	SIPA1L1	PPA1	DR1	PHF20	ANKRD12	PBX4
CCDC68	CYCS	UBE2E2	MDS2	LINC00528	ZNF451	NRROS	PHKB
THAP2	RAB29	FNBP4	INPP5F	ARHGEF10	GINM1	EFCAB13	CRTAP
MTX3	SESN1	EIF1AD	IL2RA	DNAJC5B	PCSK7	TAF4B	IL6-AS1
PPIL2	MAP3K5	G2E3	AMPD3	CDK14	MTFP1	RIN3	KLF9
UBL3	FAM162A	MDFIC	DEGS1	PIKFYVE	FBXW7	SAMSN1	PIEZO1
CLEC2D	DGKE	FARP2	ACSL1	NFAT5	DLEU1	CNNM2	ZBTB43
SLC25A37	CD40	TBX21	ADD3	MLKL	DENND4A	TMED5	GFOD1
GAS6-AS1	PTPN12	XBP1	PBX3	GALNT3	CD48	PRKD3	POU6F1
THEMIS2	GPM6A	SLAMF1	FAM49A	USP45	STEAP1B	SLC12A6	ZBP1
BAG4	TNFSF9	STEAP1	GPR65	CPEB4	BMPR2	RNF141	CD58
HLA-DPA1	CYP2U1	NDUFV2-AS1	TMEM38B	DUS2	PDE8A	MAP3K8	GNG7
PPP3CC	CLN8	MATR3	MYC	SEL1L3	LINC01588	SETDB2	EBF1
SUN1	PELI1	MATN1-AS1	DTNB-AS1	SOX5	CAPN2	IFNGR1	GPR183
EAF2	CALHM6	JADE3	TMEM156	CCR6	MAP3K7CL	ADAM28	FGR
STAMBPL1	CPNE5	ID3	TNFRSF1B	SYNJ2	FAS	PTPN22	DENND1B
BAG2	FA2H	AMIGO2	MEF2C	SELENOM	CSGALNACT1	SYNGR3	GEN1
CD1C	KLF3	DEF8	SIGLEC6	IL6	ZBTB32	SLAMF7	CD200
BTLA	LOC100507006						

Appendix Table 6. Gene ontology (GO) of functional stem cell-related categories and their respective genes.

GO ID	GO term	Genes
GO:0005020	stem cell factor receptor activity	KIT
GO:0005173	stem cell factor receptor binding	KITLG, SH2B3, SPRED1, SPRED2
GO:0017145	stem cell division	CUL3, ESRRB, GNL3, PAFAH1B1, THOC2, TIAL1, WWTR1
GO:0019827	stem cell population maintenance	ARID1A, BMPR1A, CDC73, CTNNB1, CTR9, DDX6, DIS3L2, EIF4E, EIF4ENIF1, EOMES, ESRRB, FGF4, FZD7, GNL3, KDM4C, KIT, KLF4, LEO1, LIF, LIN28A, LSM1, MED10, MED12, MED14, MED15, MED21, MED24, MED27, MED28, MED30, MED6, MED7, METTL14, METTL3, MTF2, NANOG, NIPBL, NKAP, NODAL, NOTCH2, PADI4, PAF1, PELO, PHF19, PRDM14, PRDM16, RIF1, RTF1, SALL4, SETD6, SMC1A, SMC3, STAT3, TBX3, TET1, TPT1, TRIM8, TUT4, ZNF358
GO:0030718	germ-line stem cell population maintenance	NANOS2, PIWIL2, PRDM14
GO:0035019	somatic stem cell population maintenance	ASCL2, BCL9, BCL9L, BRAF, CDX2, CUL4A, DPPA4, ELF5, EPHA1, FGF10, FGF2, FOXD3, FOXP1, GATA2, HES1, KIT, KLF10, KLF4, LDB1, LDB2, LIG4, LIN28A, LRP5, NANOG, POLR2I, POLR2J, POLR2K, POLR2L, POU5F1, PRDM14, PRDM16, RAF1, RBPJ, REST, SALL1, SALL4, SFRP1, SKI, SMAD2, SMAD4, SOX2, SOX4, SOX9, SPI1, STAT3, TDGF1, NOG, NR2E1, PBX1, POLR2A, POLR2B, POLR2C, POLR2D, POLR2E, POLR2F, POLR2G, POLR2H, VANGL2, VPS72, WNT7A, YAP1, ZFP36L2, ZHX2, ZIC3, ZSCAN10
GO:0035701	hematopoietic stem cell migration	BCL11B, GPLD1, KIT
GO:0036334	epidermal stem cell homeostasis	KIF3A
GO:0036335	intestinal stem cell homeostasis	LGR4

GO:0044338	canonical Wnt signaling pathway involved in mesenchymal stem cell differentiation	FZD1, WNT3
GO:0048103	somatic stem cell division	CDKN2A, FZD7, HOXB4, KIT, NOTCH1, TGFB2, VANGL2, WNT3A, WNT7A, ZFP36L2
GO:0048133	male germ-line stem cell asymmetric division	ETV5, ING2, STRA8, ZBTB16
GO:0048863	stem cell differentiation	A2M, DNMT3L, ELL3, EPCAM, EPOP, ESR1, FOXO4, GPM6A, HMGA2, HOXA7, JARID2, KIT, LIF, LIN28A, MSX1, MSX2, MTF2, NELFB, OSR1, PAX2, PDX1, PHF19, PHF5A, PSMD11, PUM1, RUNX2, SETD2, SETD6, SHC4, SOX10, SOX17, SOX21, ZNF281
GO:0048864	stem cell development	MSI2, PTPRC, SETD2, SHH, WNT7A
GO:0048866	stem cell fate specification	SOX17, SOX18
GO:0060218	hematopoietic stem cell differentiation	ACE, BATF, CDK6, CHD2, ERCC2, HOXB4, LMBR1L, MEOX1, SFRP1, SP7, SRF, TAL1, TP53, XRCC5
GO:0060529	squamous basal epithelial stem cell differentiation involved in prostate gland acinus development	FGFR2, TP63
GO:0061484	hematopoietic stem cell homeostasis	ADAR, CCN3, NLE1, TCIRG1, UBAP2L
GO:0071425	hematopoietic stem cell proliferation	ARIH2, CD34, CTC1, ETV6, MECOM, NKAP, RUNX1, SART3, SFRP2, WNT1, WNT10B, WNT2B, WNT5A, YTHDF2
GO:0072038	mesenchymal stem cell maintenance involved in nephron morphogenesis	SIX2, WNT9B
GO:0072089	stem cell proliferation	ABCB1, CD34, FGF2, NES, RNF43, TRIM71, WNT3, WNT7B, ZNRF3
GO:0072091	regulation of stem cell proliferation	AGO3, HMGB2, NF2, SOX17, SOX18, YAP1, ZFP36L1
GO:0097150	neuronal stem cell population maintenance	ASPM, CDH2, DLL1, FANCC, FANCD2, FOXO1, FOXO3, FUT10, HES1, HES5, HOOK3, IGF2BP1, JAG1, MCPH1, MMP24,

		NOTCH1, PCM1, PROX1, PRRX1, REST, SOX2, SRRT, SS18
GO:0097168	mesenchymal stem cell proliferation	SCRG1, SIX2
GO:0097241	hematopoietic stem cell migration to bone marrow	GAS6, GPLD1, JAM2, JAM3
GO:1902033	regulation of hematopoietic stem cell proliferation	ACE, EIF2AK2, PIM1
GO:1902034	negative regulation of hematopoietic stem cell proliferation	MIR221, MIR222
GO:1902035	positive regulation of hematopoietic stem cell proliferation	ATXN1L, KITLG, N4BP2L2, PDCD2, THPO
GO:1902036	regulation of hematopoietic stem cell differentiation	ABL1, CBFB, CDK6, EIF2AK2, GATA1, GATA2, GATA3, ITCH, KMT2A, LDB1, LMO1, LMO2, METTL3, MYB, OSM, PSMA1, PSMA2, PSMA3, PSMA4, PSMA5, PSMA6, PSMA7, PSMA8, PSMB1, PSMB10, PSMB11, PSMB2, PSMB3, PSMB4, PSMB5, PSMB6, PSMB7, PSMB8, PSMB9, PSMC1, PSMC2, PSMC3, PSMC4, PSMC5, PSMC6, PSMD1, PSMD10, PSMD11, PSMD12, PSMD13, PSMD14, PSMD2, PSMD3, PSMD4, PSMD5, PSMD6, PSMD7, PSMD8, PSMD9, PSME1, PSME2, PSME3, PSME4, PSMF1, PUS7, RUNX1, SEM1, SETD1A, TAL1, TCF12, TCF3, TP73, YAP1, YTHDF2
GO:1902037	negative regulation of hematopoietic stem cell differentiation	HSPA9, N4BP2L2, NFE2L2
GO:1902038	positive regulation of hematopoietic stem cell differentiation	FOXC1
GO:1902455	negative regulation of stem cell population maintenance	LOXL2, WNT9B, ZNF706
GO:1902459	positive regulation of stem cell population maintenance	ESRRB, KDM2B, NCOA3, PRDM14, REST, YAP1, ZNF322

GO:1902461	negative regulation of mesenchymal stem cell proliferation	MIR29B1, MIR29B2
GO:1902462	positive regulation of mesenchymal stem cell proliferation	CITED1, LTBP3, VEGFC
GO:1904672	regulation of somatic stem cell population maintenance	MYC, TAF5L, TAF6L
GO:1904673	negative regulation of somatic stem cell population maintenance	MIR145
GO:1904674	positive regulation of somatic stem cell population maintenance	LBH, TP63
GO:1904676	negative regulation of somatic stem cell division	MIR145
GO:1904677	positive regulation of somatic stem cell division	LBH
GO:1905322	positive regulation of mesenchymal stem cell migration	ACKR3, CXCR4, FBXO5
GO:1905474	canonical Wnt signaling pathway involved in stem cell proliferation	WNT3
GO:2000035	regulation of stem cell division	CDK2AP2, ESRRB, EVI2B, NAP1L2, NCOA3, PRDM15, SFRP2, SOX17
GO:2000036	regulation of stem cell population maintenance	CNOT1, CNOT2, CNOT3, ELAVL1, HMGA2, KAT2A, KDM3A, NODAL, PTN, SAV1, SMO, TAL1, WDR43, ZC3H13
GO:2000103	positive regulation of mammary stem cell proliferation	LBH
GO:2000473	positive regulation of hematopoietic stem cell migration	CCR2, PTPRC
GO:2000647	negative regulation of stem cell proliferation	FBLN1, FERMT1, KDF1, OVOL1,
		OVOL2, SNAI2
GO:2000648	positive regulation of stem cell proliferation	EPCAM, GJA1, HMGA2, HNRNPU, KDM1A, NANOG, NR2E1, PTPRC,
		SIRT6, SOX11, TBX3, TERT

GO:2000736	regulation of stem cell differentiation	GDNF, KDM3A, KDM4C, MIR146A, MIR147B, NSUN2, OCIAD1, TEAD2
GO:2000737	negative regulation of stem cell differentiation	CDK12, CDK13, ESRRB, H18, HES1, HES5, HNRNPU, JAG1, LBH, NELFB, NOTCH1, STAT3, TRIM6, YAP1, ZFP36L2
GO:2000738	positive regulation of stem cell differentiation	HOXB4, NUDT21, PTN, PWP1, RBM24, SP7, TACSTD2
GO:2000739	regulation of mesenchymal stem cell differentiation	PDGFRA
GO:2000740	negative regulation of mesenchymal stem cell differentiation	REST
GO:2000741	positive regulation of mesenchymal stem cell differentiation	LTBP3
GO:2000798	negative regulation of amniotic stem cell differentiation	REST

Appendix Table 7. Bivariate Cox regression analysis for OS in 40 leukemic MCL cases (GSE79196), using MSI2 mRNA expression levels (continuous) and different molecular prognostic factors (SOX11, high CNA, and TP53 and CDKN2A alterations) (categorical).

	HR	95% CI	P-value
MSI2 mRNA expression	2.85	[1.07-7.57]	**0.036**
SOX11 status	3.42	[1.03-11.35]	**0.045**
MSI2 mRNA expression	4.09	[1.44-11.60]	**0.008**
CNA	1.03	[0.37-2.85]	0.950
MSI2 mRNA expression	4.16	[1.54-11.21]	**0.005**
17p/*TP53*	1.86	[0.73-4.76]	0.192
MSI2 mRNA expression	4.96	[1.59-15.44]	**0.006**
9p/*CDKN2A*	7.92	[1.99-31.52]	**0.003**
PRDM15 mRNA expression	0.35	[0.07-1.73]	0.198
SOX11 status	6.46	[1.86-22.46]	**0.003**
PRDM15 mRNA expression	0.76	[0.21-2.69]	0.666
CNA	1.86	[0.67-5.17]	0.233
PRDM15 mRNA expression	0.87	[0.25-2.97]	0.826
17p/*TP53*	2.22	[0.88-5.63]	0.092
PRDM15 mRNA expression	0.98	[0.31-3.13]	0.972

9p/*CDKN2A*	7.41	[1.94-28.27]	**0.003**
SOX5 mRNA expression	0.35	[0.07-1.75]	0.200
SOX11 status	3.9	[1.20-12.74]	**0.024**
SOX5 mRNA expression	0.23	[0.04-1.18]	0.078
CNA	1.53	[0.58-4.03]	0.387
SOX5 mRNA expression	0.16	[0.03-1.02]	0.053
17p/*TP53*	2.29	[0.88-5.95]	0.087
SOX5 mRNA expression	0.25	[0.05-1.31]	0.100
9p/*CDKN2A*	6.34	[1.65-24.28]	**0.007**

HR: hazard ratio, CI: confidence interval, P value: Cox regression P value.

Appendix Table 8. Consensus motifs used for FIMO analysis.

Consensus motifs JASPAR	
MOTIF PB0177.1 Sox7_2	MOTIF MA1562.1 SOX14
MOTIF PB0176.1 Sox5_2	MOTIF MA0868.2 SOX8
MOTIF PB0073.1 Sox7_1	MOTIF MA0867.2 SOX4
MOTIF MA0143.3 Sox2	MOTIF MA1563.1 SOX18
MOTIF PB0172.1 Sox1_2	MOTIF MA0442.1 SOX10
MOTIF PB0175.1 Sox4_2	MOTIF PB0166.1 Sox12_2
MOTIF PB0174.1 Sox30_2	MOTIF PB0167.1 Sox13_2
MOTIF PB0169.1 Sox15_2	MOTIF MA0143.1 Sox2
MOTIF PB0168.1 Sox14_2	MOTIF PB0165.1 Sox11_2
MOTIF PB0171.1 Sox18_2	MOTIF MA0868.1 SOX8
MOTIF PB0178.1 Sox8_2	MOTIF MA0867.1 SOX4
MOTIF MA0077.1 SOX9	MOTIF MA0087.1 Sox5
MOTIF MA0869.1 Sox11	MOTIF PB0170.1 Sox17_2
MOTIF MA0078.1 Sox17	MOTIF MA0866.1 SOX21
MOTIF MA0143.2 Sox2	MOTIF PB0074.1 Sox8_1
MOTIF MA0870.1 Sox1	MOTIF PB0072.1 Sox5_1
MOTIF PB0063.1 Sox13_1	MOTIF MA1120.1 SOX13
MOTIF PB0062.1 Sox12_1	MOTIF PB0070.1 Sox30_1
MOTIF PB0065.1 Sox15_1	MOTIF PB0071.1 Sox4_1
MOTIF PB0064.1 Sox14_1	MOTIF PB0068.1 Sox1_1
MOTIF MA0143.4 SOX2	MOTIF PB0069.1 Sox21_1

MOTIF PB0061.1 Sox11_1	MOTIF MA0442.2 SOX10
MOTIF PB0067.1 Sox18_1	MOTIF MA1152.1 SOX15
MOTIF PB0066.1 Sox17_1	MOTIF UN0137.1 SOX7
MOTIF PB0173.1 Sox21_2	MOTIF MA0515.1 Sox6
MOTIF MA1561.1 SOX12	MOTIF MA0514.1 Sox3

Appendix Table 9. FIMO analysis on 4 SOX11+ MCL specific ATAC-seq peaks matching with Sox family consensus binding motifs.

Motif id	Motif alt id	Sequence name	Start	Stop	Strand	Score	P-value	Q-value	Matched sequence
PB0167.1	Sox13_2	ATAC_peak_2	301	317	-	12.34	8.86E-06	0.069	TTAGTGGGTGGGTGACT
MA0514.1	Sox3	ATAC_peak_2	107	116	+	14.07	1.11E-05	0.105	CCTTTGTCTG
MA1563.1	SOX18	ATAC_peak_2	62	69	-	10.77	1.47E-05	0.067	CACAATGC
MA1563.1	SOX18	ATAC_peak_4	197	204	+	10.77	1.47E-05	0.067	CACAATGC
PB0168.1	Sox14_2	ATAC_peak_2	104	118	-	12.55	1.72E-05	0.165	GTCAGACAAAGGTCC
PB0166.1	Sox12_2	ATAC_peak_2	104	119	-	12.05	1.88E-05	0.164	AGTCAGACAAAGGTCC
PB0167.1	Sox13_2	ATAC_peak_3	1215	1231	+	11.56	2.06E-05	0.069	GTGCAGGGAGGGAAGAG
PB0167.1	Sox13_2	ATAC_peak_3	202	218	-	11.22	2.95E-05	0.069	GTTGTGGGTGGGGTGAG
PB0167.1	Sox13_2	ATAC_peak_1	164	180	+	11.17	3.10E-05	0.069	ATCCCGGGTGGGAGCTG
MA1120.1	SOX13	ATAC_peak_4	1623	1633	-	12.35	3.42E-05	0.265	GTACAATGGGG
PB0166.1	Sox12_2	ATAC_peak_4	1185	1200	+	11.40	3.45E-05	0.164	AGAGAGACAAAGACAG
PB0168.1	Sox14_2	ATAC_peak_2	59	73	-	11.82	3.57E-05	0.171	CATACACAATGCTGG
PB0167.1	Sox13_2	ATAC_peak_4	2373	2389	-	11.01	3.62E-05	0.069	TTACTGGGAGGAAAATG
MA0143.1	Sox2	ATAC_peak_4	1662	1676	-	11.69	3.82E-05	0.366	CCATTGTCATAAAGA
MA0143.2	Sox2	ATAC_peak_4	1662	1676	-	11.63	3.98E-05	0.381	CCATTGTCATAAAGA
MA0143.4	SOX2	ATAC_peak_4	1668	1678	+	12.35	4.09E-05	0.205	TGACAATGGTT

PB0171.1	Sox18_2	ATAC_peak_1	471	486	-	9.94	4.19E-05	0.403	GCACCAAATGCATGAA
MA0143.4	SOX2	ATAC_peak_4	1623	1633	-	12.31	4.26E-05	0.205	GTACAATGGGG
MA0078.1	Sox17	ATAC_peak_4	1669	1677	-	11.94	4.55E-05	0.436	ACCATTGTC
MA0077.1	SOX9	ATAC_peak_4	1625	1633	+	11.22	4.77E-05	0.461	CCATTGTAC
MA0515.1	Sox6	ATAC_peak_2	107	116	+	12.53	4.96E-05	0.273	CCTTTGTCTG
MA0143.3	Sox2	ATAC_peak_2	107	114	+	13.38	5.04E-05	0.313	CCTTTGTC
MA1120.1	SOX13	ATAC_peak_4	1668	1678	+	11.75	5.50E-05	0.265	TGACAATGGTT
MA0515.1	Sox6	ATAC_peak_4	1188	1197	-	12.23	5.73E-05	0.273	TCTTTGTCTC
MA0514.1	Sox3	ATAC_peak_4	1188	1197	-	11.98	5.81E-05	0.275	TCTTTGTCTC
MA0442.2	SOX10	ATAC_peak_4	1188	1198	+	12.01	6.25E-05	0.601	GAGACAAAGAC
MA0143.3	Sox2	ATAC_peak_4	1669	1676	-	13.10	6.51E-05	0.313	CCATTGTC
PB0167.1	Sox13_2	ATAC_peak_4	2020	2036	-	10.40	6.55E-05	0.104	TGGGTGGGTGGGGGATG
MA1563.1	SOX18	ATAC_peak_4	606	613	-	10.05	6.81E-05	0.208	GACAACGC
PB0176.1	Sox5_2	ATAC_peak_1	14	28	-	9.09	8.00E-05	0.770	AGGCATAAATAAGGG
MA1152.1	SOX15	ATAC_peak_4	1667	1676	-	10.82	8.90E-05	0.856	CCATTGTCAT

ATAC_peak_1: chr17:57,440,795-57,441,325; ATAC_peak_2: chr17:57,463,187-57,463,603; ATAC_peak_3: chr17:57,499,225-57,500,470; ATAC_peak_4: chr17:57,525,240-57,527,912

Appendix Table 10. Differentially expressed genes upon MSI2 knockdown in MCL cell lines with adjusted P-value <0.1 and absolute log2-transformed fold change >0.65.

Genes upregulated in MSI2 knockdown vs MSI2 control MCL cell lines							
MEGF6	SELL	TC2N	KLRC4-KLRK1	RUNX2	GALNT9	DPYSL3	TC2N
PYHIN1	CD96	AK8	COL18A1	MAMLD1	ANXA1	WNT7B	GPR65
BTBD11	IGSF9B	RTN4RL1	SLC44A5	NPTXR	BLVRA	CD44	IL17REL
LPL	MLC1	TANC1	ARHGAP10	MET	RPS9P1	DDR1	NLRP7
HBA2	FAM171B	PTPRR	DMKN	RSPH14	POF1B	SCARA5	LDB2
NRG4	SSTR3	RAB11FIP5	CBR3	ARHGEF10	S1PR4	CSGALNACT1	ZBBX

DNM1	CCNA1	LTB	ITGB7	SMIM35	GNG3	CD52	ARHGEF10
KLRK1	FGF17	TNFRSF11A	KSR1	NAALADL2	TRAF3IP3	S100A10	TESC
TLE2	SH2D5	CD9	TSPAN15	SLCO3A1	TMEM163	RNF223	DMTN
NRP2	SERPINE2	CREB3L3	LTB	ABLIM1	EBF3	RGS7	BCAS1
CRYBG2	TMTC2	CYB561	COTL1	PLEKHG1	PRSS2	SAMD11	UBD
FBLN5	RAP1GAP2	RBFOX3	ULBP2	CELSR1	HOXC11	PALD1	DDR1
ESR1	IL32	PLEKHF1	LAMP3	ITGAM	PLAAT2	DES	ULBP3
TRABD2A	LGALS3	POGLUT2	GMFG	FAM171A1	GVINP1	CCDC151	SQOR
SPNS2	TLE1	PRF1	FOSL2	MCF2L	SEMA3F	NT5E	IGSF9
KIAA0513	C16orf74	TSPAN5	RTBDN	STEAP3	FAM78B	FSCN1	TRPV3
SAMD3	EIF4E3	CROCC2	KDF1	RNF125	BTNL8	S100A3	CARD11
MOV10L1	TRIM7	GJA3	IL7R	SSUH2	CRIP2	MISP	FAS
STK17A	FXYD5	ENPP2	TRAF5	SFN	PHLDA3	FGR	PPP1R14A
DAB2IP	PLIN5	CDHR3	EMX1	AHNAK	COL19A1	ZFYVE28	ALOX5
BMP1	PAPLN	PALM	PLEKHA1	CTSH	GNG4	ANK3	PLIN4
CAPG	ARHGEF10L	SPIC	EPCAM	CSTB	ATOH8	PPEF2	SERPINF1
FGFR3	CORO2B	ATP6V0E2	RIPOR2	B3GNT4	SYBU	TCAF2	COL9A1
CYB5R2	SMIM14	MAP7D2	HSH2D	SPACA9	TRPV2	GRK5	TUFT1
TCF7	FRY	TAS2R2P	GIPC3	FAM177B	CPNE7	ACTA2	WDFY4
CCDC113	UBXN10	RAB3B	ZDHHC14	APOL3	ANKEF1	DEPTOR	MYOM2
SLC45A3	SHISA7	FBP1	PRKCB	TNFRSF19	MAML3	LGALS9	RYR2
PPP1R16B	MLKL	CPLX1	APOBEC3H	MST1R	PLAAT4	CD22	GART
KCNQ4	KCNJ11	DENND2C	CD180	CALHM6	FLNA	ACTL8	GNB4
GPM6A	IL15RA	ARL4C	BCL6	LRIG1	JAG1	SH3BP5	APOBEC3F
TJP3	DAPL1	C2orf15	P2RX5	NFIX	SLX1B	DOK7	WNK2
TBX21	MVP	DOK4	PRR18	PRKN	MYOM2	GXYLT2	CGREF1
DNAAF3	PLSCR3	PLSCR3	TCEA3	GZMM	APOBEC3G	ITGAL	LMNA
ZC2HC1C	SNX7	RASSF4	APOBEC3D	SLC22A15	GUCD1	BLK	ACY3

Genes downregulated in MSI2 knockdown vs MSI2 control MCL cell lines							
TFDP2	SLC45A4	SDC1	PPP1R18	CORO1B	ZCCHC14	ANKRD37	NOTCH1
NAB1	MLLT3	SMAD9	SEPTIN11	NTN3	GSDME	SCARB2	MAN1A1
ITPR2	TCAF1P1	PARP2	ZNF850	ALG14	FAAH	CSF2RB	GIMAP8
ZFP3	USP18	CD84	PGAP1	LDB3	BHLHE40	PLXNC1	PPM1E
MYBPH	RAB39B	PKN3	ATP8A2	SFRP5	AXIN2	CENPS-CORT	DDIT4
PROX1	GFI1	RTKN2	FCER2	NRXN2	LDLRAD3	ARPP21	ZNF219
VLDLR	RADIL	KCNN2	KIAA0408	DLG5	CAVIN4	MSI2	CBFA2T3

SYT11	GRM4	NTNG2	KLHDC8B	GADD45G	MERTK	TSHR	ATP1B1
CEMIP	ADSS1	CD72	TMSB15A	ADGRG1	IGLL1	GPM6B	SERINC2
EFHB	AFF2	S1PR2	TCEAL4	MSANTD3-TMEFF1	HNRNPLL	RIMS2	PYGL
NR4A1	RELL1	TTC28	KALRN	ARHGEF40	ELL3	GPR162	TMEFF1
RIMKLA	SLIT1	TEC	GRASP	ROR1	AOX1	PAWR	ARHGEF25
SLC2A5	PDE9A	DUSP10	CPNE2	ACKR4	SESN3	PTPRN2	TGFBR3
MYCN	LAMA2	CDK6	HSD17B8	MTCL1	LDC1P	WASF1	CKM
GRAMD1B	TPM2	AOX3P	AOX2P	PDCD1	OSBPL6		

Appendix Table 11. Gene sets related to stemness and apoptotic process used for GSEA in Z138 MSI2 knockdown vs Z138 control.

Enriched in Z138MSI2KD VS Z138CT						
NAME	**SIZE**	**ES**	**NES**	**NOM p-val**	**FDR q-val**	**FWER p-val**
JAATINEN_HEMATOPOIETIC_STEM_CELL_DN	133	0.597	2.325	0.000	0.000	0
KEGG_HEMATOPOIETIC_CELL_LINEAGE	52	0.563	1.856	0.004	0.004	0.011
RAMALHO_STEMNESS_DN	49	0.564	1.896	0.000	0.004	0.006
HOFFMANN_IMMATURE_TO_MATURE_B_LYMPHOCYTE_UP	18	0.729	1.878	0.002	0.004	0.009
HADDAD_T_LYMPHOCYTE_AND_NK_PROGENITOR_DN	38	0.556	1.746	0.005	0.012	0.049
ALCALA_APOPTOSIS	84	0.485	1.753	0.000	0.022	0.014
CONCANNON_APOPTOSIS_BY_EPOXOMICIN_UP	199	0.358	1.457	0.003	0.052	0.214
IVANOVA_HEMATOPOIESIS_STEM_CELL_LONG_TERM	144	0.402	1.566	0.003	0.058	0.235
HAMAI_APOPTOSIS_VIA_TRAIL_DN	154	0.373	1.464	0.010	0.058	0.201
BIOCARTA_DEATH_PATHWAY	29	0.550	1.606	0.024	0.060	0.074
BIOCARTA_CASPASE_PATHWAY	21	0.534	1.481	0.060	0.063	0.184
BIOCARTA_FAS_PATHWAY	29	0.512	1.505	0.048	0.071	0.165
DUTTA_APOPTOSIS_VIA_NFKB	27	0.473	1.362	0.118	0.083	0.389
ENGELMANN_CANCER_PROGENITORS_DN	40	0.465	1.471	0.030	0.090	0.448
HOEBEKE_LYMPHOID_STEM_CELL_UP	72	0.401	1.452	0.036	0.090	0.493
HALLMARK_APOPTOSIS	136	0.386	1.510	0.005	0.091	0.16
REACTOME_APOPTOSIS	125	0.354	1.367	0.045	0.091	0.382
KEGG_APOPTOSIS	75	0.374	1.316	0.075	0.098	0.477
GAL_LEUKEMIC_STEM_CELL_DN	165	0.370	1.476	0.005	0.099	0.433
GO_APOPTOTIC_SIGNALING_PATHWAY	480	0.291	1.297	0.011	0.100	0.518
EPPERT_HSC_R	94	0.383	1.404	0.043	0.101	0.605
HADDAD_B_LYMPHOCYTE_PROGENITOR	213	0.342	1.412	0.014	0.105	0.581

KEGG_HEDGEHOG_SIGNALING_PATHWAY	34	0.437	1.346	0.112	0.138	0.756
EPPERT_CE_HSC_LSC	27	0.441	1.291	0.157	0.175	0.857
CONRAD_STEM_CELL	27	0.403	1.173	0.230	0.314	0.977
GAL_LEUKEMIC_STEM_CELL_UP	100	0.303	1.150	0.179	0.329	0.988
REACTOME_INTRINSIC_PATHWAY_FOR_APOPTOSIS	49	0.312	1.032	0.381	0.396	0.97
LIANG_HEMATOPOIESIS_STEM_CELL_NUMBER_QTL	13	0.451	1.078	0.354	0.443	0.998
BOQUEST_STEM_CELL_DN	7	0.480	1.004	0.461	0.577	1
BIOCARTA_IL3_PATHWAY	14	0.376	0.939	0.524	0.699	1
BHATTACHARYA_EMBRYONIC_STEM_CELL	65	0.259	0.905	0.623	0.744	1
ENGELMANN_CANCER_PROGENITORS_UP	34	0.274	0.844	0.723	0.798	1
RAMALHO_STEMNESS_UP	62	0.248	0.851	0.725	0.823	1
HOFFMANN_IMMATURE_TO_MATURE_B_LYMPHOCYTE_DN	25	0.275	0.771	0.787	0.869	1

Enriched in Z138CT VS Z138MSI2KD						
NAME	**SIZE**	**ES**	**NES**	**NOM p-val**	**FDR q-val**	**FWER p-val**
JAATINEN_HEMATOPOIETIC_STEM_CELL_UP	210	-0.346	-1.530	0.000	0.156	0.214
BIOCARTA_STEM_PATHWAY	4	-0.733	-1.361	0.138	0.266	0.571
IVANOVA_HEMATOPOIESIS_STEM_CELL	134	-0.290	-1.184	0.142	0.372	0.909
LAU_APOPTOSIS_CDKN2A_UP	54	-0.279	-1.000	0.440	0.446	0.929
BENPORATH_NANOG_TARGETS	764	-0.221	-1.095	0.106	0.468	0.978
WONG_EMBRYONIC_STEM_CELL_CORE	310	-0.259	-1.190	0.065	0.481	0.904
BENPORATH_NOS_TARGETS	129	-0.248	-1.009	0.443	0.581	0.993
BENPORATH_OCT4_TARGETS	214	-0.217	-0.948	0.611	0.642	1.000
CONRAD_GERMLINE_STEM_CELL	6	-0.307	-0.632	0.884	0.966	1.000

ES: enrichment score, NES: Normalized enrichment score

Appendix Table 12. Gene sets used for gene set enrichment analysis and gene ontology analysis containing differentially expressed genes upregulated and downregulated in Z138 Ro 08-2750 vs Z138 DMSO treated cells (genes with an adjusted P-value <0.1 and absolute log_2-transformed fold change >0.65).

RO_UPREGULATED_GENES							
GDF15	RGS1	FOS	SLC2A3	SYS1-DBNDD2	HOXB9	DUSP4	DUSP5
PTCH2	PPP1R15A	OSGIN1	CHAC1	CCL3	STC2	DUSP10	DDIT3
INHBE	MAFF	FBXO32	SESN2	SESN2	NUAK2	UBALD2	UPP1
DDIT4	ATF3	ROCK1P1	RASGEF1B	CUZD1	ABHD4	GADD45A	EMP1

HMOX1	TSC22D3	SPRED2	FOSB	JDP2	CREBRF	SLC7A11	RHEBL1
BIN2	SDC3	NCALD	ULBP1	GPR156	LY9	FAS	BBC3
TRPV3	CCL3	PHLDA3	ZNF703	PNRC1	RGS2	CEBPB	HBP1
HBP1	TRIB3	GABARAPL1	SEC22B4P	BHLHE40	CECR2	UBE2H	ADM2
PELI2	KLHL24	UBALD1	JUN	IL21R	IRS2	RNF122	CCNG2
NR4A1	DUSP16	DUSP16	CCPG1	FOSL1	TCP11L2	TNFRSF10B	TEX19
SGK1	DYRK1B	DYRK1B	CCL3	YPEL2	RAET1K	KLF6	SNX16
IL20RB	CD28	MTRNR2L12	PLEK	SLC25A25	HERPUD1	MTRNR2L8	SYS1
MTRNR2L4	ADPRM	WHAMM	FAM229A	NHSL1	ANKAR	EIF4A2	HECA
YPEL5	PNPLA8	ZSWIM6	INHBC	CNNM2	TMEM121B	ZNF251	ZBTB43
NFKBIE	SRXN1	MTRNR2L1	RAB30	MTRNR2L10	ZSWIM4	ZSWIM4	GEM
PMAIP1	SQSTM1	RGS3	KCNJ11	BMT2	ERO1B	SMN2	SLC3A2
HLA-DPB1	MCF2L2	VLDLR	SLC30A1	FAM83G	ZNF586	MICA	LRMP
MXD1	DTX4	FBXL20	BRF2	OSER1	PAM16	TNFRSF1A	ZNF608
CHD2	SERINC1	MT-ND4	LMNA	MTRNR2L11	MT-ND4L	RAB3A	MAFG
CHIC2	RAB39B	BNIP1	TNFRSF10A	ZNF654	RSRC2	SPECC1L-ADORA2A	BAIAP2
LONRF1	EIF1	HLA-E	HLA-E	HLA-E	HLA-E	PIM2	BRAF
ATG9A	CCT6P1	VEGFA	SPRED1	MOB3A	JMY	HRK	SLC6A9
ICOSLG	PBX4	ZNF350	MTRNR2L6	PPP3CC	RPL22L1	LONRF1	DNAJB4
BFAR	IRF2BP2	NFE2L1	ZNF791	PHF1	LINC01881	TRPM8	ANKRD33B
SH3BP2	KDM3A	HIVEP2	ERN1	IQCN	POLR2J3	NFIL3	RPS6KA5
RGS16	ZNF354B	FAM107B	FBXO30	PPP4R1L	CDKN1A	RELB	ZNF490
GKAP1	STX3	BEND5	EPC2	OTUD7B	STAT5A	LENG8	ZNF394
PPP1R18	KCNJ14	H1-10	KAT7	PRELID3A	MSMO1	POPDC2	VAMP2
SLC1A5	RIT1	CCDC28A	IFNLR1	FRAT1	MT-CO3	PIK3CA	CD48
MDM4	ZNF431	ZNF484	MTHFD2	RBM7	C16orf72	ISL2	ARID3B
DCUN1D3	TP53INP2	SESN1	MT-ND1	TNIP2	SERTAD1	MT-ATP6	UPK3BL2
CWC25	ZNF16	CCT6P3	ZNF836	CCNG1	ZNF805	NKIRAS1	CA5B
RABGGTB	HLA-E	MTCO1P12	DDX17	WTIP	ATXN7	KLHL28	UNC5B
CDK17	KANSL1	ABCB4	PHLDA1	RAB11FIP1	MAP4K3	STK17A	MT-ATP8
ZHX1-C8orf76	TRIM23	ZNF343	NAP1L4	ZNF267	TMEM267	SLC7A1	SGPP1
SGPP1	HLA-B	ANAPC1P2	PCGF1	MTATP6P1	MT-CYB	WSB1	BEND6
PDCD4	HIVEP1	KCMF1	ZNF543	CCSER2	SMG1P1	RHOG	KHDC4
MXI1	IFRD1	RNF169	TFE3	PSAT1	YAF2	ZNF738	ZNF473
ST3GAL5	OGT	ADM5	RSF1	CAMLG	AGO2	GRPEL2	CLEC7A
NR1D2	ATXN2L	ATF4	TNFAIP3	BFAR	INKA2	AMH	FAM174A
C12orf76	GID4	KIAA0355	RYBP	MICOS10-NBL1	MAP1LC3B	SDCBP	ARRDC3

PRKY	ARRDC2	BHLHE41	EPC1	MARF1	WASH7P	HSPA13	IFNGR1
ALAS1	TMEM161B	ZBTB49	AFTPH	CD55	ALKBH1	PRDM1	MAST1
DCTN4	LPIN1	GPR132	ZNF277	OSBPL2	MSR1	FAM161B	EMC3-AS1
NBR1	CERS4	RAB33B	BCL2	RNF111	ZRANB1	GPT2	MT-CO1
LENG8	USP37	TIGD7	MACO1	TIFA	RAB5A	MKNK2	MSH5
LCLAT1	NRIP1	KIAA0232	IL10RA	SMG1P2	UBOX5	STK17B	SPRY2
PIM3	GADD45B	LYSMD2					

RO_DOWNREGULATED_GENES							
AEBP1	POLR3H	CIAO3	GMPPB	HMMR	RELL1	PKIA	MMP11
DAAM1	MINK1	ACTR3B	RCOR2	UNC119B	CITED2	RARS1	CDK5R1
CIDEB	CIDEB	GEN1	CERK	IKZF1	NEURL4	NEURL4	ITSN1
SKP2	CAMKK2	MXD3	ZNF57	DLG1	BEST3	HECTD3	SLC5A6
C14orf132	SSR4P1	XYLT2	AMZ1	MKI67	HSPA1B	SCRIB	TSSC2
OSGEPL1	MLXIP	PAQR4	WNT10A	WDR35	SRSF2	ATP8B2	ATP2B1
NAGK	AGRN	ERI2	MEIS2	ABCA7	TRIM8	DUSP2	ADAM10
SRRD	CTNS	NFIB	CD3G	FBXL16	APOBEC3F	ZFP3	PFAS
DHRS13	ZNF252P	GTF2H2C_2	SOCS3	CCDC142	METTL23	H2BC11	ZDHHC14
H2AC11	SLC35F5	TPM3P9	LRRK2	TEDC2	STK38	MBLAC2	ST3GAL2
INTS1	NSFP1	FASN	RASSF2	ASPM	CRYBG3	TOMM40P4	TOMM40P4
EML5	PCYOX1	HOMEZ	AGAP2	SLX4	ALDH1B1	KLLN	KCNJ4
BCL11A	KCNA3	FAAP100	IGLC1	TLCD1	REP15	TAF15	SCRIB
AXIN2	FCGR2B	SOWAHD	SLC46A1	PITPNM1	MACF1	PIGM	ZNF599
IGLL5	PPFIA3	HDDC3	LNP1	MTFMT	CELSR2	BCL6B	AGL
CCDC85C	LPCAT1	SUMF1	SLC27A4	CHST2	EEF2KMT	TLR7	ETAA1
POP1	RCCD1	MEGF8	PLA2G2D	SAMD9L	PLPP7	SIT1	TMEM129
IGLV1-51	A4GALT	RECQL4	CLBA1	SMKR1	CHMP6	RBM43	CPT2
TUBGCP5	TSPAN14	PPP1R10	THNSL1	LOXL4	MAN1C1	SYNPO2L	ARL4C
TTC30B	NT5DC2	CENPI	SBF1	FAM217B	RXRA	LPAR5	H2AX
GOLGA7B	SPIB	DENND2A	YY2	CD1D	DOLK	BHLHB9	CDC42BPB
FCRLB	FZD1	EGLN3	ADAT3	TTYH3	ATPSCKMT	SLC5A3	FAM111B
CCDC61	RTP4	CXXC5	H2BC20P	ATG4C	GPLD1	ZMIZ1	TMEM168
TMEM177	NUDT18	SPTBN2	ABCD2	KLF2	SSTR3	MT-ND3	SDC1
BCRP2	SPATA24	GRIK3	NOTCH1	CLK2	SLFN5	EPOP	ELAC1
CAV1	C2orf74	MEX3B	PROX1	LZTS2	ETS1	NLRP6	DTD2
PRMT6	PNMA8B	IL19	GTF2A1	AHDC1	GPER1	TEAD1	CABLES2

KANK2	CEP170B	HNRNPH3	LRRC26	TPCN2	FAM86C1	PELI3	ZFPM1
GRAMD4	ATR	CEND1	OCLN	MAMSTR	PIGW	KLHDC7B	KIAA0040
CCDC71	ENC1	TLR9	BCDIN3D	IGLV6-57	DNAJC30	SLC2A6	SLC2A6
JMJD4	ARFRP1	FAM83D	PHLDB2	ZNF594	SEMA4F	PIEZO2	PLXNA1
FBXO9	NOL4L	PUDP	ACTL10	PIGW	ZNF658B	S1PR4	CIITA
LPCAT1	CDKN2C	LYSMD4	WNT10B	LHX2	HEY2	GBA	HSD17B1
PCYOX1L	SPN	CCNE2	INAFM2	BUB1B	BAHCC1	SOX18	SNAI3
FAM86EP	SLC20A1	HSPA2	PRICKLE1	ZNF658	GBA	PIK3R3	MINDY2
PDCD1	TNFRSF19	BEND3	ORAI2	ESPNL	RYR3	ABHD15	MED31
TTC3P1	PROB1	CLCN5	LRP1	PTPN3	FOXL1	ZMYM1	SOX4
NRARP	LRRC45	TTC30A	ARL10	FJX1	TLR10	INSM1	SAPCD2
DGKQ	MFSD3	NACC2	ZNF556	FAM86B1	VSNL1	MAPKBP1	COL9A3
PAQR8	KCNJ12	APAF1	WNT7B	RIPOR2	FAM78A	FZD2	CCDC65
ERBB2	H3C8	SKOR1	FOXO6	CD3EAP	HMGA1P8	BHLHA15	BCL9L
C2orf81	MARVELD1	TRIM27	JAG2	ADRB2	TEF	FAM163B	ADORA1
EPB41L4B	IFFO2	H2BC8	NANOS1	DNM1P47	DNAJC22	ELFN2	GDPGP1
ABI3	C10orf71	ALDH1A3	PYCR3	NEURL1B	LRRC20	PPP1R10	PPP1R10
PPP1R10	PPP1R10	PPP1R10	FAM86C2P	HPDL	SAMD11	DEPP1	ARHGEF40
SLA	TMEM63C	CIART	MAFA	SMAD6	LFNG	PPP1R10	SEMA3G
ZBTB42	SKIDA1	TMEM50B	ARHGEF39	IGHV5-78	IGHV5-78	H3C6	LRFN1
CXorf21	MAT2A	PYCR3	FAM86JP	IL10	DLL4	NTN3	APLN
KLHL14	TMEM169	GPR146	OPRL1	IGLVI-56			

Appendix Table 13. Functional analysis on differentially expressed genes between Z138 Ro 08-2750 vs Z138 DMSO gene expression profile (genes with an adjusted P-value <0.1 and absolute log_2-transformed fold change >0.65) by using DAVID software.

Category	Term	Count	PValue	Fold Enrichment
Pathways downregulated by Ro 08-2750				
GOTERM_BP_DIRECT	GO:0000122~negative regulation of transcription from RNA polymerase II promoter	30	2.2E-05	2.40
GOTERM_BP_DIRECT	GO:0060412~ventricular septum morphogenesis	6	1.3E-04	11.90
GOTERM_BP_DIRECT	GO:0060070~canonical Wnt signaling pathway	8	5.9E-04	5.54
GOTERM_BP_DIRECT	GO:0003151~outflow tract morphogenesis	6	1.2E-03	7.50
GOTERM_BP_DIRECT	GO:0008285~negative regulation of cell proliferation	17	1.6E-03	2.47

GOTERM_BP_DIRECT	GO:0045747~positive regulation of Notch signaling pathway	5	2.4E-03	8.71
BIOCARTA	h_hesPathway:Segmentation Clock	4	2.6E-03	13.27
KEGG_PATHWAY	hsa05217:Basal cell carcinoma	6	2.7E-03	6.11
GOTERM_BP_DIRECT	GO:0060022~hard palate development	3	4.3E-03	28.75
GOTERM_BP_DIRECT	GO:0003150~muscular septum morphogenesis	3	4.3E-03	28.75
Pathways upregulated by Ro 08-2750				
GOTERM_BP_DIRECT	GO:0070059~intrinsic apoptotic signaling pathway in response to endoplasmic reticulum stress	10	3.4E-09	17.37
KEGG_PATHWAY	hsa04010:MAPK signaling pathway	19	9.4E-07	3.97
GOTERM_BP_DIRECT	GO:0000188~inactivation of MAPK activity	7	3.5E-06	16.05
KEGG_PATHWAY	hsa04115:p53 signaling pathway	10	3.7E-06	7.90
GOTERM_BP_DIRECT	GO:0006351~transcription, DNA-templated	60	1.5E-05	1.76
GOTERM_BP_DIRECT	GO:0006915~apoptotic process	26	2.0E-05	2.63
GOTERM_BP_DIRECT	GO:0034976~response to endoplasmic reticulum stress	9	4.7E-05	6.88
GOTERM_BP_DIRECT	GO:0045944~positive regulation of transcription from RNA polymerase II promoter	34	2.2E-04	1.99
KEGG_PATHWAY	hsa04650:Natural killer cell mediated cytotoxicity	10	4.4E-04	4.34
KEGG_PATHWAY	hsa04668:TNF signaling pathway	9	8.5E-04	4.45

Appendix Table 14. Differentially expressed genes upon SOX11 overexpression in DG75 BL cell line with adjusted P-value <0.1 and absolute log_2-transformed fold change >0.65.

Genes upregulated in DG75-ERSOX11 vs DG75-ER BL cell lines							
CAPN13	CFAP47	PLXNB1	SOX11	SRL	DRAXIN	ABCB1	PREX1
FGF9	NTF3	ARNTL2	RP11-347E10.1	NOL4	IL1RAPL2	PARP14	MEX3A
CAPSL	RP11-1O10.1	RP11-299H22.3	CLEC17A	CCDC120	SLCO5A1	IGLL1	FAM159A
GALNT14	VIM	LGALS9	VIM-AS1	AMOTL1	TSKU	RP5-1092A11.5	SLFN11
HMX2	MYOF	RP3-399L15.3	ATP6V0E2	RP5-906C1.1	ZNF860	GOLGA2P11	PIK3CD-AS1
IQGAP2	MAPK10	MACROD2	TGIF1	SPINT1	DTX3L	PLEKHO1	ADAMTS7
MARCKS	RP11-620J15.1	AKR1C3	IRS2	XPNPEP2	PARP15	GNG2	PARP9
TLR4	HOMER3	SCML4	CSPG4	FAM129C	SPR	LYSMD2	PNOC
RP11-271F18.3	ZNF287	MAFA	FAM167A-AS1	GIPC2	UMODL1	CD24	EGR3
CD24P4	THSD7B	ZSCAN31	IL7R	RAP1GAP2	COL5A1	PGBD1	TRIB2

FNDC1	ITGB8	MRO	KHDRBS3	NA	MIR8089	OR13A1	ATP6V0E2-AS1
OSBPL10	MAGI1	HSPA4L	SLC2A5	RP11-734J24.1	COL15A1	VAT1L	SNAI3
SPOCK1	C19orf57	LY86-AS1	RP11-116N8.4	TTC28	LRRC46	NA	RGS12
KLF2P2	TP73	RP11-116N8.1	OR7E14P	ZNF418	KLF11	HUNK	NR4A2
CCDC141	PLAU	LINC01132	KIF5A	MEX3B	KIAA1211	CD1C	RP11-92C4.3
LY86	FAR2P2	MMP15	FAM171A2	PLEKHA7	EPN2-AS1	DENND3	TTBK1
TUBA1A	RP11-326C3.15	SMARCD3	GAS8	SYT11	P2RX1	GAB3	CNTLN
PLXNA3	GAL3ST4	AOX2P	KCNN4	CXCR5	RIMS2	ALOX5	RNF223
RP1-47M23.3	CLIP2	SLC25A24	LINC00862	LZTS1	ECEL1	FAM227A	NA
RUNDC3B	CERK	MLLT11	SBK1	RP11-197N18.8	RP11-87G24.6	CD82	AEBP1
IDH2	ZSWIM4	FBXW12	NREP	MGST3	PRR36	CBARP	RNA5SP284
ZNF608	GSTA4	AC007163.3	GPC2	PIK3CD	ETV6	UTRN	CPM
TLR2	PIK3R3	ZEB2	HGFAC	LBH	RP11-87G24.2	RP11-87G24.3	PTK7
NRROS	NA	ACSS1	CALCRL	NA	SIDT1	CTXN1	PHLDB1
RP11-4M23.4	RP11-158I9.5	TRBJ2-3	NCKAP5	C14orf37	RNF122	RP11-46D6.1	NA
TTLL7	DLL3	MILR1	KCNK15	CALHM3	SUGCT	TCL6	IFIT5
GLRXP3	FZD3	ASB9P1	FHL3	STARD4-AS1	ITM2C	SLC16A14	ATP4A
EHD3	TRIM46	RP11-13P5.1	CMTM7	TSPO	TCL1A	SP140	CFAP58
ZNF302	SEPW1	ENC1	LPAR4	BTN1A1	CD180	MCIDAS	RP11-34F13.2
ALDH3B2	ARRDC4	FADS2	HEMGN	GALNT16	HIPK2	TAF15	PHACTR1
DLG3	RP11-220I1.5	RP11-420A23.1	FADS3	ENPP3	AJUBA	ZC4H2	SYT17
NA	ENDOU	SPSB1	PITPNM2	AOX1	RP1-60O19.1	RP11-617F23.1	NHSL1
CBX2	DSE	GDAP1L1	GPR18	ZNF530	MYCL	TCN2	NA
RCOR2	SESTD1	AOX3P	CTC-559E9.8	COL9A2	NA	RP11-54O7.1	HES7
JAKMIP2	BNIP3P17	RP11-680H20.2	PAIP2B	RP11-132N15.3	ZNF783	INPP1	DFNA5
AC003092.1	GRM4	TTC16	SEMA3F	RASGRP1	MB21D1	DLG2	AC007381.3
FBXL16	RP11-495P10.9	SIPA1L2	SNX22	IL4I1	WNK2	TRIM36	APLN
POPDC2	FAM129A	CTD-2054N24.2	DUSP1	ATL1	NA	NA	TYROBP
LHFP	RP11-343H5.6	EPB41L4A	FRY	ANKRD34A	PHACTR2	TRIM2	EPB41L5
RP11-481J2.2	SSUH2	RP1-257A7.5	STS	TRPV3	DYRK3	MVB12B	PKIA
ELN	KLHL25	ARHGAP10	ICAM1	PTPN12	LINC00899	C7orf72	NCK2
RP11-54O7.3	ZAP70	FNDC5	IFT172	NOL4L	ERO1B	MIAT	RP5-1009E24.8
CCDC102A	ZNF184	AK3P3	MIDN	RP11-722G7.1	RNASEH2B-AS1	NMI	PLG
IL23A	CYP2U1	RP11-353N14.2	BAHCC1	ZNF695	FCRL2	FAR2P3	JADE3
RP11-42I10.1	ARVCF	BRD3	CCDC155	RP11-588H23.3	SLFN5	HSPA6	ZNF785
HSP90B3P	MTSS1	CTC-260E6.4	AC010524.2	LINC00598	SNN	BCORL1	SERPINB9P1
KIAA0922	IGLC2	ACSF2	RP1-257A7.4	HSPA2	PRRG4	ZNF157	PIK3C2B

RAMP1	GFI1B	ZNF710	FAM212A	ZCCHC18	RP1-283E3.4	FOXL1	KIF3C
MEX3D	KISS1R	PODXL2	KCNMA1	KIAA0040	RP11-715J22.6	SCD5	TRPM2
ZNRF3	PECAM1	TMSB10	KIF27	RP11-335F8.2	GDF11	FCRL1	PDE7A
ANO7	CAPN9	RNF175	IFI44	CTC-260E6.6	LPAL2	UBASH3B	EBF1
PANX2	ARL4D	TMEFF1	TRAJ32	PDE4B	EXOC6B	ZNF253	TMEM237
RP11-284F21.10	ACTL8	KRBA1	DUSP5	SKI	KLF1	AICDA	EVL
GNG7	CCDC136	FAM153C	GFOD1	PANK1	CTD-2555A7.1	IRF1	MARCKSL1
IQSEC1	RP13-494C23.1	ZNF385B	PDZD2	EFNA4	SPTBN2	FAM65B	ITGB4
PHC2	TTC22	SATB1	STAT5A	NA	STARD9	TPM4	DZANK1
PGAM1P5	GLRX	DDX11-AS1	ANXA2R	NA	SLC17A7	ZNF821	CYP26A1
CELF2	RP11-331F9.3	RIMKLA	C2orf16	RP11-266K4.9	VPS37D	TTYH3	GOLGA2P10
DUX4L50	SPINT2	SAMD15	STOX2	FGFRL1	R3HCC1	PIM1	IFITM3
RP5-1061H20.4	PRDM12	KCNK6	CDR2L	BAG3	LRRC32	GNAZ	ZP3
ACOT4	ZSCAN16	RP11-164H13.1	CCDC187	NA	HDAC7	B3GNT7	HES6
ACER2	SLC25A30	REM2	SOWAHD	CTD-2630F21.1	LL0XNC01-240C2.1	EGR1	RFX3
LRIG1	SERF1A	CCR7	ARHGAP31-AS1	FAM43A	HIF1A	TOX2	SYTL2
DLGAP4	TRIM22	RAD9B	SPRY2	CTC-457L16.2	TNFRSF1A	CACNB3	APOOL
RP11-51J9.5	FAM109A	CRB2	ULK1	KIAA1683	TTN	SAE1	GOLGA2P7
PDE1B	GAPT	MIR181A2HG	VGF	RASSF6	AP3M2	RP3-329A5.8	APCDD1
RP11-328P23.4	QRFP	TEX14	GPR174	RP11-326C3.13	HSPA1A	PLEKHG2	IFITM2
C1orf228	MIR635	RP11-57A19.2	CYP39A1	GRK3	SLC7A8	MYRFL	HILPDA
STAG3	PRKCH	PPM1L	CELSR1	SPIN1	WDR54	NA	HMGB3
H1FX-AS1	RP11-693J15.5	TMEM169	CTD-2319I12.10	ABHD8	FMNL2	CMAHP	RHPN1-AS1
CNOT8	FOXP1	RTKN	SYCE2	SMIM11A	ANKRD18EP	CMTM1	ULK2
RP11-326C3.11	RP11-417L19.5	RP11-134O21.1	ZBTB32	LFNG	WASF3	PGM2L1	SMTNL1
ATP2A1-AS1	RP11-30L15.4	GPR153	ABCD1	JUN	DOK1	ABL1	RBMS3
GNGT2	TIGD3	GPSM1	NEK6	ZMIZ1	CPNE5	OAS3	ARMC12
WI2-87327B8.2	ARHGAP31	DNAJB4	GLRA3	CTD-2291D10.4	FAM134B	FLNA	PGGT1B
PFKFB2	GLTSCR1	NKX6-3	TFDP2	KLHL7	APOL3	ARHGAP23P1	CTNNB1
SMAD3	BMP1	ZNF853	LMCD1	CHD7	GAB1	IGHV7-81	RP11-1149M10.2
TSHR	RP11-676J12.9	LRP1	PRF1	TMEM204	CASP10	ZNF395	ADA
ZNF627	ATG9B	RIMKLB	RAB11FIP3	ABI3	ASS1P1	MGAT5B	ZSCAN2
RAB11FIP4	SH3PXD2A	FBXO16	PTPN18	UBE2L6	STMN1	MYB	MIR181A1HG
KLHL14	RP11-222K16.1	AUTS2	ZNF84	ZNF280D	NA	CIART	NA
ITPRIP	NA	SYBU	FZD2	FGD3	BACH2	SLC35E2	CLCF1
TCONS_00029157	YWHAQ	ENO2	HPGD	USP49	SYNGR3	ZNF260	ZNF329
RAB39B	TOP2B	NA	RAB9B	RN7SL5P	PIANP	ZNF93	RP11-175P13.3

SRC	PALM2-AKAP2	FILIP1L	PARP16	PGF	MYD88	ATP11A	TRAF3IP3
ZFYVE9	TGFBR2	NA	ACY3	KCNA6	DNAJC18	DPYSL2	HSF2BP
C8orf58	NATD1	ABCB4	NA	TBC1D7	MAST4	OSCAR	CDK19
RP11-234B24.4	PLEKHA4	SP110	ZNF347	AKAP3	FCGR2B	UBE2F	TARSL2
VPREB1	REEP2	MAP1LC3A	CCNJ	ARHGAP39	DAB2IP	OAS2	ITGA6
EIF2S2P3	AC074289.1	CASP6	SLC25A53	PRR29	TNFRSF10D	GRAMD4	FKBP7
Metazoa_SRP	FOXO1	SLC35E2B	LINC01569	TES	KLHL26	PTTG1IP	GRAP
PLEKHA8	L3MBTL3	WWP2	RP11-1166P10.1	PELI2	PAIP2	SEMA3B	RIMBP3
ZNF71	OLFM2	FUT4	RP3-455J7.4	ETV4	NA	SLC7A7	IGSF6
GNB3	NTN3	SVIL	ACVR2B	H6PD	OAS1	CCDC71L	PMEPA1
TTC39C	EMILIN1	CTC-523E23.11	ZNF568	TMEM44	DBN1	TBR1	CLECL1
KIF15	ZNF30	NA	RP11-696N14.1	TNFSF10	DISP3	TRGV3	CD72
NUS1P1	IFT81	GFOD2	CTC-457L16.1	GPR176	KLHL24	CECR7	NUTM2G
SLC5A10	ANO8	SGCB	DGKA	RP5-890E16.5	ERAP2	SMARCC1	ECE1
RP1-283E3.8	LAPTM5	AP000442.1	GS1-257G1.1	BEST3	CNN2	TET3	LDOC1L
FGGY	BMP4	ZNF737	SLC22A20	RNF130	CH17-472G23.4	IPO5P1	KLHL22
RAB15	RP11-213G2.3	PDE6B	MEX3C	DLX4	MPZ	SUMO2P6	PTPRE
FGD2	CTD-2561J22.2	CTD-2201E18.3	KIF5B	HDAC2	FBXO15	DOCK4	ZNF845
LRRC37B	DGAT2	SPATA6L	LINC01138	USP3	LMNB1	TMX4	ST14
PAPSS1	MTMR9LP	NACC2	ITGB7	ZNF225	POU2AF1	FAM174B	PFN1P3
ZNF521	LIX1L	LINC00377	PNMA1	CTC-523E23.1	RASA4B	SLC44A2	LINC00237
TXNIP	SSBP3	APOL6	SAXO2	GPR75	CD80	RP11-115H13.1	CCNO
PJA1	GMFG	SEL1L3	PRSS27	DOPEY2	MYL4	RBPJ	ARID3A
BCAN	TPRG1L	KLHDC9	RP13-516M14.10	ZNF66	ABRACL	ADAM28	PSTPIP1
KDM1A	NDRG1						

Genes downregulated in DG75-ERSOX11 vs DG75-ER BL cell lines							
H2AFY2	GSTM4	MVP	GM2A	BMP3	HELLPAR	HGSNAT	ADAMTS6
LLNLR-304A6.2	MBTPS2	CACNA1C	RP11-536K7.3	KIAA0895	RP11-441O15.3	RP11-10K16.1	SLC46A1
NF1	FAM167A	RAB29	ESRRB	SLC12A5	CYFIP1	ZNF385A	CXCL8
NPM1P26	RHOV	RPS6KA2	PNPLA7	UPP1	GABRB2	PCDHGB6	RP11-91J19.2
VILL	AC079781.5	NBL1	TRIM73	CADPS	C2CD4C	LRFN4	SCART1
EP300-AS1	PAQR6	IGKV3D-20	METTL8	TRAM2	CFAP100	RP11-439E19.10	COL18A1
FERMT3	GPCPD1	RP1-92O14.3	RNF32	DIAPH1	CLDN4	HSPB7	RP5-882C2.2
PACSIN3	SLC2A6	CERCAM	INAFM2	TMC8	RELL1	RP11-1391J7.1	UGGT1
CAMK1	NA	FAM183BP	CTC-490E21.11	ARID3C	SYTL3	TYSND1	CTD-2587M2.1
ABHD3	CTB-152G17.6	IL17D	CDK14	FSD2	RP4-673M15.1	EIF5B	NA

HSPB1	SH3D21	PGGHG	PNKD	FARSA-AS1	FBXO27	IL10RA	PIGM
PAM	UBR5-AS1	CARD11	GIMAP2	MYBPHL	ZNF197	WDTC1	BICD1
CTD-3184A7.4	NDRG4	RP11-730K11.1	LEKR1	NT5C3A	CLYBL	EPHX1	MMRN2
NUTM2A	KSR2	EIF5AP2	PCAT7	KCP	HS6ST1	RP11-91K8.4	RP11-66B24.4
OMG	NRADDP	SMIM18	SNORD15B	C22orf34	PLEKHA2	CH507-513H4.4	SLC26A4
SLC44A1	PLXNA2	KCNJ11	SLC9A9	AHNAK	SIPA1L3	ALDH1A3	SLC2A13
RHBDF1	HRC	AK1	BCAR1	METRNL	RAB36	MAP1B	RP1-152L7.5
RSPH6A	SLC39A11	RAB27A	RP11-167N24.3	RTN4RL2	ARHGAP44	RP5-821D11.7	AC006946.15
AGK	EIF2AK4	LRRC26	LPAR3	FZD5	PLCB2	SLC16A7	CCDC144B
AC007285.6	NAV1	COL20A1	LRRC25	C1orf53	LINC01088	FCGRT	FIGNL1
PRX	TMPRSS13	WSB2	CCDC146	UGCG	ADAMTS7P3	FAM185BP	NTAN1P2
MDH1	CTIF	DNASE1L1	LGALS3BP	DNAJC6	SNORA5C	FAM210B	STPG3
RAPSN	NA	ZFP36L2	GALNT18	C16orf62	LUZP1	LRRC17	PCDHGB7
ANK2	RP11-163E9.1	RP11-760H22.2	RPS17	HIST1H2AI	FNBP1L	ABHD12	RAB30
UBE2FP3	PRSS21	LCMT1-AS1	SGMS1	ERLEC1	GAS6-AS1	RP11-996F15.2	MAN1B1-AS1
TBC1D27	IRAK2	FAAHP1	RP11-266L9.5	DNAJC13	SERBP1P6	ACVR1	ZNF528
RP5-1139B12.3	39692	HADHA	NFIX	SORL1	JAZF1-AS1	TMEM198	PTCH2
FAH	WBP1L	NA	ALG1L9P	GDPD5	STOML2	THTPA	DDX54
ZNF827	NA	NAALADL1	SLC23A2	RP11-262H14.4	NA	MC1R	KLRC3
GAREM1	PDLIM1	FGF22	TRIM9	NA	RP11-428G5.5	PHTF2	RHOC
RPL7P50	FAM86C2P	PQLC3	DENND1B	EPS8	ZNF331	AC010729.1	MFAP4
LRG1	ADAP1	ASPH	STK3	SH2D5	NALT1	PABPN1L	CRB3
ELOVL6	FZD8	MIR4435-2HG	H2AFJ	RP11-54C4.3	FFAR1	RPL34-AS1	FRMD6
MAP9	CKMT1B	SPDYE21P	SYT12	MFSD3	MAGEH1	EPHA8	SGMS1-AS1
MICALL2	SPIRE1	RP11-372K14.2	GRHPR	RCAN3	ATP1A3	OPLAH	ANKRD33B
BFAR	SEC31B	MTCL1	ST8SIA5	SMIM10L2A	LTBP4	NCF2	C12orf77
ARHGAP18	FAM86B3P	MAML2	RP11-326C3.2	CH507-513H4.6	WWC3	RP11-848P1.9	MYO6
STAC3	BASP1	ITGB2	COG5	CYP51A1P1	DTX1	RND2	OBSCN
SEPN1	LMAN1	PRSS30P	SSTR2	KAZN	CYP46A1	SMIM14	MID1
TPD52L1	ADAM19	NA	TBKBP1	MFHAS1	CMTM4	SPATC1	GABRR2
ADCK1	GRHL1	CLMN	S100A4	CHST11	PCDHGA6	ARHGEF37	WI2-85898F10.2
MIR193BHG	CTSW	GGT1	COL14A1	SCIMP	DGCR9	PCDHGB3	THEM4
RP4-625H18.2	NAP1L5	BIRC7	LINC01165	PLAG1	PYGL	RPL12P37	CAB39L
NBEA	POF1B	TNS3	HIST1H2BL	TGM2	C9orf129	MXRA7	SLC25A23
B4GALT5	RP11-514P8.2	TMEM63A	RPL5P1	RP11-968O1.5	PLEKHH3	LINC00278	ACSM3
SERPINB6	MTUS2-AS1	CTD-2526A2.2	LOXL2	EVI2A	RP11-861E21.2	ALOX12B	AC006960.5
TFCP2	PIK3CD-AS2	HAGHL	TSC22D3	TMEM145	TNFRSF17	RP11-713M15.2	LILRB1

HSPA8P5	ARL10	RASL11A	KB-1980E6.3	ASB13	SLC7A3	CTCFL	GFRA3
EFNA2	SUPT3H	SLC6A12	AK4	ZNF582	LA16c-313D11.9	IL6ST	MTUS2
GDF15	CST7	TCERG1L	RGS1	RITA1	CPNE2	RP11-74E22.3	USP18
DLGAP3	RP11-120K24.3	HEY2	NR2E3	AP001625.6	EML5	WWC1	AC006277.3
GDF7	RPL12P10	RECK	CSTA	FBXO6	PRKCA	SYNGR2	GLIPR1
CRYL1	RP11-77H9.1	IL21R	TMEM129	ZBTB20	CDNF	KCTD12	RP5-1033H22.2
SERPINF2	HHEX	FAM13A	AGA	RASAL1	LINC00654	DOCK7	RP11-142C4.6
AC104024.1	ZC3HAV1L	NSG1	RPL22L1	SMO	DEGS2	MOXD1	MYO1F
PDE6G	NRTN	PTGER1	TUBB2A	AK4P1	ID1	SLC6A13	PTAFR
RP11-203J24.8	GRIN1	ABHD14B	FOXP2	SMIM1	SPON2	FNDC11	SLC45A3
PARD3	CABP4	CCDC188	MCF2L-AS1	MAD1L1	PCDHGA10	PIP5KL1	ZFP41
RNF126	CTD-2575K13.6	RP11-153M7.3	RAB25	THPO	BEGAIN	NA	RP11-191G24.1
NAPSB	PLXNB3	GBGT1	TNFSF14	ARHGEF4	BCAR3	AF064858.8	AC104024.2
CCDC74A	DMD	AK4P3	UBE2E2	PDE2A	LINC00665	ID4	LRRC28
PLXNC1	PPM1H	DHRS3	CXCL16	ITGAL	IL27RA	PDK3	CCDC78
CXCL11	RP1-78B3.1	TFCP2L1	RP5-1073O3.2	PTMS	NEAT1	GATA3	CASP4
POR	UNC5A	RP11-85A1.3	MGAT4A	FHL1	LGALS1	SLC6A18	ASAP3
DNMT3B	ELL2	ZNF43	APOBEC3G	NME4	SERPINE2	HIC1	ZFYVE28
PCDHGB5	SNPH	CD4	RP11-11N9.4	PSD3	LTC4S	KLHL35	RP1-148H17.1
TNFAIP2	RP11-347C12.3	AFDN	EGFL7	SPNS2	S100A6	LZTS3	LINC01126
RNLS	ZFP3	CCDC74B	CADM2	DISP2	SHB	KCNS1	CDK7
MYO1E	TTC23	PTPRVP	RP5-1029F21.3	RP11-182J23.1	MEF2C-AS1	SCRN1	MANF
CXADR	HFE	LHFPL2	AC105052.1	SLC2A12	NKAIN4	NTNG2	LINC00304
C14orf28	TRAF1	ESRP2	AC005077.14	LAMC1	ALDH2	CHPT1	PRRT4
FAM213B	HEY1	HEBP1	MYO3B	U91319.1	SLC16A10	SLC25A42	LHFPL4
NA	BIN2	IFFO2	GRHL3	LYG2	IL4R	KCNC3	AHR
AC005682.6	PLBD1-AS1	RHPN2	RP11-10N16.2	MGLL	DNAJC22	AMIGO2	WHRN
DPF3	NOXA1	CACNA1A	FGFR3	DPY19L2P3	ITGA3	C17orf99	RAPH1
PLD4	FNBP1	MYH10	GLIDR	IL21R-AS1	RP11-103B5.4	WBSCR27	GPR65
MIXL1	PCK1	LINC01422	CH507-513H4.5	IGHG2	ANXA4	ELFN2	C6orf223
SLC41A2	RYR1	IGHGP	FCER1G	VARS	AC108463.2	RP11-603B24.1	MTERF1
AIG1	CLCNKA	CNKSR1	RP11-211C9.1	CMBL	CA2	GALNT6	FBLN1
AKAP7	GCNT1	P4HA2	OSBPL6	TIGD2	RBM47	MTUS1	CD151
PC	NR3C2	TNFRSF1B	KLRC2	MYBPC2	DEF8	RP11-33E12.2	COL8A2
VWA5A	CD58	LARGE1	PROSER2	JUP	FRMPD3	NKD2	TSPAN13
NRN1	TLR3	MYOM1	LINC01296	IGLC5	DOK5	TMEM178B	MISP
GBP2	LIN28B	RP11-573D15.1	GPR63	CENPUP2	FST	MYL9	LMO3

CEND1	AC064834.1	S100A11	SYDE2	IGLC3	GNAL	TUBB6	SHISA9
AIM2	AK5	FIRRE	GRAMD1C	BHLHA15	DNAH17-AS1	LGALSL	APOBEC3B
STEAP3	CST3	MIR34A	GPR85	HIST2H2BD	RTN4RL1	HIST2H2AC	CDYL2
PDE3B	AP000487.5	SLC27A2	SHANK2-AS1	PACSIN1	CD28	RNF43	HIST2H2BF
FAM81A	SPATA12	GSTO2	SPIRE2	ASIC1	APOBEC3F	GARNL3	THRSP
GALC	SHISA8	PEX11A	DIXDC1	STRN	KLF2	RP11-573D15.2	PNPLA4
UNC13B	PRR5	AHRR	ABHD17AP5	PTPRS	CUEDC1	TESC	CTTN
WDR31	LATS2	CA8	TRAJ45	TBC1D4	PLBD1	MLLT3	RP11-196G18.22
KIF13A	CARMIL1	BHLHE22	BSN-AS2	AC093609.1	DENND5B	KREMEN2	SMN2
HIST2H2BE	SH3RF1	LGR4	AAED1	DPEP1	CUX2	ZNF32	GEM
RUSC2	PITX2	DNER	ITM2A	FGD4	MTURN	WDR17	IRF6
KIAA1549L	ALDH4A1	RHOB	NA	RHOD	BMP6	ROR1	TSPAN15
CD7	MPP7	RIN3	RP11-410D17.2	ZNF658	SLC4A11	DUSP16	CD9
USP51	HYKK	MIR4500HG	KCNK12	ZNF486	POU4F1	SLITRK5	DUSP3
C2orf88	INA	LINC01021	USP40	SHROOM2	WNT10B	BDKRB2	GRID1
MEGF11	PDZRN3	PDE7B	DACT3	PLPP7	KREMEN1	NCALD	CLDN23
SERPINB8	GPRIN3	IGHG1	VDR	FAM198B	RP11-597D13.9	CHGB	ALDH1L2
SOX8	RP11-161M6.2	RP11-538C21.2	A4GALT	WNT7B	SLC22A31	IGHG3	GPAT3
NEXN	TMEM144	ST6GALNAC5	RMDN2	RP11-307E17.8	AFAP1-AS1	COBLL1	ZSCAN20
RNF157	NA	RP11-449J21.5	RP5-1024C24.1				

Appendix Table 15. Differentially expressed genes upon SOX11 overexpression in DG75 BL cell line with adjusted P-value <0.15 and absolute log_2-transformed fold change >0.5.

Genes upregulated in Ramos SOX11 vs Ramos CT BL cell lines							
SOX11	RAG1	RAG2	CD24	DBN1	CCDC50	HOMER3	MEX3A
PLXNB1	TNNI1	LRP5	PTPN3	RP11-87E22.2	NYNRIN	COBL	ULK1
ACTG1P22	TMEM132A	MGLL	TTYH3	KIAA1211	GJC1	MARCKSL1	MEX3B
RCOR2	MAP2	IDH2	KIAA1147	GPC2	IL23A	CKAP4	HRK
ZSCAN2	CBX2	ZNRF1	SIPA1L2	NREP	SOGA1	ZNF629	TNFRSF21
EVC2	FGFRL1	GPRIN1	STARD9	PHACTR1	FLNA	ADM	CACFD1
BRD3	JUP	ZNF627	MYB	PHC2	KIF3C	PTPN12	PHF2
RAB11FIP3	LZTS1	DENND5A	MEGF11	NARF	ZNF71	YPEL1	DAB2IP
RALGDS	SPTBN2	NAV1	GOLGA2P10	TUBA1A	CTNNA1	H1FX	SNN
RP11-255H23.4	TRIB2	TMSB10					

Genes downregulated in Ramos SOX11 vs Ramos CT BL cell lines							
GSTO2	CCDC110	EEF1E1	PTPN22	ACKR4	MSMO1	C2orf88	GLMN

DLG2	JAG2	ASZ1

Appendix Table 16. Gene sets enriched in DG75 ER-SOX11 vs DG75 ER, and Ramos SOX11 vs Ramos CT comparisons. NES, P value and FDR are shown.

Venn diagram cell lines enriched	Total	Enriched gene sets	Cell line	NES	P value	FDR
DG75 ER-SOX11 vs DG75 ER ∩ Ramos SOX11 vs Ramos CT	8	KEGG_PRIMARY_IMMUNODEFICIENCY	DG75	2.025	0.000	0.022
			Ramos	1.901	0.002	0.043
		PASINI_SUZ12_TARGETS_DN	DG75	2.163	0.000	0.003
			Ramos	2.135	0.000	0.011
		VERHAAK_GLIOBLASTOMA_PRONEURAL	DG75	2.511	0.000	0.000
			Ramos	2.548	0.000	0.000
		REACTOME_RUNX1_INTERACTS_WITH_CO_FACTORS_WHOSE_PRECISE_EFFECT_ON_RUNX1_TARGETS_IS_NOT_KNOWN	DG75	2.073	0.000	0.019
			Ramos	2.035	0.000	0.022
		HUMMEL_BURKITTS_LYMPHOMA_UP	DG75	2.233	0.000	0.001
			Ramos	1.952	0.000	0.030
		REACTOME_INTERLEUKIN_7_SIGNALING	DG75	2.028	0.000	0.024
			Ramos	2.205	0.000	0.006
		HADDAD_B_LYMPHOCYTE_PROGENITOR	DG75	2.245	0.000	0.000
			Ramos	2.014	0.000	0.025
		BENITEZ_GBM_PROTEASOME_INHIBITION_RESPONSE	DG75	1.981	0.000	0.034
			Ramos	1.901	0.002	0.043

Appendix Table 17. Genes overlapping between differential expression analysis in DG75 and Ramos SOX11-overexpressing cell lines, composing the SOX11 signature in BL.

Genes DG75 ∩ Ramos							
TMSB10	MEX3B	HOMER3	PTPN12	ULK1	TTYH3	IDH2	PLXNB1
SIPA1L2	PHACTR1	SNN	RCOR2	GSTO2	IL23A	TUBA1A	LZTS1
PHC2	ZNF627	RAB11FIP3	MEGF11	CBX2	FGFRL1	DLG2	MGLL
CD24	ZSCAN2	MEX3A	DAB2IP	ZNF71	NAV1	DBN1	SPTBN2
GOLGA2P10	GPC2	JUP	KIAA1211	MARCKSL1	NREP	STARD9	SOX11
C2orf88	BRD3	KIF3C	FLNA	TRIB2	MYB		